10.14751/SZIE.2013.005

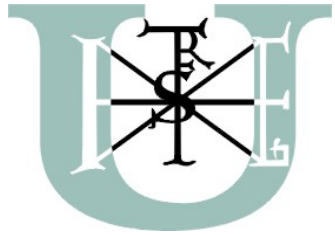

SZENT ISTVÁN UNIVERSITY

KINETICS AND KINEMATICS OF THE HUMAN KNEE JOINT UNDER STANDARD AND NON-STANDARD SQUAT MOVEMENT

PhD dissertation

by

Gusztáv Fekete

Gödöllő, Hungary
2013

10.14751/SZIE.2013.005

Doctoral School: Mechanical Engineering PhD School

Thematic group: Basics of Agriculture Machine Engineering

Director: Prof. Dr. István Farkas
Doctor of Technical Science
Faculty of Mechanical Engineering
Szent István University, Gödöllő, Hungary

Supervisor: Prof. Dr. Béla Málnási-Csizmadia
Candidate of Technical Science
Faculty of Mechanical Engineering
Szent István University, Gödöllő, Hungary

Co-supervisor: Prof. Dr. Patrick De Baets
Doctor of Philosophy
Faculty of Engineering and Architecture
Ghent University, Ghent, Belgium

…… ……
Director of the Doctoral School Supervisor

10.14751/SZIE.2013.005

CONTENTS

10.14751/SZIE.2013.005

10.14751/SZIE.2013.005

NOMENCLATURE AND ABBREVIATIONS

F_{pf} :	Patellofemoral compression force (N)
F_{tf} :	Tibiofemoral compression force (N)
F_q :	Quadriceps tendon force (N)
F_{pt} , F_{pl} :	Patellar tendon force (N)
F_s :	Friction force (N)
F_N :	Normal force (N)
F_h :	Hamstring muscle force (N)
F_{re} :	External force for knee extension (N)
F_{rh} :	External force for knee flexion (N)
F_{GR} :	Measured ground reaction force (N)
$T_{extension}$:	Extension torque (Nm)
$T_{flexion}$:	Flexion torque (Nm)
BW:	Body weight force (N)
D_h :	Moment arm of hamstrings muscle (mm)
D_{pl} :	Moment arm of patellar tendon (mm)
D_r :	Moment arm for external force (mm)
M_q :	Moment arm of the quadriceps force about the patellofemoral contact point (cm)
M_{pt} :	Moment arm of the patellar tendon force about the patellofemoral contact point (cm)
M_{act} :	Actual moment arm of patellar tendon about the tibiofemoral contact point (cm)
M_{eff} :	Effective moment arm (cm)
d :	Moment arm of the net knee moment in case of standard squat (m)

L_{eff} :	Effective moment arm of quadriceps tendon (mm)
M_N :	Net knee moment (m)
$g(\alpha)$:	Approximate function of $\boldsymbol{F_{pt}/F_q}$ ratio (-)
$k(\alpha)$:	Approximate function of $\boldsymbol{F_{pf}/F_q}$ ratio (-)
$C_{1\text{-}2\text{-}3\text{-}4}$:	Constants for approximate functions (-)
l_{10} :	Length of the tibia (cm)
l_{30} :	Length of the femur (cm)
l_1 :	Intersected length of the axis of tibia and the instantaneous line of action of the ***BW*** (cm)
l_3 :	Intersected length of the axis of femur and the instantaneous line of action of the ***BW*** (cm)
l_p :	Length of the patellar tendon (cm)
l_t :	Perpendicular length between the tibia and the tibial tuberosity (cm)
l_f :	Perpendicular length between the femoral axis and the line of action of quadriceps tendon force (cm)
λ_1 :	Dimensionless, intersected tibia length function (-)
λ_3 :	Dimensionless, intersected femur length function (-)
λ_p :	Dimensionless length of patellar tendon (-)
λ_t :	Dimensionless thickness of shin (-)
λ_f :	Dimensionless thickness of thigh (-)
α :	Flexion angle of the knee (°)
β :	Angle between the patellar tendon axis and the tibial axis (°)
γ :	Angle between the axis of tibia and the line of action of the ***BW*** force (°)
δ :	Angle between the axis of femur and the line of action of the ***BW*** force (°)
φ :	Angle between the tibial axis and tibiofemoral force (°)
ρ :	Angle between the patellar tendon and the patellar axis (°)
ε :	Angle between the patellar axis and the femoral axis (°)

ψ: Angle between the quadriceps tendon and the femoral axis (°)

ξ: Angle between the quadriceps tendon and the patellar axis (°)

ϕ: Dimensionless function of the angle between the axis of tibia and the line of action of the ***BW*** force (-)

θ: Flexion of femur relative to the tibial axis (°)

θ_q: Quadriceps force angle with respect to tibial axis (°)

θ_p: Patellar axis angle with respect to tibial axis (°)

η_{1-2-3}: Patellar rotation, twist and tilt (°)

τ: Change in patellofemoral mechanism angle (°)

ϑ'': Angular acceleration (1/s^2)

y_{COP}: Position of center of pressure in the *y* direction (m)

x_c: Position of center of gravity in the *x* direction (m)

y_c: Position of center of gravity in the *y* direction (m)

z_c: Position of center of gravity in the *z* direction (m)

s^2_{ycj}: Variance of center of gravity in the *y* direction (m^2)

$s^2_{\lambda 1}$: Variance of the dimensionless, intersected tibia length function (-)

$s^2_{\lambda 3}$: Variance of the dimensionless, intersected femur length function (-)

$s^2_{fit.\lambda 1}$: Fitting variance of the dimensionless, intersected tibia length function (-)

$s^2_{fit.\lambda 3}$: Fitting variance of the dimensionless, intersected femur length function (-)

s_{ycj}: Standard deviation of center of gravity in the *y* direction (m)

Y_s: Moment arm of the net knee moment in case of non-standard squat (cm)

Δy_c: Standard error of y_c (m)

t: Constant for *t*-tests (-)

r^2: Linear correlation coefficient between the original and modelled data values (-)

ΔK: Percentage difference between standard and non-standard squat quantities (-)

d_{b1}: Basic circle of the driving gear (m)

d_{b2}: Basic circle of the driven gear (m)

V_1: Contact velocity of the driving gear (m/s)

V_2: Contact velocity of the driven gear (m/s)

ω_1: Angular velocity of the driving gear in the contact (1/s)

ω_2: Angular velocity of the driven gear in the contact (1/s)

χ: Sliding-rolling ratio (-)

ρ_{r-s}: Rolling-sliding ratio (-)

$\bar{r}_{Ci}$: Displacement vector describing the path of the contact points (m)

$\bar{r}_{CMF}$: Displacement vector of the center of mass regarding the femur (m)

$\bar{r}_{CMT}$: Displacement vector of the center of mass regarding the tibia (m)

$\bar{v}_{CMF}$: Velocity vector of the center of mass regarding the femur (m/s)

$\bar{v}_{CMT}$: Velocity vector of the center of mass regarding the tibia (m/s)

$\bar{\omega}_{CMF}$: Angular velocity vector of the center of mass regarding the femur (1/s)

$\bar{\omega}_{CMT}$: Angular velocity vector of the center of mass regarding the tibia (1/s)

$\bar{e}_{Ci}$: Tangential unit-vector of the contact path (-)

$\bar{r}_{CF}$: Displacement vector determining the contact point with respect to the center of mass of the femur (m)

$\bar{r}_{CT}$: Displacement vector determining the contact point with respect to the center of mass of the tibia (m)

$\bar{v}_{CF}$: Velocity vector of the contact point with respect to the center of mass of the femur (m/s)

$\bar{v}_{CT}$: Velocity vectors of the contact point with respect to the center of masses of the tibia (m/s)

v_{CFt}: Tangential velocity components in the contact point regarding the femur (m/s)

v_{CTt}:	Tangential velocity components in the contact point regarding the tibia (m/s)
v_{CFn}:	Normal velocity components in the contact point regarding the femur (m/s)
v_{CTn}:	Normal velocity components in the contact point regarding the tibia (m/s)
s_{femur}:	Arc length of femur (m)
s_{tibia}:	Arc length of tibia (m)
μ_s:	Static coefficient of friction (-)
μ_d:	Dynamic coefficient of friction (-)

TKR:	Total knee replacement
ACL:	Anterior cruciate ligament
PCL:	Posterior cruciate ligament
MCL:	Medial cruciate ligament
LCL:	Lateral cruciate ligament
SD:	Standard deviation
COP:	Center of pressure
COG:	Center of gravity
ODE:	Ordinary Differential Equations
DAE:	Differential-Algebraic Equations
CCD:	Charge-couple device

10.14751/SZIE.2013.005

1. INTRODUCTION AND OBJECTIVES

1.1. Involved Research Partners

Two research partners are involved into this doctoral work, namely:

- Institute of Mechanics and Machinery (Department of Mechanics and Engineering Design), Szent István University, Gödöllő, Hungary. The Department participates in different research fields such as mechanics of composite materials, granular assemblies modelled by Discrete Element Method, and biomechanics of the human knee joint. The topic related to the biomechanics has been the latest one at the department since it started in 2003, and during the past years, mostly experimental work has been carried out regarding the kinematics of cadaver knee joints with the cooperation of the Semmelweis University of Medicine.

- Labo Soete (Department of Mechanical Construction and Production), Ghent University, Ghent, Belgium. The Department carries out various researches in numerous fields such as tribology, fatigue and fracture mechanics of mechanical structures and machine elements. The Department started the biomechanics research in 2006, and it has been expanded with several institutes (UZ in Gent, Hogeschool West-Vlaanderen in Kortrijk). The work, which was started at Szent István University, Hungary, has been complemented and finished Ghent University.

1.2. Motivation

Although knee implants perform well in restoring and maintaining good strength and functionality of the knee joint, the large number and type (posterior-stabilized design, cruciate-retaining design, unicompartmental design, etc.) of knee prostheses indicate that the behaviour of the knee joint is not yet fully understood.

Nevertheless, the satisfaction of the patients is not unanimous according to the published survey results. While in the study of Kwon et al. [Kwon et al., 2010], only 0.9% of the patients (from 438 patients) declared to be unsatisfied, Blackburn et al. [Blackburn et al., 2012] stated, based on several other studies as well [Gandhi et al., 2008, Scott et al., 2010], that approximately the 18% of the patients were unsatisfied with the outcome of the total knee arthroplasty (TKA).

At the same time, patient satisfaction is a highly complex issue that is affected by many factors that determine health-related quality of life [Ethgen et al., 2004, Noble et al. 2006]. Therefore, it is a challenging task to assess the patient satisfaction in an objective and reliable manner.

The design of knee prosthesis is based on functionality, correct kinematics, determination of the operational loads and choosing adequate materials that can withstand the arising stresses.

Among the various human locomotions (gait, running, squatting) we set the emphasis on the squat. We squat if the shoelaces are untied, or something is dropped on the floor. Besides the every day use, squat movement is a basic strengthening exercise, which is vital to train primarily the muscles of the thighs, hips and buttocks.

It is obvious that squatting is very much involved into our lives, therefore, it has to be correctly taken into account during the design.

The primary focus on squatting is based on three significant facts:

1. Except kicking, jogging or jumping the highest forces appear in the knee joint under squatting movement,
2. Under squatting movement, almost the complete flexion angle (0˚ to 120-130˚) is used while during gait, running or other activities, it is limited to its one-third, one-fourth of the complete range,
3. While patients with total knee replacements can carry out e.g. gait fairly well, kneeling or squatting often means difficulty due to the imperfection of the implants.

These are the main reasons why this study deals exclusively with squatting.

The kinetic description of squatting is limited to the so-called *standard squat* in the literature, where the torso is restrained to carry out only vertical motion, which means that practically the centre of gravity does not change its position during the squat. This simplification has been widely used and so far, only a few authors pointed out, that the moving centre of gravity might have a significant effect on the kinetics of the knee joint.

On the grounds of this hypothesis, it will be demonstrated in this thesis how significantly the movement of the centre of gravity alters the knee kinetics under squatting movement. This new movement will be titled as *non-standard squat*.

Nevertheless, there are also questions in the kinematics of the knee that studies have not yet dealt with, for example the *sliding-rolling ratio* in the active functional arc, which expands from 20˚ to 120˚ of flexion angle. The sliding-rolling ratio is not only interesting in case of spur, helical or other gear connections, but in any engineering systems where components have to withstand long-term varying loading conditions and wear.

Human knee prostheses are such elements, and for this reason, tribological tests are carried out on them before the actual production. Naturally, to obtain reliable results, experiments have to be carried out with realistic kinetic and kinematic boundary conditions.

Due to the multiple studies about the kinetics of the knee joint under different movements, the loading issue is well-known and fundamentally researched.

Problems rise, when certain parameters, such as the sliding-rolling parameter has to be set for a test. Regarding its ratio, only rough estimations are available in the literature, and that is related to the beginning of the motion between 0˚ to 20-30˚ of flexion angle. These results claim that in this initial segment, rolling is dominant, while above these certain angles sliding is primer.

So far, sliding-rolling results related to 0-30˚ segment have been widely applied throughout tribological experiments, although if this ratio is underestimated, the actual wear will be much higher than the expected. For this reason, another fundamental aim of this thesis is to answer the question of the applicable sliding-rolling ratio in the functional arc of the knee joint (20-120˚ of flexion angle).

1.3. Aims of the PhD thesis

In this doctoral thesis, two main questions are set as primary goals.

The first question is related to a significant everyday motion, the non-standard squatting, and its kinetics.

What is the difference between the standard and non-standard squatting?

In case of standard squatting, the horizontal displacement of the center of gravity is neglected during the movement (it is supposed to be fixed in one point). However, this parameter is considered in the non-standard squat and its position depends on the flexion angle.

So far, only the standard squat has been substantially investigated, which lacks this significant parameter. For this reason, the choice fell on the non-standard squat since the horizontal movement of the centre of gravity, or in other words the forward movement of the trunk, may considerably alter the kinetics of this type of movement. The forward-backward movement of the trunk as a factor, has been recognized and mentioned in earlier studies, but it was always left out of consideration.

A new analytical-kinetical model that involves this parameter answers the question of how the forward movement of the trunk may affect the patellofemoral forces. By having involved the effect of moving center of gravity (movement of the trunk) into the model, the patellofemoral force, the tibiofemoral force, the patellar tendon force and the quadriceps force can be derived in case of standard and non-standard squatting alike.

The output of this question serves more as a fundamental understanding of the knee joint, where the results can be used as initial conditions, related specifically to the loading conditions in the replacement design.

The second question deals with a more practical-orientated issue, namely the sliding-rolling ratio. This ratio actually defines the relative motion between the condyles of the femur and the tibia. For this reason, it is in a close interrelation with wear and therefore it has an essential effect on the lifetime and the survivorship of the knee implants.

The foregoing phenomenon has also a fundamental side. Only a limited number of studies (analytical, numerical, and experimental) have dealt comprehensively with the question of sliding-rolling, and exclusively only but one study investigated this phenomenon on both lateral and medial sides of prostheses geometries.

Preliminary results have already been published, for example in the beginning of the motion up to 20-30˚ of flexion angle the relative motion is dominantly rolling, while above these angles sliding is prevailing.

As for an output, this phenomenon is substantially essential in the tribological tests on actual prostheses. The presence of sliding-rolling produces different wear phenomenon on the connecting surfaces and for this reason a proper ratio has to be applied during these experiments. So far, these preliminary results were normative for tribological tests regardless of the applied domain (20-30˚ of flexion angle or above).

Considering that a ratio, which is applicable for lower angles, would also be appropriate at higher angles is most certainly incorrect. For this reason, the ratio has to be investigated between 20˚ and 120˚ of flexion angle in order to provide valid results for experimental tests.

The result of the second question is a multibody model, which can predict the sliding-rolling ratio of different prostheses. By the summary of these models, a general range about the ratio is appointed.

2. LITERATURE REVIEW

2.1. Anatomical review of the human knee joint

In this chapter, the major structures of the knee joint will be presented anatomically, followed by some important elements regarding their biomechanics. The review is intended to assist in the modelling, since a thorough knowledge of the complex anatomy and biomechanical function of the structures of the knee is essential to make adequate assumptions and simplifications.

2.1.1. Structural build-up of the bone

Osseous tissue, or bone tissue, is the major structural and supportive connective tissue of the human body [Standring, 2008]. Osseous tissue forms the rigid part of the bone organs that build up the skeletal system. If we look at the structure of the femur, two specific compositions occur in the bone: a solid part and a cancellous (spongy) part (Figure 2.1).

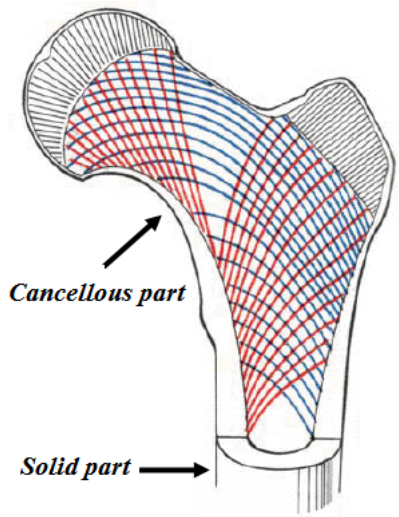

Figure 2.1. Structure of the femur [Standring, 2008]

The solid part frames the outer part of the bone, while the spongy part composes the inner part.

The buildup of the bone is not irregular, but structured, in a so-called trajectory system, accordingly to the normal forces that affect the bone. This means that due to the load, the frame has equivalent arrangement related to the static force lines.

By considering all these features, the modelling becomes rather difficult if all the aspects of mechanics (material, structure, etc.) are about to be investigated [Szentágothai, 2006].

Apart from the theory of elastic or plastic deformation, if the deformations of the bones are disregarded and they are modelled as rigid bodies, the mechanical investigation becomes significantly simpler.

2.1.2. Structural build-up of the knee and the major bones

The knee joint is a closed system, built up from ligaments and muscles. This system is generally defined as one of our organs (Figure 2.2). Often, it is considered in the modelling as a simple hinge that carries out planar motion, while in reality, it is the largest and most complex (related to its function and its geometry as well) mechanism of our body [Standring, 2008].

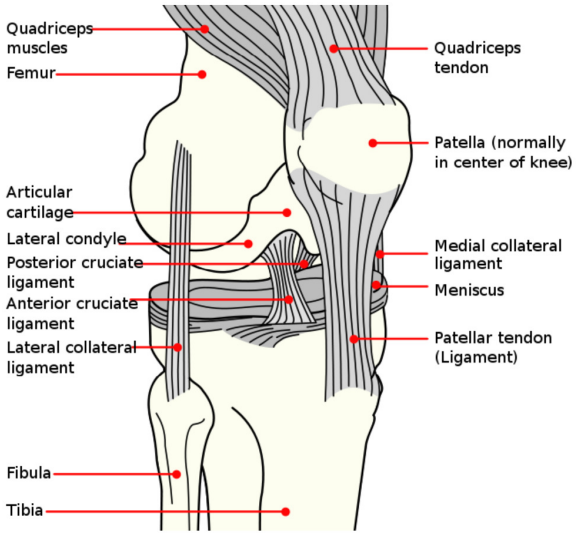

Figure 2.2. Anterolateral aspect of the knee joint [Standring, 2008].

Functionally, it is not a gynglymus (planar joint) but strictly trochogynglymus (spatial joint) joint type [Szentágothai, 2006].

The knee joint allows both flexion and extension about a virtual transverse axis of the femur and a slight medial-lateral rotation about the tibial axis (the lower leg) during the movement. The knee joint carries out local movement as well, since rolling and sliding occurs between the condyles of the femur and tibia during extension-flexion.

Three major bones can be distinguished concerning the bones of the knee joint: femur, tibia and patella (Figure 2.3 and Figure 2.6). The joint baths in a synovial fluid, which is responsible for the proper lubrication between the sliding-rolling contact surfaces, the so-called condyles.

2.1.2.1. Femur and Tibia

The femur is the largest and longest bone of the human body. The length of an average adult male femur is about 43.85 ± 3.549 cm while a female is 42.19 ± 3.127 cm [Özaslan et al., 2003]. The femur has the ability to support up to 30 times the full body weight of an adult. The structure of the bone can be divided into three parts such as, body part and the two extremities: the proximalis part (upper) and distalis part (lower) (Figure 2.3). The tibia has a prismoid form and it expands at the top where it enters into the knee joint. It also contracts in the lower third and then again enlarges but to a lesser extent towards the ankle joint (Figure 2.3). The length of an average adult male tibia is about 38.37 ± 2.398 cm while a female is 35.13 ± 2.215 cm [Özaslan et al., 2003]. The highest internal load during gait can reach 4.7 times of the bodyweight

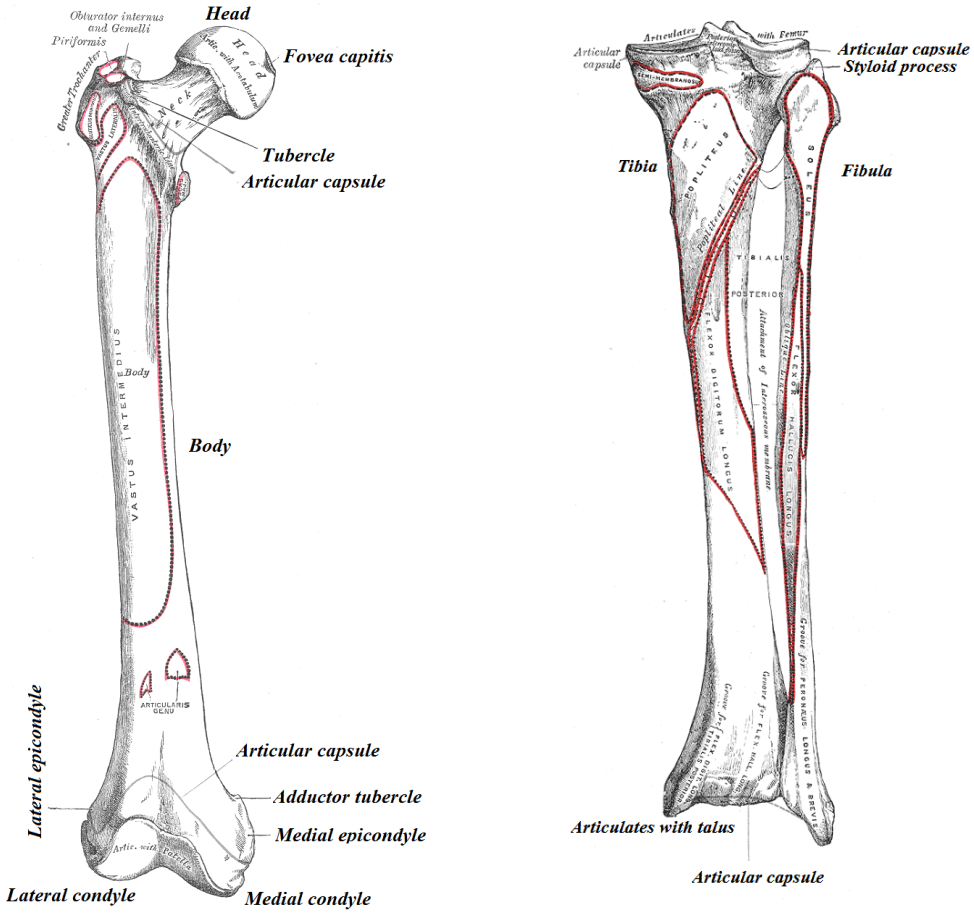

Figure 2.3. The femur and the tibia [Standring, 2008]

The proximalis part joints the hip similarly to a socket-ball connection, while the distalis part connects the tibia and the patella together. By looking at the distalis part from the front (Figure 2.4), the different surfaces such as the lateral or medial condyles can be fairly well distinguished.

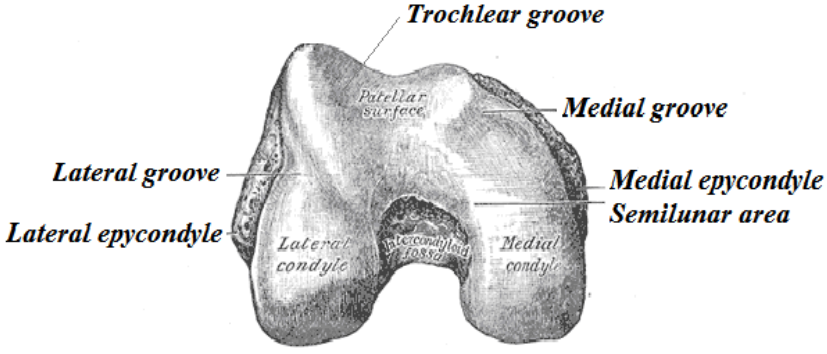

Figure 2.4. Condyles of the femur (right leg) [Standring, 2008]

Between the lateral and medial groove, the patellar surface is situated. This concave region at the lower end of the femur is commonly called as trochlea or trochlear groove [Szentágothai, 2006]. In this groove (trochlea), the patella carries out a rotating-sliding motion.

The condyles of the knee joint are covered by cartilage, which is a thin, elastic tissue that protects the bone and assures that the joint surfaces can easily slide (and roll) over each other. Cartilage ensures the correct knee movement as well.

One remarkable feature of the femur that the internal structure is formed in an efficient manner to withstand the internal stress that occurs due to the load on the femur-head. Throughout the femur, with the load on the femur-head, the bony material is arranged in the paths of the maximum internal stresses, which are thereby resisted with the greatest efficiency, and hence with maximum economy of material [Girgis et al., 1975].

The tibia has also a body part and two extremities.

The upper extremity is large, and expanded into two eminences, the medial and lateral condyles (Figure 2.5). The superior articular surface presents two smooth articular facets. The medial facet, oval in shape, is slightly concave from side to side, while the lateral, nearly circular and it is concave from side to side [Szentágothai, 2006].

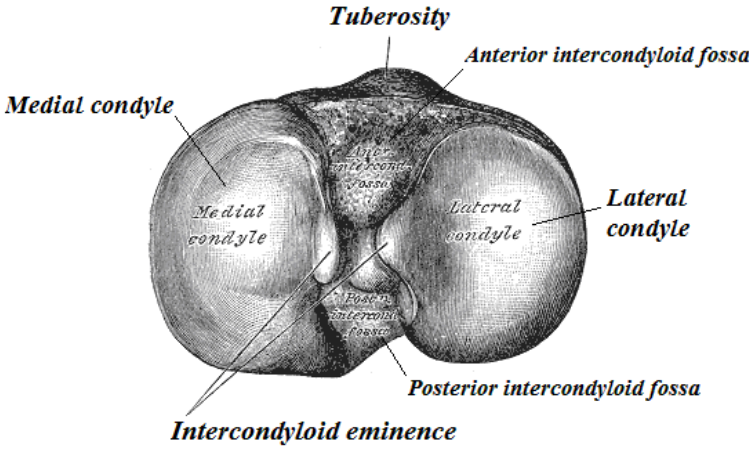

Figure 2.5. Condyles of the tibia [Standring, 2008]

Between the articular facets, but nearer the posterior than the anterior aspect of the bone, is the intercondyloid eminence (*spine of tibia*), surmounted on either side by a prominent tubercle (small eminence or outgrowth), on to the sides of which the articular facets are prolonged. Rough depressions situate in front of and behind the intercondyloid eminence for the attachment of the anterior and posterior cruciate ligaments and the menisci [Szentágothai, 2006].

2.1.2.2. Patella

The patella (also called kneecap) is a flat, chestnut-like bone, situated on the front of the knee joint (Figure 2.6). It serves to protect the front of the joint, and increases the leverage of the quadriceps tendon by altering the angle between the femoral axis and the quadriceps tendon during the movement. It has an anterior and a posterior surface, three borders and an apex (pointy lower part) [Standring, 2008].

Figure 2.6. Patella from anterior and posterior view [Standring, 2008]

Unlike the femur or tibia, the patella consists of a nearly uniform dense cancellous tissue, covered by a thin compact layer.

2.1.3. The cartilage system

Two types of joint cartilage can be differentiated in the knee joint: fibrous cartilage, or better known, the meniscus and hyaline cartilage. As for their role in the knee, the meniscus has tensile strength and can resist pressure, while the hyaline cartilage covers the surface along which the joint moves [Standring, 2008].

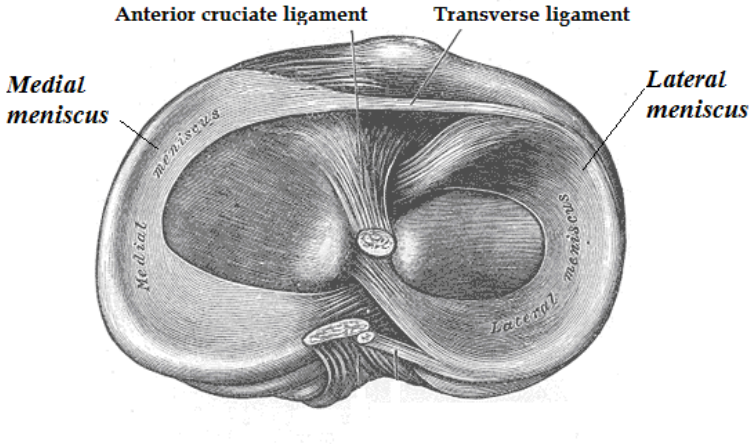

Figure 2.7. Medial and lateral meniscus of the knee joint [Standring, 2008]

The menisci have two parts: lateral and medial (Figure 2.7). Both are cartilaginous tissues that provide structural integrity and stability to the knee joint when it undergoes tension and torsion. The menisci are also known as *semi-lunar* cartilages due to their half-moon *"C"* shape. Although this term has been largely dropped by the medical profession, still led the menisci being called knee "*cartilages*" by the lay public [Szentágothai, 2006].

The function of the menisci is to distribute the body weight and to reduce friction during extension or flexion. This transmission is carried out as follows: the patella, due to the constraining force of the patellar tendon, slowly slips out of the patellar surface into the intercondylaris fossa (Figure 2.5). Since the condyles of the femur and tibia meet at one point (which changes during flexion and extension), the menisci distribute the load of the body [Szentágothai, 2006].

Natural tendency that cartilage wears over the years and unfortunately likewise the human teeth, it has a very limited capacity for self-restoration. The newly formed tissue will generally consist for a large part of fibrous cartilage of lesser quality than the original hyaline cartilage. As a result, new cracks and tears will form in the cartilage over time.

2.1.4. Ligaments and tendons

The cruciate ligaments are very strong intracapsular structures. Originally referred as a crucial ligament due to the cruciate, or crossed, arrangement of the anterior and posterior ligaments within the knee. The crossing point is located slightly posterior to the articular centre. They are entitled as anterior- and posterior ligaments with reference to their tibial attachments (Figure 2.2). The synovial membrane almost surrounds the ligaments but it is reflected posteriorly from the posterior cruciate to adjoining parts of the capsule, therefore the intercondylar part of the posterior region of the fibrous capsule has no synovial covering.

The anterior cruciate ligament (later on ACL) is attached to the anterior intercondylar area of the tibia, just anterior and slightly lateral to the medial tibial eminence, partly blending with the anterior horn of the lateral meniscus [Standring, 2008]. It ascends postero-laterally, twisting on itself and fanning out to attach high on the postero-medial aspect of the lateral femoral condyle [Girgis et al., 1975]. The average length and width of an adult anterior cruciate ligament are 38 mm and 11 mm respectively [Girgis et al., 1975, Wehner et al., 2009]. It is formed of two, or possibly three, functional bundles that are not apparent to the naked eye, but can be demonstrated by micro dissection techniques. The bundles are named anteromedial, intermediate, and posterolaterally, according to their tibial attachments [Mommersteeg et al., 1995].

Compared to the ACL, the posterior cruciate ligament (later on PCL) is thicker and stronger, while the average length and width of an adult posterior cruciate ligament is 38 mm and 13 mm respectively [Girgis et al., 1975, Wehner et al., 2009].

The PCL is attached to the lateral surface of the medial femoral condyle and extends up onto the anterior part of the roof of the intercondylar notch. Its fibres are adjacent to the articular surface. Both anterolateral and posteromedial bundles are named according to their femoral attachments. The anterolateral bundle tightens in flexion while the posteromedial is tight in extension of the knee joint. Each bundle slackens as the other tightens. Unlike the anterior cruciate ligament, it is not isometric during knee motion, thus the distance between the attachments varies as a function of knee position. The PCL rupture occurs less commonly than the ACL and patients usually tolerate it better than that of the ACL.

The quadriceps femoris is the major extensor muscle of the leg, which covers almost the complete front and side part of the knee. This muscle is divided into four individual parts namely: rectus femoris that travels straight down the middle of the thigh, vastus lateralis, which is lateral to the femur, vastus medialis, which is medial to it and vastus intermedius that lies in front of the femur (Figure 2.8).

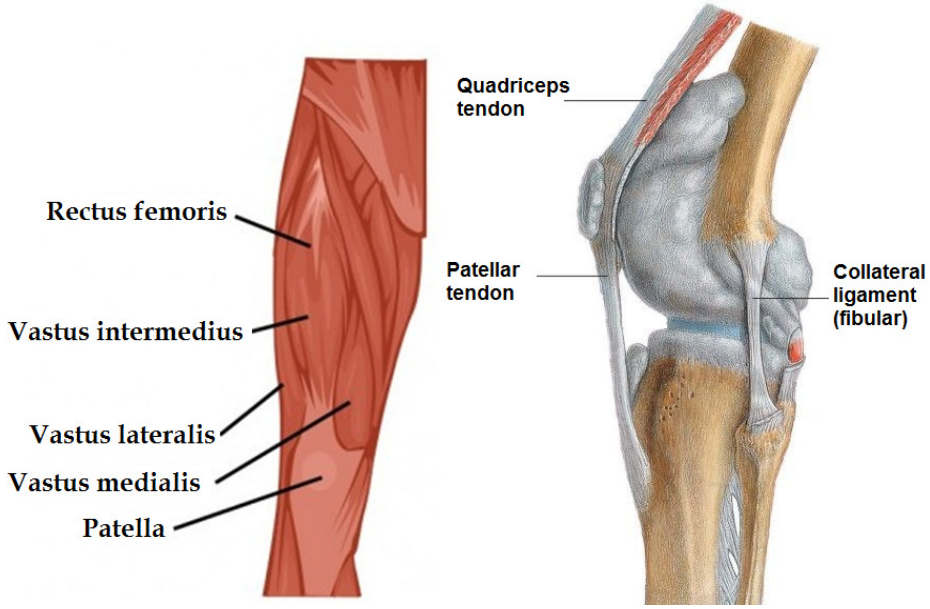

Figure 2.8. Components of the quadriceps and patellar tendon [Standring, 2008]

The four components of the quadriceps muscle unite in one tendon at the lower part of the thigh. This tendon then goes over the patella and ends in the tubercle of the tibia as a continuation of the main tendon. The role of the patellar tendon is essential in the locomotion of the knee, since it transmits the force from the quadriceps through the patella to the tibia (Figure 2.9).

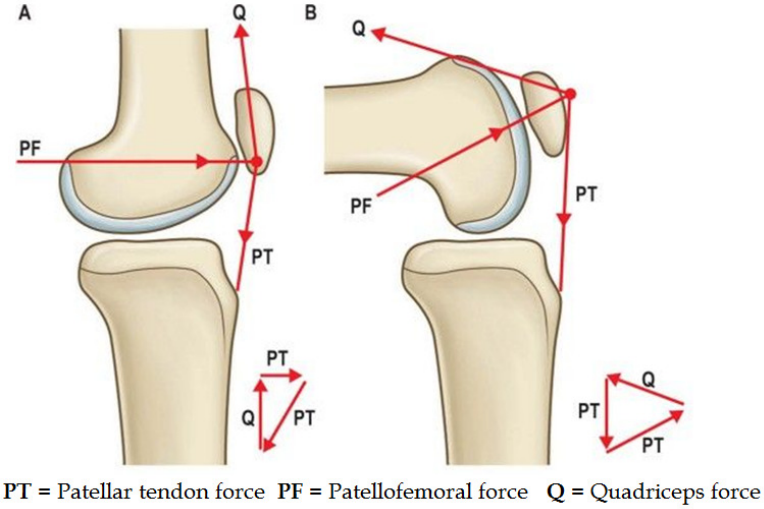

Figure 2.9. Force acting on the knee joint [Standring, 2008]

2.1.5. Major segments of the flexion angle

The range of knee flexion used in the everyday activities extends from about 20˚ ± 10˚ to 110-120˚ of flexion angle. In this range, or arc, the human knee corresponds to the quadrupedal (land animal locomotion) mammalian [Freeman, 2001].

The flexion of arc in case of human beings can be divided into three major segments: the “screw home” arc, the “active arc” and the “passive arc” (Figure 2.10).

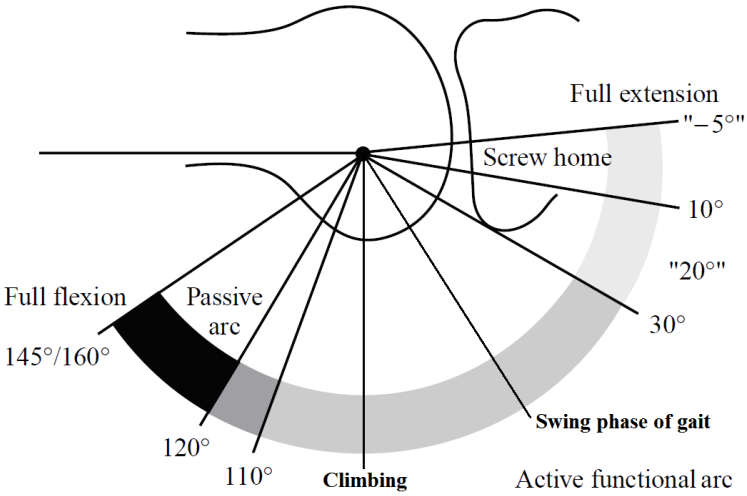

Figure 2.10. Major segments of human arc [Freeman, 2001]

The arc between 20-120˚ of flexion angle is considered as the fundamental active arc, which is totally under muscular control and involves most of our daily activities. Approximately 67˚ is required for swing phase of gait, 83-90˚ for climbing up and descending stairs and 93˚ for rising up from a chair [Laubenthal et al., 1972, Kettelkamp et al., 1970].

The knee joint carries out the „screw-home mechanism” between 5-20˚ degree of flexion. In this arc, rotation between the tibia and femur occurs automatically.

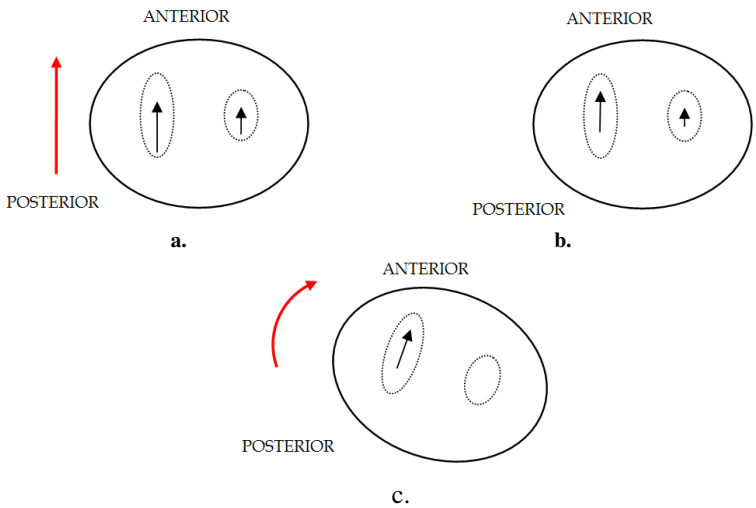

Figure 2.11. Illustration of the screw-home mechanism (a, b, c)

The knee carries out the following pattern during knee extension: the tibia slides anteriorly on the femur surface (Figure 2.11-a) starting from 0˚ angle, then in the last 20˚ of knee extension, anterior tibial slide persists on the medial condyle of tibia because its articular surface is longer in that dimension than the lateral condyle (Figure 2.11-b). At the last part, the prolonged anterior slide on the medial side produces external tibial rotation, which is the so-called "screw-home" mechanism (Figure 2.11-c).

Finally, there is the “passive arc” between 120-160˚ of flexion angle, which is most commonly used in the Asian population [Thambyah, 2008]. It is important to know that the thigh muscles have no effective moment arm after 120˚ of flexion angle and for this reason to maintain the motion and carry the tibia into another flexed position an external force has to be applied, which is the body weight itself [Freeman, 2001].

Since this arc is less often practiced (except in the Asian countries), the accent will be set in this thesis on the active arc between 20-120˚ of flexion angle.

2.2. Analytical-mechanical models of squat

2.2.1. Introduction

Mathematical models mean comprehensive tools to expand the possibilities of analysing complicated structures in any field of science.

The investigation of the musculoskeletal system, like those of any system, usually requires the development of a model. A model is used to answer some questions about the behaviour of a system. It may be constructed as a physical apparatus, or alternatively it may be theoretical or computational.

The ability to devise the best model to answer a specific question is one of the hallmarks of excellence in scientific investigation. Neither should the model be so complex that the inputs cannot be measured, nor should it be so simple that the predictions are too obvious. Creating a model that balances these two aspects requires knowledge of modelling tools, and how they may be applied [Csizmadia and Nádori, 2003].

Naturally, it also requires judgment and experience. In order to give a hint about the modelling, five simple but concrete statements can be summarized [Csizmadia and Nádori, 2003], which will be applied in our further investigations:

1. **None of the investigations – theoretical or experimental – should be over-emphasised. Only the proper combination of the two leads to solution.**
2. **The observed phenomenon can be divided into parts. Useful information can be gained by only investigating the individual parts and not the complete system.**
3. **The laws of nature are constant in space, valid in every field, can be summarized in mathematical formulas, independent respectively of the observer or the state of the phenomenon. These laws are parts of the nature, not made-up mathematical formulations.**
4. **The model is defined by the aim of the investigation as well. The aim of the model – in the view of the related laws of nature – is to determine the behaviour of the investigated phenomenon. The knowledge, related to the phenomenon, can only be expanded by the model results.**
5. **Through the new models, new information can be gained regarding the phenomenon in interest, but the obtained results must be always compared to experiments. This is the adequate way to conclude whether the model is correct or not.**

Although, it is not mentioned as an individual statement, another relevant comment has to be added to the modelling issues. Since a model only follows some major similarity with the observed phenomenon, eventually it will not be able to describe it entirely. There is always a range where the model gives a good approximation related to the phenomenon but beyond that, due to the lack of perfect description, the obtained results are not in agreement with reality.

This is the *applicability range* of the model. In any case, if a theoretical model is used, this range has to be appointed.

It is well known, that patellofemoral problems are common causes of failure after total knee replacement (TKR). Patellar resurfacing implants have often shown loosening or wear of their polyethylene surfaces [Garcia et al., 2009, Sharkey et al., 2002]. Besides that large increases in anterior patellar strain have been reported after total knee replacements, suggesting, that joint replacements may have adverse effects on the mechanics of the extensor mechanism of the knee joint [McLain et al., 1986, Reuben et al., 1991].

For this reason, the acting forces in the knee joint have to be known in most of the cases of the movements. In order to address the problem regarding the kinetics of the knee joint, a comprehensive overview have been carried out about all the available (current and early) analytical-mechanical models.

In this overview, the models are substantially reviewed and analyzed. At the end of each review, the important findings, related to the shortcomings or problems still undealt with, are summarized and some remarks are outlined.

By this approach, the common and long-standing features of the earlier models can be utilized, the ones that are proven irrelevant disregarded, and the missing links complemented in a new analytical-kinetical model.

2.2.2. Human locomotion and kinetics

Peak forces acting in the knee joint under various activities were calculated as long ago as the 1950s. Different knee models with input of gait analysis, force plate data, EMG data, or geometric measurements of the limb were used in these investigations. In order to see how the magnitude of the forces depends on the different locomotion types a table has been assembled with the type of activities and the peak patellofemoral compression forces (Table 2.1).

AUTHOR	ACTIVITY	FLEXION ANGLE	F_{pf}/BW
Bresler and Frankel, 1950	Level walking	20°	1.2
Reilly and Martens, 1972	Level walking	10°	0.5
Morra and Greenwald, 2006	Walking gait	15°	0.6
Nisell, 1985	Lifting (12.8 kg)	90°	2.2
Ericson and Nisell, 1987	Cycling	83°	1.3
Reilly and Martens, 1972	Stair walking	55°	3.3
Andriacchi et al., 1980	Stair ascent and descent	60-65°	2.1-5.7
Morra and Greenwald, 2006	Stair ascent	45°	2.5
Smidt, 1973	Isometric quads contraction	75°	2.6
Kelley et al., 1976	Rising from a chair	90°	5.5
Ellis et al., 1979	Rising from a chair	120°	3.1
Morra and Greenwald, 2006	Rising from a chair	90°	2.8
Huberti and Hayes, 1984	Isometric extension	90°	6.5
Nisell, 1985	Isometric extension	90°	9.7
Kaufman et al., 1991	Isokinetic exercise	70°	5.1
Reilly and Martens, 1972	Squatting	130°	7.6
Dahlqvist et al., 1982	Ascending/descending from squat	140°	6-7.6
Winter, 1983	Jogging	50°	7.7
Wahrenberg et al., 1978	Kicking	100°	7.8
Smith et al., 1972	Jumping	-	20
Nisell, 1985	Quadriceps tendon rupture	-	14.4-24.2
Zernicke et al., 1977	Patellar tendon rupture	90°	25

Table 2.1. Patellofemoral force (F_{pf}) divided by body weight (BW) in case of different movements

As we look at the table, the patellofemoral values start from 0.5 of the body weight (***BW***) in case of level walking and end around 25 ***BW***, in case of the patellar tendon rupture-test. Obviously, everyday life does not involve rupture tests, but it does movements like walking, running, jogging, squatting, or jumping.

Let us analyse the above-mentioned table. During walking, the peak patellofemoral force varies between 0.5 and 1.2 ***BW*** combined with low flexion angle. Stair ascend and descent, alongside with arising from a chair give forth higher forces, typically between 2.8 and 5.7 ***BW***, with relative high flexion angle domain (between 65° and 120° of flexion angle).

According to the literature, squatting movement brings forth forces, which are 6 to 7.6 times higher than the body weight, combined with a high flexion angle. Only Nisell [Nisell, 1985] reported higher patellofemoral forces under isometric extension (approximately 9.7 times ***BW***) than under squatting.

Considering the fact that squatting induces almost the greatest forces in the knee joint, beside the jogging and kicking, and the peak forces appear in the highest flexion angles, this movement is an adequate choice for further investigations.

2.2.3. Mathematical, phenomenological models

These models mainly aim to understand the dynamic-mechanical (load-displacement) response of the knee joint under external forces as inputs. In addition, they also enable to study the effect of the ligaments, both normal and injured, under the movement of the knee joint and the effect of the inaccurate condyle positioning.

In order to contribute to the above-mentioned objectives, Andriacchi et al. [Andriacchi et al., 1983] and Crowninshield et al. [Crowninshield et al., 1976] created quasi-static, analytical phenomenological models with the purpose to reveal the overall stiffness of the joint as a function of flexion angle. Their models consisted of a collection of spring elements interconnecting with the rigid body representations of the femur and tibia (Figure 2.12).

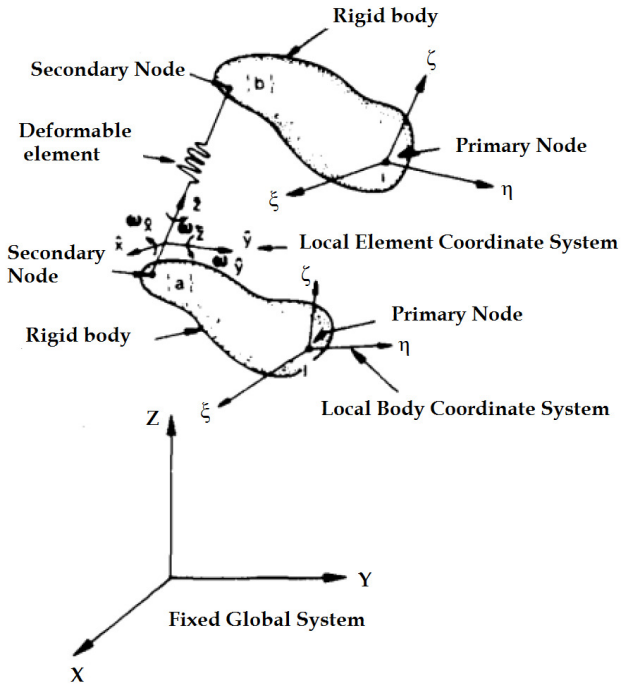

Figure 2.12. Three-dimensional model [Andriacchi et al., 1983]

Soon after this model, Wisman et al. [Wisman et al., 1980] introduced a three-dimensional model of the knee joint, where they considered three important parameters (Figure 2.13):

1. the geometry of the joint surface,
2. the material properties of the ligaments (anterior, posterior, lateral, medial),
3. the material properties of the patellar tendon.

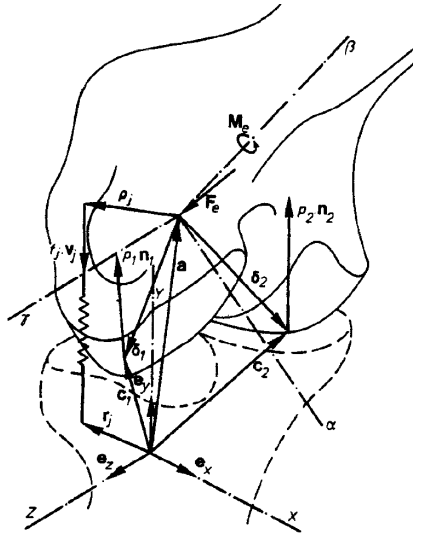

Figure 2.13. Three-dimensional model [Wisman et al., 1980]

The surfaces were approximated with polynomial functions, while the ligaments and the knee capsule were represented by multiple non-linear springs (Figure 2.13). Compared to the earlier studies [Andriacchi et al., 1983, Crowninshield et al., 1976], the model of Wisman et al. [Wisman et al., 1980] was more complex by means of having less restrain in the kinematical boundary conditions.

The investigation of the flexion-extension movement in these studies was done by prescribing these flexion-extension angles. The ligament forces and the other dependent values were determined from the geometric compatibility- and equilibrium equations.

In case of non-linear problems of this kind, there can be more than one equilibrium configuration for a prescribed flexion-extension angle, unless it is counterbalanced with a force. For example, if we are interested of the contact point, force etc. at 15° of flexion angle, than to keep the stability of the above-mentioned non-linear equations and to gain solution, an additional member has to complement the mathematical system. The physical meaning of this additional member is a force.

According to Wisman et al. [Wisman et al., 1980], it is necessary to apply an external force for the preferred equilibrium configuration.

Due to these restrictions in the quasi-static modelling, Manssour et al. [Manssour et al., 1983] proposed a solution by creating a so-called biodynamic model (Figure 2.14). By their model, the artificial restrictions of the quasi-static state could be elaborated alongside with the necessity to specify the preferred configuration if the dynamics of the problem is incorporated into the model.

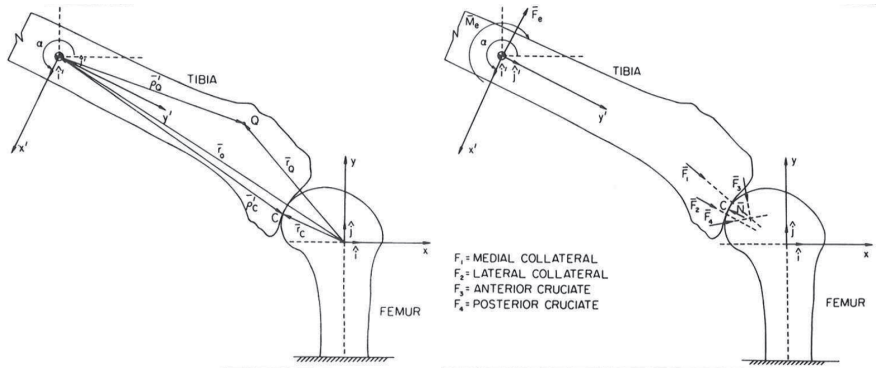

Figure 2.14. Two-dimensional dynamic model [Manssour et al., 1983]

Naturally, this work contains simplifications as well, for example:

a) The model is two-dimensional,

b) Only ligaments in the sagittal plane can be investigated,

c) The femur is fixed, thus the tibia carries out relative movement compared to it,

d) Friction between the femoral and tibial surfaces is ignored, since the coefficient of friction due to the synovial fluid is very low [Radin and Paul, 1972].

These studies offered a wide range of investigations related to the contact point of the femur and tibia, mechanism of the ligaments, including the determination of the material properties, or the stability questions of the knee joint.

As a short overview of the above-mentioned models, the authors [Crowninshield et al., 1976, Wisman et al., 1980, Andriacchi et al., 1983, Manssour et al., 1983] presented the following findings:

I. The authors provided numerical solution about the contact position of the femur and the tibia.

II. The authors provided numerical results how the knee, as a system, responds to dynamically applied loads, e.g. ligaments force-trend in case of a pulse loads.

III. The authors provided numerical results about the initial strain in the ligaments and their elongation during the movement.

IV. These models can provide information about the boundary conditions or parameters of numerical models such as the spring- and damping constant of the ligaments and menisci.

2.2.4. Mathematical, anatomical models

The basic analytical investigation of the knee forces can be dated to the work of Smidt [Smidt, 1973], who combined his mathematical approach with X-ray images and a force platform in order to locate the axis of instantaneous rotation, the moment arm of the extensor mechanism and the maximum averaged torque in the knee joint. The data acquisition was carried out by taking several lateral X-ray images and measuring the torque generated by the extensors and flexors of the knee.

During the experiments, the subject was side lying, approximately in the same position as the X-ray images were taken (Figure 2.15), so the influence of gravity was eliminated.

The movement during the experiments was carried out up to 90˚ of flexion angle, with the constant radial velocity of 13˚ per second.

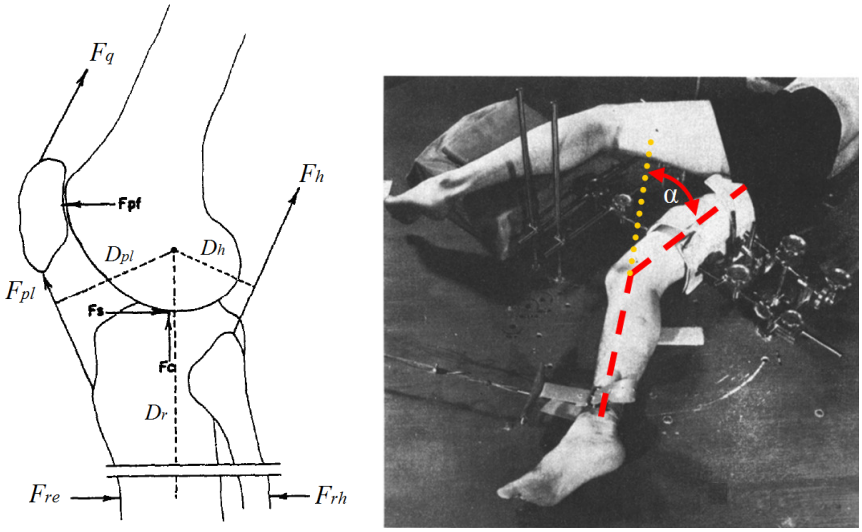

Figure 2.15. Mathematical model and measurement setup [Smidt, 1973]

Regarding the mathematical modelling, a concurrent force system was assumed: the lines of action of the forces coincide at a common point, otherwise patellar movement would occur. The magnitude of the patellar tendon force and the quadriceps tendon force were considered equal. The forces were derived using simple equilibrium equations (six equations). The author [Smidt, 1973] published the following results:

I. The change of the patellar tendon (D_{pl}) moment arm and the hamstrings moment arm (D_h) as a function of flexion angle (Figure 2.16)

II. The change of the torque ($\boldsymbol{T_{extension}} = \boldsymbol{F_{re}} \cdot D_r$ or $\boldsymbol{T_{flexion}} = \boldsymbol{F_{rh}} \cdot D_r$) as a function of flexion angle (Figure 2.17),

III. The change of the patellofemoral ($\boldsymbol{F_{pf}}$) and tibiofemoral forces ($\boldsymbol{F_{tf}}$) as a function of flexion angle. They were measured from the center of rotation (Figure 2.18 and Figure 2.19),

IV. An explanation and calculation of the instantaneous centre of rotation with regard to the knee joint.

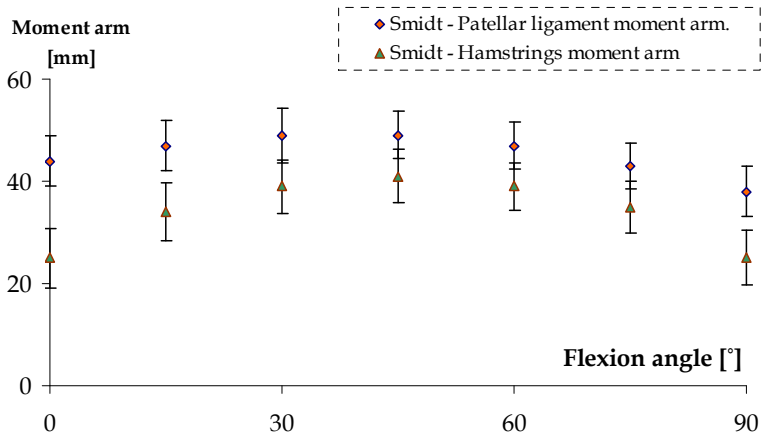

Figure 2.16. Moment arms [Smidt, 1973]

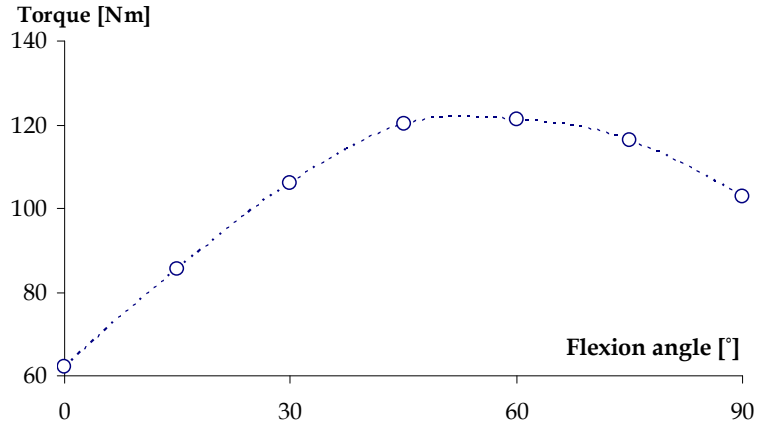

Figure 2.17. Torque during extension [Smidt, 1973]

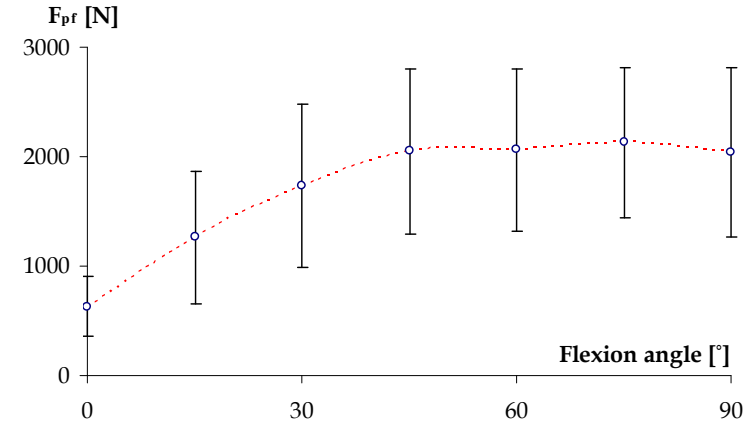

Figure 2.18. Patellofemoral compression force [Smidt, 1973]

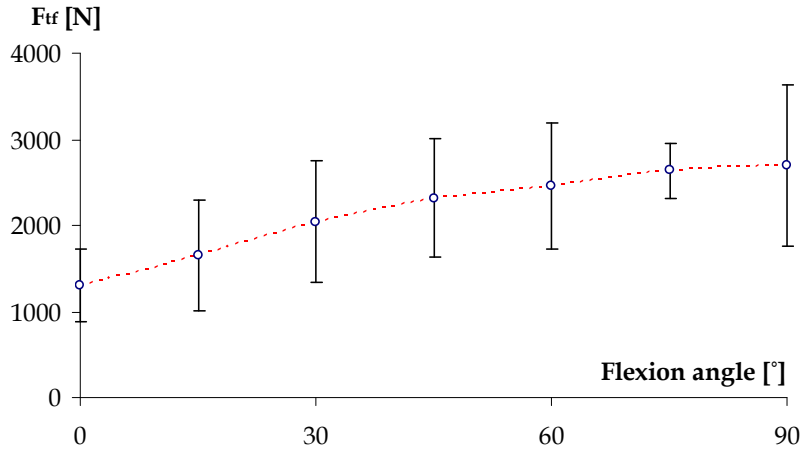

Figure 2.19. Tibiofemoral compression force [Smidt, 1973]

The following remarks have to be mentioned related to Smidt's study [Smidt, 1973]:

- The author supposed that the force in the patellar tendon and in the quadriceps is equal. This assumption is invalid, which was confirmed by Denham and Bishop [Denham and Bishop, 1978].
- The model requires to measure external forces ($\boldsymbol{F_{re}}$ and $\boldsymbol{F_{rh}}$ in Figure 2.15) in order to calculate the above-mentioned forces.

With the use of radiographic and other experimental measurements, Denham and Bishop [Denham and Bishop, 1978] composed an analytical-kinetical model to calculate the patellofemoral forces (Figure 2.20). The forces were derived using equilibrium equations (three equations).

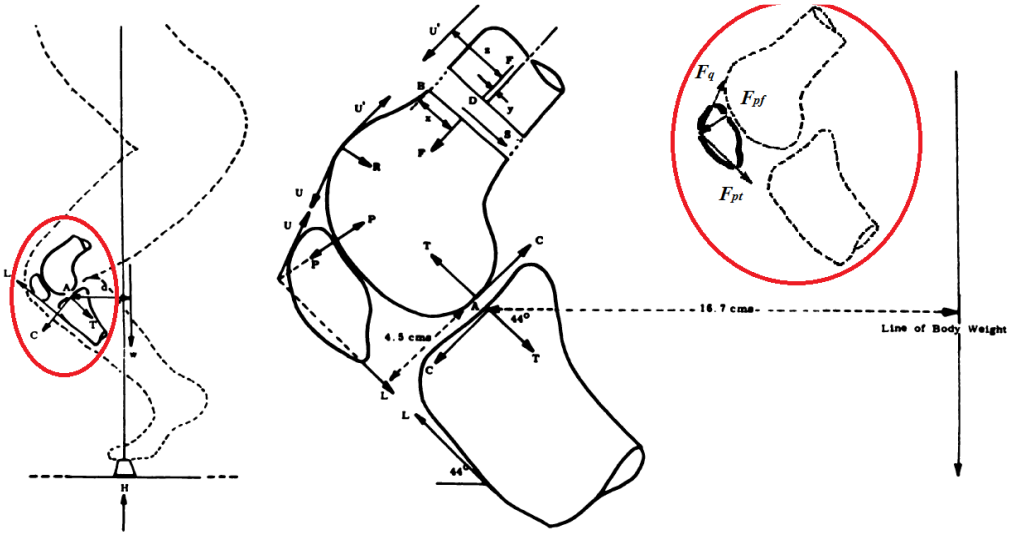

Figure 2.20. The mechanical model [Denham and Bishop, 1978]

Through this study, the authors pointed out several, fundamentally important statements about the kinetics and kinematics of the knee joint:

I. They demonstrated with simultaneous electromyograph tracings that in case of balanced equilibrium the extensor effect upon the knee is minorly affected by the actions of the hamstrings or the gastrocnemius (Figure 2.21). Major activity is seen only in the quadriceps and the soleus. Only the occasional burst of activity (which helps to maintain balance) is seen in these muscle groups, so their effect can be safely disregarded.

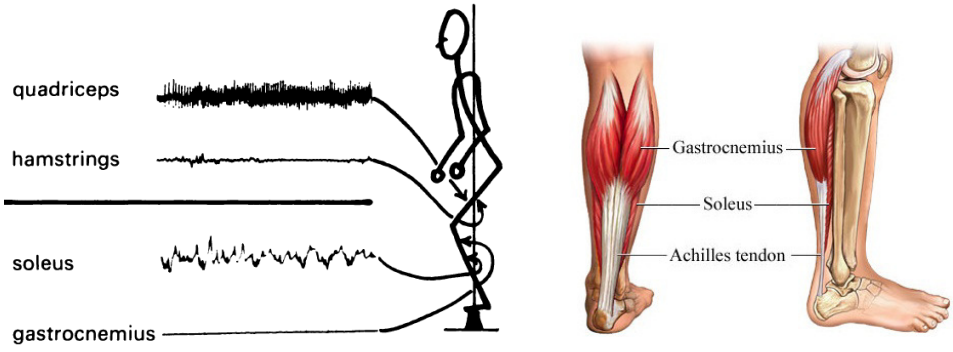

Figure 2.21. Electromyograph recording about the acting muscles [Denham and Bishop, 1978]

II. The patella can be isolated as a system, thus the equilibrium of the acting forces on it, such as the patellofemoral compression force ($\boldsymbol{F}_{pf}$), the quadriceps tendon force ($\boldsymbol{F}_{q}$) and the patellar tendon force ($\boldsymbol{F}_{pt}$) can be examined.

III. The authors introduced firstly the concept of force ratios (the patellofemoral forces always compared to the quadriceps force) in quasi-static state ($\boldsymbol{F}_{pf}/\boldsymbol{F}_{q}$, $\boldsymbol{F}_{pt}/\boldsymbol{F}_{q}$).

IV. It it shown by this report [Denham and Bishop, 1978] and by an earlier study [Bishop and Denham, 1977] that the tension in the patellar tendon is not equal with the tension in the quadriceps tendon ($\boldsymbol{F}_{pt} \neq \boldsymbol{F}_{q}$) which was widely held earlier due to the low friction between the patella and the femoral condyle. This result does not state that friction should be always neglected.

V. The most important finding of the authors was that they revealed the major effect of the position of the centre of gravity on the kinetics of the patellofemoral forces (the centre of gravity in two positions is visible in Figure 2.22). According to them, leaning forward a few centimeters can halve the patellofemoral forces passing through the knee.

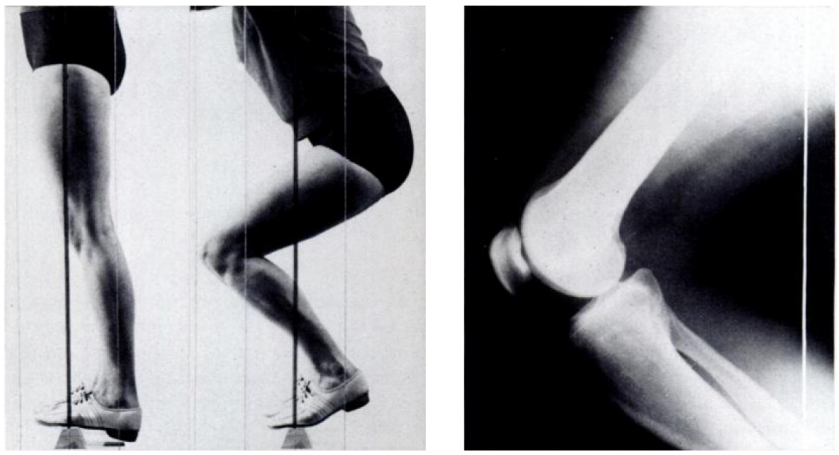

Figure 2.22. The centre of gravity during movement [Denham and Bishop, 1978]

The following remarks have been made related to the study of Denham and Bishop [Denham and Bishop, 1978]:

- Although the authors appointed a very important parameter, the moving centre of gravity, as a so far undiscussed topic, they did not investigate further this parameter and its accurate effect on the kinetics.
- Their results are only available until 80˚ of flexion angle, but in some cases only until 30˚ of flexion angle.

Van Eijden et al. [Van Eijden et al., 1986] introduced the most comprehensive kinematical-kinetical study about the patellofemoral knee joint of that period. They only took the movements and the forces of the sagittal plane into account in their model (Figure 2.23).

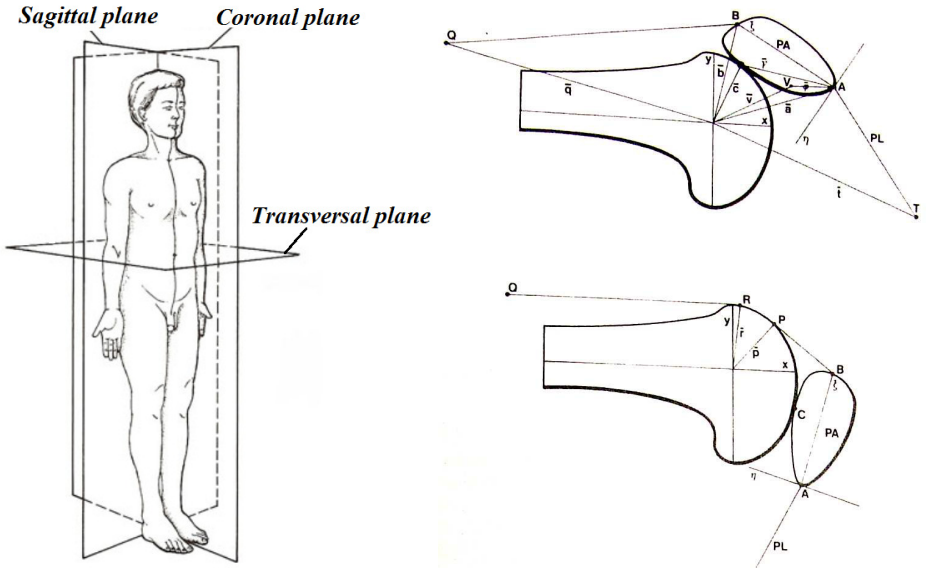

Figure 2.23. Patellofemoral model [Van Eijden et al., 1986]

Van Eijden et al. [Van Eijden et al., 1986] had two main goals with their model:

1. From the kinematic point of view, to enable the calculation of the relative contact location between the patella and the femur,
2. From the kinetic point of view, to calculate the F_{pf}/F_q and F_{pt}/F_q ratios as a function of flexion angle.

The model includes some simplifications as follows:

a) The femur, tibia and patella elements are considered rigid,

b) The patellar tendon is assumed inextensible, while the quadriceps tendon is represented as a string with variable length,

c) Due to the two-dimensional nature of the model, the condyles are reduced to two-dimensional profiles and the surfaces to points,

d) Friction between the femoral and tibial surfaces is ignored, since the coefficient of friction due to the synovial fluid is very low [Paul and Radin, 1972]. Gravitational forces or other forces are not taken into account.

The presented model [Van Eijden et al., 1986] describes a set of non-linear equations (nine equations), which was solved by Newton-Raphson iteration process [Newton, 1711, Raphson, 1690]. The model can be applied primarily for static situations, and the transmission of the forces is realized by the followings: a force $\boldsymbol{F_q}$ exerted by the quadriceps tendon is counteracted by a force $\boldsymbol{F_{pt}}$ in the patellar tendon. The resultant force of these two forces is the $\boldsymbol{F_{pf}}$, the patellofemoral compression force, which is the reaction force between the patella and the femur.

The most important findings of the authors are the followings:

I. The authors found the relationship of the angle between the patellar tendon axis and the tibial axis (β) as a function of flexion angle (Figure 2.25).

II. The authors found the relationship of the angle between the patellar tendon and the patellar axis (ρ) as a function of flexion angle (Figure 2.26).

III. The authors found the relationship of the angle between the patellar axis and the femoral axis (ε) as a function of flexion angle (Figure 2.27).

IV. The authors found the relationship of the angle between the quadriceps tendon and the femoral axis (ψ) as a function of flexion angle (Figure 2.28).

V. The authors found the relationship of the angle between the quadriceps tendon and the patellar axis (ξ) as a function of flexion angle (Figure 2.29).

VI. The authors provided the $\boldsymbol{F_{pt}/F_q}$ and $\boldsymbol{F_{pf}/F_q}$ ratios as a function of flexion angle (Figure 2.30 and Figure 2.31).

The above-mentioned angles are represented on Figure 2.24.

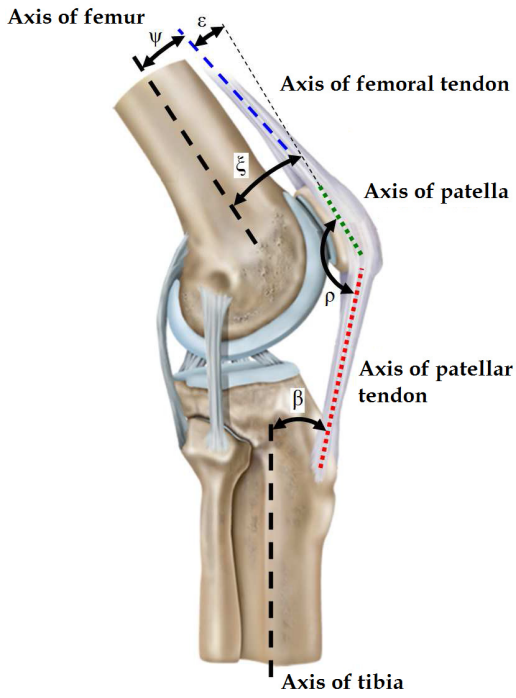

Figure 2.24. Anatomical angles

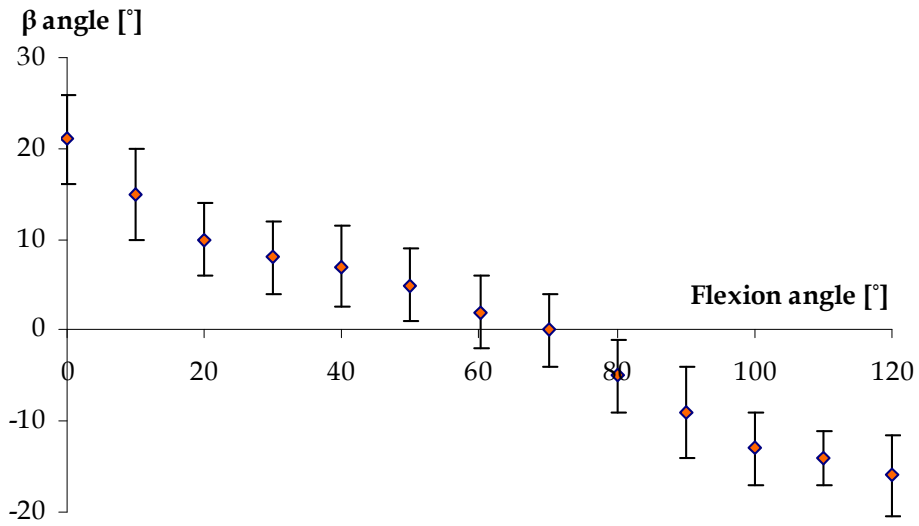

Figure 2.25. Angle between patellar tendon and tibial axis (*β*) [Van Eijden et al., 1986]

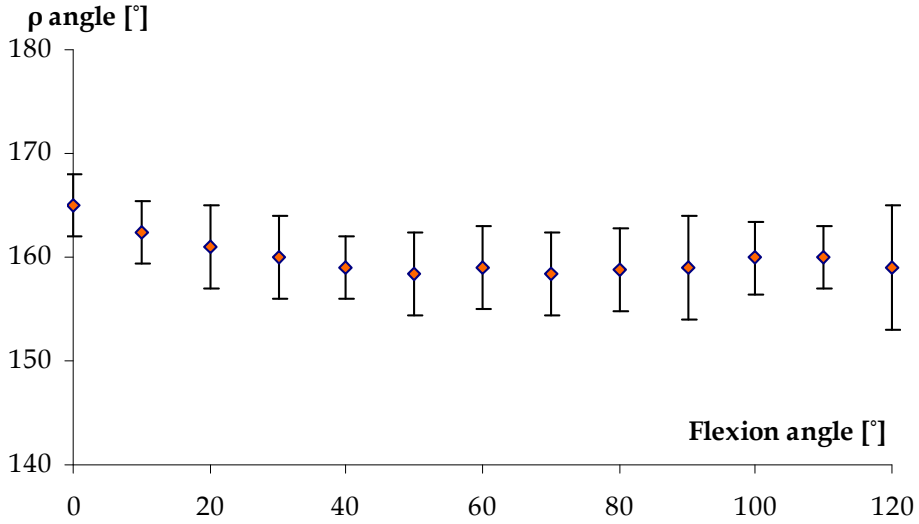

Figure 2.26. Angle between patellar tendon and patellar axis (*ρ*) [Van Eijden et al., 1986]

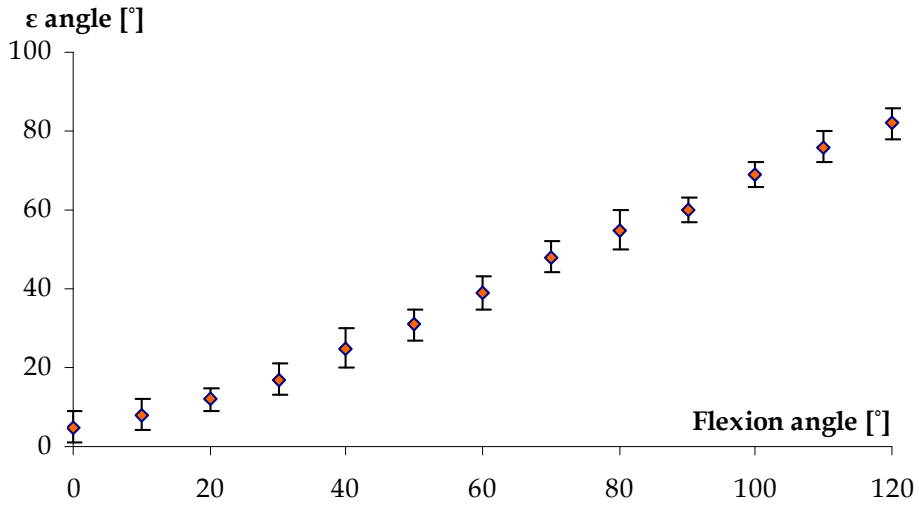

Figure 2.27. Angle between patellar axis and femoral axis (*ε*) [Van Eijden et al., 1986]

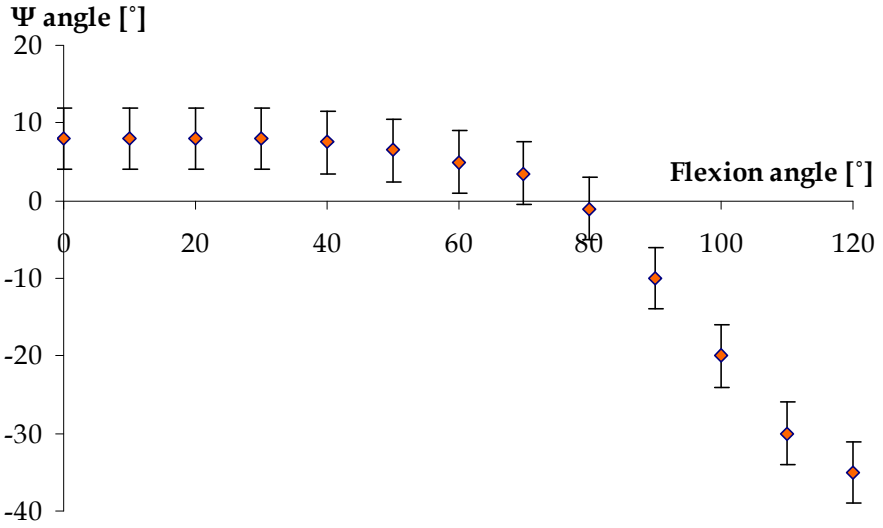

Figure 2.28. Angle between quadriceps tendon and femoral axis (*δ*) [Van Eijden et al., 1986]

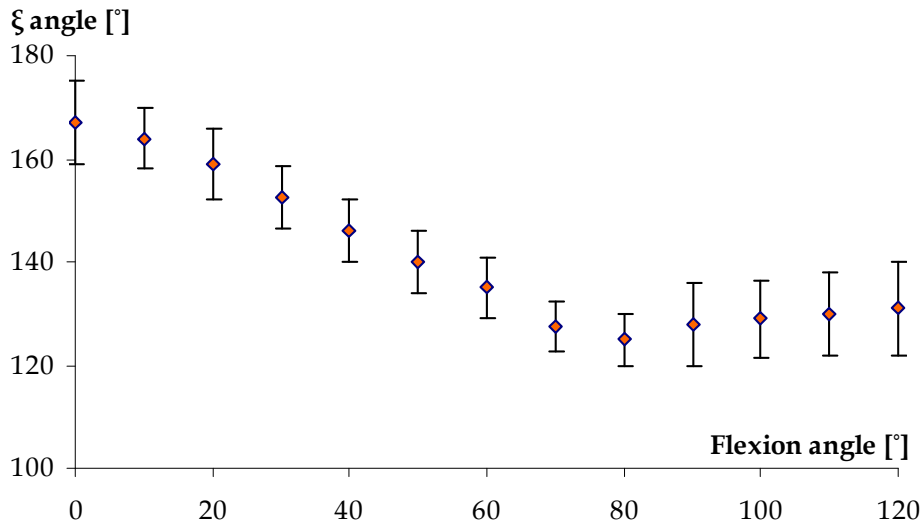

Figure 2.29. Angle between quadriceps tendon and patellar axis (ξ) [Van Eijden et al., 1986]

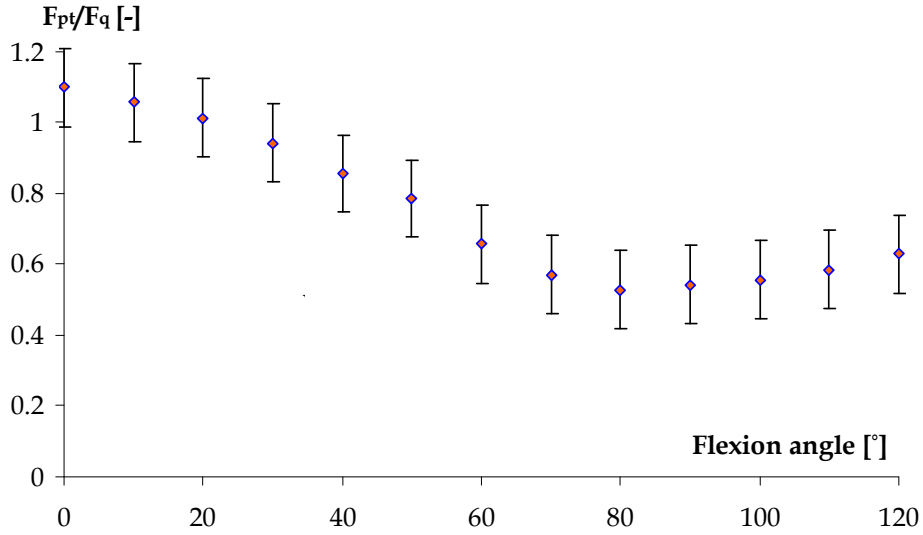

Figure 2.30. F_{pt}/F_q relationship [Van Eijden et al., 1986]

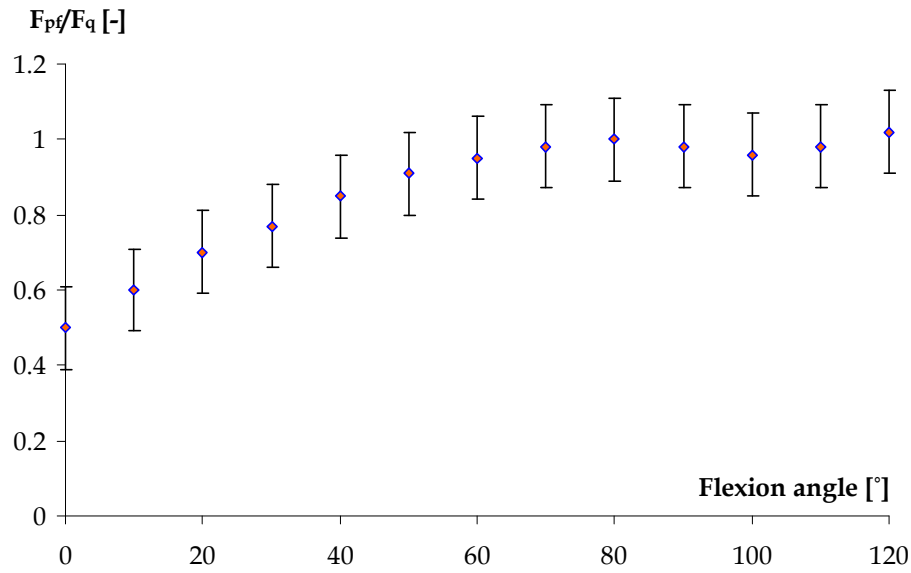

Figure 2.31. F_{pf}/F_q relationship [Van Eijden et al., 1986]

Van Eijden et al. [Van Eijden et al., 1986] validated their results experimentally by involving ten cadaver knees into their investigations. The obtained results soon became widely accepted and often cited in the field of biomechanics, although some remarks have to be mentioned:

- The quadriceps force is arbitrarily chosen and its nature is unknown during the movement. In this approach, the quadriceps force has only the function to impose the motion, but by doing so, no information can be gained about how the individual quadriceps force changes under the motion.
- The model is described by non-linear equations which solution can be only found by numerical solvers but not analytical way.

As a conclusion, the model provides significant findings about the kinematics of the patellofemoral knee joint in the sagittal plane such as the relationship between the main anatomical angles (β, δ, ε) and the flexion angle (α), sliding-rolling (roll-slide in the article), and the basic relationship regarding the patellofemoral forces.

However, the provided information was obtained under a special movement when the femur is fixed and the tibia carries out relative motion around it. This motion is equal to the open kinetic chain leg extension [Cohen et al., 2001], when the leg is not loaded with the complete body weight but the weight of the lower leg. In addition, the relationship between the individual $\boldsymbol{F_q}$, $\boldsymbol{F_{pf}}$, $\boldsymbol{F_{pt}}$ and the $\boldsymbol{BW}$, as a function of flexion angle, is unknown.

It is also unknown, and not mentioned in the study, whether the kinetical results are valid for any kind of everyday motions (squat, modified squat, rising from chair, etc)?

Nisell et al. [Nisell, 1985, Nisell et al., 1986] aimed to define a general, two-dimensional mechanical model of the knee joint in a way that the model is not limited to one particular situation. In their research, they carried out morphological investigation on cadavers combined with radiographic landmarks on healthy individuals (Figure 2.32). The patellar tendon is modelled as a rigid link and its length does not change as the patella moves along the femur.

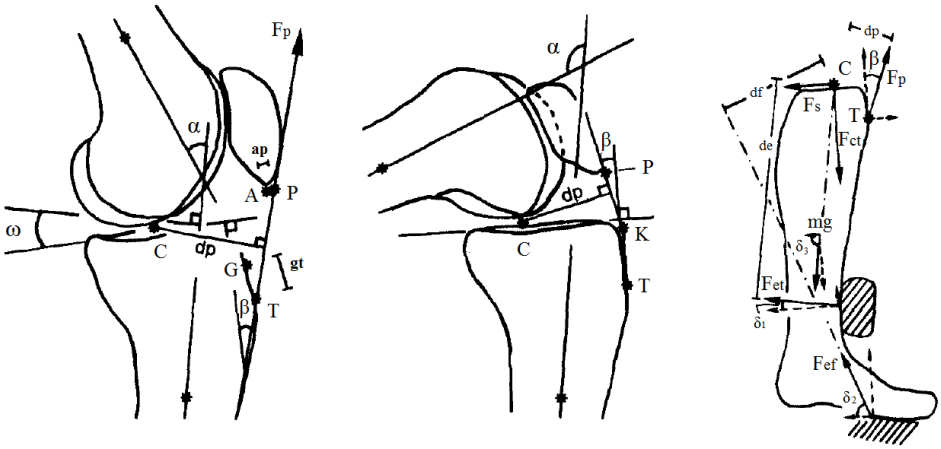

Figure 2.32. Mechanical model [Nisell et al., 1986]

According to the authors, the model can be used in case of isometric exercise against a resistance applied to the anterior side of the distal leg.

The authors have given an analytical approach to calculate the forces, although some forces and moment arms ($\boldsymbol{F_{et}}$, d_e) are not determined but arbitrarily taken. Altogether, ten algebraic equations were derived to investigate the kinetics and kinematics.

By this model, it could be demonstrated that the precise determination of the contact point is sturdily important since 10 mm anterior movement would cause 22% of decrease in the patellar tendon force while the same amount of movement in the posterior direction would increase the same force by 40%.

Since some parameters are arbitrarily chosen, the model only gives an approximation how the sensitivity of the output parameters depends on these input parameters. However, the obtained forces hold some uncertainty due to the random values.

As a summary, the authors published the following findings related to the knee joint:

I. Rolling appears beyond 30° of flexion angle as well. The sliding-rolling motion as a factor is not sufficiently considered in the design and in the current research.

II. 10 mm of anterior or posterior movement of the contact point (C) can increase the magnitude of the forces by 20-40%.

III. The β function (angle between the patellar tendon and the tibial axis) intersects the zero line at about 100° of flexion angle (Figure 2.33).

IV. The authors determined actual moment arms for the patellar tendon with regard to male and female subjects (Figure 2.34).

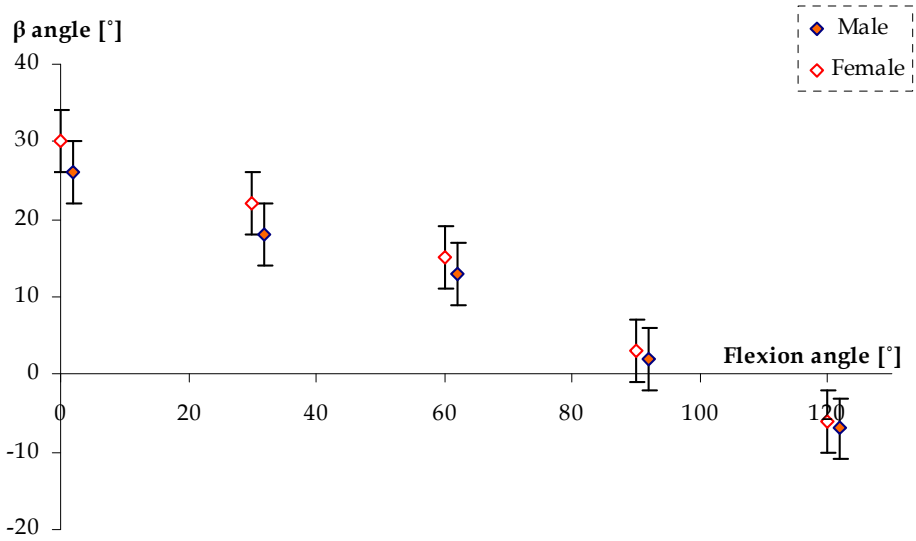

Figure 2.33. Angle between patellar tendon and tibial axis (*β*) [Nisell et al., 1986]

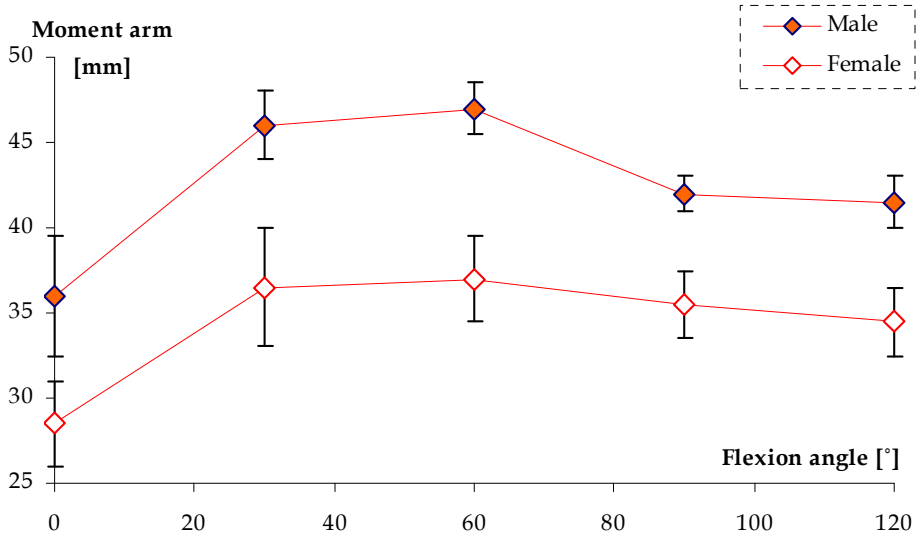

Figure 2.34. Actual patellar tendon moment arm [Nisell et al., 1986]

In their study, the authors [Nisell, 1985, Nisell et al., 1986] only dealt with the question of patellar tendon moment arm by comparing their results to other earlier results [Smidt, 1973, Haxton, 1945, Kaufer, 1971, Bandi, 1972] with fairly good agreement.

Regarding the study of Nisell et al. [Nisell, 1985, Nisell et al., 1986], a few remarks have to be mentioned:

- In their study, they only investigated the kinetics (load moment of the knee) in case of two very specific motions, namely: firstly, machine milking operation, when the operator has to lean forward his/her trunk with bent knee to carry out the milking process and secondly, lifting a 12.8 kg box with bent knees.

- The kinetic equations related to the $\boldsymbol{F_{pt}/F_q}$ and $\boldsymbol{F_{pf}/F_q}$ relationships are derived from a simple knee extension where the $\boldsymbol{F_q}$ is considered as a known external force, although during activity the $\boldsymbol{F_q}$ force changes as well.
- Several angles and moment arms, which may depend on the flexion angle ($\delta_{1\text{-}2\text{-}3}$, ω, ψ, d_m, etc.), are referred to, but not found in the articles as diagrams or equations. The calculation method is not clear or possible without these parameters.

In case of this certain model, the authors gave an explanation how the figure could be used to calculate the force ratios, but analytical calculation itself cannot be executed due to the above mentioned missing parameter values.

Yamaguchi and Zajac [Yamaguchi and Zajac, 1989] similarly to Van Eijden et al. [Van Eijden et al., 1986] created a two-dimensional, mathematical-mechanical model to determine both the moment arms of the quadriceps- and the patellar tendon and to investigate the influence of the patella on the knee joint.

It is known, that the moment arms depend on the position of the contact point(s) between the connecting condyles. Since the contact points are constantly on the move, the determination of the instantaneous position is quite challenging.

To answer the second aim, related to the influence of the patella on the knee joint, it was already considered that the patella behaves as a spacer and a lever. The role as a spacer means that the patella forces the extensor muscles ($\boldsymbol{F_q}$, $\boldsymbol{F_{pt}}$) away from the center of rotation thus increasing their moment arms [Stiehl et al., 2001], while the lever role means that the patella can alter the magnitude and the direction of the forces [Kaufer, 1971].

Likewise, in the earlier models, the patellar tendon is modelled as a rigid link and its length does not change as the patella moves along the femur. Grood et al. [Grood et al., 1984] defined a so-called effective moment arm, which expresses the extensor moment arm in terms of the quadriceps force. Simply said, the effective moment arm is the product of the actual moment arm and the ratio of the patellar tendon force and the quadriceps force.

Results related to the effective moment arms are, however, not in every way in agreement. The result of Grood et al. [Grood et al., 1984] reported peak sharply between 20-30° of flexion angle, more or less the same what other authors' published [Smidt, 1973, Bandi, 1972], although at large flexion angles the moment arm was found small compared to the results of other authors [Smidt, 1973, Bandi, 1972].

Yamaguchi and Zajac [Yamaguchi and Zajac, 1989] wanted to answer two additional questions regarding the kinetics of the knee joint:

1. How does the direction of the quadriceps force influence the effective moment arm of the patellar tendon, and the quadriceps tendon?
2. How significant is this influence, compared to the levering action of the patella?

The patella was modelled as a rectangular rigid body. Both femur and tibia were assumed to be rigid as well. Their model was also created in the sagittal plane with the following concern: the patella has to fulfill the role of a spacer and a lever (Figure 2.35).

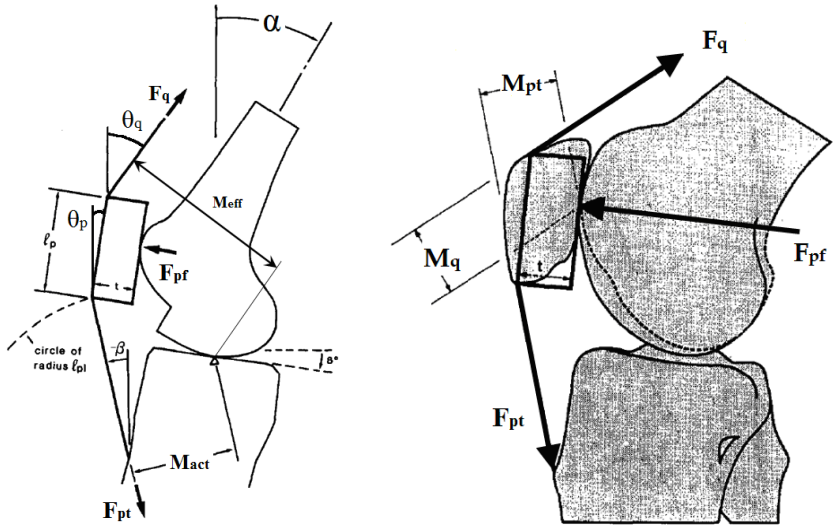

Figure 2.35. Mechanical model [Yamaguchi and Zajac, 1989]

Similar to the model of Van Eijden et al. [Van Eijden et al., 1986], a numerical iteration was carried out from 0° to 90° of flexion angle. The increment was set to 1° per step, and the friction was ignored similar to the earlier authors [Nisell, 1985, Denham and Bishop, 1978, Van Eijden et al., 1986].

In their model, $\boldsymbol{F_q}$ represents the applied arbitrary force, while the magnitude of $\boldsymbol{F_{pf}}$ and $\boldsymbol{F_{pt}}$ are unknown (patellofemoral compression- and patellar tendon force). θ_p, β, are to be calculated or used from other source as a function of flexion angle (α). Since the direction of the applied quadriceps force (θ_q) and the orientation of the femur with respect to the fixed tibia are also prescribed functions of the flexion angle, only α remains the single independent parameter describing the joint (Figure 2.35). The following equations (Eq. (2.1) and Eq. (2.2)) have to be solved to obtain the forces and the moment arms:

$$\begin{bmatrix} \cos\theta_p & \sin\beta \\ -\sin\theta_p & \cos\beta \end{bmatrix} \cdot \begin{bmatrix} F_{pf} \\ F_{pt} \end{bmatrix} = \begin{bmatrix} \sin\theta_q \\ \cos\theta_q \end{bmatrix} \cdot F_q \tag{2.1}$$

After the iteration, the forces are available. The moment equilibrium requires that:

$$F_{pt} \cdot M_{pt} = F_q \cdot M_q \tag{2.2}$$

where M_{pt} and M_q are the moment arms of the patellar tendon force and the quadriceps force about the contact point.

The actual moment arm (denoted as M_{act}), is the perpendicular distance between the patellar tendon force and the contact point, and it can be derived as follows:

$$M_{eff} = \frac{F_{pt} \cdot M_{act}}{F_q} \tag{2.3}$$

The estimated actual and effective moment arm has been plotted with the result of Nisell et al. [Nisell et al., 1986] and showed good correlation (Figure 2.36 and Figure 2.37). The results of Yamaguchi and Zajac [Yamaguchi and Zajac, 1989] can be summarized as follows:

I. Their results confirmed that the levering action of the patella is at least as important as its spacer function.

II. The thickness of the patella has only minor effect on the extensor moment arm under 35° of flexion angle, while above that angle, it does not change the effective moment arm.

III. The length of the patellar tendon has major effect on the patellar axis orientation (denoted θ_p [Yamaguchi and Zajac, 1989]), the $\boldsymbol{F_{pf}/F_q}$ and $\boldsymbol{F_{pt}/F_q}$ relationships, and on the effective moment arm.

IV. The orientation of the quadriceps force affects only minorly the effective moment arm at high flexion angle.

V. The authors results agreed with result of Van Eijden et al. [Van Eijden et al., 1986] related to the $\boldsymbol{F_{pf}/F_q}$ and $\boldsymbol{F_{pt}/F_q}$ relationships.

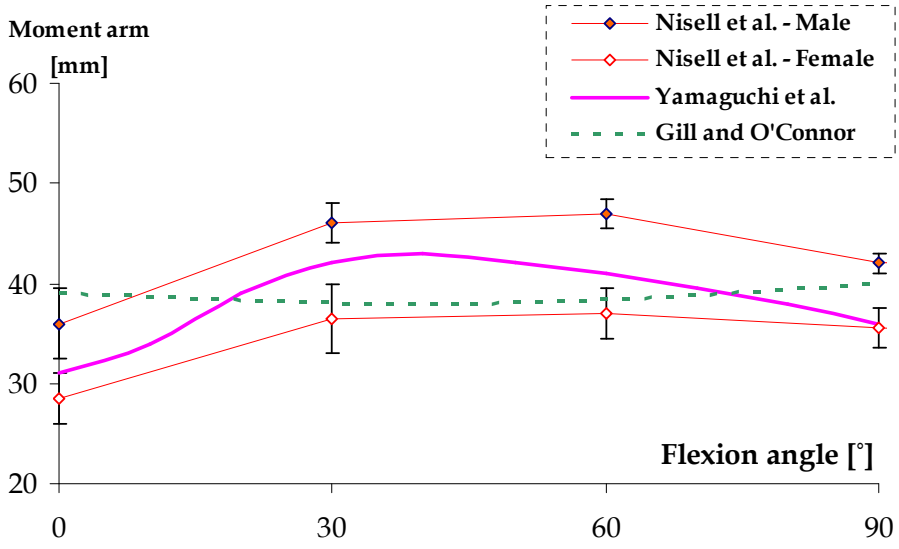

Figure 2.36. Actual patellar tendon moment arm [Yamaguchi and Zajac, 1989]

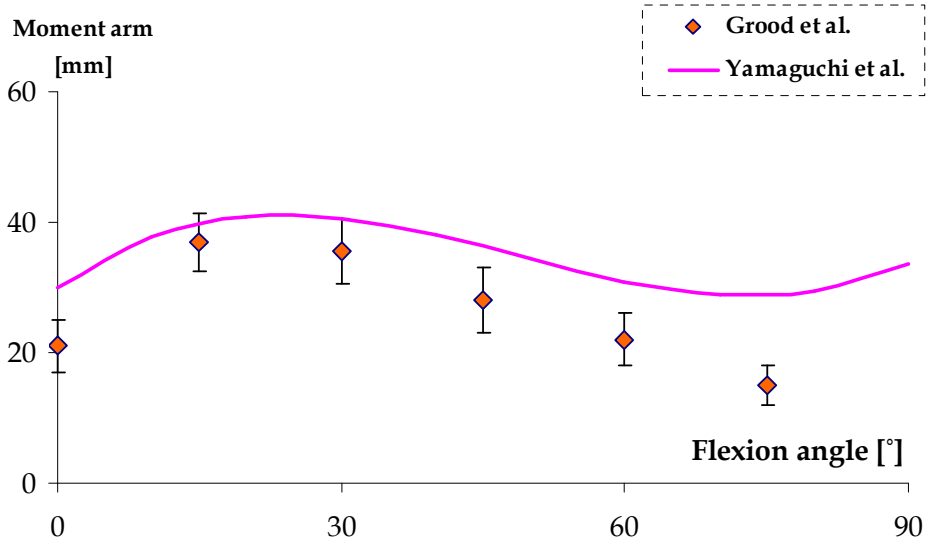

Figure 2.37. Effective patellar tendon moment arm [Yamaguchi and Zajac, 1989]

After the results, let us point out some important remarks related to the model of Yamaguchi and Zajac [Yamaguchi and Zajac, 1989]:

- Similar to the model of Van Eijden et al. [Van Eijden et al., 1986], the model of Yamaguchi and Zajac [Yamaguchi and Zajac, 1989] can only be solved numerically.
- Similar to other models [Van Eijden et al., 1986, Nisell, 1985, Nisell et al., 1986] the F_{pt}/F_q and F_{pf}/F_q relationships are derived from a simple knee extension, where F_q is considered as a given external force. Although their results agree well, they also cannot provide individual force calculation.

Hirokawa [Hirokawa, 1991] made the first substantial step by creating the first three-dimensional mathematical-mechanical model, which included the articular surface geometry and the mechanical properties of the ligaments. Hefzy and Yang [Hefzy and Yang, 1993] have also developed a three-dimensional, anatomical-mathematical, patellofemoral joint model that determines how patellofemoral motions and patellofemoral contact forces change with the knee flexion. Furthermore, a unique two-point contact was assumed between the femur and tibia, on the medial and lateral sides.

Similarly to the model of Van Eijden et al. [Van Eijden et al., 1986,] both Reithmeier and Plitz [Reithmeier and Plitz, 1990] and Gill and O'Connor [Gill and O'Connor, 1996] turned back to the two-dimensional models. The latter authors decided to carry out the modelling in two-dimension due to the convincing studies of Singerman et al. [Singerman et al., 1994] and Miller [Miller, 1991], who cogently emphasized the importance of the sagittal plane effects in the patellar mechanics.

These models [Reithmeier and Plitz, 1990, Hirokawa, 1991, Hefzy and Yang, 1993, Gill and O'Connor, 1996] and their results can be found in the Appendix.

Mason et al. [Mason et al., 2008] published a comprehensive review about the patellofemoral joint forces, in which they combined the results and models of other authors in order to give a fully analytical approach for calculating the patellofemoral forces (Figure 2.38). They derived the patellofemoral forces from a so-called net knee moment, which is the moment about the instantaneous center of rotation of the knee joint generated by the body weight. To derive the equations, they used the kinetic model of Cohen et al. [Cohen et al., 2001].

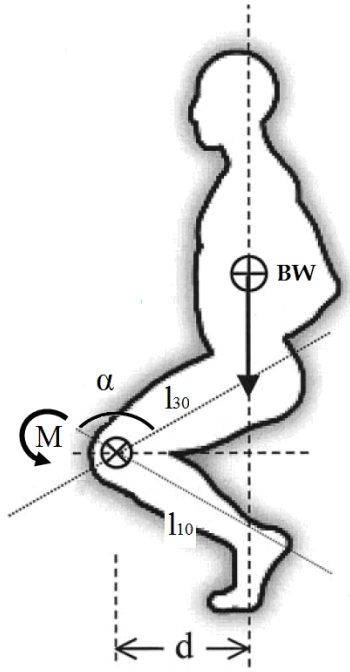

Figure 2.38. Free body diagram of squat movement [Mason et al., 2008]

The following simplifications were considered related to the model of Mason et al. [Mason et al., 2008]:

a) The model is quasi-static,

b) The model is two-dimensional,

c) The inertial forces during the movement are neglected,

d) No contact forces ($\boldsymbol{F}_s$, $\boldsymbol{F}_N$) are considered,

e) Only the standard squat is investigated with the model,

f) The load is derived from the total weight of the person,

g) The body weight vector ($\boldsymbol{BW}$) can only move vertically,

h) The femur and tibia are symmetrically positioned (their rotation during the movement is equivalent).

The model is based on the assumption, that under squatting movement the center of gravity does not change its line of action horizontally (the trunk does not lean forward of backward), consequently the net knee moment can be derived as a simple function of flexion angle.

Let us follow the description of Mason et al. [Mason et al., 2008]. Note that l_{30} represents the length of the femur (in their actual calculations they considered it 0.45 m) while l_{10} represents the length of the tibia. The flexion angle is denoted as α. The moment arm is represented as d, while the body weight vector as $\boldsymbol{BW}$ (Figure 2.38):

$$d(\alpha) = l_{30} \cdot \sin(\alpha / 2) \tag{2.4}$$

$$M_N(\alpha) = 0.5 \cdot BW \cdot d(\alpha) = 0.5 \cdot BW \cdot l_{30} \cdot \sin(\alpha / 2) \tag{2.5}$$

The quadriceps tendon force ($\boldsymbol{F_q}$) can be derived from the net knee moment ($\boldsymbol{M_N}$) and the effective moment arm (L_{eff}) of the quadriceps tendon according to Salem and Powers [Salem and Powers, 2001]:

$$F_q(\alpha) = \frac{M_k(\alpha)}{L_{eff}(\alpha)} \tag{2.6}$$

Where, L_{eff} can be found in Table 2.2.

Several authors have investigated the ratio of the patellofemoral forces under extension and flexion exercises, and obtained very similar results [Denham and Bishop, 1987, Van Eijden et al., 1986, Yamaguchi and Zajac, 1989, Hirokawa, 1991, Miller, 1991, Hefzy and Yang, 1993, Gill and O'Connor, 1996]. These have been gathered and plotted in Figure 2.39 and Figure 2.40:

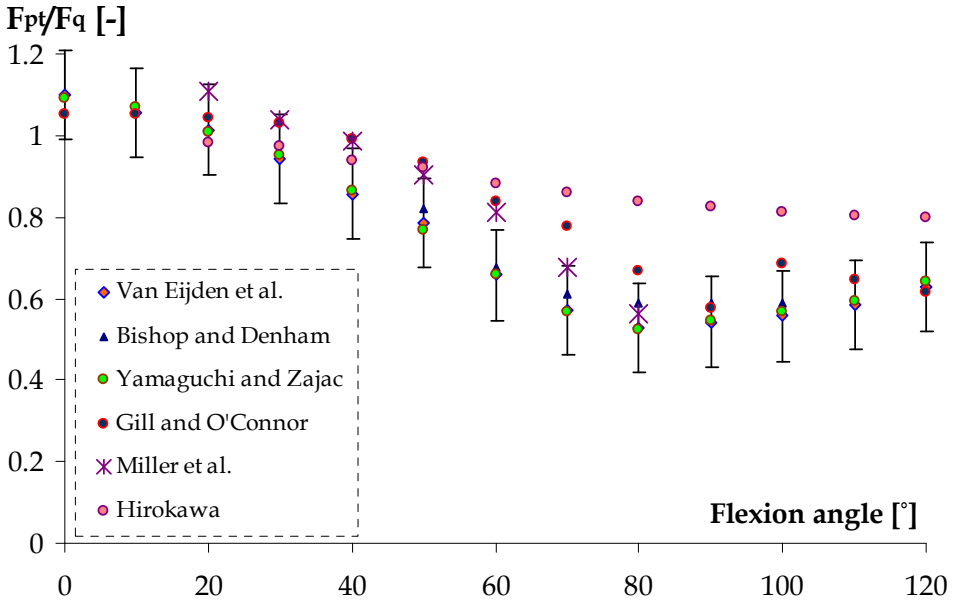

Figure 2.39. F_{pt}/F_q relationship

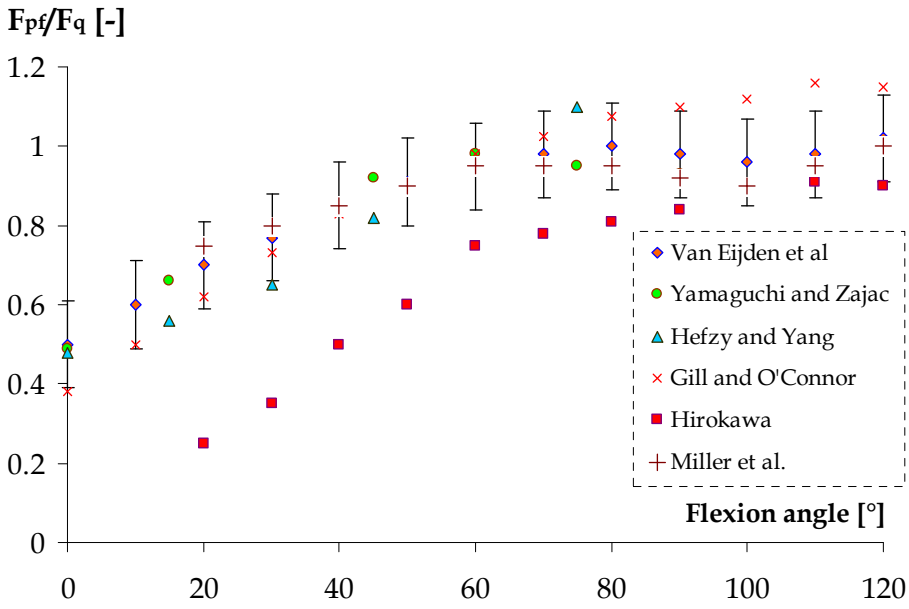

Figure 2.40. F_{pf}/F_q relationship

Since the obtained results are mostly in the range of the result of Van Eijden et al. [Van Eijden et al., 1986], it is adequate to use further on their relationship regarding the patellar tendon force and the patellofemoral compression force:

$$\frac{F_{pt}}{F_q}(\alpha) = g(\alpha) \tag{2.7}$$

$$\frac{F_{pf}}{F_q}(\alpha) = k(\alpha) \tag{2.8}$$

Where $g(\alpha)$ and $k(\alpha)$ are cubic approximate functions of the flexion angle and can be found in Table 2.2.

	C1	C2	C3	C4	SD	r^2	SAMPLE	p
g(α) [-]	1.102	-2.21E-3	-1.49E-4	1.14E-6	0.1	0.98	13	$p < 0.05$
k(α) [-]	0.486	1.32E-2	-1.15E-4	3.35E-7	0.1	0.98	13	$p < 0.05$
L_{eff} (α) [mm]	0.046	2.8E-4	-1.3E-5	8E-8	N/A	0.98	N/A	N/A

Table 2.2. Functions* of the mathematical model

* The following equation is used: $f(\alpha) = C1 + C2 \cdot \alpha + C3 \cdot \alpha^2 + C4 \cdot \alpha^3$

The patellofemoral compression force (F_{pf}) can be expressed as a product of the quadriceps tendon force (Eq. (2.6)) and the patellofemoral compression force-quadriceps force ratio (Eq. (2.8)):

$$F_{pf}(\alpha) = F_q(\alpha) \cdot k(\alpha) = \frac{M_k(\alpha)}{L_{eff}(\alpha)} \cdot k(\alpha) \tag{2.9}$$

Finally, the patellar tendon force ($\boldsymbol{F_{pt}}$) can be derived by multiplying Eq. (2.7) with Eq. (2.6).

$$F_{pt}(\alpha) = F_q(\alpha) \cdot g(\alpha) = \frac{M_k(\alpha)}{L_{eff}(\alpha)} \cdot g(\alpha) \tag{2.10}$$

The following major findings have been summarized from the study of Mason et al. [Mason et al., 2008] with regard to the patellofemoral forces under squatting movement:

I. The authors successfully synthesized the results of the earlier authors related to the kinetics of the patellofemoral joint.

II. The authors provided an easy and fully analytical approach to calculate individually the patellofemoral compression force ($\boldsymbol{F_{pf}}$), the patellar tendon force ($\boldsymbol{F_{pt}}$) and the quadriceps tendon force ($\boldsymbol{F_q}$).

Regarding the remarks, it has to be mentioned that:

- The obtained results can only be used to investigate the standard squat, where the centre of gravity does not change its position horizontally.

The formulas (Eq. (2.7) and Eq. (2.8)) of the model of Van Eijden et al. [Van Eijden et al., 1986] are widely used in the calculation of patellofemoral forces, even in the recent literature [Mason et al., 2008, Powers et al., 2006]. However, the authors [Van Eijden et al., 1986] only stated that their model is able to calculate the relative position of the patella, patellar tendon and the quadriceps tendon, the location of the patellofemoral contact point and the magnitude of the patellofemoral compression force and the force in the patellar ligament as a function of flexion angle, but not specifically under deep squat motion.

2.2.4.1. Special modelling issue – Is the hinge-model applicable for the knee?

Several important questions have to be considered regarding the analytical-kinetical models of the knee joint. Most importantly, it has to be decided that to what extensions can the joint be simplified.

Although there are many pros and contras regarding the two- or three-dimensional models, the effect of the contact geometry itself was not investigated by the earlier mentioned authors. This question can lead us to consider whether a simple hinge or a more elaborated bone-shaped connection is adequate for the kinetical or kinematical investigations.

Powers et al. [Powers et al., 2006] pointed out in their study that it has not been examined whether contact geometry should be considered or not in the modelling of the patellofemoral knee joint due to its possible influence on the contact forces. They investigated this significant question by means of in-vitro cadaveric setup and a computer model that did not consider the contact geometry of the patellofemoral joint (Figure 2.41).

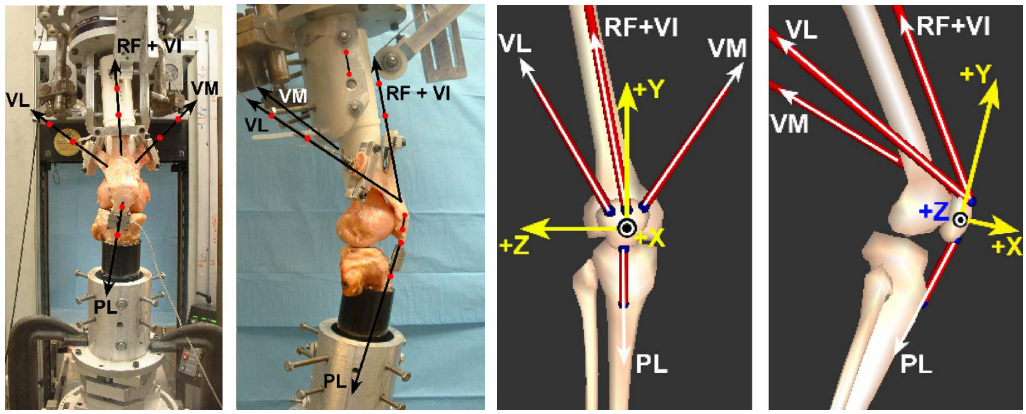

Figure 2.41. Experimental setup and computational model [Powers et al., 2006]

According to their results, the averaged patellofemoral joint reaction force (***PFJRF***), which is the resultant force of the knee joint, was estimated only a slightly higher than the measured (Figure 2.42).

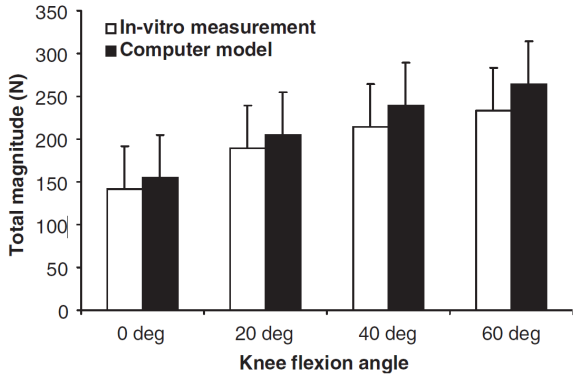

Figure 2.42. Magnitude of the *PFJRF* [Powers et al., 2006]

The reported highest difference in the resultant force was 30 N, which contributes to only about 10% of error between experiment and simulation. It is quite convincing how the simulated resultant force correlates with the measured values, although some discrepancies have to be mentioned as well. The computational model has over- and underestimated the forces in the superior and lateral directions, however the study suggest that the accurate patellofemoral forces, regarding their magnitudes, can be obtained by using computer-based models that neglect joint contact geometry.

Still connecting to the question of how the knee joint should be modelled, another study investigated how the different kind of prostheses, ergo, mechanical models, might alter the patellofemoral forces.

Innocenti et al. [Innocenti et al., 2011] studied the contact forces of several total knee replacements during squatting by means of numerical models. Their sensitivity analysis examined the following total knee replacement types: fixed bearing posterior stabilized prosthesis, high flexion bearing guided motion prosthesis, mobile bearing prosthesis and a simple hinge prosthesis (Figure 2.43).

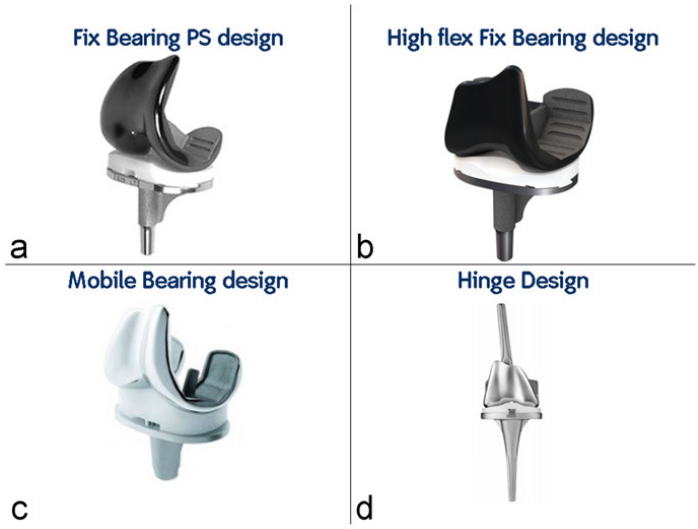

Figure 2.43. Total knee replacement models [Innocenti et al., 2011]

Their aim was to investigate the sensitivity of the patellofemoral and tibiofemoral contact forces with regard to patient-related anatomical factors. Beside their original aim, their results also let us see how the patellofemoral force changes if different, more and less complex prostheses are used under squatting movement (Figure 2.44).

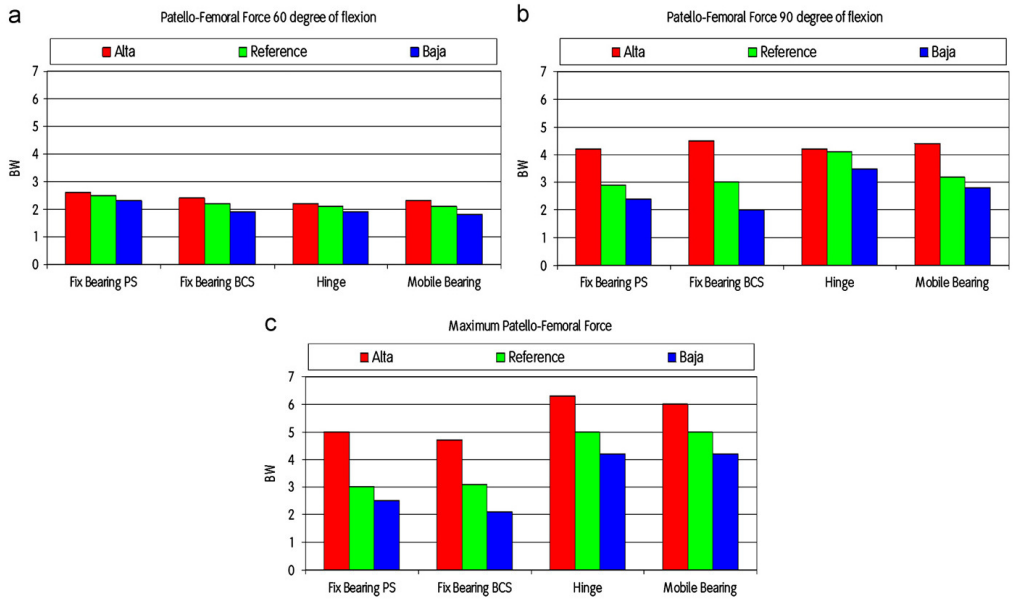

Figure 2.44. Histograms of patellofemoral contact forces [Innocenti et al., 2011]

If we look at Figure 2.44, at 60˚ of flexion angle, the patellofemoral forces have almost the same magnitude regarding all the four prostheses, while at 90˚ of flexion angle the prostheses can be divided into two groups. These groups are the fixed bearing types and the mobile bearing-simple hinge types. Although the hinge type is the simplest in the matter of kinematics, still it shows only slight difference regarding the kinetics compared to the mobile bearing type, and negotiable difference compared to the fixed bearing types.

It is also important to consider how hinge-type modelling appears in the contemporary design as well.

Earlier studies insisted that the total knee replacement design should take multiple instantaneous centers of rotation into account [Gunston, 1971, Frankel et al., 1971]. This means that the femoral replacement has several different radiuses (Figure 2.45), which meant to follow the geometry of the normal pathological knee. Opposite to this approach, the single-radius design (Figure 2.45) is based on the following theory: there is only one location for the flexion-extension axis and that is fixed to the femur [Churchill et al., 1998, Pinskerova et al., 2000].

Both of them have some advantages and disadvantages.

On one hand, the single-radius design keeps the femur and tibia rotate around each other in a constant radius, similarly to a hinge, which results a simplified motion. On the other hand, it clearly reduces the patellofemoral force [D'Lima et al., 2001] and allows less change in the exerting force through the quadriceps during flexion and extension [Wang et al., 2005].

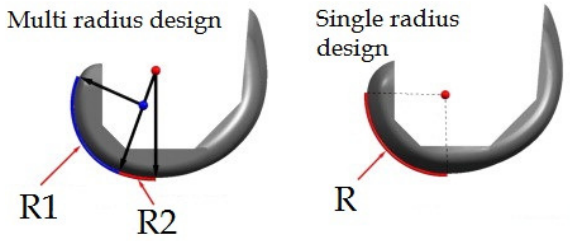

Figure 2.45. Multi- and single-radius design

The multi-radius design leaves more freedom in the movement, therefore less patellar symptoms occur due to its more elaborated geometry [Gómez-Barrena et al., 2010]. Nevertheless, it also has a kinetic-related disadvantage: during flexion-extension, the different radiuses cause greater shifts in the extensor, which might lead to temporary medio-lateral instability [Wang et al., 2005]. In details, this instability takes place when the knee motion reaches the transition between *R1* and *R2*, thus momentarily the tension drops in the collateral ligaments, and this might result instability or patellar dislocation.

Due to the fixed radius attribute of the single-radius design, the tension is better maintained in the collateral ligaments, which provides more stability to this type of design.

Among other global prosthetic developers, the Stryker® introduced a new type of prosthesis, the GetAroundKnee™, where the single-radius design is applied (Figure 2.46) therefore the motion of the knee becomes very similar to the hinge-type model [Stryker®, 2012].

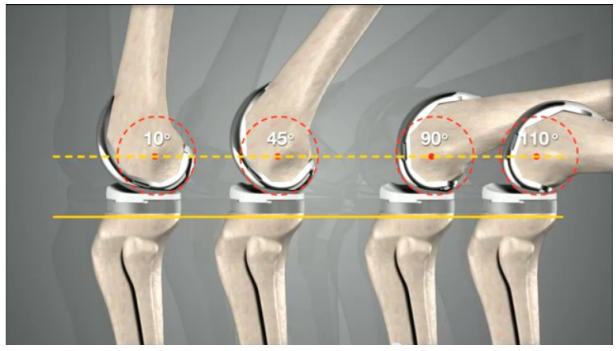

Figure 2.46. GetAroundKnee™ during flexion motion

One great advantage of this new type of prosthesis lies in the fact that the movement requires less knee moment to initiate the motion, and it restores the knee so-called circular motion [Wang et al., 2005, Gómez-Barrena et al., 2010].

After the reviewing the contemporary literature and the currently applied directions in total knee replacement design, it can be concluded that under certain circumstances the hinge-type modelling is applicable.

2.3. Numerical-mechanical models of squat

2.3.1. Introduction

In this part, numerical and experimental models of the sliding-rolling phenomenon will be analyzed, in order to establish a new three-dimensional multibody model, which will be introduced in the followings.

Sliding-rolling phenomenon appears in many fields of engineering, but maybe it is most known in the field of Machine Elements e.g. gear connections. As one of the earliest author and inventor of the involute gearing, Leonard Euler [Euler, 1760] established the kinematical fundaments of the gear-tooth action for further investigations.

The mechanism of the gear-tooth action is partly rolling and partly sliding. Pure rolling only appears in the pitch point, while before and after, sliding and rolling are jointly present (Figure 2.47).

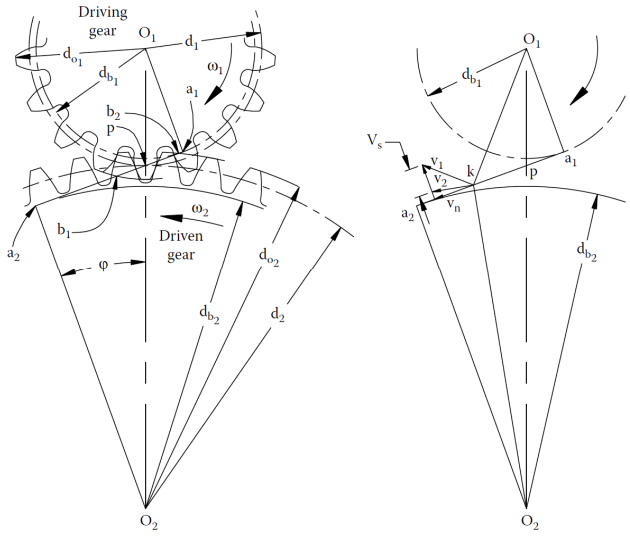

Figure 2.47. Gear connection [Klebanov et al., 2008]

It has been determined by the fundamental law of gear-tooth action that at the instantaneous contact point the two profiles have equal velocities ($\boldsymbol{V}_1$ and $\boldsymbol{V}_2$):

$$V_1 = d_{b_1} \cdot \omega_1 = V_2 = d_{b_2} \cdot \omega_2 \tag{2.11}$$

These velocities can be broken up to normal and tangential components, where the difference of the tangential velocity components is the sliding velocity. The sliding component of the movement causes noise, loss of power and most of all wear.

Therefore, in the design the sliding feature of the connection has to be carefully taken into account by keeping it as low as possible, since the more rolling the connection has, the longer it lasts.

In the knee joint itself, sliding and rolling appears alike, but as long as the connecting surfaces (cartilages) are intact, a natural balance prevails. Problems arise when – due to an external trauma or simply to ageing – the natural balance is split and more sliding starts appearing in the condyles.

If this case is an actuality in someone's life, then upcoming knee arthritis can be well handled by means of unicondylar (one-sided implant) or total knee replacements (TKR) (Figure 2.48).

Figure 2.48. Unicondylar (left) and Total knee replacement (right)

Naturally, these knee replacements have to comply with many strict requirements. The three most important ones are the followings:

- Being able to carry out closely the same locomotion as a normal non-pathological knee,
- Relieve pain,
- Good rate of survivorship.

Even though that manufacturers and researchers provide more and more studies about the efficiency and reliability of the current prostheses, failures still occur. Major causes of failure can be classified as follows:

- Infection of the joint,
- Loose components (either femoral or tibial),
- Fracture of components,
- Wear of the components.

It is considerably difficult to give a complete answer to each segment, since these above-mentioned problems are probably – to a certain extent – dependent on each other. Thus, let us limit our investigation to the last problem, related to the wear and within that, to the phenomenon of sliding-rolling.

Implant wear is the main mechanical factor that limits the lifetime duration of the knee replacements [Kurtz, 2009, O'Brien et al., 2013, Blunn et al., 1992, Hood et al., 1983]. It has also been confirmed that the kinematics of the knee joint has critical influence on the wear of the replacements [Wimmer and Andriacchi, 1997, Wimmer et al., 1998].

The wear in implants, due to occurring particle debris, is in relation with multiple and interrelated factors (Figure 2.49), therefore it has to be studied as a system not as a material property [Karlhuber, 1995].

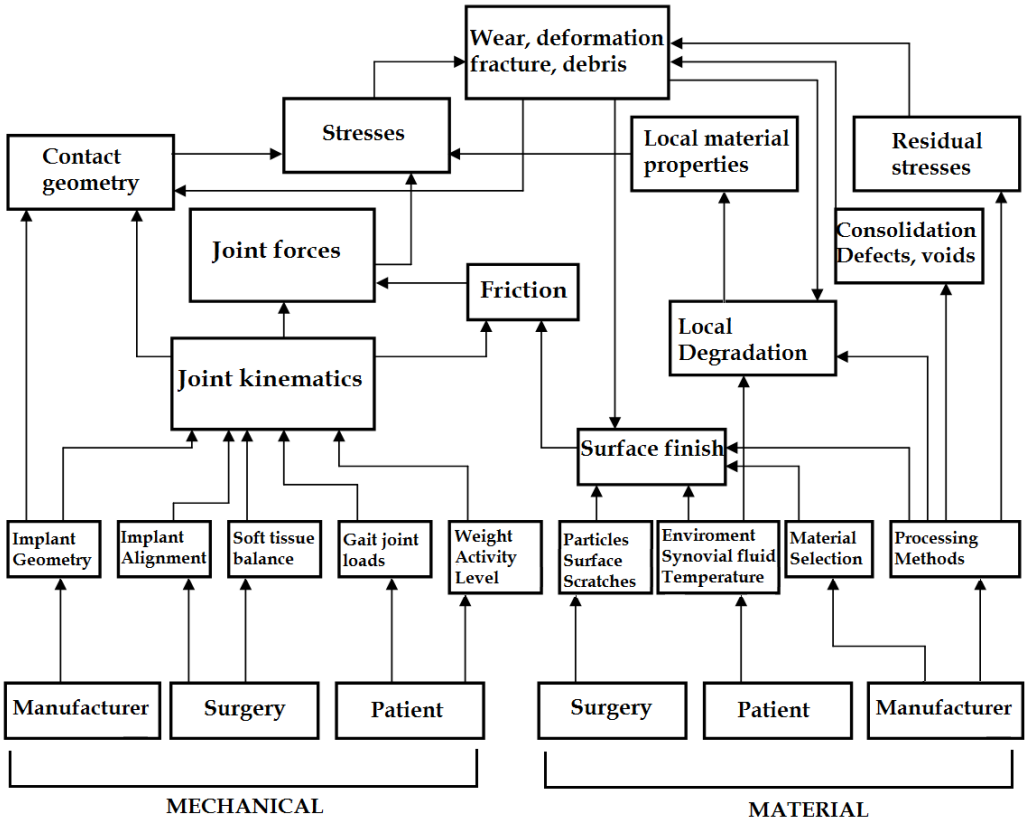

Figure 2.49. System of implant wear [Karlhuber, 1995]

The system of implant wear – suggested by Karlhuber [Karlhuber, 1995] – is very complex to involve completely in a numerical analysis, therefore only some parts will be taken into account in this study. The rolling-sliding factor is not a frequently applied and investigated element in the system, although, it has been suggested that a very similar movement, the cyclic sliding, is the most damaging kinematic motion [Blunn et al., 1991].

Sliding-rolling can be a key-factor, and also an answer why several authors [Blunn et al., 1994, Davidson et al., 1992], who have carried out wear studies on different test setups, obtained results which did not exactly correspond with the damage seen in the retrieved TKRs.

It has also been considered that high slip velocity during gait cycles causes increased sliding motion on the tibiofemoral surfaces and therefore generates greater volume of wear debris [Andriacchi et al., 2003].

One possible interpretation of the difference in the actual and expected wear can be originated to the fact, that the sliding-rolling ratio is not correctly taken into account, or if it is possible to set on the test setup, than it is incorrectly adjusted to the motion.

Laurent et al. [Laurent et al., 2003] also suggested that the wear mechanism is highly dependent not only on the loading of the connecting surfaces but the interfacial contact kinematics, which consist a cyclic multidirectional path of motion and the rolling-sliding ratio.

However, how is the sliding-rolling ratio involved into tribological tests?

A wear study on TKRs is carried out similarly as other wear tests. Load, number of cycles, in some studies sliding-rolling ratio and other factors, have to be set before the test and after the experiment, according to these parameters, wear can be estimated.

However, while the load (which is represented as the tibiofemoral force between a femoral and tibial compartment) is a well-known parameter or at least the maximum of the load is known, the sliding-rolling ratio in the active functional arc (where most of the locomotion is carried out) is currently unknown.

For this reason, this part of the thesis is dedicated to the sliding-rolling phenomenon of total knee replacements. With the obtained results, (minimum and maximum values of the ratio, evolution along the flexion angle) valuable information can be provided about this significantly influencing wear.

The applied methods are numerical, since computer models proved to be useful tools for predicting human kinematics especially if the motion has to be modelled in three-dimension.

In the followings, a review of different models (numerical and experimental) will be presented, while the second part of the study describes a new multibody model, which can estimate the sliding-rolling phenomenon and the kinetics between the contact surfaces (condyles) under squatting movement.

2.3.2. General numerical models

Although the knee is statically unstable structure, the surrounding ligaments, menisci, and muscles sustain its stability. In case of investigating local kinematics and/or kinetics of the knee joint, an adequately complex model has to be created. By importing realistic geometry of the condyles into a modelling software, muscle forces or contact pressures (in case of deformable bodies) can be predicted. Since computational models outnumber analytical models, only the most cited three-dimensional multibody and finite element models are summarized in Table 2.3.

AUTHORS	DYNAMIC / QUASI-STATIC	MODEL TYPE	CONTACT
Wismans et al., 1980	Quasi-static	Knee	Rigid
Blankevoort et al., 1991	Quasi-static	Knee	Deformable
Pandy et al., 1997, 1998	Quasi-static	Knee	Deformable
A-Rahmann and Hefzy, 1998	Quasi-static	Knee	Rigid
Kwak et al., 2000	Quasi-static	Knee	Deformable
Piazza and Delp, 2001	Dynamic	Full-body	Rigid
Cohen et al., 2003	Quasi-static	Knee	Deformable
Dhaher and Kahn, 2002	Quasi-static	Knee	Rigid
Chao, 2003	Quasi-static	Knee	Deformable
Guess et al., 2010	Dynamic	Knee	Deformable
Bíró et al., 2010	Dynamic	Knee	Rigid

Table 2.3. Numerical knee models

It is clear from the table that both rigid- and deformable models are frequently used. Most of the cases, the authors were in agreement – as an adequate approximation – to model only the knee itself, not the complete leg or body.

The rigid body models or multibody models generally lack the ability to calculate contact pressures, but have the advantage of providing precise contact definition, not only static but real dynamic simulation and quick iteration.

On the other hand, finite element models, due to the considerable simulation time, are often used for static simulation but they offer more calculation options against the multibody models.

2.3.3. Sliding-rolling phenomenon – Numerical models

In this subsection, a review has been assembled, similarly to the earlier section, where the early models are revised, highlighting their advantages, disadvantages and their results related to sliding-rolling.

Compared to other questions, the sliding-rolling phenomenon, with regard to physiological knee joints or TKRs, earned the interest of lesser authors, which is apparent due to the low number of studies about this specific area.

Van Eijden et al. [Van Eijden et al., 1986] constituted remarkably not only in the kinetics of the human knee joint, but also in the kinematics, by being the first ones who gave local description about the sliding-rolling phenomenon (denoted in their paper as rolling-gliding) between the femur and the patella (Figure 2.50).

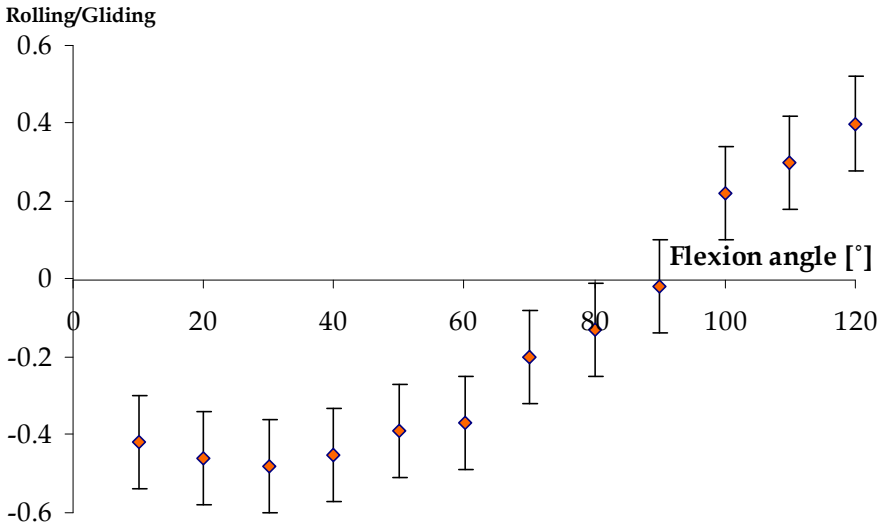

Figure 2.50. Sliding-rolling between the femur and the patella [Van Eijden et al., 1986]

Some remarks have to be mentioned related to their results:

- Van Eijden et al. [Van Eijden et al., 1986] did not define mathematically how they calculated the sliding-rolling ratio,
- They only calculated the ratio between the patella and the femur, although the phenomenon is more relevant between the femur and the tibia.

Although the model of Chittajallu and Kohrt [Chittajallu and Kohrt, 1999] is more like a phenomenological model that considers all the major ligaments (ACL, PCL, MCL and LCL), it can also calculate the slip ratio. Their mathematical model can describe the range of passive knee joint motion, which is the basis of all motion of the knee joint, and be a helpful tool in diagnosing the extent of ligament injury by matching clinically observed laxity in the knee joint to a variety of ligament conditions with the response of their model (Figure 2.51).

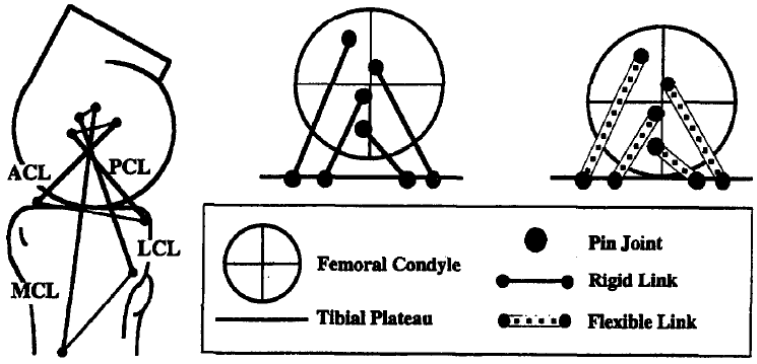

Figure 2.51. Numerical model [Chittajallu and Kohrt, 1999]

The slip ratio is defined as follows: one represents pure rolling, infinite represents pure sliding, while intermediate values represent the combination of the two.

The authors made several simplifications, which are namely:

a) The tibia plateau is a flat surface,

b) The surface of the femoral condyle is circular,

c) Ligaments are one-dimensional bodies without mass and they are connected to the bone by revolute/pin joints,

d) Ligaments can change in length, but only in case of tension,

e) No penetration of the tibia or femur is allowed,

f) No friction is assumed.

As for the findings, the author published the following results:

I. Strain values of the various ligaments as the function of flexion angle.

II. The slip ratio has been calculated as a function of flexion angle (Figure 2.52).

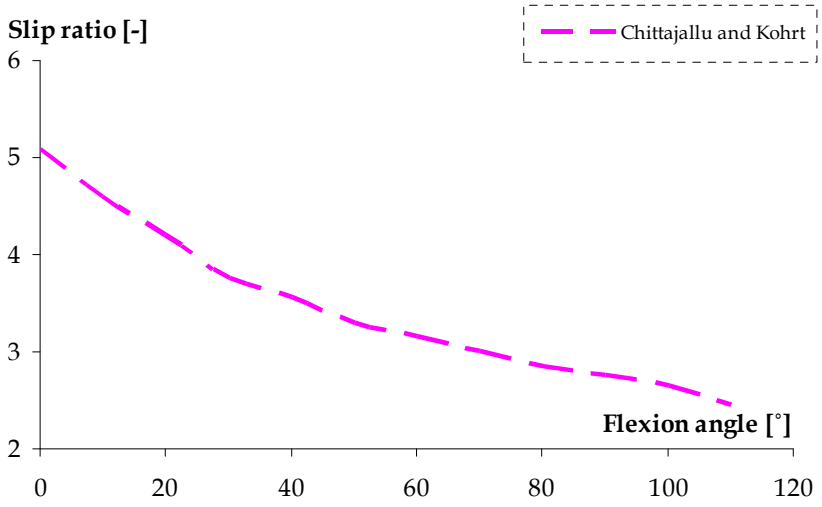

Figure 2.52. Slip ratio [Chittajallu and Kohrt, 1999]

The remarks related to the results of this model are the followings:

- Although Chittajallu and Kohrt [Chittajallu and Kohrt, 1999] reported that their slip ratio corresponded well with the result of O'Connor et al. [O'Connor et al., 1990], the result lacks providing an easily understandable physical meaning regarding the phenomenon
- Their model is far too simple to give an accurate prediction about the sliding-rolling phenomenon due to the applied geometrical simplifications.
- The model is only two-dimensional.

Ling et al. [Ling et al., 1997] introduced a similar model in order to study the behaviour of a knee joint with the effect of inertia, articular surfaces, and the patella (Figure 2.53).

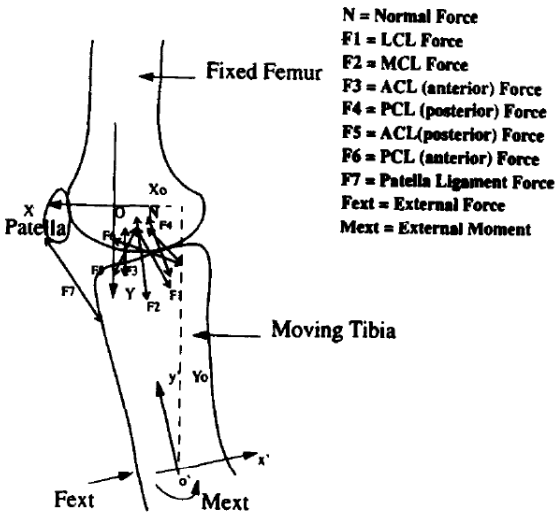

Figure 2.53. Numerical model [Ling et al., 1997]

They applied the following simplifications:

a) The model is planar, created in the sagittal plane,

b) Ligaments are one-dimensional bodies without mass,

c) Ligaments can change in length, but only in case of tension,

d) No penetration of the tibia or femur is allowed,

e) No friction is assumed.

As an incompleteness of the earlier models, the authors appointed that the articular surfaces of the femur are often assumed circular. To improve this problem, they used fourth order and root functions to describe the connecting surfaces (denoted by f_i parameter). The authors determined the sliding-rolling ratio by calculating the arc lengths travelled on the surface of the tibia and femur between each simulation step:

$$s = \int_{lower}^{upper} \sqrt{1 + \left(\frac{df_i}{dx} \right)^2} \, dx \tag{2.12}$$

If $i = 1$, then it is the curve of the tibia, if $i = 2$, then it is the curve of the femur. The sliding-rolling ratio is defined as the difference between the larger distance (s_l) and the smaller distance (s_s) travelled on the femur and tibia over the smaller of the two arc lengths travelled (s_s).

$$sliding / rolling = \frac{s_l - s_s}{s_s} \tag{2.13}$$

The problem with this definition is that e.g.: s_l equals to 6 mm and s_s equals to 2 mm, then if we calculate the sliding-rolling ratio from Eq. (2.13), we obtain 2. By knowing s_l and s_s, then by common sense it is obvious that the sliding-rolling ratio is distributed as 66% sliding and 33% of rolling. However, from the above-mentioned formula (Eq. (2.13)), we can only obtain the number of two, which grants no clear physical interpretation about the ratio.

From their calculation (Ling et al., 1997), the authors stated that in the beginning of flexion, rolling is dominant and as the flexion angle increases, sliding becomes the dominant factor (Figure 2.54).

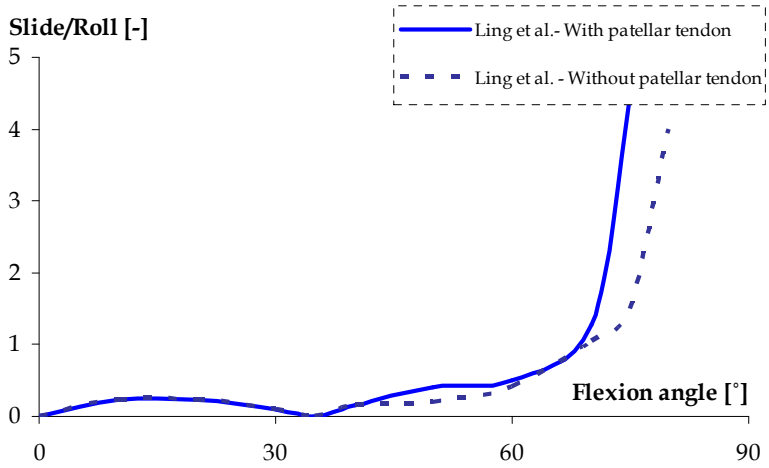

Figure 2.54. Sliding-rolling ratio [Ling et al., 1997]

The following remarks can be concluded regarding their results:

- In their study, they gave a description how the sliding-rolling ratio was calculated, although the ratio itself lacks to interpret the physical meaning of the obtained results (e.g., what does the ratio of zero, one or number above that mean?)
- By comparing their results to Chittajallu and Kohrt [Chittajallu and Kohrt, 1999], no correlation can be noticed.

Wilson et al. [Wilson et al., 1998] aimed to prove the hypothesis that the passive knee joint is guided by the articular contact and isometric fascicles of the ACL, MCL and PCL (anterior-, medial and posterior cruciate ligaments). To perform their simulation they created a mechanism based on anatomical considerations (Figure 2.55):

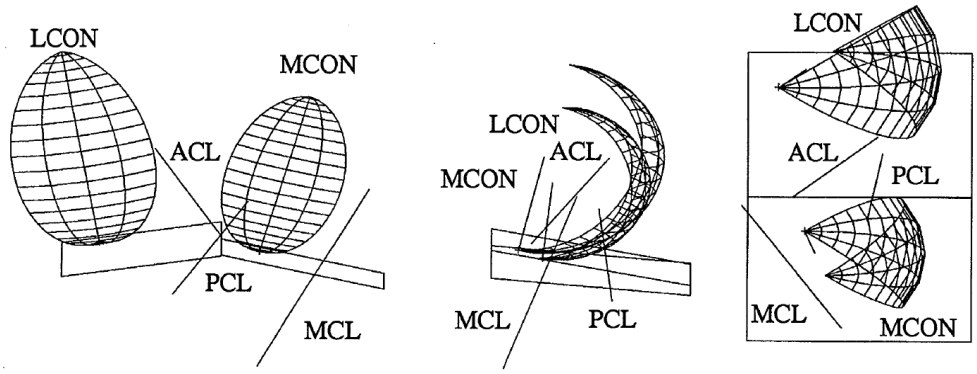

Figure 2.55. Numerical model [Wilson et al., 1998]

The authors applied the following simplifications:

a) The femoral condyles are spherical,

b) The tibial condyles are planar,

c) Ligaments are represented by kinematic pairs (links),

d) No penetration of the tibia or femur is allowed,

e) No friction is assumed.

Regarding the slip ratio, Wilson et al. [Wilson et al., 1998] used the description of O'Connor et al. [O'Connor et al., 1990], but Wilson et al. [Wilson et al., 1998] described the slip ratio slightly differently: slip ratio of zero indicates pure slipping, while one indicates pure rolling. Slip ratio above one indicates "skidding". The slip ratios, provided by the above-mentioned authors, are summarized in Figure 2.56:

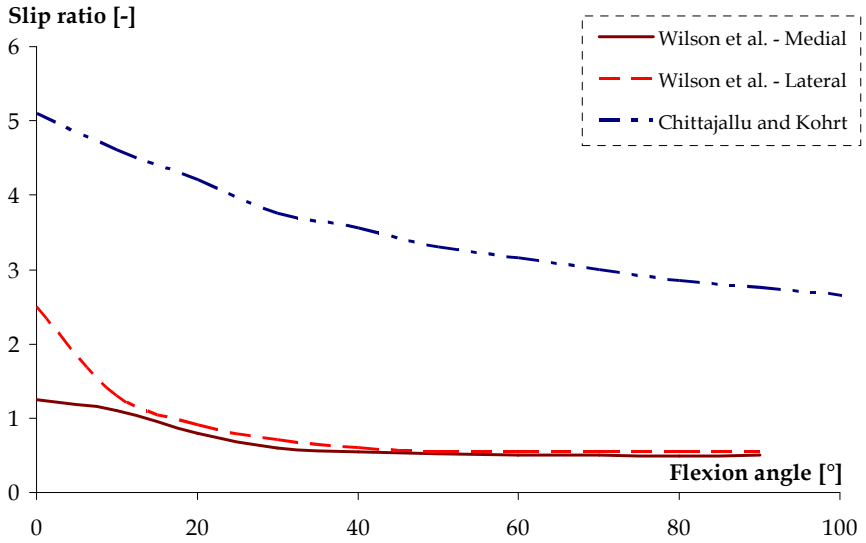

Figure 2.56. Slip ratio [Wilson et al., 1998]

The following remarks can be concluded regarding their results:

- The connecting surfaces, especially the tibial, are oversimplified,
- The authors described the slip ratio between zero and one but above one, the "skidding" phenomenon is unclear and the authors did not explain it further.

A mention must be made that by neglecting the non-interpreted "skidding" zone, the slip ratio starts growing, which means that the local movement changes from pure rolling to the mixed sliding-rolling phase. This corresponds with the early results of Zuppinger [Zuppinger, 1904], who stated that in the beginning of the motion, e.g. in stance, the knee only carries out rolling motion, and then slowly more sliding appears.

This statement has been widely accepted as a very possible trend of the sliding-rolling phenomenon, thus we can assume that the result of Wilson et al. [Wilson et al., 1998] stands closer to reality than the result of Chittajallu and Kohrt [Chittajallu and Kohrt, 1999].

Although a similar trend appears in the result of Chittajallu and Kohrt [Chittajallu and Kohrt, 1999] as well, their magnitude is completely in the so-called "skidding" zone, which makes it difficult to understand or interpret.

Hollman et al. [Hollman et al., 2002] investigated how the electromyographic activity and sliding-rolling phenomenon differ between patients with injured ACLs and patients without knee pathology in case of weight bearing movement (WB) and non-weight bearing movements (NWB). In their research, the determination of the sliding-rolling ratio has been carried out by an analytical approach, based on the concept of the path of instantaneous center of rotation (PICR). The model is shown in Figure 2.57.

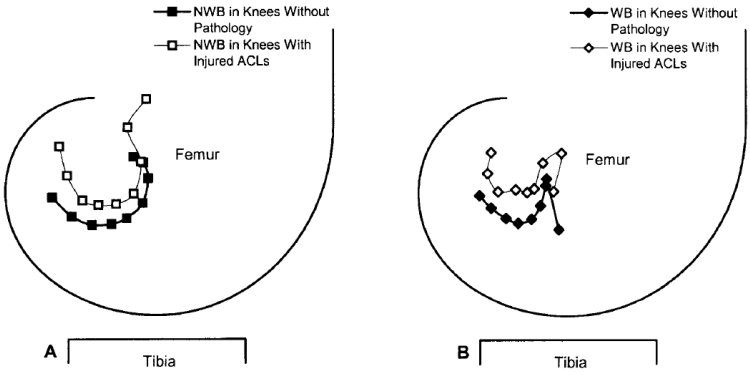

Figure 2.57. PICR model [Hollman et al., 2002]

Hollman et al. [Hollman et al., 2002] used certain simplifications regarding to the calculation of the sliding-rolling ratio:

a) The knee joint is primarily a joint with a single degree of freedom,

b) The knee joint is modelled in the sagittal plane,

c) The femur line is represented by average condylar geometries,

d) The tibia line is represented by linear straight line,

e) The condyles – lateral and femoral – are not distinguished,

f) No friction is taken into account.

The authors calculated the contact coordinates of the femur and tibia at 10˚ of flexion angle intervals along the surface of the model. Based on the experimentally obtained ICR data the sliding-rolling ratio has been determined.

The sliding has been specified in percentage, and the weight-bearing ratio is plotted in Figure 2.58.

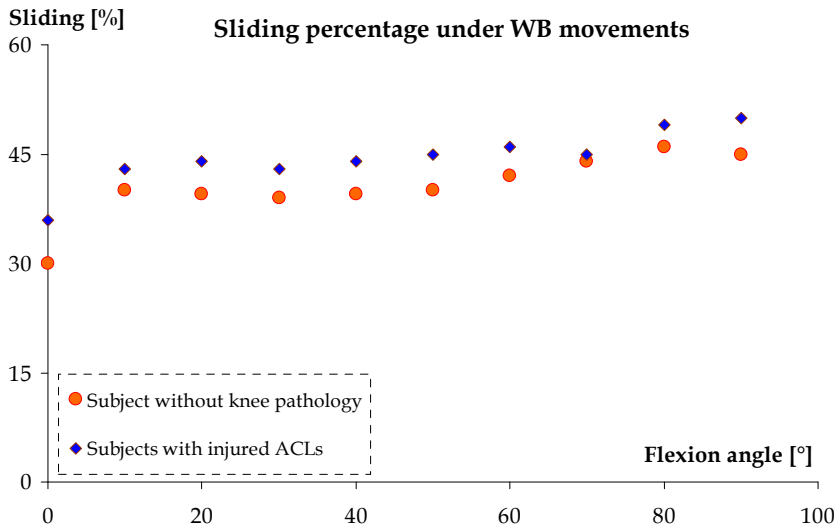

Figure 2.58. Sliding-rolling ratio [Hollman et al., 2002]

The following remarks must be mentioned regarding the results of Hollman et al. [Hollman et al., 2002]:

- The connecting surfaces are oversimplified,
- The investigated motion is reduced to planar,
- The model is not suitable for kinetical calculation.

Nägerl et al. [Nägerl et al., 2008] re-investigated the question of rolling-sliding (R-S) ratio based on the experiments carried out by Iwaki et al. [Iwaki et al., 2000] and Pinskerova et al. [Pinskerova et al., 2004] on loaded, unloaded and cadaver knees. Analytical and numerical techniques were mutually applied in the investigation, and new results were found regarding the lateral and medial compartments (Table 2.4).

R-S ratio	Flexion angle	Medial compartment		Lateral compartment	
		Loaded	Unloaded	Loaded	Unloaded
$\rho_{r\text{-}s}$	0-20°	0.96	0.8	1.24	0.17
$\rho_{r\text{-}s}$	45-90°	0.1	0.09	0.2	0.43

Table 2.4. Various rolling-sliding ratios [Nägerl et al., 2008]

They defined a rolling-sliding ratio (ρ), where one represents pure rolling and zero represents pure sliding. In contrary to other authors [Wilson et al., 1998, Hollman et al., 2002], Nägerl et al. [Nägerl et al., 2008] assumes that at higher flexion angles the sliding goes beyond 40-50%. This assumption has been verified by their simulations on the AEQOUS-G1 model (Figure 2.59, for later use, here the sliding-rolling ratio is plotted, thus the reverse of ρ).

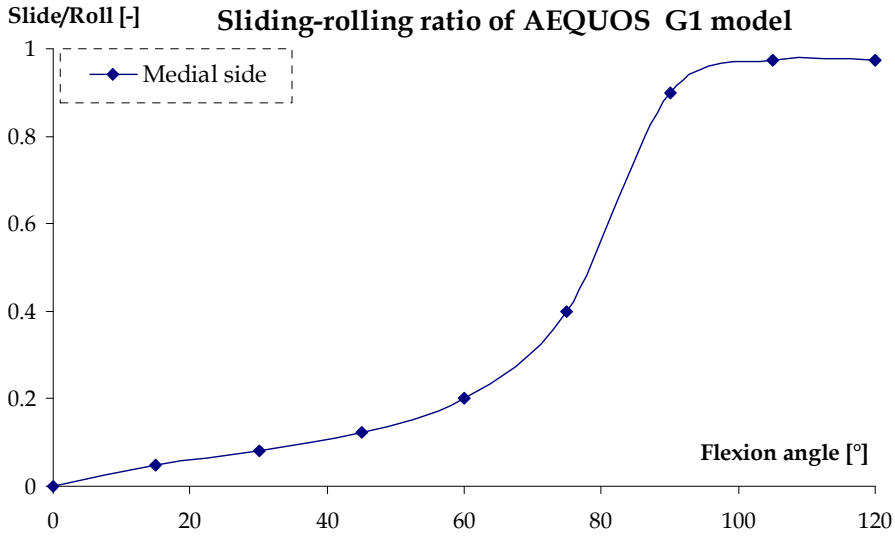

Figure 2.59. Sliding-rolling ratio [Nägerl et al., 2008]

As for the approach of Nägerl et al. [Nägerl et al., 2008], the followings can be mentioned:

- Their approach can calculate the sliding-rolling ratio on both lateral and medial side, but the motion is reduced to planar.
- The results of AEQOUS-G1 is only the result of a single prosthesis.
- The model is not suitable for kinetical calculation.

As a closure of this review, a mention must be made that the available results from the literature [Van Eijden et al., 1986, O'Connor et al., 1990, Ling et al., 1997, Wilson et al., 1998, Chittajallu and Kohrt, 1999], with few exceptions [Hollman et al., 2002, Nägerl et al., 2008], are controversial and no comprehensive study has been published to unfold and determine the governing phenomenon of sliding-rolling between different prostheses.

2.3.4. Sliding-rolling phenomenon – Experimental methods

Sliding-rolling is tightly connected to several fields such as Machine Design – especially gear drives – or the contact between femoral and tibial condyles. The connecting point between these fields is the wear.

As it was earlier mentioned, wear is the most determining lifetime factor regarding gear teeth or the current TKRs. Wear is also highly affected by the presence of sliding-rolling and for this reason, it cannot be neglected. The reason lies in the fact that this phenomenon causes different material abrasion (with a possible effect of adhesion) compared to pure sliding or rolling alone [Wimmer, 1999]. Several test setups and techniques are available [Saikko and Calonius, 2002, Laurent et al., 2003, Kellett et al., 2004, Lancin et al., 2007, Schwenke et al., 2009, Kretzer et al., 2011, Van Ijsseldijk et al., 2011] to quantify the wear on the prosthesis surfaces, but it is partially known what forces appear on the surface or how much sliding-rolling ratio should be applied during standard tests.

Beside the actual load (which represents the tibiofemoral force), the sliding-rolling ratio is one of the most important parameters of the wear tests, since if it is set incorrectly high or low, than wear will be heavily over- or underestimated.

With regard to the experimental approaches, McGloughlin and Kavanagh [McGloughlin and Kavanagh, 1998] designed and built a three-station wear test rig in order to assess the influence of kinematic conditions on quantitative wear on the basis of TKR materials (Figure 2.60).

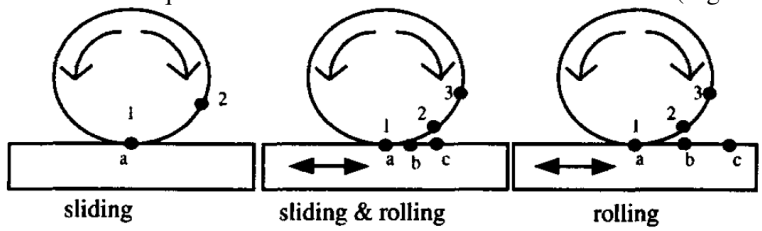

Figure 2.60. Motion conditions [McGloughlin and Kavanagh, 1998]

In their study, they used a flat plate and a cylinder to measure how wear rate is influenced by different sliding-rolling conditions. According to their results, at 0.95-0.99 sliding-rolling ratio the wear rate reached the maximum.

As a conclusion they assumed that on the one hand high sliding-rolling ratio generates fatigue type mechanism and on the other hand it influences the wear rate, thus this specific kinematic condition has design significance.

Reinholz et al. [Reinholz et al., 1998] developed a revolving simulator which allows setting the sliding-rolling ratio between 0 to 1 (between 0 and 100% of sliding). In their experiments they investigated the change of the coefficient of friction as a function of sliding.

Schwenke et al. [Schwenke et al., 2005] developed a setup which allows the parametric analysis of various slip velocity ranges in order to study the polyethylene wear relative to the sliding-rolling ratio (Figure 2.61).

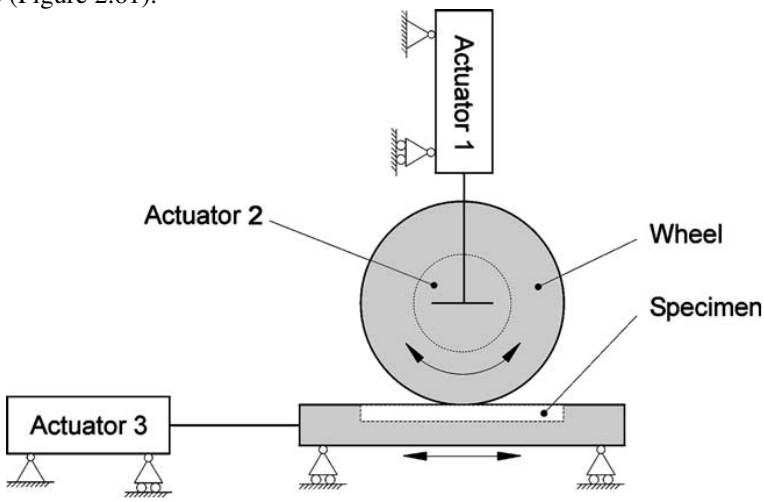

Figure 2.61. Wear test setup [Schwenke et al., 2005]

They concluded that high slip velocities under the condition of pure sliding, and the transition between pure rolling and sliding (tractive rolling) generated the highest amount of wear. Their tests also revealed that the amount of sliding rolling has critical effect on the wear.

Van Citters et al. [Van Citters et al., 2004] designed a six-station tribotester that is able to test six specimens simultaneously (Figure 2.62). In their tests, the sliding-rolling ratio was set to maximum 0.4 by means of creating 40% of sliding and 60% of rolling [Van Citters et al., 2004, Van Citters et al., 2007].

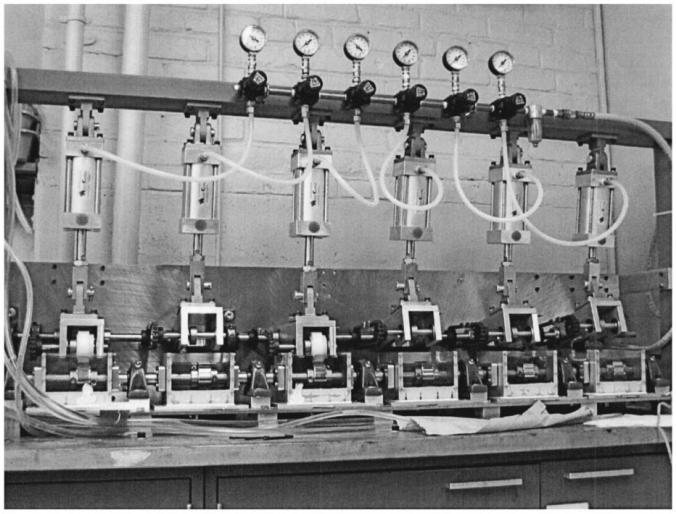

Figure 2.62. Multi-station test rig [Van Citters et al., 2004]

According to these studies, in case of experimental testing of prosthesis materials, the sliding-rolling ratios are widely applied between 0.3-0.4 in the range of 0-30˚ flexion angle. Above this certain angle only McGloughlin and Kavanagh [McGloughlin and Kavanagh, 1998] carried out experiments and proved that the sliding-rolling ratio can reach higher values, although they did not use real prosthesis components but a cylinder and a flat plate.

3. MATERIALS AND METHODS

3.1. Methodology

Generally, four major methods can be used to solve a scientific problem, namely: *analytical, numerical, experimental,* and *complex method* that involves all the earlier mentioned three methods [Csizmadia, 1998].

Analytical methods are applied when it is possible to describe the phenomenon with algebraic or differential equations, therefore a closed-form mathematical solution can be obtained.

Numerical methods are used when the descriptive equations of the phenomenon are known, but it is impossible to provide a closed-form solution for the problem.

Experimental methods are based on observations and measurements on the phenomenon. Although it is widely used in both industrial works and researches, it might not always be an optimal way to solve the problem.

In the case of *complex method*, the phenomenon is approached by mostly analytical or numerical techniques, but experiments are also involved.

In this doctoral work, the complex method is applied. The thesis begins with a purely analytical-kinetical model that is based on Newton's second law and aims to describe the kinetics of both standard and non-standard squat. Earlier published models were surveyed, analyzed and utilized in the modelling in order to answer questions that were neglected or oversimplified. Finally, a new model has been created. By this new model the patellofemoral compression force, the patellar tendon force, the quadriceps tendon force and the tibiofemoral compression force can be derived by means of algebraic equations.

Every theoretical model has a certain number of parameters that splices the model with reality. The more parameters it has, the more accurately it describes the phenomenon of interest.

Bearing in mind that too many parameters are also not advised (for example in Hanavan's model forty-one anthropometrical parameter appears [Hanavan, 1964]), the new analytical-kinetical model, described later in this chapter, includes seven anthropometrical parameters that were experimentally obtained.

Regarding the experiments: several human male and female subjects participated in a series of non-standard squats, where human anthropometrical data was gathered and processed to serve as inputs to the analytical-kinetical model.

In the second half of the thesis, a special part of the local knee kinematics was investigated, namely the sliding-rolling. Due to the complexity of the connecting femoral and tibial condyles, analytical methods were insufficient to draw accurate conclusions. For this reason, the phenomenon was investigated by means of numerical methods with the MSC.ADAMS software.

As a minor result, a new sliding-rolling ratio has been introduced, since the ones given in several publications do not give clear view about the phenomenon. Regarding the major result, the sliding-rolling ratio has been obtained in the functional arc of the knee joint (between 20-120˚ of flexion angle) on four commercial- and one prototype prosthesis.

3.2. Conclusions about the early analytical-kinetical models

After the comprehensive review of these models, general conclusions have to be drawn in order to create a new model that is able to answer questions that until now have not been dealt with.

In order to establish this new model, let us look at the main modelling questions and make decisions towards the model creation with a brief explanation.

1st QUESTION: Which human locomotion should be modelled?

ANSWER: Considering three simple facts, it is adequate to choose the locomotion of squatting:

a) According to the studies of Reilly et al. [Reilly et al., 1972] and Dahlqvist et al. [Dahlqvist et al., 1982], the greatest magnitude of the patellofemoral forces ($\boldsymbol{F}_{pf}$, $\boldsymbol{F}_{pt}$, $\boldsymbol{F}_{q}$) appears during squatting motion,

b) Squatting is an frequently (everyday) practiced movement, which also has clinical importance as being a rehabilitation exercise,

c) From the mathematical point of view, the squatting movement provides more possibility to create a simpler but accurate analytical model.

For these reasons, the chosen locomotion is the squat.

2nd QUESTION: Should numerical or analytical model be used?

ANSWER: Although most of the earlier published mathematical models are considered as analytical models, only the work of Denham and Bishop [Denham and Bishop, 1978], Nisell et al. [Nisell et al., 1986] and Mason et al. [Mason et al., 2008] provide closed-form analytical solutions regarding the patellofemoral forces.

The rest of the mathematical models describe the phenomenon by non-linear equation systems that make the calculation clumsy. In addition, if a numerical model is used, no closed form analytical correspondence can be created between the biomechanical factors such as patellar length-height, patellar tendon length or the anatomical angles.

As a major aim of this thesis, an analytical-kinetical model will be created, thus the forces can be analytically derived from equilibrium equations.

3rd QUESTION: Should we consider static of dynamic model?

ANSWER: A significant question in the biomechanical research whether the human locomotion should be modelled with static or dynamic models.

The static-dynamic choice actually depends more on the locomotion. Regarding the running, it is adequate that the model is dynamic since the motion is carried out rapidly, hence significant inertial forces may arise.

In contrary, squatting is rapid only in special cases. The clinical relevance of the squatting on the one hand is a lower-extremity strengthening exercise, while on the other hand a postoperative ACL rehabilitation program. A mention must be made that for patients with total knee arthroplasty, rapid squatting is contraindicated.

For the sake of clarity, the following duration(s) can be credited to normal squat exercise: Innocenti et al. [Innocenti et al., 2011] reported 20 sec of descending time in their study from 0° to 120° of flexion angle, while Fukagawa et al. [Fukagawa et al., 2012] discovered age-related correlation about deep squat kinematics. Their findings showed that the average normal deep squat duration situates between 3 and 6 sec as a function of age.

Due to the slow motion, how generally the squat is carried out, the inertial forces can be safely disregarded. This fact was more comprehensively confirmed by the study of Krabbe et al. [Krabbe et al., 1997], who dealt thoroughly with the importance of the inertial forces of the lower extremity joints (hip, knee and ankle) during running. They stated that the inertial forces could be neglected, if the horizontal velocity of the subject is not more than 5 m/s. During squatting, no horizontal velocity can be interpreted, but the average vertical speed is much lower than 5 m/s. Based on this fact, we can conclude that the inertial effect on the patellofemoral forces under squat movement can be neglected as well.

Consequently, a static squat model will be used.

4th QUESTION: Should two- or three dimensional model be used?

ANSWER: Two-dimensional modelling is widely accepted and used in case of kinetic investigation, since the forces have their major effect in the sagittal plane and minor effect in the coronal plane [Singerman et al., 1994, Miller, 1991].

Furthermore, the change of the force-transmission can be explained as follows: the patellofemoral forces directly depend on the distance between the line of body weight (the centre of gravity line) and the instantaneous point of rotation of the patellofemoral joint [Schindler and Scott, 2011].

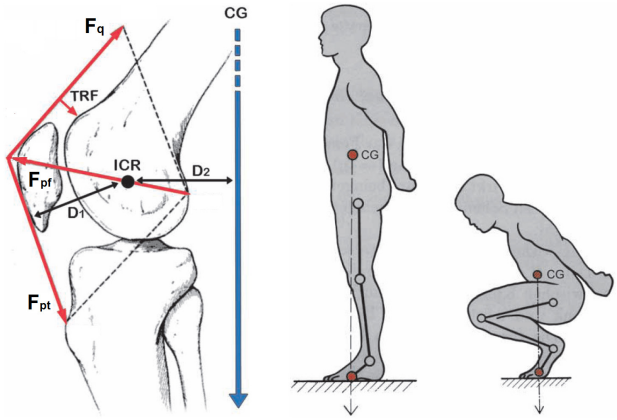

Figure 3.1. The patellofemoral forces and centre of gravity [Schindler and Scott, 2011]

If the posture changes (e.g. leaning forward or backward), then this distance alters as well which leads to substantial changes in the force transmission. In the coronal plane this influence is negligible (Figure 3.1).

Naturally, a three-dimensional model has the advantage that it is more similar to the real human knee joint. Nevertheless, according to the models in the literature [Wisman et al., 1980, Hirokawa, 1991, Hefzy and Yang, 1993], they are also more difficult to handle. As for the modelling point of view, regarding the patellofemoral and tibiofemoral forces, a two-dimensional model can also provide accurate results with the advantage of easy handling.

Thus, the new analytical-kinetical model is consequently two-dimensional.

5th QUESTION: Should the geometry of the contact be considered?

ANSWER: The analytical-kinetical model is meant to examine only the patellofemoral and tibiofemoral kinetics. The studies of Powers et al. [Powers et al., 2006], Innocenti et al. [Innocenti et al., 2011] and some practical applications regarding prostheses (GetAroundKnee™) suggest that a simple connection such as the hinge is applicable and satisfactory, if only the kinetics is considered.

Therefore, the connection between the femur and tibia is represented with a hinge in the new analytical-kinetical model.

6th QUESTION: What muscles should be taken account and what can be disregarded?

ANSWER: The roll of the quadriceps tendon and the patellar tendon are indispensable, but ultimately what other ligaments and tendons can be neglected?

In the study of Denham and Bishop [Denham and Bishop, 1978], it was well demonstrated with simultaneous electromyograph tracings that in case of balanced equilibrium, the extensor effect upon the knee is minorly affected by actions in the hamstrings or in the gastrocnemius muscles (Figure 2.21).

Major activity was only reported in the quadriceps and in the soleus, while only occasional burst of activity, which helps to maintain balance, was noticed in the other muscle groups. Therfore their effects can be safely disregarded.

The roll of the anterior and posterior crucial ligaments (ACL and PCL) is neglected in the modelling, since these ligaments are more responsible for keeping the stability, rather than force transmission.

According to the above-mentioned facts, only the quadriceps tendon and the patellar tendon are considered in the new analytical-kinetical model.

7th QUESTION: Should rigid of flexible bodies be used in the modelling?

ANSWER: Among other aims, the goal of this thesis is to provide an easy, preferably completely analytical way to calculate the change of the patello- and tibiofemoral forces in the knee joint under squatting movement.

Firstly, disregarding the deformation of the bones considerably simplifies the calculation while only associates a moderate error to it, and secondly, it is a commonly applied simplification which was demonstrated by the earlier presented models from the literature review.

In the new analytical-kinetical model, the bodies are considered rigid.

8th QUESTION: Should force ratios or individual forces be used?

ANSWER: In several studies [Denham and Bishop, 1978, Van Eijden et al., 1986, Yamaguchi and Zajac, 1989, Hefzy and Yang, 1993, Gill and O'Connor, 1996] only the ratio of the patellofemoral forces can be obtained in a way that the quadriceps force is always assumed as a constant known force.

To all intents and purposes, these models neglect the fact that the quadriceps force changes during the motion and the change could be derived analytically.

In spite of the common assumption, another major aim of the new analytical-kinetical model is to derive the patello- and tibiofemoral forces individually, thus the change could be monitored and further studied.

9th QUESTION: Should the moving centre of gravity be implemented into the model?

ANSWER: The movement of the centre of gravity is a known phenomenon although it has been only slightly investigated how it alters the forces in the knee joint.

Firstly, it was shortly discussed by Perry et al. [Perry et al., 1975] that according to clinical experiences by locking the hip bone and leaning forward, practically moving the centre of gravity towards the knee, the amount of quadriceps force needed to stabilize the posture will be decreased. Therefore, the knee flexion can be carried out easier, which in indicated for patients with paresis. Although it was an appreciation of necessity, the question was not further analyzed.

Denham and Bishop [Denham and Bishop, 1978] recognized that the position of the centre of gravity has the most significant effect on the patellofemoral forces. By taking radiographs of the knee joint, they measured the extensor moment arms and the position of the centre of gravity in an arbitrary posture. According to their studies, finding the accurate position of the centre of gravity line is based on the following considerations [Denham and Bishop, 1978]:

- If equilibrium is established, the centre of gravity line passes through the feet,
- The smaller the area of contact with the ground, the greater is the accuracy with which the line of body weight can be located.

The authors included this shifted centre of gravity into their model, but only in one certain position without investigating how the centre of gravity function changes during the squat as a function of flexion angle. They suspected that leaning forward a couple of centimetres could halve the patellofemoral forces, although they did not prove this hypothesis.

Amis and Farahmand [Amis and Farahmand, 1996] also posed a similar question related to the knee extensor mechanism in the sagittal plane by assuming a length between the centre of rotation of the knee joint and the centre of gravity line.

Likewise the earlier authors, they did not propose a solution or expand the question.

After a long period, Schindler and Scott [Schindler and Scott, 2011] brought the importance of the moving centre of gravity related to the patellofemoral forces to the surface in their comprehensive study. They gave numerous examples (squat, gait or stair descent and ascent) where the role of the moving centre of gravity is incontrovertible (Figure 3.2).

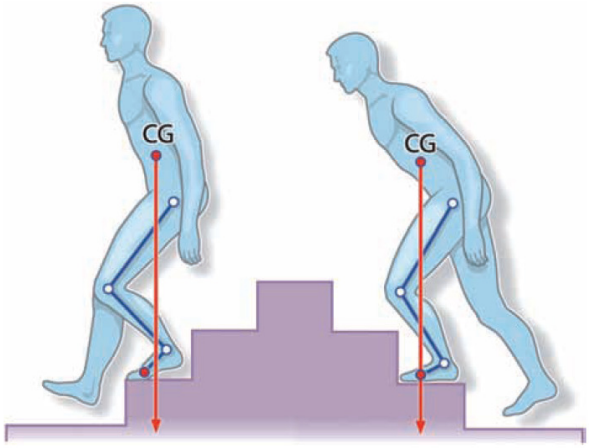

Figure 3.2. Movement of the centre of gravity during stair descent/ascent [Schindler and Scott, 2011]

While Schindler and Scott [Schindler and Scott, 2011] only discussed the possibilities and the importance of the moving center of gravity, Farrokhi et al. [Farrokhi et al., 2008] carried out kinetic and kinematic analysis under forward lunge exercise based on surface electromyographic (EMG) data involving the effect of the trunk movement.

At last but not least, the most comprehensive and current study is originated to Kulas et al. [Kulas et al., 2012] who investigated how minimal and moderate forward trunk movement affects the anterior cruciate ligaments together with the quadriceps- and hamstring muscle forces by means of inverse dynamics.

Their findings clearly pointed out that the forward trunk movement effectively reduces the force in the anterior cruciate ligaments, but also that only a few authors have explored or dealt with the influence of trunk position and/or trunk load on knee biomechanics [Kulas et al., 2008].

From the summary of the above-mentioned studies, it becomes apparent that the role of the moving centre of gravity has not been described and implemented into any numerical or analytical model. It has to be also clarified, that the movement of the center of gravity significantly alters the patellofemoral forces: hypothetically, it reduces them.

Due to the currently unknown effect of the horizontally moving center of gravity on the patellofemoral forces, this phenomenon, as a novel factor, will be implemented into the new analytical-kinetical model.

GENERAL COMMENTS

In order to give an interdisciplinary answer to all the above-mentioned questions, a new two-dimensional analytical-kinetical model is presented. This model is able to investigate forces in the knee joint such as: quadriceps force ($\boldsymbol{F_q}$), patellar ligament force ($\boldsymbol{F_{pt}}$), patellofemoral compression force ($\boldsymbol{F_{pf}}$) and the tibiofemoral compression force ($\boldsymbol{F_{tf}}$) as a function of the flexion angle, relative to the body weight ($\boldsymbol{BW}$).

The horizontally moving center of gravity – the trunk motion effect – is also incorporated into the model.

The examined motion regarding this part of the thesis is the standard and non-standard squat. The reason why this specific movement has been chosen for investigation is based on its clinical importance, the good modelling aspects, and the fact that under this movement the forces in the knee joint reach extremity.

3.3. New analytical-kinetical model

3.3.1. Introduction

The results of Van Eijden et al. [Van Eijden et al., 1986] regarding the particular kinetics of a fixed femur and a sliding-rolling patella (Eq. (2.7) and (Eq. (2.8)) are widely cited and applied, however, the motion described by the authors is not kinematically equivalent with squatting. One the on hand, they initiated the movement by applying a given $\boldsymbol{F_q}$ force and on the other hand, the femur was fixed. In contrary under squatting movement both the femur and the tibia rotate about the knee joint (Figure 3.3).

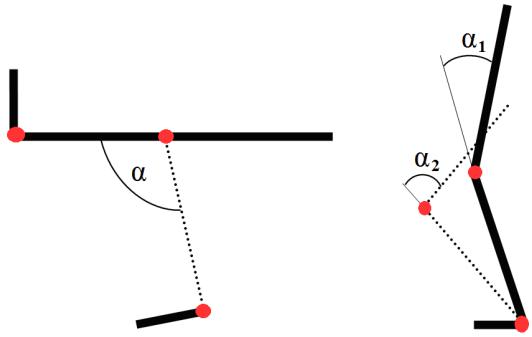

Figure 3.3. Knee movement by Van Eijden et al. [Van Eijden et al., 1986] (left), and normal squatting (right)

A mention must be made that the $\boldsymbol{F_q}$ force (50 N) was arbitrarily chosen by the authors [Van Eijden et al., 1986], although $\boldsymbol{F_q}$ itself also depends on the position of the knee joint. The novelty of the present model, compared to the model of Van Eijden et al. [Van Eijden et al., 1986] or Mason et al. [Mason et al., 2008], is based on two considerations:

1. Firstly, the incorporation of the movement of the trunk, which appears in this model as a horizontal movement of the center of gravity,
2. Secondly, the movement of the femur and tibia relative to each other are not constrained (none of them are fixed but can freely rotate during the squat).

As demonstrated in the model of Mason et al. [Mason et al., 2008], the net knee moment directly depends on the position of the body weight vector, which has the same line of action as the center of gravity. If the center of gravity moves towards the knee, namely the d moment arm decreases, then the net knee moment decreases as well. Due to this phenomenon, the magnitude of the patellofemoral forces decreases [Bishop and Denham, 1978, Schindler and Scott, 2011].

Since none of the earlier models [Bishop and Denham, 1978, Van Eijden et al., 1986, Nisell et al., 1986, Yamaguchi and Zajac, 1989, Reitmeier and Plitz, 1990, Hirokawa, 1991, Miller, 1991, Hefzy and Yang, 1993, Gill and O'Connor, 1996, Mason et al., 2008] considered the forward trunk motion, no accurate results are available about its effect on the patello- and tibiofemoral forces.

To reveal and analyze their effect, these additional attributes will be implemented into the new analytical-kinetical model.

3.3.2. Limitations and advancements of the model

Some of the simplifications are similar compared to the model of Mason et al. [Mason et al., 2008] while several other factors (anatomical angles, etc.) are also considered:

a) The model is quasi-static,

b) The femur, tibia and patellar are considered as rigid bodies,

c) The patellar tendon and the quadriceps tendon are inextensible,

d) The line of action of the quadriceps is parallel with the femoral axis,

e) The model is two-dimensional,

f) The forces are only investigated in the sagittal plane,

g) No contact forces ($\boldsymbol{F}_s$, $\boldsymbol{F}_N$) between the surfaces are considered,

h) The connection between the femur and tibia is described with a hinge with one degree of freedom (no instantaneous center of rotation is considered),

i) The load is derived from the total body weight of the person.

The new model is built to complement the earlier models, thus it holds several new features:

1. Both standard and non-standard squatting movement can be investigated with this model,
2. The body weight vector ($\boldsymbol{BW}$) can move vertically and horizontally,
3. The angle between the axis of tibia and the patellar tendon (β) is considered,
4. The angle between the axis of tibia and the line of action of $\boldsymbol{BW}$ (γ) is considered,
5. The angle between the axis of femur and the line of action of $\boldsymbol{BW}$ ($\delta = \alpha - \gamma$) is considered,
6. The angle between the axis of tibia and the tibiofemoral force vector (φ) is considered,
7. The rotation of the femur and tibia are not synchronized, but independent of each other,
8. The experimentally determined dimensionless moment arms of the quadriceps force (λ_f) patellar tendon force (λ_p) and tibiofemoral force (λ_t) are taken into account.
9. The patellofemoral compression force ($\boldsymbol{F}_{pf}$), the patellar tendon force ($\boldsymbol{F}_{pt}$), the quadriceps force ($\boldsymbol{F}_q$) and the tibiofemoral force ($\boldsymbol{F}_{tf}$) can be derived analytically in a closed form.

The clinical relevance of this analytical-kinetical model lies in the multiple factors that are considered. By the analytical formulas, the effect of each factor on the patello- and tibiofemoral forces can be individually studied.

3.3.3. Free-body diagram of the analytical-kinetical model

Three interconnected bodies build up the analytical-kinetical model: femur, tibia and patella. The model consists of equilibrium equations, which describe the forces, connected to the femur, tibia and patella under squatting (Figure 3.4).

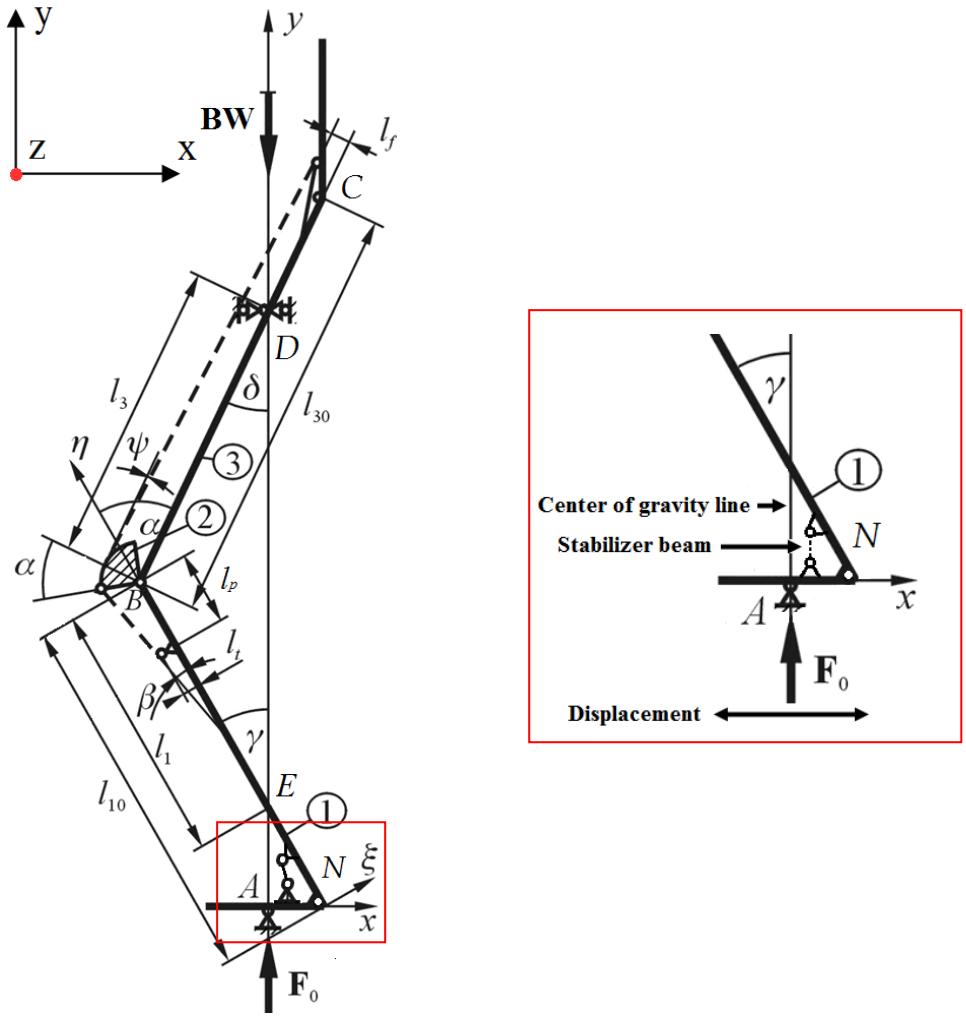

Figure 3.4. Analytical-kinetical model with the geometric parameters

Figure 3.4 shows an arbitrary knee position at angle α where the ***BW*** force is derived from the body weight.

The patella is assumed to rotate about *z*-axis at point *B* and so does the tibia, similar to the model of Smidt [Smidt, 1973], Denham and Bishop [Denham and Bishop, 1978] or Mason et al. [Mason et al., 2008]. The line of action of ***BW*** intersects with the theoretical line of femur and tibia in point *D* and *E*. In order to keep the balance of the system, a stabilizer element has been incorporated into the model (Figure 3.4). The stabilizer beam has the feature that its length can change during the movement, thus moment can be transmitted at the ankle. Mention must be made that the kinetics of the ankle is not considered in this thesis.

Let the *y* component of the coordinate system be fixed to the line of action of ***BW***, while the origin is at the ground in point *A*. The roller in point *A* can move along the feet in the *x* direction as the center of gravity changes its position.

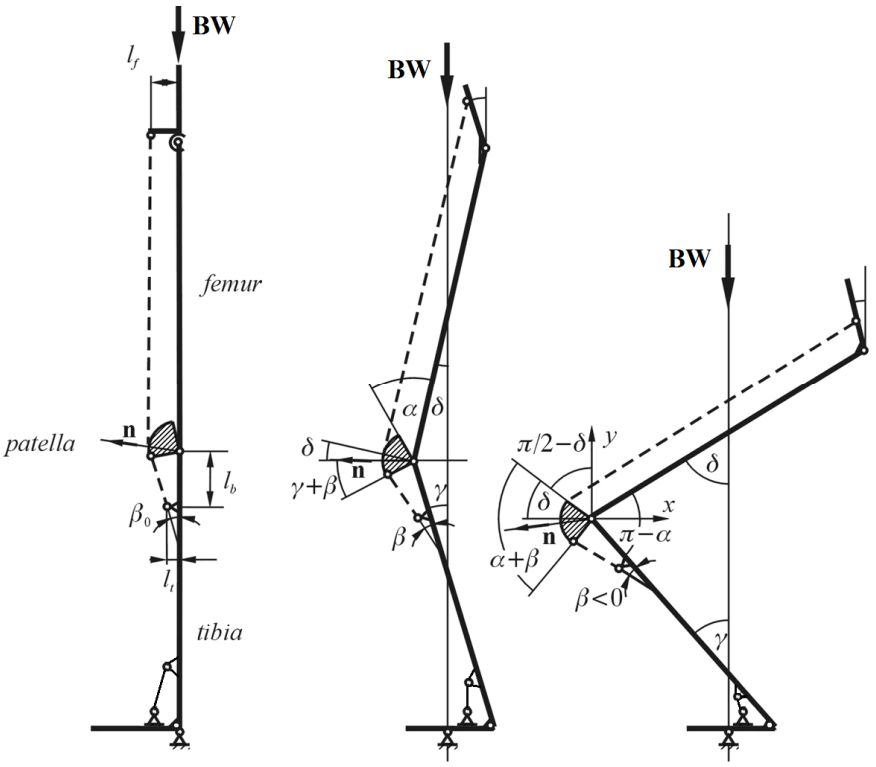

Figure 3.5. Human leg in three different positions

Rigid linkages represent the femur (3), the patella (2), and the tibia with the foot (1). The tibia is connected to the foot by a hinge of one degree of freedom (point *N*, Figure 3.4). The line of action of the center of gravity intersects with the femur at point *D* and with the foot at point *A*. These points are not fixed, since the center of gravity carries out horizontal motion during the squat, thus the intersected points have different positions at each angle (Figure 3.5).

At point *D*, a roller is applied which can move along the axis of femur, while another roller is applied at point *A* which can move along the axis of foot.

At point *A*, the ground reaction force is represented as $\boldsymbol{F_0}$ force, which equals to ***BW***. Strings, representing the quadriceps and patellar tendons, attach the rigid bodies to each other. The elongation of these strings is neglected.

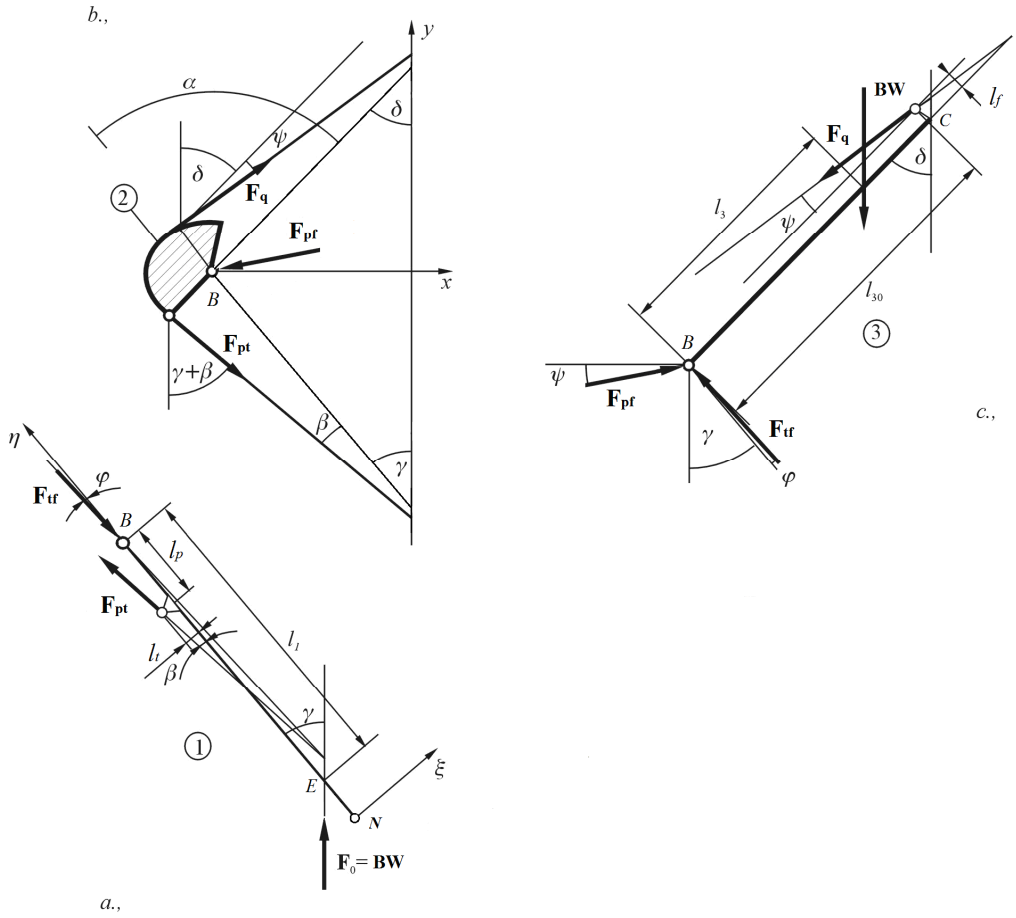

Figure 3.6. Free-body diagram (a, b, c).

The three elements are plotted as free-body diagrams, where the forces, angles, and the different lengths are shown in Figure 3.6 (a-b-c). The specific geometric form of the patella is not considered in the present model. The relationship between the patella and the tendons are taken into account by dimensionless moment arms. The model includes several constants and variables: the denotations of the geometric lengths are listed in Table 3.1 and Table 3.2.

DESCRIPTION	DENOTATION
Length of tibia	l_{10}
Length of femur	l_{30}
Length of patellar tendon	l_p
Moment arm between the axis of tibia and the tibial tuberosity	l_t
Moment arm between the axis of femur and the line of action of the quadriceps force	l_f
Angle between the axis of femur and the quadriceps tendon force	ψ

Table 3.1. Parameters of the analytical-kinetical model

DESCRIPTION	DENOTATION
Intersected length of the axis of tibia and the instantaneous line of action of the ***BW***	l_1
Intersected length of the axis of femur and the instantaneous line of action of ***BW***	l_3
Angle between the axis of tibia and the patellar tendon	β
Angle between the axis of tibia and the line of action of ***BW***	γ
Angle between the axis of femur and the line of action of ***BW***	δ
Angle between the axis of tibia and the tibiofemoral force vector	φ

Table 3.2. Variables of the analytical-kinetical model

3.3.4. Mathematical description of the model

The aim is to derive the $\boldsymbol{F_q}$ quadriceps tendon force, the $\boldsymbol{F_{pf}}$ patellofemoral compression force, the $\boldsymbol{F_{pt}}$ patellar tendon force and the $\boldsymbol{F_{tf}}$ tibiofemoral compression force. The calculation is carried out by the use of static equilibrium equations as a function of flexion angle.

The moment equation applied about z-axis through point B on the tibia (Figure 3.6-a):

$$\sum M_{B1z} = 0 = -l_p \cdot F_{pt} \cdot \sin\beta(\alpha) - l_t \cdot F_{pt} \cdot \cos\beta(\alpha) + l_1(\alpha) \cdot BW \cdot \sin\gamma(\alpha) \tag{3.1}$$

From Eq. (3.1), the patellar tendon force can be derived as:

$$F_{pt}(\alpha) = BW \cdot \frac{l_1(\alpha) \cdot \sin\gamma(\alpha)}{l_p \cdot \sin\beta(\alpha) + l_t \cdot \cos\beta(\alpha)} \tag{3.2}$$

In order to simplify the results, dimensionless variables are introduced (Table 3.3):

DESCRIPTION OF GEOMETRIC PARAMETERS	FORMULA
Dimensionless, intersected tibia length function	$\lambda_1(\alpha) = l_1(\alpha)/l_{10}$
Dimensionless, intersected femur length function	$\lambda_3(\alpha) = l_3(\alpha)/l_{30}$
Dimensionless length of patellar tendon	$\lambda_p = l_p / l_{10}$
Dimensionless thickness of shin	$\lambda_t = l_t / l_{10}$
Dimensionless thickness of thigh	$\lambda_f = l_f / l_{30}$

Table 3.3. Dimensionless functions and constants

The patello- and tibiofemoral forces will be calculated in a normalized form with respect to the force derived from the body weight (***BW***). Ideally, the forces are compared to the bodyweight [Mason et al., 2008] as an internationally accepted method to normalize forces [Innocenti et al., 2011, Komistek et al., 2005].

By the introduction of these quantities, the normalized force in the patellar tendon is:

$$\frac{F_{pt}(\alpha)}{BW} = \frac{\lambda_1(\alpha) \cdot \sin\gamma(\alpha)}{\lambda_p \cdot \sin\beta(\alpha) + \lambda_t \cdot \cos\beta(\alpha)} \tag{3.3}$$

The scalar equilibrium equations related to the ξ - η coordinate system (fixed to the tibia) are the followings (Figure 3.6-a):

$$\sum F_{i\eta} = 0 = -F_{tf} \cdot \cos\varphi(\alpha) + F_{pt} \cdot \cos\beta(\alpha) + BW \cdot \cos\gamma(\alpha) \tag{3.4}$$

$$\sum F_{i\xi} = 0 = F_{tf} \cdot \sin\varphi(\alpha) - F_{pt} \cdot \sin\beta(\alpha) + BW \cdot \sin\gamma(\alpha) \tag{3.5}$$

First, Eq. (3.3) is substituted into Eq. (3.4) and Eq. (3.5), thus $\boldsymbol{F_{pt}}$ disappears from the equations. Second, Eq. (3.4) is set to $\boldsymbol{F_{tf}}$, and then it is substituted into Eq. (3.5).

By performing the substitution, $\boldsymbol{F_{tf}}$ vanishes from the equation as well. The substitution is followed by some additional simplification and finally the angle between the axis of tibia and the tibiofemoral compression force of the upper condyles can be derived as:

$$\varphi(\alpha) = arctg\left[\frac{\left(\lambda_1(\alpha) - \lambda_p\right) \cdot tg\beta(\alpha) - \lambda_t}{\lambda_1(\alpha) \cdot tg\gamma(\alpha) + \lambda_p \cdot tg\beta(\alpha) + \lambda_t} \cdot tg\gamma(\alpha)\right] \tag{3.6}$$

By the use of angle φ the tibiofemoral force can be derived from Eq. (3.4) or Eq. (3.5) as:

$$\frac{F_{tf}(\alpha)}{BW} = \frac{F_{pt}}{BW} \cdot \frac{\cos\beta(\alpha)}{\cos\varphi(\alpha)} + \frac{\cos\gamma(\alpha)}{\cos\varphi(\alpha)} \tag{3.7}$$

The moment equilibrium equation applied about z-axis through point B on the femur (Figure 3.6-c):

$$\sum M_{ib3} = 0 = l_f \cdot F_q \cdot \cos\psi(\alpha) + l_{30} \cdot F_q \cdot \sin\psi(\alpha) - l_3(\alpha) \cdot BW \cdot \sin\delta(\alpha) \tag{3.8}$$

Taking into account that $\delta = \alpha - \gamma$, and assuming that $\psi = 0$, the quadriceps tendon force is:

$$\frac{F_q(\alpha)}{BW} = \frac{\lambda_3(\alpha) \cdot \sin\left(\alpha - \gamma(\alpha)\right)}{\lambda_f} \tag{3.9}$$

The $\psi = 0$ assumption means that the direction of the resultant acting forces in the quadriceps muscle are parallel to the axis of femur.

Since the muscle is connected under the hip bone and stretches out until the frontal surface of the patella (facies patellaris) [Szentágothai, 2006], this approximation is acceptable. Another mention must be made to clarify that this type of approximation – assuming the quadriceps force to be parallel with the femoral axis – is widely accepted and used in current researches.

Luyckx et al. [Luyckx et al., 2009] investigated the effect of the patellar height by dynamic knee simulator with the assumption of neglecting the femoral ψ angle.

Similarly, Didden et al. [Didden et al., 2010] and Victor et al. [Victor et al., 2010] used knee simulators with the same simplification to study the effect of the tibial component positioning on the patellofemoral contact mechanics, and the influence of the muscle load on the tibiofemoral knee kinematics.

All these, and other authors widely use the hypothesis that the line of action of the quadriceps force and the femoral axis can be well approximated if they are considered parallel.

The scalar equilibrium equations related to the patella in the *x* - *y* coordinate system (Figure 3.6-b):

$$\sum F_{ix} = 0 = F_q(\alpha) \cdot \sin \delta(\alpha) + F_{pt}(\alpha) \cdot \sin\big(\gamma(\alpha) + \beta(\alpha)\big) + F_{pf_x} \tag{3.10}$$

$$\sum F_{iy} = 0 = F_q(\alpha) \cdot \cos \delta(\alpha) - F_{pt}(\alpha) \cdot \cos\big(\gamma(\alpha) + \beta(\alpha)\big) + F_{pf_y} \tag{3.11}$$

From Eq. (3.10) and Eq. (3.11) the magnitude of the patellofemoral compression force can be derived by using *x,y* coordinates with respect to the body weight force:

$$\frac{F_{pf}(\alpha)}{BW} = \frac{\sqrt{F_{pf_x}^2 + F_{pf_y}^2}}{BW} = \frac{\sqrt{F_q(\alpha)^2 + F_{pt}(\alpha)^2 - 2 \cdot F_q(\alpha) \cdot F_{pt}(\alpha) \cdot \cos(\beta(\alpha) + \delta(\alpha) + \gamma(\alpha))}}{BW} \tag{3.12}$$

3.3.5. Remarks about the model

Since all the forces are mathematically described by the use of the above-mentioned equations, the patellofemoral forces can be estimated in the knee joint during squatting.

Nevertheless, the derived equations include multiple dimensionless functions and constants such as $\lambda_1(\alpha)$, $\lambda_3(\alpha)$, λ_p, λ_t, λ_f, $\beta(\alpha)$, $\gamma(\alpha)$, which are currently unknown.

Without these parameters, the analytical-kinetical model cannot be solved, thus as another aim of this thesis that these certain parameters and variables have to be determined by means of experiments.

3.4. Experiments on human subjects

3.4.1. Introduction

In subsection 3.2, the new analytical-kinetical model of the non-standard squat has been fully described, but as it was mentioned, seven important factors and variables ($\lambda_1(\alpha)$, $\lambda_3(\alpha)$, λ_p, λ_t, λ_f, $\beta(\alpha)$ and $\gamma(\alpha)$) are missing to solve the equations.

Among the above mentioned functions, only $\beta(\alpha)$ function has been investigated and published earlier by several authors [Van Eijden et al., 1986, Yamaguchi and Zajac, 1989, Gill and O'Connor, 1996, Victor et al., 2010], while the $\lambda_1(\alpha)$, $\lambda_3(\alpha)$ and $\gamma(\alpha)$ functions have not yet appeared in other models or publications. Thus, by all means, they have to be determined experimentally. Regarding the $\beta(\alpha)$ function, the authors were all in agreement.

The dimensionless constants raise another issue. The length of the patellar tendon (l_p) has already been investigated in multiple works [Neyret et al., 2002, Lemon et al., 2007, Gellhorn et al., 2012]. The patellar length is constant in case of healthy knee but shortening appears after knee surgery in several cases starting from cruciate ligament reconstruction [Dandy and Desai, 1994, O'Brien et al., 1991] to knee arthroplasty [Tanaka et al., 2003, Weale et al., 1999]. The mechanism of the patellar tendon shortening is currently unclear and it is considered multifactorial [Noyes et al., 1991, Wojtys et al., 1997, Weale et al., 1999]. For this reason, the elongation of the tendon is not studied in this thesis, but it is considered constant throughout the investigations.

Although the patellar tendon length is known, and varies between 4.6 cm and 6.1 cm [Neyret et al., 2002], no authors have compared this length to the tibial length as a dimensionless patellar tendon length (Table 3.3). It is clearly possible to take a set of data from one author about the patellar length and from another author about the length of the tibia, then creating the dimensionless λ_p constant for the mathematical model, but it is a question how adequate or valid is using and mixing two different sets of data from different human subjects. Therefore, it is more realistic if the same lengths are measured on each subject, and then the dimensionless value of λ_p is created.

The same problem stands for the two additional dimensionless parameters (λ_t, λ_f). The height of the tibial tuberosity (l_t), which is measured from the tibial axis (or from the averaged tibial surface) has not been either compared to the tibial length, therefore this ratio can only be created by using two different data set from different authors. The perpendicular distance between the line of action of the quadriceps force and the femoral axis (l_f) has the same problem.

Due to the absence of these data (the lack of dimensionless form), an experimental study is required, where all these parameters can be measured on human subjects.

In order to place confidence in our measurements, the experimental results will be compared to the averaged results of other authors from different literatures as follows: if author **A** published results about l_p and author **B** published results about l_{10}, then from their results an averaged λ_{pvalid} can be created, which will be compared to the obtained experimental results.

3.4.2. Aims of the experiment

If the magnitude of the patellofemoral forces in the knee joint, or in the ligaments and tendons connected to the knee joint are to be predicted, the load case (how the center of gravity lines changes its position horizontally) must be known as well.

The different type of human motor tasks indicates many types of load transmission throughout the knee joint. The load, derived from the bodyweight (***BW***), always intersects with the center of gravity, and during the locomotion is constantly moving.

The path of the center of gravity is mostly investigated experimentally, in two-dimension [Hasan et al., 1996] or three-dimension [Tesio et al., 2010] as a function of gait cycles. Gait cycles can be measured as a function of walking speed [Gard et al., 2004], while in standing case, the path is given as a function of time [Caron et al., 1997].

There are analytical methods to calculate the line of action of the center of gravity (or shortly the center of gravity line) of the human body by taking all body parts into account [Hanvan, 1964, Dempster, 1955]. In order to use these methods, 41 anthropometric parameters have to be measured. On the one hand, multiple parameters make the calculation challenging, and on the other hand, specifying the accurate position of all body parts during e.g. squatting is also difficult. Obviously, the describing function of center of gravity depends on the motion carried out, thus in case of gait, running, squatting, etc. the function is altered.

For the new analytical-kinetcal model, three dimensionless parameters (λ_p, λ_t, λ_f), two anatomical angles ($\beta(\alpha)$, $\gamma(\alpha)$) and the dimensionless center of gravity functions ($\lambda_1(\alpha)$, $\lambda_3(\alpha)$) must be determined under non-standard squatting.

These constants and functions come from Table 3.1 and Table 3.2, but beside the motivation to comply the analytical-kinetcal model with the necessary functions they are also meant to prove the following hypotheses:

1. The horizontal movement of the center of gravity line changes its position during squatting, in contrary with other assumption [Cohen et al., 2001],
2. The horizontal movement of the center of gravity line can be derived with empirical function during squatting.

3.4.3. Description of the experimental model

In order to validate these hypotheses and gaining the necessary constants and functions for the analytical-kinetical model, an experiment has to be carried out.

As a first step, the experiment has to be planned and measurable parameters must be appointed. Our experimental model creation begins with the following simplifications:

a) The bones are considered as straight lines,

b) The center of gravity line goes through the hip bone, the knee joint and the ankle in case of standing position (stance) [Szentágothai, 2006],

c) The model is quasi-static, the inertial forces are neglected during the movement,

d) Since the analytical-kinetical model is two-dimensional, only the horizontal component (y_c) of the center of gravity line is investigated during the movement (Figure 3.7),

e) Only the bodyweight is considered (***BW***), which points downwards along the z-axis.

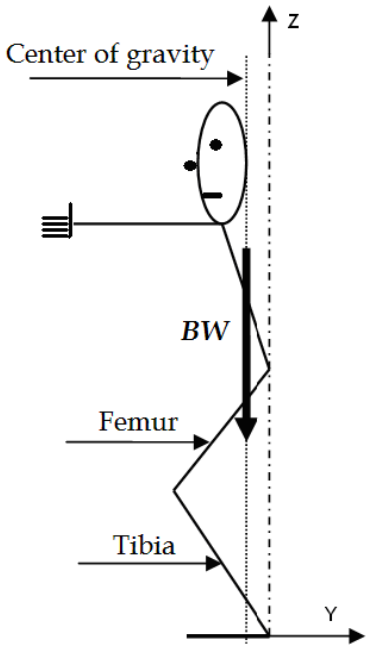

Figure 3.7. Center of gravity line

In stance, the kinetic state of the body is quite simple, but if only the simplest kind of motion is considered, like the squatting with specific boundary conditions (stretched arms, heels kept down), the first problem occurs: the center of gravity changes its position.

If the above-mentioned experimental model is created, where the bones are modelled as simple co-planar links, the forces can be determined by simple equilibrium equations as it described in the analytical-kinetical model in subsection 3.3. In order to solve the equations, the length of the bones have to be considered as known constants, and the solution of the equations will be the patello- and tibiofemoral forces, the force in the quadriceps tendon and the force in the patellar tendon as a function of the flexion.

Nevertheless, the position of the center of gravity is known in the function of cycle, time, etc. during several types of motion [Zok et al., 2004, Abe et al., 2010, Gutierrez-Farewik et al., 2006], but not in some human-bound kinematic quantity such as the angle of flexion. Without the center of gravity line, the load cannot be described with the equilibrium equations in the analytical-kinetical model.

Throughout the experiments, the phenomenon will be explained, and the obtained functions and constants will be presented. In the followings, the measurement setup will be shown with the applied theory, then the measurements, and in the last section, the experimental results are presented.

3.4.4. The measurement setup

Since the investigation of any locomotion is very complex, it is better to divide the complete motion into phases [Ren et al., 2008], which means different positions, to model the whole phenomenon. Let us consider the lower frame of a human, where the limbs are simplified by two-dimensional linkages, and the joints are modelled as hinges with one degree of freedom (Figure 3.7).

During squatting, the center of gravity line changes its position as the function of flexion angle, thus the magnitude of the load on the legs constantly changes. As long as a human person is balanced during squatting, the center of gravity line must intersect with his/her feet [Szentágothai, 2006].

If the position of intersection can be measured at the feet at any arbitrary α angle in a defined coordinate system, then a straight line (representing the center of gravity) can be plotted on the frame through, and the intersections of femur and tibia (Figure 3.8) can be determined.

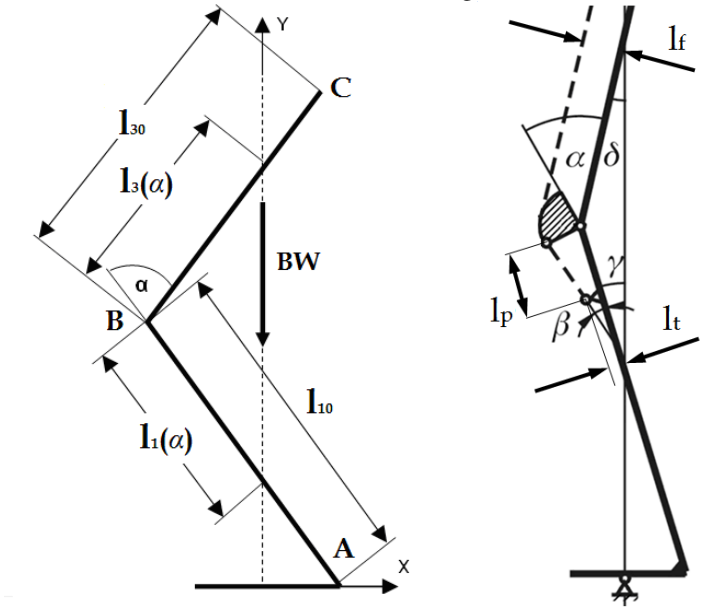

Figure 3.8. Geometrical lengths

Let us denote the intersected parts as follows (Figure 3.8):

MEASUREABLE PARAMETERS AND VARIABLES	DENOTATION
Intersected length of center of gravity line with tibia	$l_1(\alpha)$
Intersected length of center of gravity line with femur	$l_3(\alpha)$
Patellar tendon angle	$\beta(\alpha)$
Angle between tibia and the center of gravity line	$\gamma(\alpha)$
Perpendicular length between the tibial axis and tibial tuberosity	l_t
Perpendicular length between the femoral axis and line action of the quadriceps force	l_f
Length of the patellar tendon	l_p
Length of tibia	l_{10}
Length of femur	l_{30}

Table 3.4. Parameters and variables

These are the parameters and variables needed for the analytical-kinetical model (Table 3.4).

All of the parameters and variables (except β angle) are given in a dimensionless form in the description of the analytical-kinetical model in section 3.2, thus further on in the experiments, these values would be put in a dimensionless form as well.

The aim of the experiment is to create these functions and constants experimentally based on different "from standing to squatting" positions, involving multiple human subjects.

To carry out the measurements of the center of gravity, force platforms were manufactured out of two wooden plates. The dimensions of the platform are 258 mm x 400 mm with 13 mm of thickness. One of the platforms has three bores for the dynamometers, and a coordinate system is engraved in it as well (Figure 3.9).

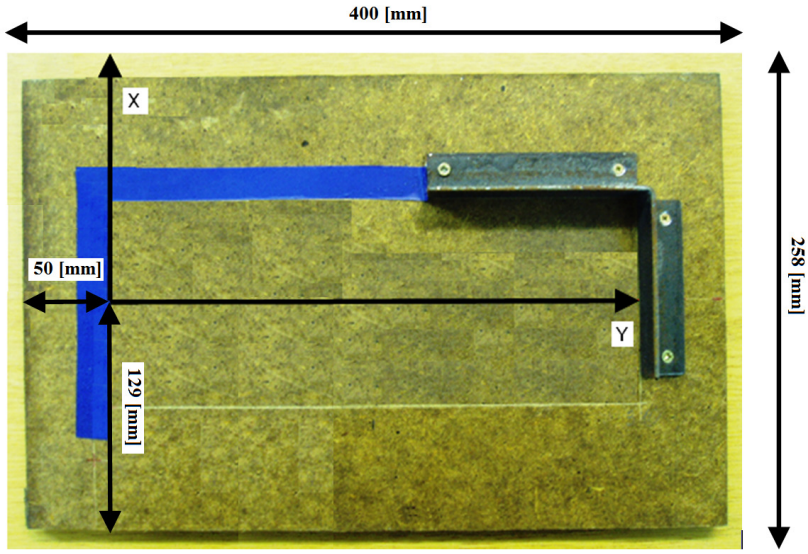

Figure 3.9. Force platform

The zero point of the coordinate system is located at x_0 = 129 mm, y_0 = 50 mm. This point is measured from the left low corner of the force platform (Figure 3.9). The human subjects had to stand on these platforms during the measurements by adjusting their heels to the metal frame (Figure 3.9). This metal frame assured that all the participants stood on the same position on the frame.

For the experiments, MOM type "A" class ETP 7922 dynamometers [Kaliber] were used from the Kaliber Ltd, which have the following parameters:

- Range of load: 0-1000 N,
- Cell coefficient: 1 mV/V ± 0.1,
- 0.05 % accuracy on total range.

The dynamometer is shown in Figure 3.10.

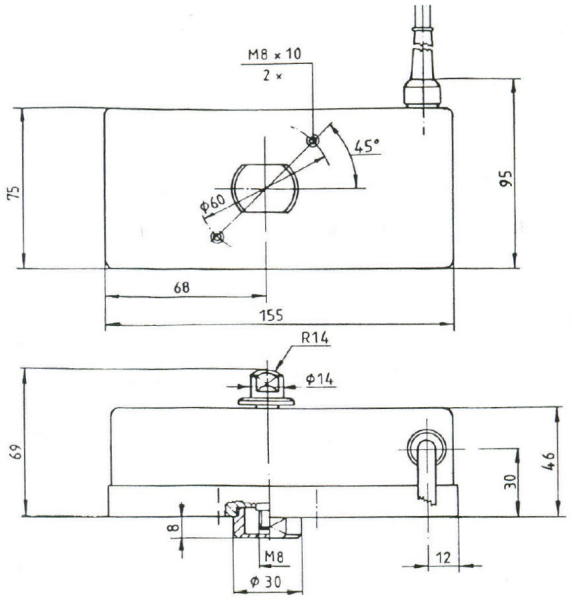

Figure 3.10. MOM type dynamometer

For data process, a Spider 8 multi-channel PC measurement electronics [HBM] was used from the HBM GmbH, which is capable for parallel dynamic data acquisition with the following parameters:

- 0.1% accuracy on total range,
- Maximum number of channels: 8/device,
- Digital measurement rate: 9600/s/channel.

The Spider is controlled by the Catman Express 3.0 program, and developed by the HBM.

3.4.5. Measurement of the center of gravity line

The experiments were carried out on 16 persons (9 males and 7 females) between 21 and 27 years old (Figure 3.11). The mean (± standard deviation) weight of all participants was 72.2 ± 17.4 kg respectively. The measurements were carried out in two parts. 9 people at the first experiment and couple of weeks later the other 7.

Figure 3.11. Subjects of the experiment

The dynamometers had been calibrated with standard weights and their equilibrium ($\Sigma \mathbf{F}_i = \mathbf{F_1} + \mathbf{F_2} + \mathbf{F_3} = \mathbf{BW}$) had been checked before the measurements were carried out (the load, derived from the body weight is represented by ***BW***). During the measurements the dynamometers were set under the force plate, and while a human subject was standing on it, the forces (***F*** $_1$, ***F*** $_2$, ***F*** $_3$ are the forces induced in the dynamometers) were continuously measured in the three points (Figure 3.12).

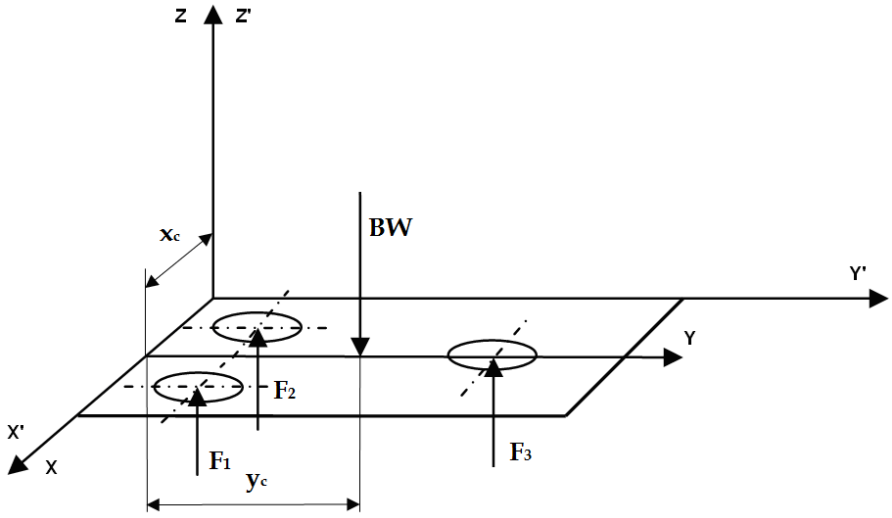

Figure 3.12. Arrangement of the dynamometers

The position of the measured resultant force is very precisely called as the center of pressure (*COP*). The center of pressure and the center of gravity is not in the same position under the movement due to the dynamic forces acting on the body. In order to determine the position of the center of gravity (*COG*) along an arbitrary direction (*y*), the following equation has to be concerned [Hamilton and Luttgens, 2002]:

$$F_{GR} \cdot y_{COP} - BW \cdot y_c = l \cdot \vartheta'' \tag{3.13}$$

Where $\boldsymbol{F_{GR}}$ is the measured resultant ground reaction force, ***BW*** is the body weight force, y_{COP} and y_c are the moment arms, ϑ'' is the angular acceleration and l is a constant. It is assumed that the body is in still position, then the right side of the equation equals to zero, since $\vartheta'' = 0$. By setting the equation, the following is obtained:

$$F_{GR} \cdot y_{COP} = BW \cdot y_c \tag{3.14}$$

Since the measured resultant ground reaction force and the body weight is the same ($\boldsymbol{F_{GR}} = \boldsymbol{BW}$) the equation is simplified to:

$$y_{COP} = y_c \tag{3.15}$$

In the case of our experiment, the subjects remained still during the measurement, thus the position of the center of gravity and the center of pressure, under these specific boundary conditions of this measurement, is the same. The position of the center of gravity was derived according to the law of spatial force system [Csizmadia and Nándori, 2009]. If this theory is applied on the three dynamometers, the obtained formulas are:

$$x_c = \frac{\sum F_i \cdot x_i}{F_i} = \frac{F_1 \cdot x_1 + F_2 \cdot x_2 + F_3 \cdot x_3}{BW} \tag{3.16}$$

$$y_c = \frac{\sum F_i \cdot y_i}{F_i} = \frac{F_1 \cdot y_1 + F_2 \cdot y_2 + F_3 \cdot y_3}{BW} \tag{3.17}$$

Where x_c and y_c are the coordinates of the center of gravity line defined in the coordinate system of the force plate. From these formulas, both x_c and y_c position of the center of gravity line can be located, although only the y_c component will be investigated. Measuring the z_c direction is not possible with this instrument.

The simple linkage model, which was introduced in the subsection 3.3.4, must be applied on the subjects as well. In order to carry out the experiment, cross markers were attached to known anatomical points namely: the ankle (lateral malleolus), the knee (lateral epicondyle), and the femur proximalis (trochanter major) (Figure 3.13).

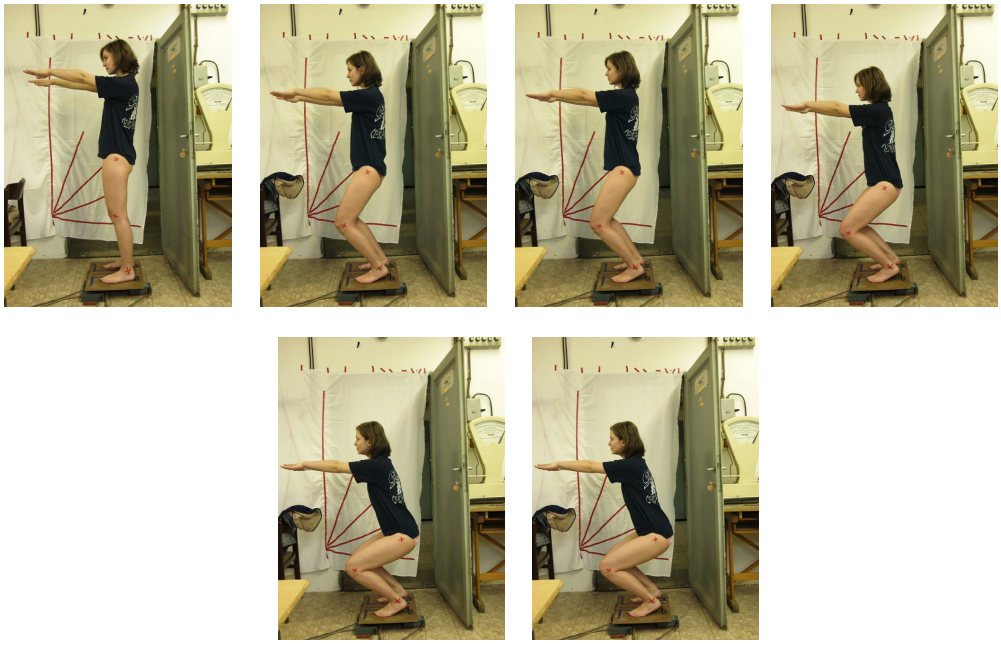

Figure 3.13. Squat positions

It is fairly easy and accurate to find these well palpable anatomical points. If a straight line intersects the crosses, the lines will appoint the theoretical axes of femur and tibia, and the same model is obtained as it is in Figure 3.7.

When the markers are fixed, the subject steps up on the plates and his/her center of gravity will be measured in six positions (Figure 3.13).

During the squatting motion, the subject has to keep three conditions:

1) stretched arms,
2) heels adjusted to the metal frame at initial standing position,
3) keeping the different positions for 3 seconds.

This type of squatting is not a standardized movement. During squatting, the heel naturally ascends which is allowable for the experiment. The metal frame has the purpose to provide the same initial position for each subject, not to restrain the heel from its natural movement.

The squatting plane (see in the background in Figure 3.13) is not meant to calibrate angles, only to distinguish the six squatting positions during the measurement. Measuring the parameters strictly at the very same angles in case of all subjects is irrelevant regarding the aims.

The x_c and y_c coordinates of the center of gravity were measured in six positions, and in each position a photo was taken as well. The measured data were processed in Excel. As an example, the following kind of graphs was obtained as it can be seen in Figure 3.14.

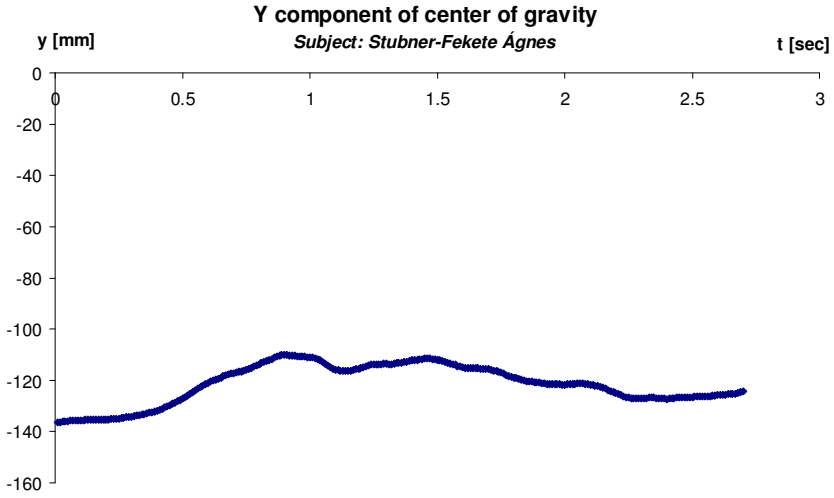

Figure 3.14. Measured *y* component of the center of gravity

The graph shows the change of the y_c component of the center of gravity line in one position as a function of time. As it is seen, some fluctuation appears during the measurement due to the effect of the balancing nerve system. The average value of y_c coordinate was determined in each position:

$$\overline{y}_{cj} = \frac{\sum_{i=1}^{n} y_{ci}}{n} \tag{3.18}$$

Where, j denotes the numbers of the positions (1-6), i denotes the particular sample while n denotes the sample size during the predetermined time period (3 second). The variance (denoted by s^2) was also calculated in each position:

$$s_{ycj}^2 = \frac{\sum_{i=1}^{n} \left(y_{ci} - \overline{y_c}\right)^2}{n-1} \tag{3.19}$$

The data distribution was checked and proven to be normally distributed (Figure 3.15).

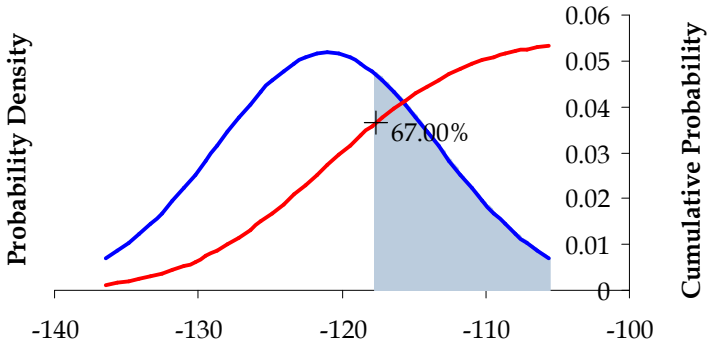

Figure 3.15. Distribution check of Stubner-Fekete's data

The standard error can be deduced from the standard deviation and the *t*-value:

$$\Delta y_c = t \cdot s_{yc} \tag{3.20}$$

The *t* value can be found by the use of *t*-test tables [Stephens, 2004]:

- in case of 95% confidence,
- the degree of freedom of the experiment is beyond 120,

then $t = 1.96$ [Stephens, 2004].

According to these calculations the y_c coordinate of the center of gravity line is determined alongside with its standard error.

3.4.6. Construction of the dimensionless quantities and angles

After measuring the y_c coordinate of the center of gravity line of all persons, the theoretical lines of the bone axes and the intersection of the center of gravity had to be constructed. The constructions were carried out in the AUTOCAD by importing the photos into the program. Since all of the dimensions of the platforms were known, the measured *y* component of the center of gravity could be drawn in each position by the software (Figure 3.16).

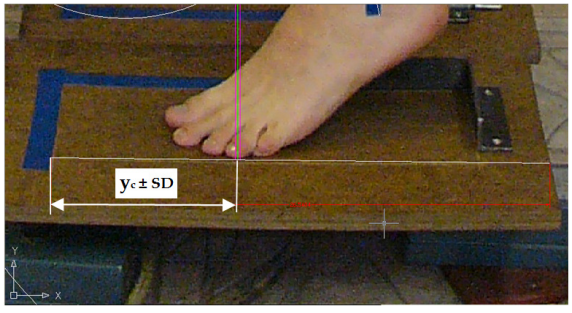

Figure 3.16. y_c coordinate with it standard deviation

Only a conversion coefficient (ζ) had to be calculated between the photo scale and the real scale, and the line of action of the center of gravity could be plotted (Figure 3.17).

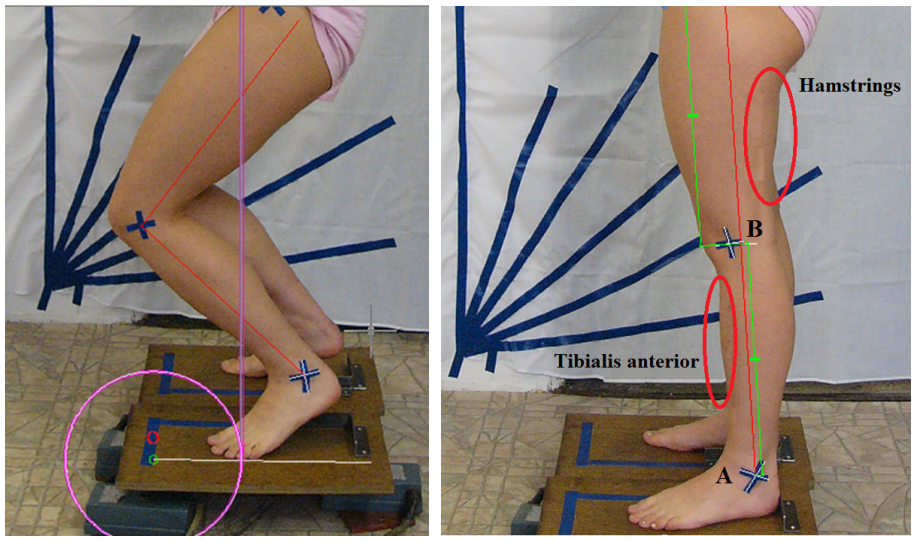

Figure 3.17. Plotted y_c on the model

Problem occurred, when we simply tried to connect the markers with a line in other positions then standing, since the markers on the knee and the femur proximalis were shifted. Due to this shift during the motion, the markers (at point *B* and *C*) did not show the proper position of the bone endings.

Only the marker on the ankle (point *A*) did not alter its position during squatting. In order to evade this problem, a new construction procedure was developed to find the correct positions of the markers in other squatting status. This method is presented now in details.

Additional auxiliary points have to be specified in order to construct the shifted point *B* and *C*. Let us denote these shifted points now on as *B'* and *C'*. At the initial standing position (Figure 3.18), the length of *AB* and *BC* section can be easily allocated. Two more auxiliary points are needed, which have the attribute of not changing their position during the movement (like point *A*), thus they can be used to construct the shifted point *B'* and *C'*. To carry out this construction segments have to be found on the leg, where the tissue does not move significantly under squatting motion.

During squatting, the muscular activity is low in the hamstrings and tibialis anterior muscles [Bishop and Denham, 1978]. This fact can be used as follows: in the appointed areas, due to the lack of muscle activity, the deformation of the tissue surroundings is fairly low. Therefore, these areas can be modelled during the construction as rigid bodies (Figure 3.17). By considering these segments as rigid bodies, two auxiliary points (*P* and *Q*) can be appointed and measured by radius $R_{1\text{-}2\text{-}3\text{-}4}$. With the help of these two extra points (*P* and *Q*), the shifted points (*B'* and *C'*) can be determined in any position.

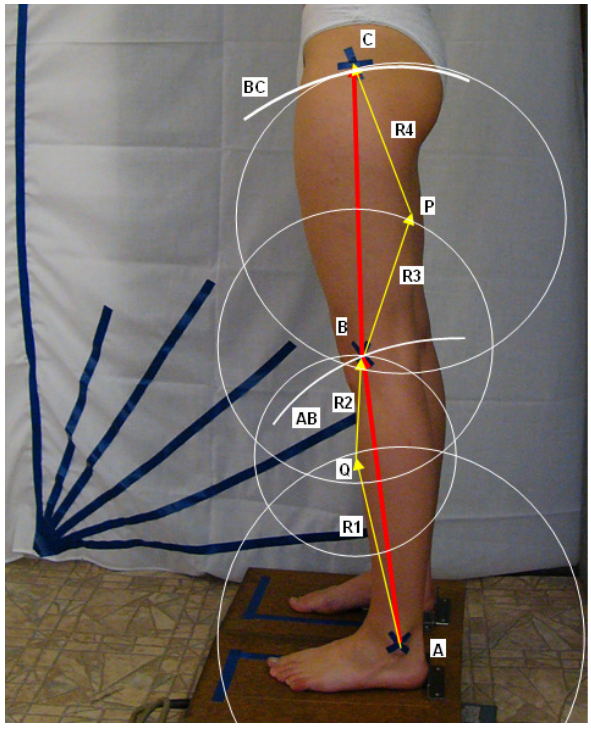

Figure 3.18. 1st construction position

To carry out the construction, six constants (*AB* and *BC* length, $R_{1\text{-}2\text{-}3\text{-}4}$ radiuses) have to be determined by the following steps (Figure 3.18 and Figure 3.19):

- Let us denote the point of ankle as *A*, the femur distalis as *B*, and the femur proximalis as *C*.
- *AB* and *BC* length must be measured (from point *A* and *B*) and stored in AUTOCAD.
- Let us draw a circle from point *A*, denoted by R_1, which crosses the anterior part of the shin in an arbitrary point. Let the R_1 radius be stored, and the arbitrary point denoted as *Q*.
- From the intersection of R_1 and the shin (point *Q*), let us draw another circle, denoted by R_2, which intersects point *B*. This radius must be stored as well.
- Let us draw again a circle from point *B*, denoted by R_3, which crosses the posterior part of the thigh in an arbitrary point. Let the R_3 radius be stored, and the arbitrary point denoted as *P*.
- From the intersection of R_3 and the thigh (point *P*), let us draw another circle, denoted by R_4, which intersects point *C*. This radius must be stored as well.

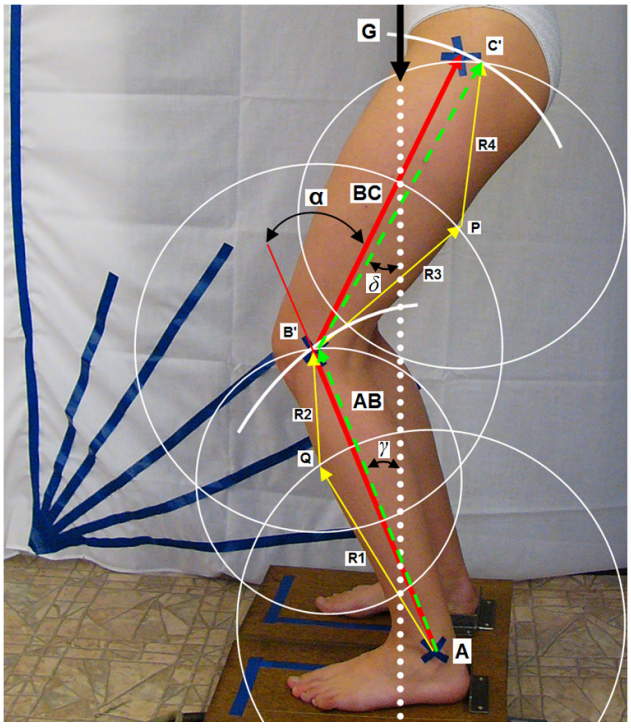

Figure 3.19. 2nd construction position

A mention must be made that all measured constants (*AB* and *BC* length, $R_{1\text{-}2\text{-}3\text{-}4}$ radiuses) are used in the following steps as well. Then in each position, the shifted *B* and *C* points (*B'* and C') can be allocated by using the following steps (Figure 3.19):

- From the point *A,* a circle is drawn with equal radius as the original *AB* length.
- From point *A,* another circle is drawn with R_1 radius, which intersects the anterior part of the shin. This is point *Q*.
- From this intersection, point *Q*, another circle has to be drawn with radius R_2, which intersects with the *AB* circle. That intersection will be the shifted point *B*, denoted by *B'*.
- Since point *B'* is available, a circle with R_3 radius has to be drawn which intersects with the posterior part of the thigh. This is point *P*.
- From point *P*, a circle with radius R_4, while from point *B'*, another circle with *BC* radius has to be drawn. Their intersection is the shifted position of point *C,* denoted now as *C'*.

Now, all requested points are available, thus the *AB* and *BC* lines can be connected and they represent the theoretical axes of the femur and the tibia.

A particular mention must be made of the fact that these *A-B-C* points are well palpable anatomical points where experiment shows that the deviation (error) between two persons' points is higher than the deviation (error) caused by the palpation.

After all constructions were carried out, the measured and averaged center of gravity lines are plotted as dashed vertical line on the theoretical femur and tibia axes.

By doing so, the l_{30}, l_3, l_{10}, l_1 lengths become measurable in each status, and the specific $\lambda_1(\alpha)$, $\lambda_3(\alpha)$ functions can be determined as a function of flexion angle.

Naturally, these constructions and the measured averaged center of gravity lines are applied individually on each subject, using their individually measured data. Not only one data set was applied on all participants, but also each participants own measured data.

The flexion angle alongside with $\delta(\alpha)$ and $\gamma(\alpha)$ were also measured in every position as it is seen in Figure 3.19.

After the construction of the specific lengths, the $\beta(\alpha)$ angle and the parameters had to be measured as well. The construction of $\beta(\alpha)$ angle was carried out as follows: a tangent was laid on the patellar tendon, thus the angle between the ligament and the tibial axis could be immediately measured in any position (Figure 3.20 and Figure 3.21).

The l_p length is known to be constant from the earlier studies [Neyret et al., 2002, Lemon et al., 2007, Gellhorn et al., 2012] and so is the l_t, the height of the tibial tuberosity.

The l_p and l_t lengths were measured in stance position.

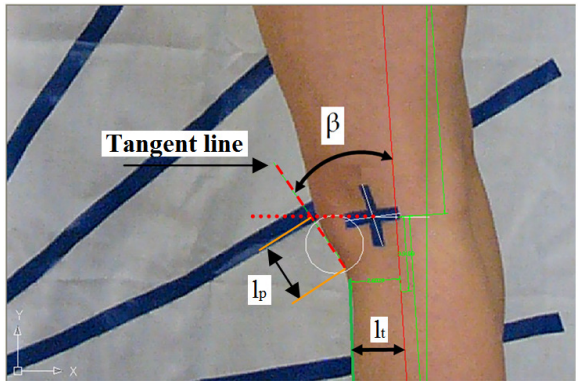

Figure 3.20. Determining $\beta(\alpha)$ angle and l_t in stance position

This construction and measurement has been carried out in each position and on every person individually.

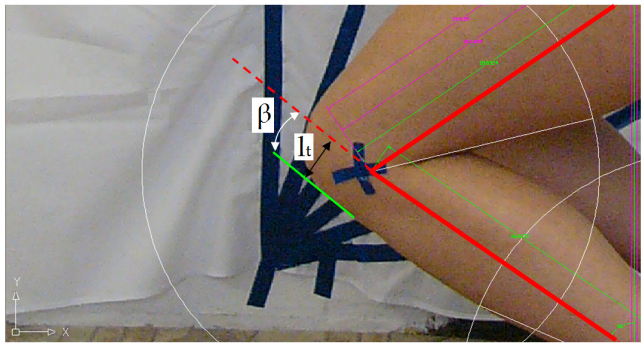

Figure 3.21. Measuring the $\beta(\alpha)$ angle and l_t in squat position

At the end of the construction, the l_f constant has also been measured (Figure 3.22).

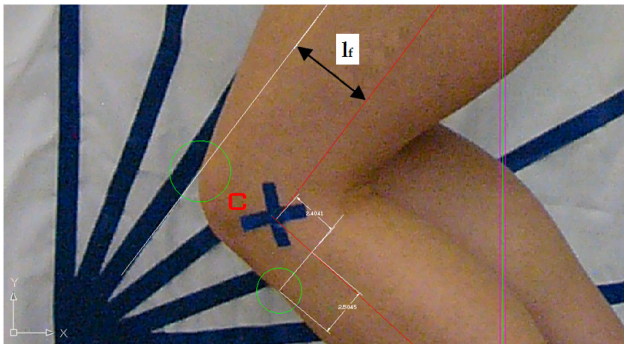

Figure 3.22. Measuring l_f in squat position

3.4.7. Data processing

3.4.7.1. Fundamentals

The analysis of variance is a method to investigate whether the variance of an observed phenomenon during an experiment varies significantly – caused by unknown factors – or remains approximately the same, therefore only the same factors are taken into account in each experimental set. The method includes two steps:

1. Homogeneity analysis: Are the variances weighted with the same factors? If yes, then an averaged variance can be calculated. If no, the phenomenon cannot be approximated by only one function.
2. Curve fitting.

In the following steps, a homogeneity method will be presented on the data of a human subject in order to identify the mathematical model that best fits the data set. Further on, the *F*-test [Stephens, 2004] or so-called *Fisher-test* will be applied on the data of each human subject. The test is very sensitive to non-normality [Box, 1953, Markowski and Markowski, 1990] but in that case, the *Bartlett's test* [Csizmadia, 1998] can also be used.

Let the y_c component of the center of gravity line be examined by the *F*-test, whether the homogeneity of variances is applicable and valid. For the test, the maximal and minimal value of the variances must be calculated:

$$F_{Exp.} = \frac{s^2_{\max}}{s^2_{\min}} \tag{3.21}$$

And if

$$F_{Exp.} \leq F_{Table} \tag{3.22}$$

then the homogeneity of variances is valid. This means, that e.g. an averaged variance (and hereby the averaged standard deviation) can be determined for each y_c component.

3.4.7.2. Steps of the approach

Let us take, as an example, one person's data – Anonym I. – and present the test (Table 3.5). The variance of y_c (s_{yc}^2) was calculated from the measured data of each squatting status. Since the momentary result is important in this experiment, only the first 15-25 samples were taken.

Due to the occasional swing of the human body (which maintains balance), the measured data included higher amplitudes. These amplitudes can be considered as disturbances in the measured data, therefore they were neglected as follows: during the sampling, the measured data was mostly similar to Figure 3.14, but in certain cases, higher jumps appeared in the measured set. These jumps were detected by statistical methods as gross errors, due to extreme balancing movements, and therefore removed from the data set.

The variance number related to the λ_1 and λ_3 values are relatively low, and for this reason, all the digits were necessary to use.

Status / s^2 / F	s_{yc}^2 [mm^2]	$s_{\lambda 1}^2$ [mm^2]	$s_{\lambda 3}^2$ [mm^2]	DoF [-]
2nd	0.764	0.004147	0.003106	15
3rd	0.8354	0.003298	0.002505	23
4th	0.9187	0.002309	0.002543	12
5th	0.8407	0.002253	0.001807	14
6th	0.7559	0.001756	0.001421	14
s^2_{max}	0.9187	0.04147	0.003106	-
s^2_{min}	0.7559	0.001756	0.001421	-
F_{exp}	1.21	2.36	2.18	-
F_{table}	2.53	2.46	2.46	-

Table 3.5. Table of calculation for homogeneity analysis of Anonym I.

In the 1st position, when the subject is standing, no deviation can be defined. As it is seen, the result of Table 3.5 satisfies the condition of Eq. (3.22), so the homogeneity is valid. Now, the averaged variance of Anonym I. can be calculated:

$$s_{yc}^2 = \frac{\sum_{j=1}^{n} s_{ycj}^2}{n} = 0.8298 \tag{3.23}$$

Since the determined variance of the center of gravity (s^2_{yc}) is convincingly homogeneous, the same way the variance ($s^2_{\lambda 1\text{-}3}$) of the derived geometrical values (λ_1, λ_3) were also checked and proven to be homogeneous (see data of Anonym I. s^2_{yc} and $s^2_{\lambda 1\text{-}3}$ data of in Table 3.5).

The following step is to find an approximate function, which properly fits on the data set. It is always beneficial to use the simplest approximate function, which is the linear function. In order to check the validity of the linear function let us introduce a so-called fitting variance [Csizmadia, 1998].

In Eq. (3.24) n - 2 stands for the linear approximation. In case of quadratic approximation, the subtracted value is 3.

$$s^2_{fit.\lambda i} = \frac{\sum_{i=1}^{n} \left[\overline{\lambda}_i - (b - a \cdot \alpha_i)\right]^2}{n-2} \tag{3.24}$$

The result can be derived by substituting λ_i values in each experimental status, and the value, given by the approximate function in that specific angle, will be subtracted from it.

After calculating the fitting variances in all status, the maximum fitting variance has to be divided with the variance of the derived geometrical values:

$$F_{Exp.} = \frac{s^2_{fit.\max.\lambda 1}}{s^2_{\lambda 1}} = \frac{3.988 \cdot 10^{-3}}{1.756 \cdot 10^{-3}} = 2.27 \tag{3.25}$$

$$F_{Exp.} = \frac{s^2_{fit.\max.\lambda 3}}{s^2_{\lambda 3}} = \frac{8.76 \cdot 10^{-4}}{1.421 \cdot 10^{-3}} = 0.59 \tag{3.26}$$

while the table value is, $F_{table} = 3.11$,

$$F_{Exp.\lambda 1-3} \leq F_{Table} \tag{3.27}$$

Thus, the linear approximation is acceptable. The quadratic approximation was also tried, but the difference of the fitting was only 0.5% better, which does not justify its use.

After fitting a linear curve to both $\lambda_{1\text{-}3}$ values, the following functions were determined:

$$\lambda_1(\alpha) = 0.0024 \cdot \alpha + 0.4925 \pm t \cdot s_{\lambda 1} \tag{3.28}$$

$$\lambda_3(\alpha) = -0.0022 \cdot \alpha + 0.86 \pm t \cdot s_{\lambda 3} \tag{3.29}$$

Where $t = 1.96$ [Stephens, 2004] in case of 95%.

The calculation was carried out on all human subjects' data. The s_{yc} deviation values varied between 0.5-4 mm among the persons. The $s_{\lambda 1}$-$s_{\lambda 3}$ deviations varied between 0.0035-0.032 in the whole set and they were plotted in Figure 3.23 and Figure 3.24.

These values mean maximum 4.9% of error, considering the average value of λ_1 or λ_3 functions. The measurement error itself, due to the accurate instrument, is insignificantly low. The major part of the deviation is due to the human synthesis, namely the constant sway (swing) of the human body during the measurement of the six positions. However, these results show proper accuracy and reliability, since the measurements were carried out in different time and the instrument was recalibrated.

Besides the $\lambda_1(\alpha)$ or $\lambda_3(\alpha)$ functions, the $\beta(\alpha)$ and $\phi(\alpha)$ (for practical reason γ function is also put into a dimensionless form) approximate functions have been determined with their standard deviation:

$$\beta(\alpha) = -0.3861 \cdot \alpha + 26.56 \pm t \cdot s_{\beta} \tag{3.30}$$

$$\phi(\alpha) = \frac{\gamma}{\alpha} = -0.0026 \cdot \alpha + 0.567 \pm t \cdot s_{\phi} \tag{3.31}$$

Both the one- and two-tailed probability (p-value) of the functions were examined according to the sample size and the Pearson correlation coefficient. Eventually they were found significantly less then 0.05.

All the functions and standard deviation have been summarized in Table 3.6.

FUNCTION OR CONSTANT	C1	C2	SD	r^2
$\lambda_1(\alpha)$ [-]	0.492	0.0024	0.15	0.65
$\lambda_3(\alpha)$ [-]	0.86	-0.0022	0.22	0.63
$\beta(\alpha)$ [°]	26.56	-0.3861	14	0.95
$\phi(\alpha)$ [-]	0.567	-0.0026	0.081	0.735
λ_t [-]	0.11	0	0.018	-
λ_p [-]	0.1475	0	0.043	-
λ_f [-]	0.164	0	0.028	-

Table 3.6. Functions* and constants of the analytical-kinetical model

* The following equation is used: $f(\alpha) = C1 + C2 \cdot \alpha$

Where r^2 is the linear correlation coefficient between the original and modelled data values regarding the $\lambda_1(\alpha)$, $\lambda_3(\alpha)$, $\beta(\alpha)$ and $\phi(\alpha)$ functions and *SD* denotes the standard deviation. The standard deviation and the correlation coefficient are considered normal compared to other biomechanical measurements [Abe et al., 2010, Eames et al., 1999, Fukagawa et al., 2012].

3.4.8. Experimental results

The $\lambda_1(\alpha)$ or $\lambda_3(\alpha)$ functions give a view about the horizontal movement of the center of gravity line under squatting motion. By substituting any α into the λ functions, the intersection of the center of gravity line with the femur and tibia is obtained (Figure 3.23 and Figure 3.24).

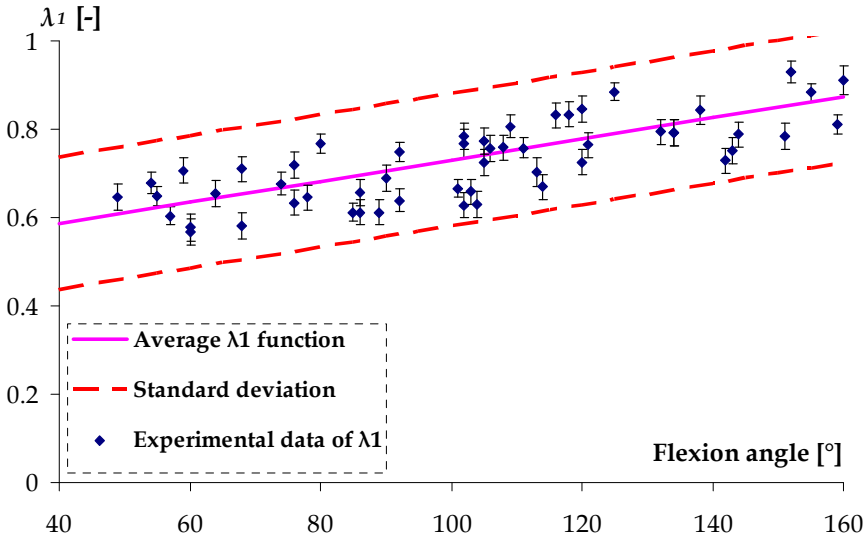

Figure 3.23. Dimensionless λ_1 functions

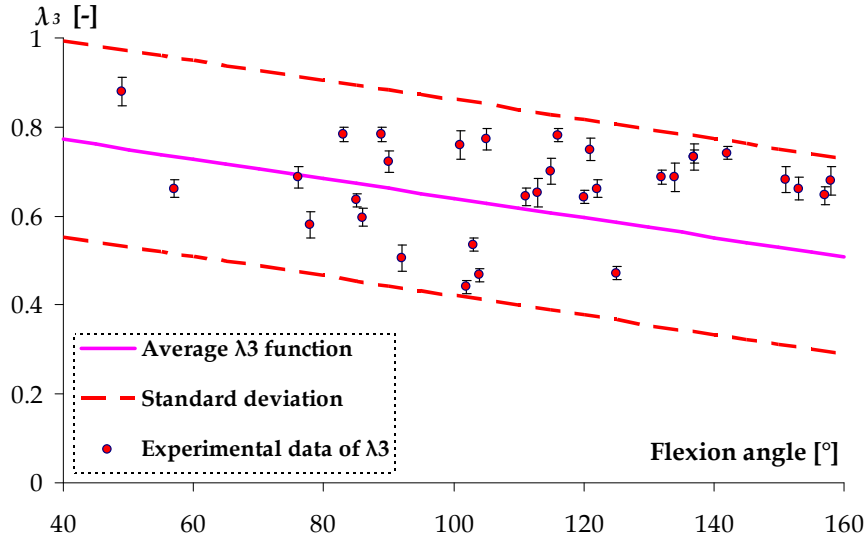

Figure 3.24. Dimensionless λ_3 functions

The $\phi(\alpha)$ and $\beta(\alpha)$ functions are also plotted with their standard deviation (Figure 3.25 and Figure 3.26).

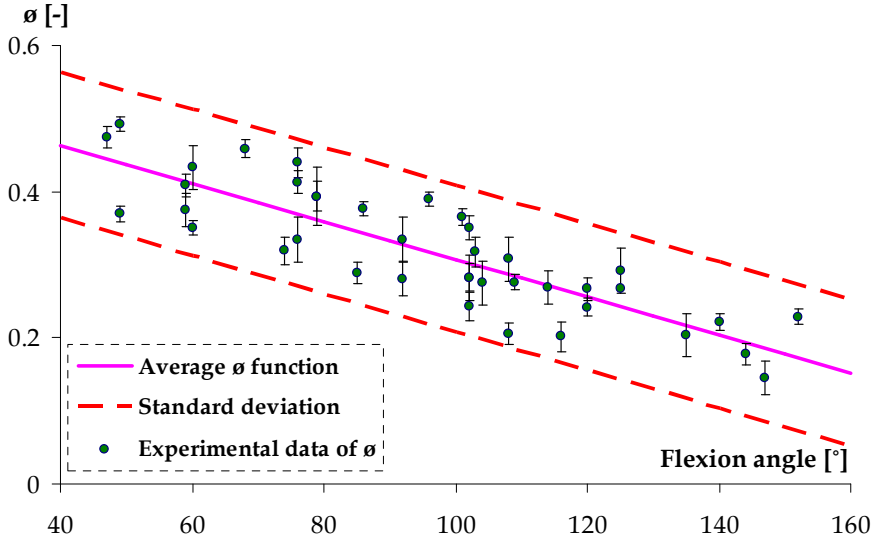

Figure 3.25. Dimensionless ϕ function

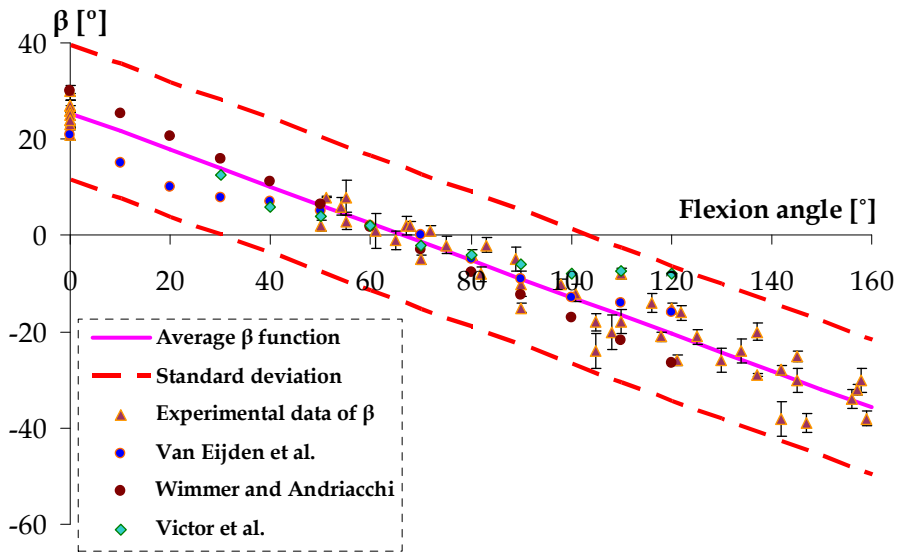

Figure 3.26. Dimensionless *β* function

The results were compared to the results of other authors in case of the *β(α)* function. As it is seen, the correlation between the own measured results, the results of other authors [Van Eijden et al., 1986, Wimmer and Andriacchi, 1997, Victor et al., 2010] is remarkably good.

The higher deviation of the $\lambda_1(\alpha)$, $\lambda_3(\alpha)$ and $\phi(\alpha)$ functions can be originated to three factors:

1. The variety of the subjects (regardless of males or females)
2. Small, but inevitable differences in the carried out motion,
3. The constant fluctuation of the center of pressure, which is directly connected to the center of gravity under standing, walking or squatting movement.

Let us explain these factors in details.

The aim of the experiment was to derive universal descriptive functions with regard to the horizontal movement of the center of gravity. The obtained results were inspected if noticeable difference could be observed on the male or female results, but seemingly, they were randomly located in the data field with similar trend.

Naturally, in contempt of the prescribed three conditions, small differences always appear in biomechanical measurements, since humans implicitly are not able to carry out a motion exactly the same way as a machine. This incident obviously increases the standard deviation in the biomechanical measurements.

To maintain balance, the human body has to move constantly towards a balance point, which appears physically as a body sway. This neural control [Masani et al., 2006, Loram et al., 2005] can be perceived as constant fluctuation in the center of pressure. Due to this constant interference of the neural balance control, more deviation is experienced in the measured data.

Beside these factors, one more remark has to be added.

A visible gap appears in the functions between 0˚ and 50˚ of flexion angle, which can be explained as follows: the subjects were asked to bend their knees slightly, however, a bent knee at 20˚ of flexion angled can be perceived as someone being in normal stance position.

Since the aim was to carry out squatting measurement, the subjects were ordered to take on a well-visible bent position, which involuntarily always exceeded 50˚ of flexion angle.

Regarding the constants (λ_p, λ_t, λ_f) of the analytical-kinetical model, the λ_p factor (the dimensionless length of the patellar tendon) has been also created from the results of other authors to validate our measurement method and its accuracy. The λ_p dimensionless parameter, which has been determined by our experiment:

$$\lambda_p = 0.1475 \pm 0.043 \tag{3.32}$$

While the average patellar and tibial length from the data of Neyret et al. [Neyret et al., 2002] and Özaslan et al. [Özaslan et al., 2003] (data are in mm):

$$l_{p-Neyret} = 53 \pm 7 \text{ and } l_{10-Özaslan} = 383.7 \pm 23.98 \tag{3.33}$$

From these data $\lambda_{p\text{-}Neyret\text{-}Özaslan}$ can be created:

$$\lambda_{p-Neyret-Özaslan} = 0.1381 \tag{3.34}$$

The difference between the averaged constants is 6.3%, which confirms the validity of the determined constants.

In order to gain a view about the movement of the center of gravity, let us draw the lower human frame in two positions (Figure 3.27 (a-b)).

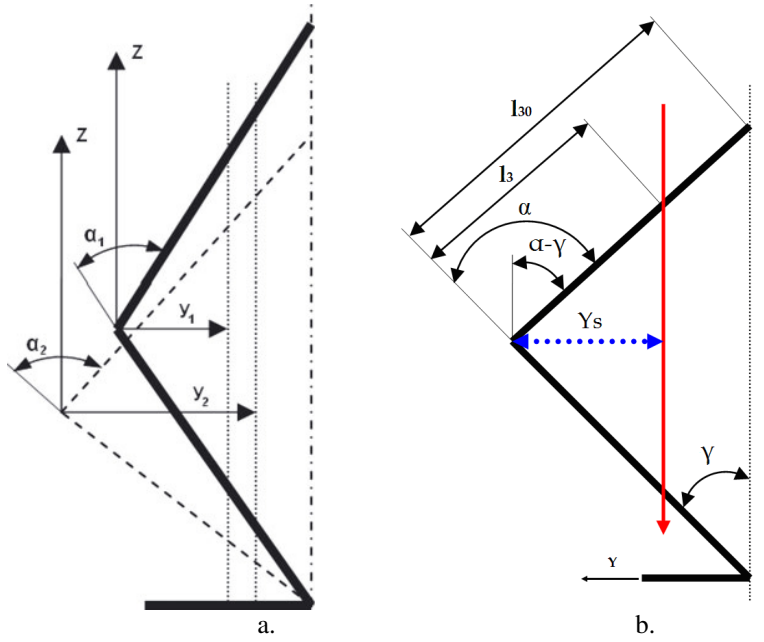

Figure 3.27 (a-b). Dimensions of the knee joint and the moment arm

The coordinate system is attached to the knee joint, and it moves constantly during squatting.

If the center of gravity line is given at angle α_1, then the horizontal distance between the knee joint and the center of gravity can be denoted by y_1. Accordingly, at a different angle α_2 the horizontal distance will be y_2. If all y distances of the center of gravity are plotted as a function of α, then the horizontal movement becomes clear and visual.

Let us denote the describing function as $Y_s(\alpha)$. The calculation of $Y_s(\alpha)$ function can be carried out as follows: first the $l_3(\alpha)$ functions has to be determined. Since,

$$\lambda_3(\alpha) = l_3(\alpha) / l_{30} \tag{3.35}$$

Then by setting Eq. (3.35) we obtain,

$$l_3(\alpha) = l_{30} \cdot \lambda_3(\alpha) \tag{3.36}$$

With a simple trigonometrical equation, finally we obtain:

$$Y_s(\alpha) = l_3(\alpha) \cdot \sin(\alpha - \gamma) = l_{30} \cdot \lambda_3(\alpha) \cdot \sin(\alpha - \gamma) \tag{3.37}$$

Where, l_3 is the actual femur length.

In order to determine the $Y_s(\alpha)$ function, the λ_3 function together with the length of the femur and tibia are required. These anthropometrical data can be found in Table 3.7.

	AVERAGE	**SD**	**r^2**	**SAMPLE**	**p**
Length of Femur (Male) [cm]	45.15	2.32	-	9	-
Length of Tibia (Male) [cm]	41.46	1.32	-	9	-
Length of Femur (Female) [cm]	40.12	1.64	-	7	-
Length of Tibia (Female) [cm]	36.27	1.89	-	7	-
$\lambda_1(\alpha)$ function	See Eq. 3.28	See Table 3.6	0.65	55	$p < 0.05$
$\lambda_3(\alpha)$ function	See Eq. 3.29	See Table 3.6	0.63	31	$p < 0.05$

Table 3.7. Anthropometrical data of the subjects

The obtained data regarding the length of femur and tibia is in good agreement with the data found in the literature, since the average length of the femur and tibia are approximately 43.85 ±3.549 and 38.37 ±2.398 cm (males) and 42.29 ±3.127 and 35.13 ±2.215 cm (females) [Özaslan et al., 2003]. By the use of the length of the bones, the average movement of the center of gravity line, with its standard deviation, as a function of flexion angle can be obtained (Figure 3.28). In addition, the result from Mason et al. [Mason et al., 2008] has been added to the Figure 3.28.

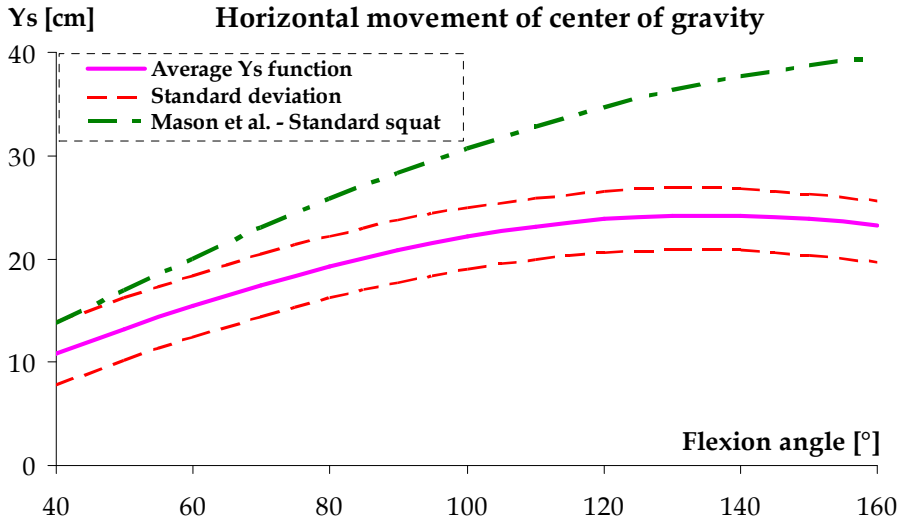

Figure 3.28. $Y_s(\alpha)$ function with its standard deviation

As it is seen, the difference between the two graphs is quite significant. In order to show how the two models differ in numbers, a small calculation has been carried out as follows:

$$\Delta K = \left(1 - \frac{K_{\text{non-standard}}}{K_{\text{standard}}}\right) \cdot 100 \tag{3.38}$$

Where, K can be any quantity (force, moment or displacement). ΔK can provide a percentage difference of a standard quantity compared to a non-standard quantity (here standard and non-standard relates to the type of squat motion). The results were summarized in Table 3.8.

FLEXION ANGLE	ΔYs
40°	21%
80°	25%
120°	31%
160°	41%

Table 3.8. *Ys* difference between standard and non-standard squat

The displacement of center of gravity line, as it was mentioned earlier in the introduction, is usually bounded to external non-human geometric quantities. The novelty of these graphs that they present functions, which are easy to apply in any mathematical model, since they are only dependent on one physical quantity: the flexion angle of the knee joint.

Although Mason et al. [Mason et al., 2008] also created a similar function (Eq. (2.4)), their function supposes that:

- the movement of the femur and the tibia are always symmetric to each other,
- the center of gravity does not move horizontally.

These hypotheses are major simplifications and the difference evidently appears.

By the use of the experiment, the range of the functions is estimated between 40° and 160° of flexion angle. Due to the multiple human subjects, an acceptable domain has been appointed about the phenomenon of the center of gravity line movement in case of squatting.

The major aims of the experiments were on the one hand to determine how the horizontal movement of the center of gravity line changes its position under squatting movement, and on the other hand to provide the other missing parameters and variables related to the analytical-kinetical model. By these results, the model described in subsection 3.2 is ready for use.

3.4.9. Conclusions about the experiment

In summary, a new method was presented to experimentally determine the horizontal movement of the center of gravity line and other anthropometrical constants-functions.

Multiple human subjects participated in this experiment, and the results of the individuals showed good accordance with the whole set. It was also demonstrated that the horizontal movement of the center of gravity line could be described with dimensionless, linear functions as a function of flexion angle. The standard deviation of the functions was also determined.

By knowing the above-mentioned parameters, the results can be extended for further use: the earlier introduced analytical-kinetical model in subsection 3.2 – where the load case is based on the obtained λ functions – is able to predict now all the patellofemoral and tibiofemoral forces.

3.5. Conclusions about the early numerical models

After reviewing the advancements of other authors in the modelling of sliding-rolling phenomenon, several questions were conceived regarding the white spots of the literature.

By gathering these questions, solid directions about the properties of the new model could be drawn and controversial or disregarded factors could be re-evaluated.

1st QUESTION: Should numerical or analytical model be used?

ANSWER: The complex geometry of the condyles and the challenging contact issue between the bodies make the description of the phenomenon impossible with algebraic equations, thus an analytical model is not advised.

Due to the complexity of the geometry and the phenomenon itself, only a numerical model is fitting for use.

2nd QUESTION: Which human locomotion should be modelled?

ANSWER: On the one hand, our analytical-kinetical model is based on the squatting movement, thus it is adequate to use this motion as basis. Moreover, the load of the knee joint during squatting is certainly higher than in most of other activities (subsection 3.2, 1st Question), therefore it is a good reason to work further on this movement.

For these reasons, the chosen locomotion is the squat.

3rd QUESTION: Should rigid or flexible bodies be used in the modelling?

ANSWER: Several authors carried out an evaluation between model accuracy and computational time using both deformable and rigid contact formulations. It has been proven that the use of rigid bodies causes negligible error in the kinematical [Baldwin et al., 2009, Halloran et al., 2005a, Halloran et al., 2005b] or in the kinetical [Baldwin et al., 2009] investigations, while the calculation time is only the half, one forth of the simulations with flexible bodies. Naturally, if e.g. one has to carry out fatigue or wear estimations, which requires the contact surfaces and their deformations, then only the finite element modelling is adequate. Nevertheless, this thesis only deals with one kinematic factor of the wear (sliding-rolling) and for this reason the rigid body approach is also suitable.

In summary, disregarding the deformation of the bones is a commonly applied simplification if we look at the earlier presented models in the literature review [Van Eijden et al., 1986, O'Connor et al., 1990, Ling et al., 1997, Wilson et al., 1998, Chittajallu and Kohrt, 1999, Hollman et al., 2002, Nägerl et al., 2008], while it only associates a moderate error to our investigations. It also has to be mentioned that the examination of the deformation in the contact is not among the aims.

In the new, proposed numerical-kinematical model, the bodies are rigid.

4th QUESTION: Should two- or three dimensional model be used?

ANSWER: The human knee joint is practically a three-dimensional joint that incorporates secondary rotations in the frontal (represented as abduction/adduction) and transverse (represented as axial rotation) planes of motion. The assumption that knee joint movements can be represented by planar motion in the sagittal plane excludes the potential effect of axial rotation (the so-called "screw home mechanism") on the calculation of the sliding-rolling phenomenon.

Thus, one principal limitation of the earlier published models [Van Eijden et al., 1986, O'Connor et al., 1990, Ling et al., 1997, Wilson et al., 1998, Chittajallu and Kohrt, 1999, Hollman et al., 2002] is that the contact geometry of the knee joint is oversimplified. Wilson et al. [Wilson et al., 1998] considered the femoral condyles spherical and the tibial plateau as a plate, while the natural knee condyles are aspherical and the tibial plateau cannot be modelled as a simple plate in the sagittal and coronal planes. According to O'Connor et al. [O'Connor et al., 1990] the slip ratio (thus the sliding-rolling ratio as well) is sensitive to the shape, or the assumed shape, of the tibia plateau. Considering this fact, simplification of the geometry very likely has a significant effect on the sliding-rolling ratio.

In addition, several authors agree, that their approach [Wilson et al., 1998, Hollman et al., 2002] is only a rough approximation due to the simplified geometry.

Thus, the new numerical-kinematical model is consequently three-dimensional.

5th QUESTION: Should the sliding-rolling phenomenon be examined between the tibiofemoral or the patellofemoral connection?

ANSWER: Typically, wear (regarding knee replacements) appears between the tibiofemoral contact due to the constant sliding and rolling motion. For this reason, almost with no exceptions, most studies put the emphasis on the tibiofemoral connection [Wimmer and Andriacchi, 1997, O'Brien et al., 2013, Blunn et al., 1992, Hood et al., 1983, Wimmer et al., 1998, Blunn et al., 1991, Blunn et al., 1994, Davidson et al., 1992]. According to these studies, the new numerical-kinematical model will also be designed to examine the tibiofemoral contact with regard to the sliding-rolling phenomenon.

According to the above-mentioned studies, the new numerical model sets the emphasis on the tibiofemoral connection.

6th QUESTION: What muscles should be taken account and what can be disregarded?

ANSWER: The quadriceps tendon and the patellar tendon are absolute necessity, thus we have to consider what other ligaments and tendons can we neglect? It has been demonstrated with simultaneous electromyograph tracings that in case of balanced equilibrium the extensor effect upon the knee is minorly affected by actions in the hamstrings or the gastrocnemius muscles (Figure 2.21).

The roll of the anterior and posterior crucial ligaments (ACL and PCL) is neglected in the modelling, since these ligaments are more responsible for the stability, rather than force transmission.

According to the above-mentioned facts, only the quadriceps tendon and the patellar tendon are considered in the new numerical-kinematical model, similarly to the analytical-kinetical model.

7th QUESTION: Should friction between the bodies be defined?

ANSWER: The earlier authors [Van Eijden et al., 1986, Yamaguchi and Zajac, 1989, Reithmeier and Plitz, 1990, Hirokawa, 1991, Hefzy and Yang, 1993, Gill and O'Connor, 1996, Singerman et al., 1994, Chittajallu and Kohrt, 1999, Ling et al., 1997] were in agreement that, due to the synovial fluid, the friction between the condyles can be neglected, although no studies were reported about the possible effect of friction on the sliding-rolling ratio.

Since multibody models can easily incorporate contacts with friction, it is worth involving this specific factor.

For this reason, friction is incorporated into the numerical-kinematical model.

8th QUESTION: Should the slip ratio or other quantity be used to define the sliding-rolling phenomenon?

ANSWER: In the literature, several types of slip ratios, sliding-rolling ratios, etc, appear. Many of these sources refer to a so-called slip ratio defined by O'Connor et al. [O'Connor et al., 1996]:

$$\text{Slip ratio} = \frac{s_m}{s_f} \tag{3.39}$$

Where

$$s_m = \int_{\alpha_1}^{\alpha_2} R \cdot d\alpha \text{ and } s_f = \int_{\alpha_1}^{\alpha_2} (R - r_{icr}) \cdot d\alpha \tag{3.40}$$

R is the radius of the curvature; r_{icr} is the radius from the ICR (instantaneous center of rotation) location and α is the flexion angle. s_m is the displacement between successive convex points on the convex femoral surface and s_f is the displacement between successive convex points on the flat tibial surface.

The slip ratio is defined as follows: the slip ratio of one represents pure rolling, and a slip-ratio of infinity represents pure slip while intermediate values represent combination of roll and slip together.

This definition does not make the phenomenon easily understandable, or gives a well-defined ratio, since between one and infinity the difference is infinite. Another ratio has to be introduced, which can describe this local motion preferably as a percentage.

For this reason, a new ratio will be introduced which can describe the sliding-rolling phenomenon as a percentage.

9th QUESTION: Should real bone structure geometry be examined or prosthesis geometry?

ANSWER: The condyles are covered by meniscus, which fulfil several purposes: on the one hand, it stabilizes the knee that no severe lateral or medial slip would occur, and on the other hand, it disperses the load on the surface. In order to model real human bone geometry, the meniscus system should be modelled as well, which highly complicates the work.

It is more advisable to work with current prosthesis geometries, where no meniscus modelling is included.

Therefore, prosthesis geometries are used in the numerical-kinematical model.

10th QUESTION: Between what angles should the sliding-rolling ratio be examined?

By summarizing the findings of the experimental and mathematical (numerical) literature, in case of experimental testing of prosthesis materials the sliding-rolling ratios are widely applied between 0.3-0.46 [Hollman et al., 2002, Van Citters et al., 2007] but only in the range of 0° to 30° flexion angle due to the firm belief that in the beginning of the motion, rolling is dominant. This assumption has been proven correct, although at higher flexion angles, presumably, the sliding-rolling ratio changes significantly [Nägerl et al., 2008, Reinholz et al., 1998], but the results related to the sliding-rolling ratio above 30° of flexion angle are rather limited.

Since the pattern of the sliding-rolling phenomenon has not been thoroughly investigated in full extension, the aims are the followings:

I. The pattern and magnitude of the sliding-rolling ratio have to be determined between 20-120˚ of flexion angle on several prosthesis geometries. This segment is considered as the fundamental active arc (Figure 2.10), which is totally under muscular control and involves most of our daily activities [Freeman, 2001].

    a. The arc between zero and 20˚, where the so-called "screw home mechanism" happens, is a great interest for anatomist although it may have a little importance in the daily living activities [Haines, 1941] as being only used in such activities as one-legged stance [Smith, 1956] or normal stance.

    b. The arc between 120˚ and 160˚ is not considered due to two reasons: there is no increment in the patellofemoral forces above 120˚ of flexion angle, and it only appears in the Asian cultures as an everyday activity, thus it has smaller relevance [Thambyah, 2008].

II. The change of the sliding-rolling ratio has to be investigated, as a function of different commercial and prototype prostheses. This should help to find the lower and upper limit of the sliding-rolling ratio between the condyles.

III. The possible effect of the lateral and medial collateral ligaments on the sliding-rolling ratio should be examined. It is unknown how much influence has the ligaments on the local kinematics, therefore as a first step, an investigation will be carried out by involving them into the multibody system.

GENERAL COMMENTS

By summarizing the above-mentioned conclusions, a new multibody model will be constructed which includes three important, but earlier neglected factors: valid three-dimensional geometry, friction between the condyles and as a modelling experiment, collateral ligaments.

The modelling of the condylar geometries will be based on four commercial prostheses and one prototype prosthesis. The spring constants and damping constant of the ligaments will be obtained from the literature.

In addition, a new definition will be introduced to characterize simply and precisely the sliding-rolling phenomenon in contrast to the earlier applied, less obvious and descriptive slip ratio.

The examined motion throughout this part of the thesis is the standard squat. For the same reason as it was in the case of the analytical-kinetical model, we chose to investigate the squatting for the following facts: under this movement the patellofemoral and tibiofemoral forces in the knee reach extremity, squatting is a daily used motion, and it has great clinical importance as a rehabilitation exercise.

3.6. The new numerical-kinematical model

3.6.1. Introduction

The currently applied numerical approaches in contact mechanics can be divided into two main groups: Finite Element Method and approaches based on Multibody dynamics.

The Finite Element Method is undisputedly the most powerful numerical method in the field of contact mechanics. It is well suited for particularly high accuracy requirements but with that, a very high computational effort is coupled for contact treatment that causes some practical difficulties e.g. very long computation times, divergence problems, etc.

In certain situation when a modestly decreased accuracy is suitable and deformation is not primarily in interest, multibody approach can also model the contact with acceptable precision and considerably less computational effort compared to Finite Element methods.

In addition, considering the practicality how multibody software can deal with very complex geometries in dynamic contact situations, it is a suitable choice for modelling the knee joint during squatting.

As for the software, MSC.ADAMS has been chosen to carry out kinematical and kinetical simulations. MSC.ADAMS is worldwide used program that helps engineers to study moving parts, elements, or even complete systems and improve their performances.

In contrast with simple CAD systems, MSC.ADAMS incorporates real physics by simultaneously solving linear or non-linear Ordinary Differential Equations (ODE) and non-linear Differential-Algebraic Equations (DAE) for kinematics, statics, quasi-statics, and dynamics.

3.6.2. Limitations and advancements of the model

In this part of the thesis, the investigation is restricted to the sliding-rolling ratio and the contact kinetics under standard squat movement. The new numerical-kinematical model includes some simplifications as follows:

a) The bones, such as the tibia, patella and femur were assumed as rigid bodies, since the influence of deformation in this study is neglected,

b) The patellar tendon modelled as an inextensible spring,

c) The quadriceps is modelled as one single linear spring,

d) No cruciate ligaments were modelled.

The new model complements the earlier models in some extent, thus it holds new features:

α The numerical-kinematical model is three-dimensional, based on commercial prosthesis geometries,

β Both lateral and medial sliding-rolling ratio can be studied due to the three dimensional surfaces,

γ Realistic friction condition is considered between the contact surfaces e.g. patellofemoral and tibiofemoral connection,

δ Kinetical investigation is also possible with this model.

3.6.3. Geometrical models

Geometric models were mapped by CCD camera system by the use of five prosthesis geometries. These prostheses are namely:

- Prosthesis 1.: Prototype from the SZIU, non-commercial,
- Prosthesis 2.: Biotech TP Primary knee,
- Prosthesis 3.: Biotech TP P/S Primary knee,
- Prosthesis 4.: BioMet Oxford Partial knee,
- Prosthesis 5.: DePuy PFC.

The geometric models were mapped with a Breuckmann OptoTop-HE 3D monochrome scanner with the 75 µm of resolution at the Szent István University, by the following steps (Figure 3.29 and Figure 3.30).

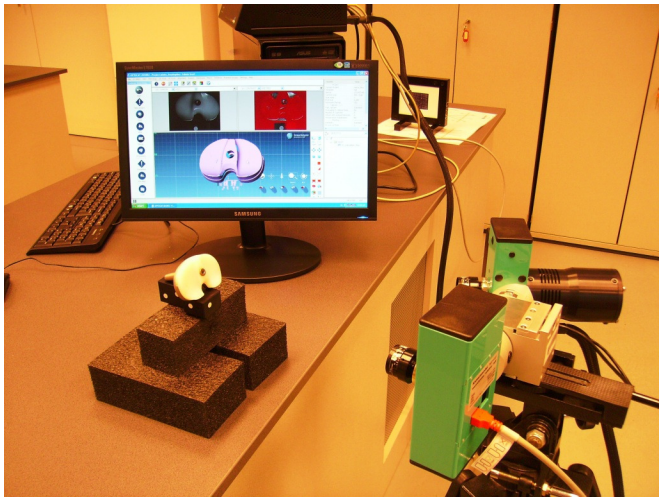

Figure 3.29. Scanning settings

Figure 3.30. Setting the focus (left) and actual scanning (right)

The scanned surfaces were processed and assembled in the OptoCat 2010 program and saved as STL files. The STL files (Stereolithography) are widely used in the 3D prototyping or computer aided manufacturing. However, the STL is built up as an unstructured, triangulated surface, which cannot be directly used in a CAD system, but needs to be converted into either a surface or a body model.

One problematic issue, that although the MSC.ADAMS program should accept several graphic files like IGS, STEP or PARASOLID, practically only the PARASOLID works properly. PARASOLID files can be created in Solid Edge or Solid Works software. Unfortunately, these software cannot convert STL files.

Theoretically, the solution is the following:

1. The obtained raw STL files have to be repaired (holes, singularities) and then converted into IGS files with the Catia software.
2. The IGS files have to be converted into PARASOLID format by the use of the Solid Edge/Works software.

Practically, some other factors – inside the CAD software – have to be taken into consideration in order to evade the upcoming errors in the file import process. This method was carried out in Solid Edge V16 and Catia V5R17, and it is systematically explained in the Appendix.

3.6.4. Multibody models

After creating the geometrical models, multibody models were built with MSC.ADAMS program system. The following boundary conditions were applied on each model (Prosthesis 1, 2, 3, 4, 5) identically:

- Only the patellar tendon and the rectus femoris were considered in the numerical model. Both of them were modeled as simple linear springs (SPRING element see Figure 3.32). According to the literature, the stiffness coefficient of the rectus femoris can be found between 15 and 83 N/mm [Conceição et al., 2002, Thelen et al., 2005], therefore this parameter was set to 40 N/mm, as an average value, while a damping coefficient of 0.15 Ns/mm was attributed to all tendons to prevent oscillations in the system [Frigo et al., 2010, Granata et al., 2002]. The patellar tendon was set to inextensible.
- A FORCE VECTOR was applied on the femur distalis (Figure 3.32) which represented the load of the body weight (***BW***). The magnitude was set to 800 N (1 ***BW***). The application of the vector was defined by a STEP function (STEP (A, x_0, h_0, x_1, h_1)), which means that the force magnitude proportionally increased in a certain period of time (STEP (time, 0.0, 0.0, 0.03, -800)) until it reached its maximum value (Figure 3.31). By loading the model with this method, initial unbalances could be evaded.

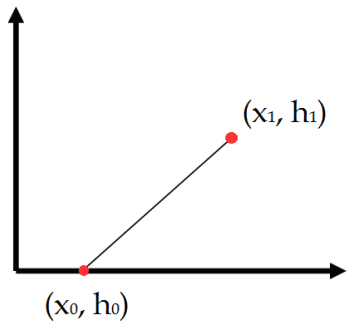

Figure 3.31. Step function in MSC.ADAMS

- The femur distalis was constrained by a GENERAL POINT MOTION, where all the coordinates can be prescribed (Figure 3.32). Only one prescription was set: the endpoint of the femur (distalis) can only perform translational motion along the *y*-axis.
- The ankle part of the model was constrained by a SPHERICAL JOINT, which allows rotation about all axes, but no translational motions are permitted in that point (Figure 3.32). By applying this constraint, the tibia can perform a natural rotation and a kinematic analysis can be carried out in a further study.
- Between the femur, tibia and patella, CONTACT constraints were set according to Coulomb's law with respect to the very low static and dynamic friction coefficients (μ_s = 0.003, μ_d = 0.001) similarly to real joints [Mow and Soslowsky, 1991, Quian et al., 2006] (Figure 3.32). With this constraint, the kinetic relationship between the normal and friction forces ($\boldsymbol{F_n}$, $\boldsymbol{F_s}$) and the flexion angle can be analyzed.
- The following material properties were set [Guess and Maletsky, 2004]: Young modulus$_{Femur}$: 19 GPa, Poisson ratio$_{Femur}$: 0.3, Young modulus$_{Tibia}$: 1 GPa, Poisson ratio$_{Tibia}$: 0.46. The material properties are necessary if CONTACT is used between the surfaces (see in CONTACT section).

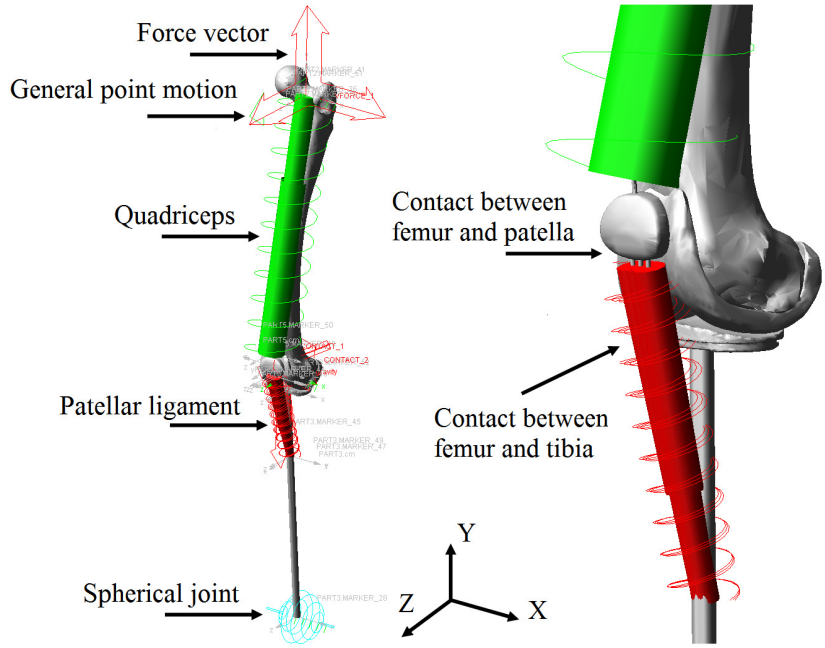

Figure 3.32. Multibody model in the MSC.ADAMS

3.6.4.1. Applied forces – FORCE VECTOR [MSC.ADAMS]

Applied forces in MSC.ADSMS can have one, three, or six components (three translational and three rotational) that define the resultant force. For example, a single-component force or moment defines the force using a single component, while a multi-component force or moment defines the force using three or more components.

Forces can be:

- Space fixed: Sets the force direction so it is applied to a part. The force direction is fixed on ground. In this PhD work, this type of force was applied.
- Moving with the body: Sets the force so it is applied to a part. The part defines the direction of the force.
- Between two bodies: Creates a force between two parts. One of the parts can be ground.

The characteristic of the force can be:

1. Constant force: In this case, we enter a constant value that will define the magnitude of the force in the MSC.ADAMS. In this PhD work, this type of force was applied.
2. Bushing-like force: In this case, the MSC.ADAMS creates a function expression that can be defined by linear stiffness and damping coefficients.
3. Custom: By selecting this option, the force can be defined as a function of velocity, displacement, other applied forces, user-defined variables, or time.

3.6.4.2. Point motion – GENERAL POINT MOTION [MSC.ADAMS]

Two types of point motion can be created by this option:

- Single point motion: Prescribes the motion of two parts along or around one axis.
- General point motion: Prescribes the motion of two parts along or around the three axes (six degrees of freedom (DOF)).

When a point motion is created, the user can specify the parts to which the motion is to be applied and the location/orientation of the motion. MSC.ADAMS creates markers on each part at the location of the motion. The *z*-axis of the reference point defines the positive direction using the right-hand rule. When choosing a point motion, MSC.ADAMS creates a motion at the specified location as follows:

1. For a single point motion, MSC.ADAMS defines the motion as a constant velocity over time, based on the entered value. This can be a numerical value, function expression or user-written subroutine.
2. For general point motion, MSC.ADAMS creates a motion around or along all six coordinates of the markers created on the selected parts. It does not define the magnitude or the motion, both of them have to be defined by the user. In this PhD work, this type of Point Motion was applied.

3.6.4.3. **Contact** [MSC.ADAMS]

During contact detection, as a simplification, MSC.ADAMS assumes that the volume of intersection between two solids is much less than the volume of either solid. After contact occurs between two solids, MSC.ADAMS computes the volumes of intersection. Once there is contact, the program finds the centroid of the intersection volume. This is the same as the center of mass of the intersection volume (assuming the intersection volume has uniform density).

After this step, MSC.ADAMS finds the closest point on each solid to the centroid. The distance between these two points is the penetration depth (P_d).

MSC.ADAMS then puts this distance into a formula where K is the material stiffness (for this reason the material property of the bone has to be set), n is an exponent while $\boldsymbol{F}$ is the contact force.

$$F_c = K \cdot P_d \cdot n \tag{3.41}$$

By this method, the contact forces between any connecting bodies can be calculated alongside with the contact position.

As the simulation starts, the forces acting on the femur distalis drives the model (FORCE VECTOR in Figure 3.32). The kinematical constraint (GENERAL POINT MOTION in Figure 3.32) has the only role to keep the structure in balance thus is could carry out a translational motion along the y-axis. Since the model is dynamic and not static, the equilibrium of the forces during the motion is not imperative.

Before the simulation, some important parameters have to be set such the FACETING TOLERANCE. Faceting is the process of approximating the surface of an object by a mesh of triangles. All polygon-based geometry engines used faceted representations of surfaces. The default value of this parameter is 300. Higher value will result in a finer mesh of triangles, which gives a more accurate representation of surfaces that are curved. Setting the faceting tolerance to values greater than 1000 is not recommended [MSC.ADAMS].

3.6.4.4. **Model verification** [MSC.ADAMS]

It is recommended to inspect the model before the actual run. By using the MODEL VERIFY tool, hidden erroneous conditions in the model, such as misaligned joints, unconstrained parts, or massless parts can be detected and fixed. This tool not only shows errors in the model, but it also calculates the degrees of freedom of a kinematical chain, such as our model.

The MSC.ADAMS determined that the current model (Figure 3.32) has 13 degrees of freedom (DoF), which can also be manually controlled. The DoF of any structure (S_{DoF}) can be determined by the following formula [Csizmadia and Nándori, 2009]:

$$S_{DoF} = C_{DoF} - (c_i + c_e) \tag{3.42}$$

Where C_{DoF} is the degree of freedom of the kinematic chain, c_i is the degree of freedom of the internal constraints (the ones that connect the links-bodies together) while c_e is the degree of freedom of the external constraints (the ones that connect the kinematical chain to its surroundings).

One single rigid body in a spatial system has six degree of freedom, while we have three, three-dimensional rigid bodies. That gives 3 x 6 = 18 degrees of freedom ($s_{DoF} = 18$).

There is only one external constraint, namely the SPHERICAL joint which allows three degrees of freedom (the three rotations), thus $c_e = 3$. There are two internal constraints, one between the patella and femoral surface and one between the femoral and the tibial surfaces. These special constraints (in the literature "higher pair") allow any motion on the connecting surfaces but no penetration. This reduces the degrees of freedom to one per higher pair. Since there are two connections of this type, the $c_i = 1 + 1 = 2$.

Finally the DoF of the current model is: $S_{DoF} = 18 - (3+2) = 13$.

Regarding the solver part of the program, GSTIFF type integrator [Gear, 1971] was used in the MSC.ADAMS for solving the ODE and DAE of the motion. The solver routine was set to work maximum 10^{-3} tolerance of error, while the maximum order of the polynomial was defined as 12. The solution converged very well with these parameters; the model in different positions during simulation is presented in Figure 3.33.

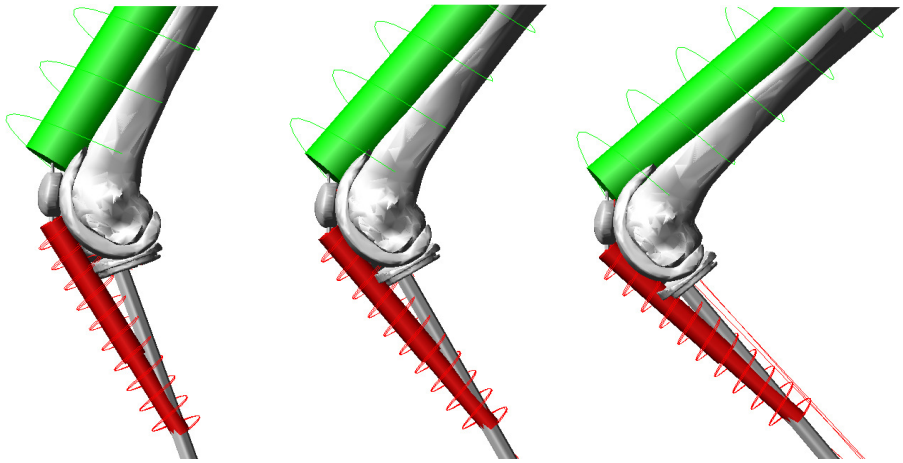

Figure 3.33. Multibody model in different positions during simulation

3.6.5. Calculation method

The following kinematic quantities can be directly calculated by the MSC.ADAMS during the simulation of the motion as a function of time:

- $\bar{r}_{Ci}(t)$: Vector-scalar function, which determines the instantaneous position of the connecting points of two bodies defined in the absolute coordinate system (Figure 3.34). If i = 1, contact between femur and tibia, if i = 2, contact between femur and patella.
- $\bar{r}_{CMF}(t)$, $\bar{r}_{CMT}(t)$, $\bar{v}_{CMF}(t)$, $\bar{v}_{CMT}(t)$, $\bar{\omega}_{CMF}(t)$, $\bar{\omega}_{CMT}(t)$: Vector-scalar functions, which determine the instantaneous position of the center of mass (CM_i), velocity and angular velocity of the femur (F) and the tibia (T) defined in the absolute coordinate system (Figure 3.34).
- $\bar{e}_{Ci}(t)$: Vector-scalar function (unit-vector), which determines the instantaneous tangent vector respectively to the contact path defined in the absolute coordinate system (Figure 3.35).

Besides the kinematic quantities, MSC.ADAMS software can calculate kinetic quantities as well, for example:

- Contact forces between the contact surfaces, reaction forces and moments in the applied constraints or forces in the springs.

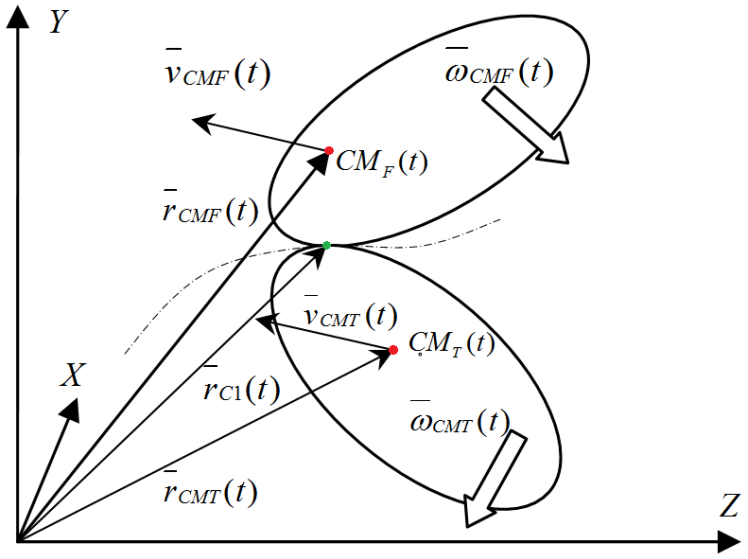

Figure 3.34. Kinematic quantities between the femur and tibia

In order to calculate the sliding-rolling ratio, additional kinematic quantities have to be determined as well (these quantities cannot be calculated directly with MSC.ADAMS):

- $\bar{r}_{CF}(t)$, $\bar{r}_{CT}(t)$, $\bar{v}_{CF}(t)$, $\bar{v}_{CT}(t)$: Vector-scalar functions, which determine the instantaneous position and velocity in the contact point (*C*) of the connecting femoral or tibial surfaces respectively (Figure 3.35).

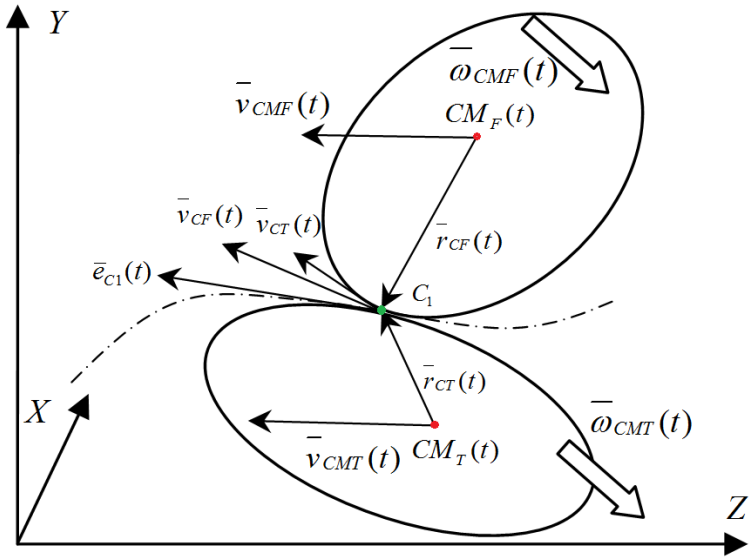

Figure 3.35. Kinematic quantities between the femur and tibia

Since the multibody model is considered rigid, the rigid body kinematics is applicable. The sliding-rolling ratio is only determined between the femur and the tibia therefore the patella does not appear in the calculation or in the figures.

To obtain the velocity of a point – in our case point C_1 – the following calculation algorithm is applied [Csizmadia and Nándori, 1997]:

$$\bar{v}_{CF}(t) = \bar{v}_{CMF}(t) + \bar{\omega}_{CMF}(t) \times \bar{r}_{CF}(t) \tag{3.43}$$

$$\bar{v}_{CT}(t) = \bar{v}_{CMT}(t) + \bar{\omega}_{CMT}(t) \times \bar{r}_{CT}(t) \tag{3.44}$$

where,

$$\bar{r}_{C1}(t) = \bar{r}_{CMF}(t) + \bar{r}_{CF}(t) \rightarrow \bar{r}_{CF}(t) = \bar{r}_{C1}(t) - \bar{r}_{CMF}(t) \tag{3.45}$$

$$\bar{r}_{C1}(t) = \bar{r}_{CMT}(t) + \bar{r}_{CT}(t) \rightarrow \bar{r}_{CT}(t) = \bar{r}_{C1}(t) - \bar{r}_{CMT}(t) \tag{3.46}$$

By substituting Eq. (3.45) into Eq. (3.43) and Eq. (3.46) into Eq. (3.44) we obtain:

$$\bar{v}_{CF}(t) = \bar{v}_{CMF}(t) + \bar{\omega}_{CMF}(t) \times \left(\bar{r}_{C1}(t) - \bar{r}_{CMF}(t)\right) \tag{3.47}$$

$$\bar{v}_{CT}(t) = \bar{v}_{CMT}(t) + \bar{\omega}_{CMT}(t) \times \left(\bar{r}_{C1}(t) - \bar{r}_{CMT}(t)\right) \tag{3.48}$$

Now, the velocities with respect to the femur and tibia are determined in the contact point, in the absolute coordinate system (Figure 3.36).

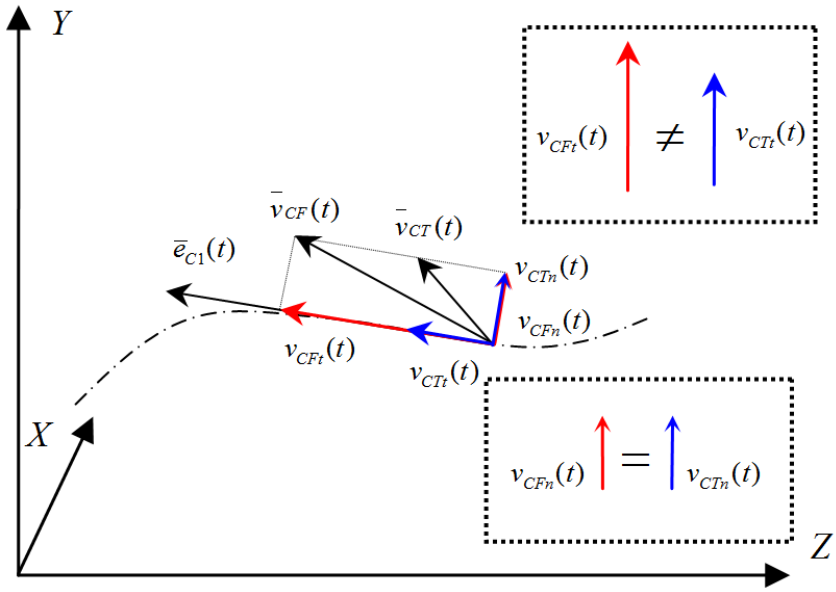

Figure 3.36. Velocities of the femur and tibia in the contact point

By multiplying equation (3.47) and (3.48) with the $\bar{e}_{C1}(t)$ unit vector, we can derive the tangential scalar component of the femoral and tibial contact velocities with respect to the contact path:

$$v_{CFt}(t) = \bar{v}_{CF}(t) \cdot \bar{e}_{C1}(t) = \left[\bar{v}_{CMF}(t) + \bar{\omega}_{CMF}(t) \times \left(\bar{r}_{C1}(t) - \bar{r}_{CMF}(t)\right)\right] \cdot \bar{e}_{C1}(t) \tag{3.49}$$

$$v_{CTt}(t) = \bar{v}_{CT}(t) \cdot \bar{e}_{C1}(t) = \left[\bar{v}_{CMT}(t) + \bar{\omega}_{CMT}(t) \times \left(\bar{r}_{C1}(t) - \bar{r}_{CMT}(t)\right)\right] \cdot \bar{e}_{C1}(t) \tag{3.50}$$

The tangential scalar components are only valid, if the following condition is satisfied [Szendrő, 2007, Vörös, 1970]:

$$v_{CF\,n}(t) = v_{CT\,n}(t) \tag{3.51}$$

This means that the normal scalar components of the femoral and tibial contact velocities have to be equal, otherwise, the two surfaces either would be crushed into each other or would be separated.

Since the scalar contact-velocities are available, by integrating them over time the connecting arc lengths with respect to the femur and tibia can be calculated as:

$$s_{femur}(t) = \int v_{CFt}(t) \cdot dt = \int \left[\bar{v}_{CMF}(t) + \bar{\omega}_{CMF}(t) \times \left(\bar{r}_{C1}(t) - \bar{r}_{CMF}(t)\right)\right] \cdot \bar{e}_{C1}(t) \cdot dt \tag{3.52}$$

$$s_{tibia}(t) = \int v_{CTt}(t) \cdot dt = \int \left[\bar{v}_{CMT}(t) + \bar{\omega}_{CMT}(t) \times \left(\bar{r}_{C1}(t) - \bar{r}_{CMT}(t)\right)\right] \cdot \bar{e}_{C1}(t) \cdot dt \tag{3.53}$$

By having determined the arc lengths on both connecting bodies, the sliding-rolling ratio can be introduced and denoted as follows:

$$\chi(t) = \frac{\Delta s_{tibiaN}(t) - \Delta s_{femurN}(t)}{\Delta s_{tibiaN}(t)} \tag{3.54}$$

where,

$$\Delta s_{femurN}(t) = s_{femurN}(t) - s_{femurN-1}(t) \tag{3.55}$$

$$\Delta s_{tibiaN}(t) = s_{tibiaN}(t) - s_{tibiaN-1}(t) \tag{3.56}$$

are the corresponding incremental differences of the connecting arc lengths.

The sliding-rolling function, or sliding-rolling ratio, is defined as the difference between of an incremental distance travelled (Δs_{tibiaN}) on the tibia and the incremental distance travelled (Δs_{femurN}) on the femur over the incremental distance travelled (Δs_{tibiaN}) on the tibia. *N* denotes an arbitrary arc length during the connection.

By this function, exact conclusions can be drawn about the sliding and rolling features of the motion. A sliding-rolling ratio of zero indicates pure rolling, while one describes pure sliding. If the ratio is between zero and one, the movement is characterized as partial rolling and sliding. For example, a sliding-rolling ratio of 0.4 means 40% of sliding and 60% of rolling. A positive ratio shows the slip of the femur compared to the tibia. If the sign is negative, than the tibia has higher slip compared to the femur.

It is desirable to determine the sliding-rolling ratio as a function of flexion angle rather than as a function of time. To do so, the flexion angle (α) was derived by integrating the angular velocities of the femur and tibia about the *x*-axis over time and taking into account that the model was set in an initial 20 degree of squat at the beginning of the motion.

$$\alpha(t) = \int \omega_{CMFx} \cdot dt + \int \omega_{CMTx} \cdot dt + 20 \tag{3.57}$$

Since $\alpha(t)$ function has been determined, time can be exchanged to flexion angle and the sliding-rolling function can be plotted as a function of flexion angle:

$$\chi(\alpha) = \frac{\Delta S_{tibiaN}(\alpha) - \Delta S_{femurN}(\alpha)}{\Delta S_{tibiaN}(\alpha)} \tag{3.58}$$

4. RESULTS

4.1. Results regarding the analytical-kinetical model

4.1.1. Effect of the center of gravity – Standard squat model

Since the required parameters and variables are available, the analytical-kinetical model of subsection 3.2 can be evaluated and compared to the results of other authors. However, let us first investigate the effect of the horizontally moving center of gravity on the standard squat model described by Mason et al. [Mason et al., 2008] from subsection 2.2.

As it has been proven by other authors [Cohen et al., 2001, Mason et al., 2008], the patellofemoral forces directly depend on the net knee moment in case of the standard squat. Therefore, it is interesting to see how this moment depends on the position of the center of gravity. As it was mentioned earlier, the standard squat model is based on the following three assumptions:

1. During squatting the line of action of the center of gravity does not change its position horizontally,
2. The femur and tibia are symmetrically positioned (their rotation during the movement is equivalent),
3. The net knee moment can be derived as a simple function of the flexion angle (Eq. (2.4) and Eq. (2.5)).

The movement of the center of gravity has been described empirically as a linear function of the flexion angle (Eq. (3.28) and Eq. (3.29)). In subsection 3.3, an equation has been created (Eq. (3.37)) to define the moment arm for the net knee moment. This equation, as an amendment, includes the horizontal movement of the center of gravity (λ_3) and the rotation of the tibia (γ).

Let us substitute Eq. (3.37) into Eq. (2.5) in order to determine the net knee moment with horizontally moving center of gravity:

$$M_k(\alpha) = 0.5 \cdot BW \cdot Y_s(\alpha) = 0.5 \cdot BW \cdot l_{30} \cdot \lambda_3(\alpha) \cdot \sin(\alpha - \gamma) \tag{4.1}$$

After analytically deriving this net knee moment with the moving center of gravity, and considering that the femur and tibia are not symmetrically positioned, a new calculation was carried out. In Figure 4.1, two net knee moments are compared: the original net knee moment without the effect of the horizontally moving center of gravity, and a modified (non-standard) net knee moment described in Eq. (4.1).

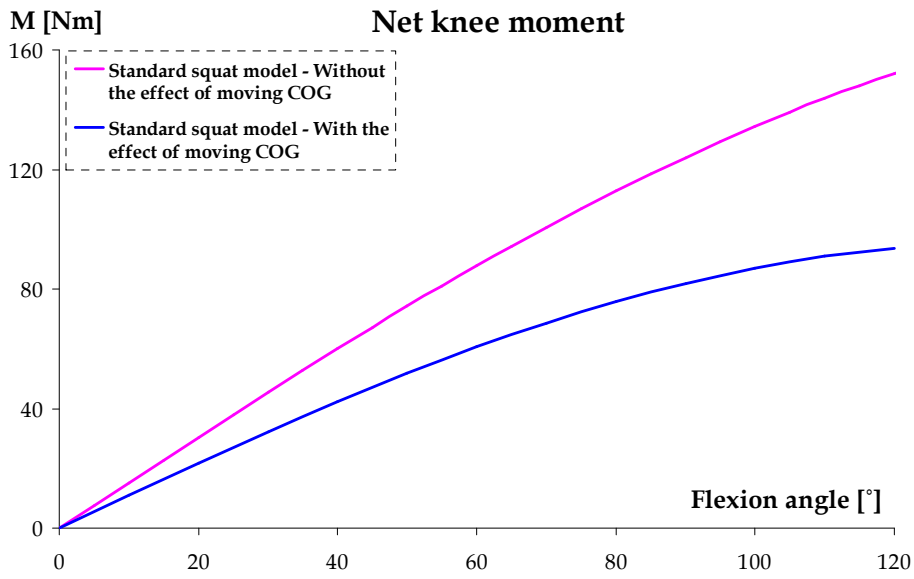

Figure 4.1. Net knee moments of the model of Mason et al. [Mason et al., 2008]

In order to see the influence of the moving center of gravity in numbers, the patellofemoral forces and the net knee moments have been recalculated, as percentage difference, and compared between the standard (fixed center of gravity) and non-standard (moving center of gravity) squat in this model [Mason et al., 2008].

$$\Delta K = \left(1 - \frac{K_{\text{non-standard}}}{K_{\text{standard}}}\right) \cdot 100 \tag{4.2}$$

Where, K can be any quantity (force, moment or displacement). ΔK can provide a percentage difference of a standard quantity compared to a non-standard quantity (here standard and non-standard relates to the squat motion). The obtained results were summarized in Table 4.1.

FLEXION ANGLE	ΔM_N	ΔF_q	ΔF_{pf}	ΔF_{pt}
30°	20%	17%	17%	18%
60°	28%	24%	24%	24%
90°	34%	38%	38%	38%
120°	44%	25%	25%	25%

Table 4.1. Percentage difference between Standard and Non-standard squat

While only 17-20% deviation is noted at 30˚ of flexion angle, a clear difference, approximately 44% can be noted at 120˚ of flexion angle. The significant difference between the net knee moments has also considerable impact on the measurable forces.

The incorporation of the moving center of gravity significantly lowers the patellofemoral forces (17-38%) along the calculated domain. This lowering effect on the patellofemoral forces (average 27.5%) corresponds very well with the result of Kulas et al. [Kulas et al., 2012] who also investigated the effect of the moderate forward trunk lean condition and observed 24% lower peak ACL forces!

This closely equal percentage-difference between the ligaments and forces is a remarkable match regarding the effect of the moving center of gravity.

Several authors [Denham and Bishop, 1978, Schindler and Scott, 2011, Perry et al., 1975, Amis and Farahmand, 1996] bethought and assumed that the movement of the center of gravity should influence the patellofemoral forces by means of decreasing them. By these results, not only the necessity of this factor in the modelling has been confirmed, but it also has been shown that this factor surely decreases the forces in the tendons (and ligaments). The average decrease is approximately 25%.

4.1.2. Effect of the center of gravity – Non-standard squat model

In the followings, the new analytical-kinetical model will be compared to the available analytical, inverse-dynamics and oxford-type models from the literature.

In Figure 4.2, Figure 4.3, Figure 4.4 and Figure 4.5, the calculated forces of the standard and non-standard squat models are plotted and compared with the results of other authors. The calculations are carried out between 0˚ and 120˚ of flexion angle due to three reasons:

- This is the so-called active functional arc of the knee joint, where most movements are carried out [Freeman, 2001],
- The available experimental data in the literature does not exceed this specific domain (0-120˚ of flexion angle),
- The pattern, how the patellofemoral forces behave as a function of flexion angle, is the following [Sharma et al., 2008]:
    - Between 0-90˚: Monotonic increase,
    - Between 90-120˚: Reaching the maximum,
    - Between 120-160˚: Decrease until maximum flexion.
- The new analytical model predicts the maximum force at a 120˚ of flexion angle (beyond that angle the forces start decreasing).

The reason of the decrease beyond 120˚ of flexion angle is due to the wrap of the quadriceps which starts approximately at 90˚ of flexion angle. When the quadriceps tendon begins to wrap around the femur, the quadriceps force angle, with respect to the femoral axis, does not change.

In the meanwhile, the moment arm of the quadriceps starts increasing due to the posterior movement of the tibiofemoral contact, therefore the amount of force in the quadriceps decreases and so do the patellar tendon force and the patellar compression force [Sharma et al., 2008].

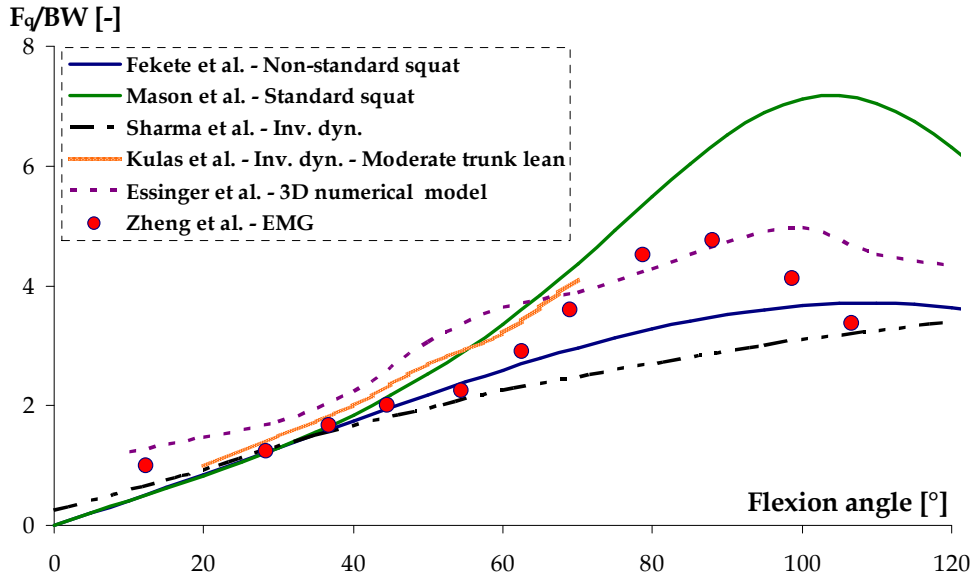

Figure 4.2. Quadriceps tendon force as a function of flexion angle

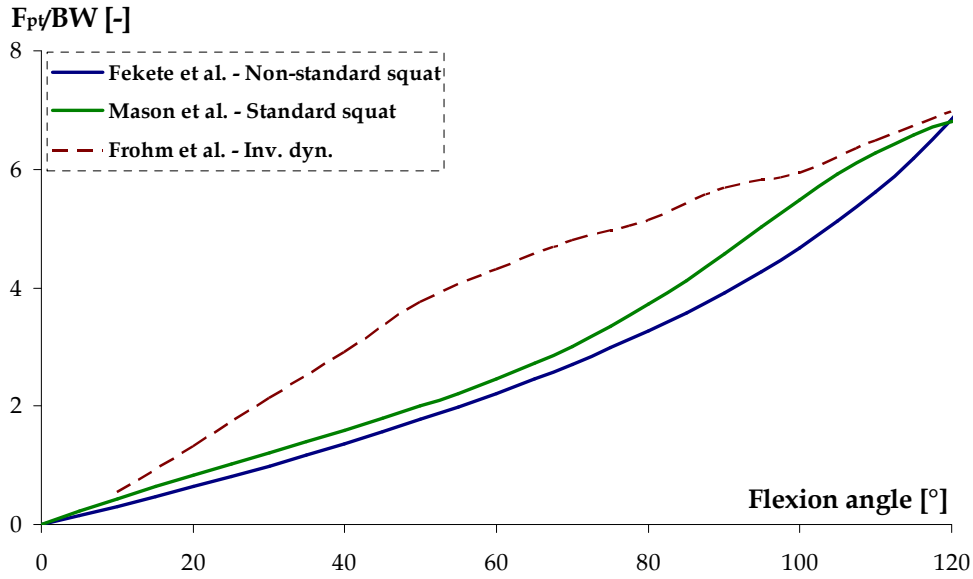

Figure 4.3. Patellar tendon force as a function of flexion angle

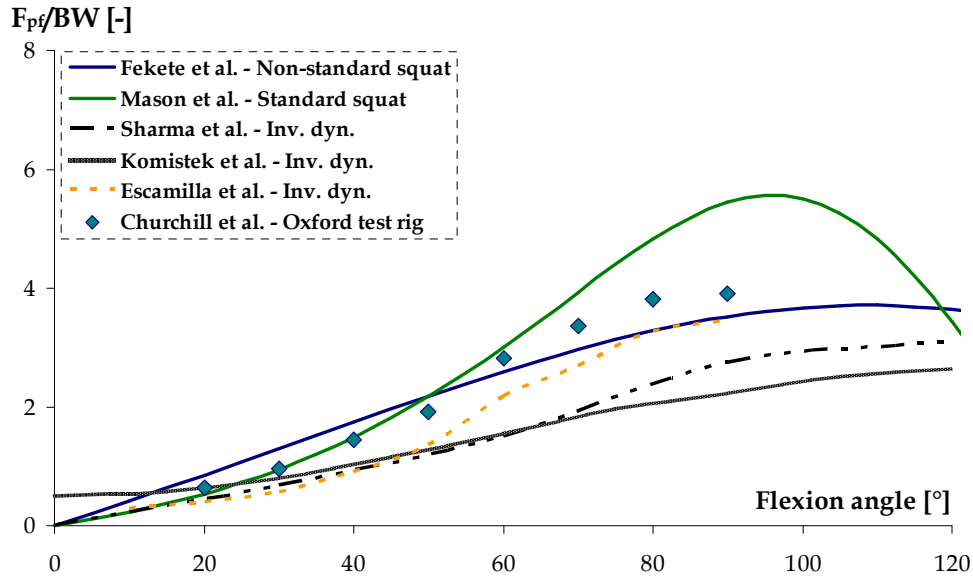

Figure 4.4. Patellofemoral compression force as a function of flexion angle

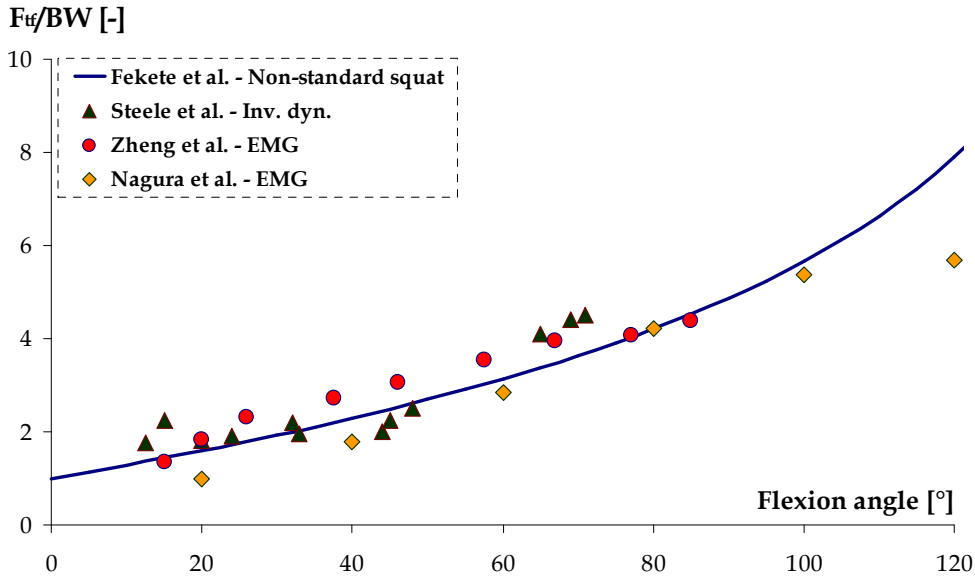

Figure 4.5. Tibiofemoral compression force as a function of flexion angle

The incorporation of the moving center of gravity (the forward and backward movement of the trunk) is an absolute novelty among the existing analytical models. The former analytical models were mainly validated by Oxford test rigs [Singerman et al., 1999, Petersilge et al., 1994, Churchill et al., 2001] that had load systems similar to the standard squat model in Figure 2.38, which permits the center of gravity to move only vertically under squat movement. This restriction prevents us to observe how the patello- and tibiofemoral forces change with the moving center of gravity.

As a validation, the analytically obtained forces are compared to results derived by inverse dynamics approach, oxford-type test rigs, and other analytical models.

The inverse dynamics approach is based on the following method: if the acting force-system (or acting moments) and the moment of inertia (or mass) are known, then by double-integration the displacement of the body (or particle) can be deduced:

Forward dynamics

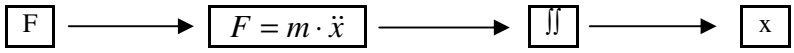

On the other hand, if the moment of inertia (or mass) and the displacement are known, then similarly with a double derivation the acting force-system (or moments) can be deduced:

Inverse dynamics

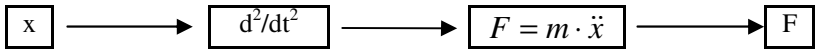

With regard to human locomotion, the limbs are represented as rigid links, where given the kinematics of each part, the inverse dynamics approach determines the forces (and moments) responsible for the individual movements. The movements are detected by sensors, while the moment of inertia can be taken from experimentally determined tables [Hanavan, 1964, Dempster, 1955].

By the use of inverse dynamics approach [Robertson et al., 2004], all the movements of the human body can be taken into consideration, thus the effect of the center of gravity as well. By knowing (measuring) the kinematics of a person during non-standard squat, the measured forces will involve the effect of the moving center of gravity as well. For this reason the results are best compared to the results of inverse dynamics method.

In Figure 4.2, the quadriceps tendon force of the non-standard squat model corresponds well with the result of Kulas et al. [Kulas et al., 2012], Essinger et al. [Essinger et al., 1989] and Zheng et al. [Zheng et al., 1998]. Among the three authors, the most important comparison is considered with Kulas et al. [Kulas et al., 2012], since their study involves the effect of moderate forward movement of the trunk. The non-standard squat model and the model of Sharma et al. [Sharma et al., 2008] estimate the peak force at 120˚ of flexion angle, while the model of Essinger et al. [Essinger et al., 1989] approaches the peak at 100˚ of flexion angle. The peak force of the non-standard squat model is estimated to 3.63 ***BW***.

In contrast, the standard squat model predicts that the peak magnitude is 7.2 ***BW*** and the peak location is between 90˚ and 100˚ of flexion angle.

In case of the analytical model of Mason et al. [Mason et al., 2008] and similar approaches, the following explanation can be derived related to the overestimation of the forces. Let us look at Figure 2.38 again.

The $\boldsymbol{F_q}$ force is calculated from the net knee moment (Eq. (2.5)), where it is supposed that the line of action of the center of gravity does not change its position. In the calculation of the moment arm (d) it is assumed that l_{30}, which represents the length of the femur, the length between the point of rotation and the applied ***BW*** force does not change its length. Since l_{30} has constant length, the moment is changed only by the different flexion angle. This approach assumes that the subject stays in perfectly vertical position during squatting.

In reality, human subjects do lean forward during squatting, which besides helping them to keep their balances, it also alters the patellofemoral forces by means of reducing them.

The solution is the following: the length between the point of rotation and the acting ***BW*** force has to be considered as a function of flexion angle ($l_3(\alpha)$), which reduces the net knee moment.

Due to this reason, every model, experimental, analytical or numerical, which does not incorporate the moving center of gravity into their model tends to overestimate the net knee moment and results higher forces in the quadriceps (and in the other muscles or tendons).

Generally speaking: our new model has also the limit that the input parameters, regarding the motion (standard or non-standard squat), only describes one specific squatting movement carried out on a set of people. All the same, this parameter has not yet been investigated thoroughly by any other author (except Kulas et al., 2012), thus until now, there was no data about how the horizontal movement of the center of gravity interferes with the patellofemoral forces. In addition, the model is capable to investigate other types of squat, if other λ functions (determined by other measurements) are incorporated.

In Figure 4.3, the patellar tendon force is plotted. The correlation is very strong between the standard and non-standard models regarding this force. Their characteristics, magnitudes and peak locations are in good accordance with each other. The experimental result of Frohm et al. [Frohm et al., 2007] shares more or less the same location and magnitude, but it has different, degressive, characteristic. According to these corresponding results, the estimated peak force is 6.8 ***BW*** and the peak location is at 120˚ of flexion angle.

In Figure 4.4, the patellofemoral compression force is plotted. The deviation between the forces is higher, compared to other forces ($\boldsymbol{F_q}$ or $\boldsymbol{F_{pt}}$). By considering the plotted results, the non-standard squat model correlates with the results of Sharma et al. [Sharma et al., 2008], Komistek et al. [Komistek et al., 2005] and Escamilla et al. [Escamilla et al., 2008], although with some overestimation. Komistek et al. [Komistek et al., 2005] and Escamilla et al. [Escamilla et al., 2008] estimated the peak force between 2.6 and 3.5 ***BW***. The estimated peak angle of the non-standard squat model, in this case, is located around 110˚ of flexion angle and the peak force is approximately 3.6 ***BW***. The only exception is the result of Escamilla et al. [Escamilla et al., 2008], which was only carried out up to a 90˚ of flexion angle.

If we compare the standard squat results with the results provided by the inverse dynamics method and the non-standard squat model, the significant difference becomes quite apparent related to this force.

In Figure 4.5, the tibiofemoral force is presented. The standard squat model by Mason et al. [Mason et al., 2008] is not able to predict this force, thus no comparison could be carried out between the two analytical models. The new analytical-kinetical model was compared to the results of Zheng et al. [Zheng et al., 1998], Nagura et al. [Nagura et al., 2010] and Steele et al. [Steele et al., 2012]. As it is seen, the four results have very good correlation with each other, although the experimental result of Zheng et al. [Zheng et al., 1998] and Steele et al. [Steele et al., 2012] provide prediction only until 90˚ and 70˚ of flexion angle. Here, the peak force is estimated between 7.8 ***BW***.

Although, no direct measurement was performed to validate the obtained results, a comparison between the current predictions and the ones found in the literature can estimate the validity of this new analytical-kinetical model (Table 4.2). The comparison was done at 90˚ of flexion angle, since that was the angle until all sources had results.

AUTHOR	MODEL TYPE	F_{pf}/BW	F_{pt}/BW	F_{tf}/BW	F_q/BW
Mason et al., 2008	Hinge	5.4	4.5	-	7.1
Dahlkvist et al., 1982	Hinge	7.4	-	5.1	5.3
Steele et al., 2012	Hinge (OpenSim)	-	-	7.6	9.6
Essinger et al., 1989	Three-dimensional	-	-	-	4.7
Kulas et al., 2012	Inverse dynamics	-	-	-	4.1
Sharma et al., 2008	Inverse dynamics	2.7	1.5	-	3
Frohm et al., 2007	Inverse dynamics	-	5.7	-	-
Escamilla et al., 2008	Inverse dynamics	3.5	-	-	-
Komistek et al., 2005	Inverse dynamics	2.5	-	-	-
Nagura et al., 2006	EMG	-	-	4.7	4.5
Zheng et al., 1998	EMG	-	-	4.4	4.7
Churchill et al., 2001	Oxford	3.9	-	-	-
Mean		4.3	3.9	5.45	5.37
SD		1.86	2.16	1.46	2.06
Present model	**Hinge**	**3.51**	**3.9**	**4.86**	**3.52**

Table 4.2. Peak muscle force predictions from literature and present model at 90˚ of flexion angle

According to Table 4.2, the present model shows very good correlation with the results from the literature. In spite of the simplicity of the model, the predicted forces, compared to the calculated mean values, only differed by 0-1.85 SD respectively.

4.2. Results regarding the numerical-kinematical model

4.2.1. Individual results of the prosthesis models

After all of the simulations have been carried out on all the five prostheses, the following results were obtained related to the sliding-rolling ratio and the tibiofemoral force:

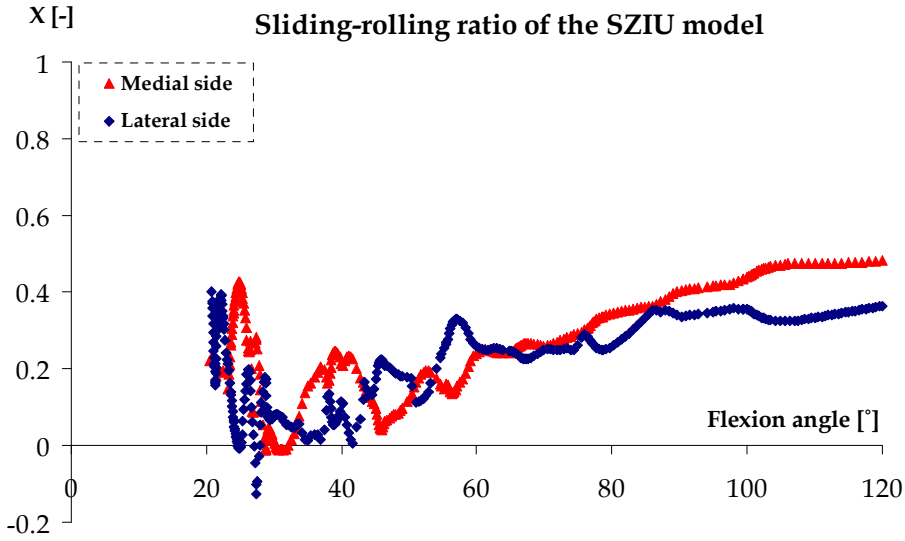

Figure 4.6. Sliding-rolling ratio of SZIU model

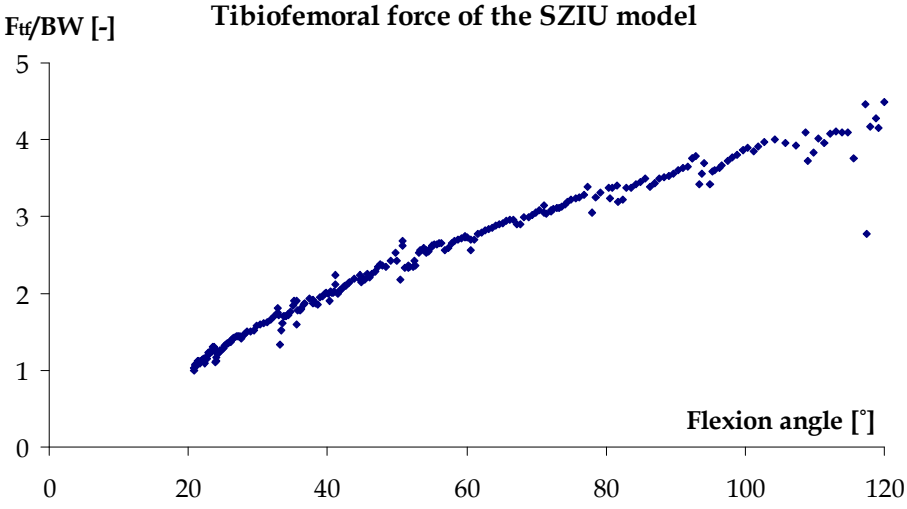

Figure 4.7. Tibiofemoral force of SZIU model

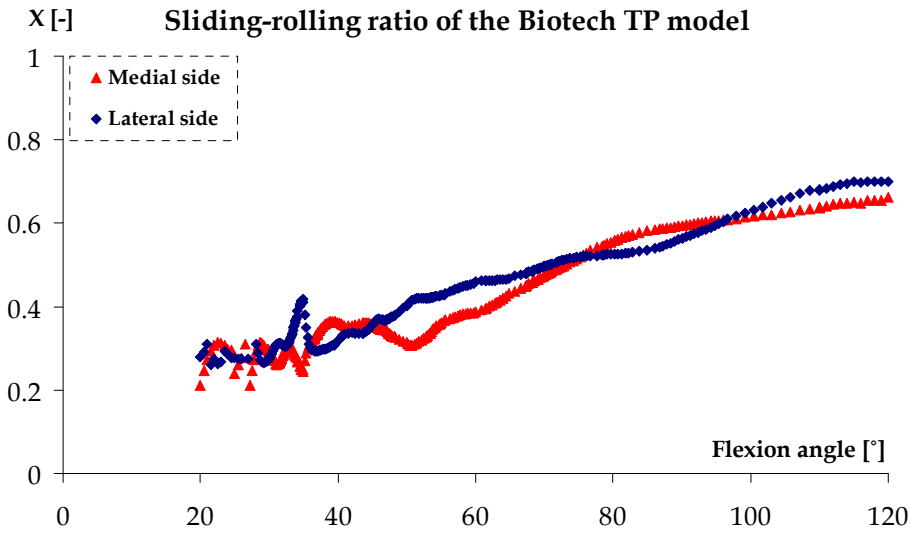

Figure 4.8. Sliding-rolling ratio of Biotech TP model

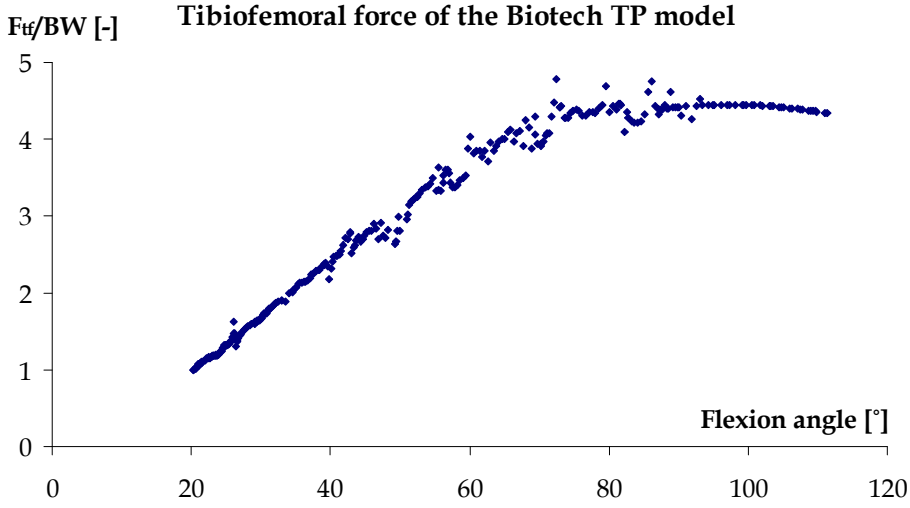

Figure 4.9. Tibiofemoral force of Biotech TP model

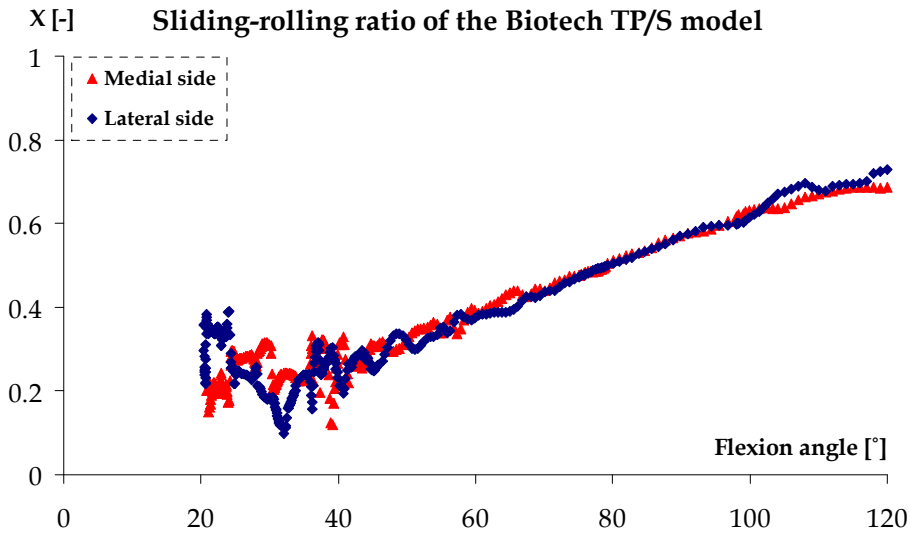

Figure 4.10. Sliding-rolling ratio of Biotech TP P/S model

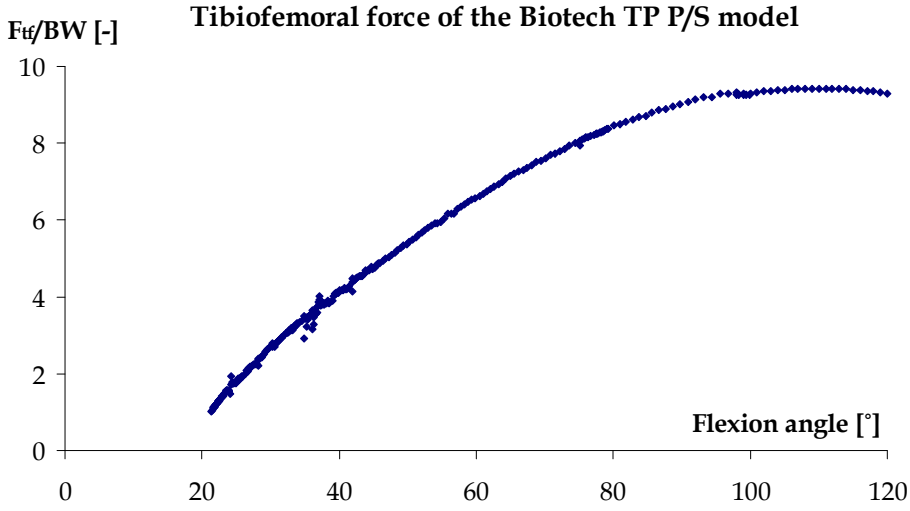

Figure 4.11. Tibiofemoral force of Biotech TP P/S model

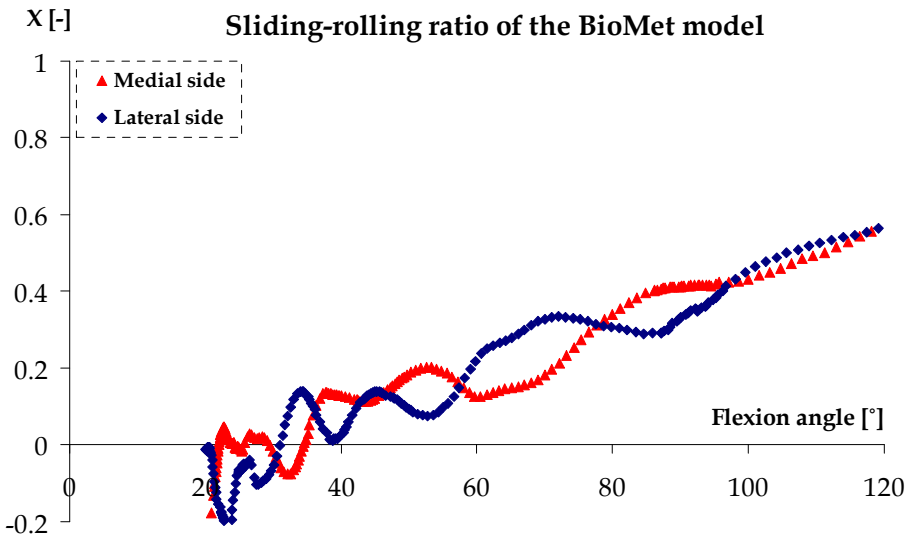

Figure 4.12. Sliding-rolling ratio of BioMet Oxford model

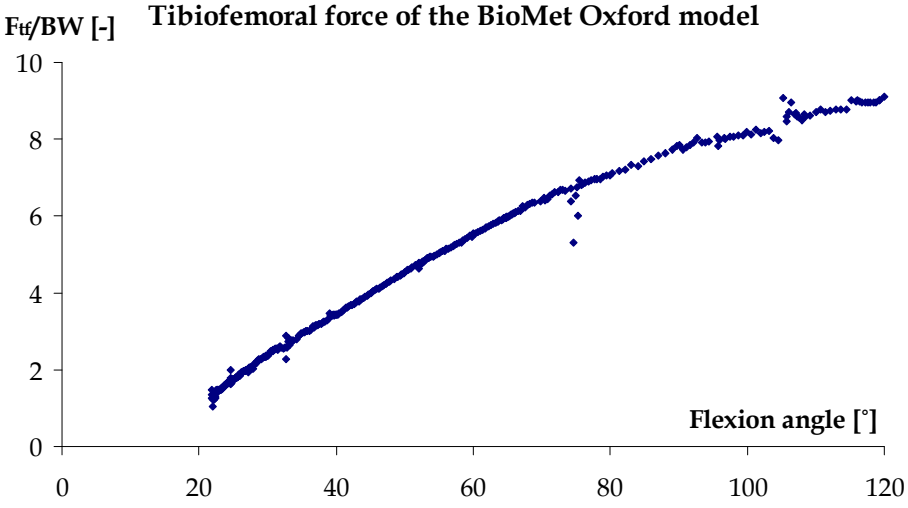

Figure 4.13. Tibiofemoral force of BioMet Oxford model

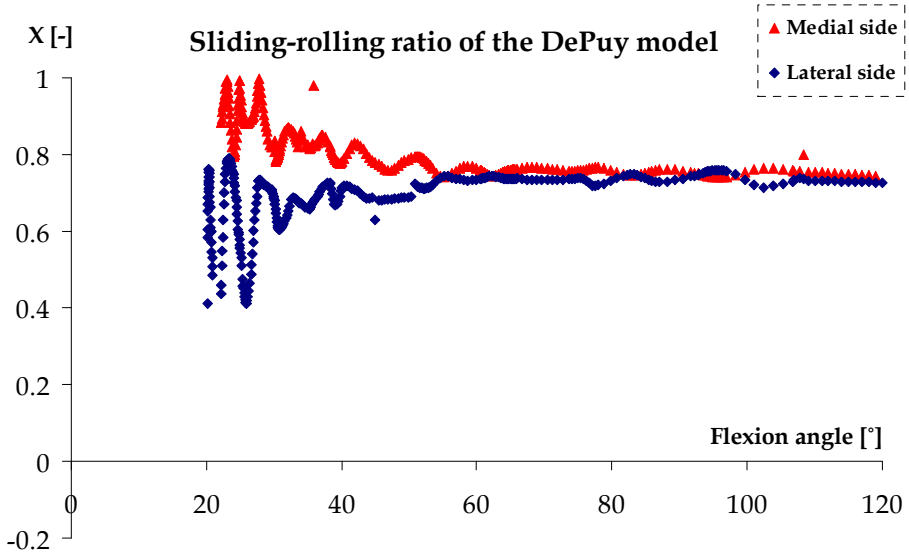

Figure 4.14. Sliding-rolling ratio of DePuy model

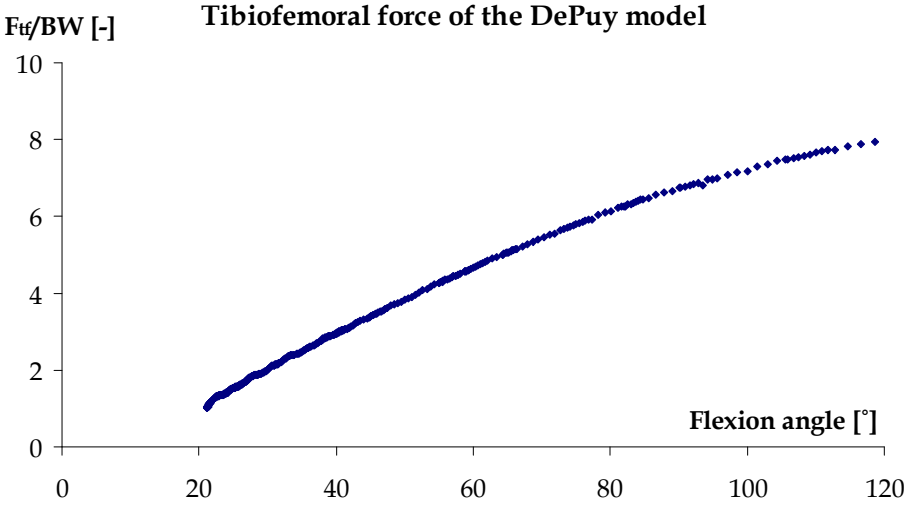

Figure 4.15. Tibiofemoral force of DePruy model

4.2.2. Discussion and interpretation of the results

Let us first look at the magnitude and the pattern of the sliding-rolling ratio of the different prostheses and then at the tibiofemoral contact forces. The calculation of the sliding-rolling is considered on both sides of the condyles (lateral and medial) and involves the slip in every direction (spatial).

In the case of the SZIU prototype model (Figure 4.6), both of the lateral and medial sides start from a positive sliding-rolling ratio of 0.2. The functions gradually increase with occasional irregularities to 0.42 at the medial side and 0.38 at the lateral side.

The irregularity during the motion is originated to the contact of the complex geometries. These mapped geometries are numerically approximated curves, thus their smoothness is also a factor that can cause less smooth functions. In Figure 4.16, an approximated prosthesis curve is visible from the sagittal view. The original analytical curve is represented with continuous line, the tangents with dotted lines, and the numerical curve with a dashed line.

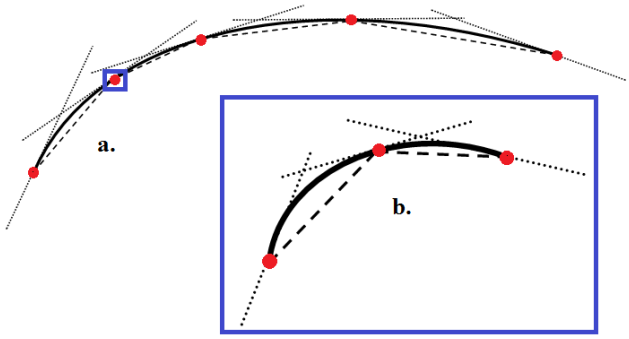

Figure 4.16. Approximated prosthesis curve

As the two bodies establish a contact and they start moving along these curves, the sharp approximating lines (Figure 4.16 a-b) may cause small jumps, skips on the bodies, which appear mainly on the sliding-rolling functions.

If we neglect these irregularities, the increment shows closely linear growth. With regard to the kinetics, namely the tibiofemoral force (Figure 4.7), between the condyles, the evolution of the force can be described as closely linearly increasing, with a maximum of 4.5-8.5 times of the ***BW***.

The Biotech TP and the TP P/S models (Figure 4.8 and Figure 4.10) are from the same manufacturer. They have quite similar characteristics both in their kinematics and their kinetics. In both cases the sliding-rolling evolution is quite smooth along the complete segment (0˚ to 120˚) compared to the SZIU model which is more hectic. However the tibiofemoral force of the TP model (Figure 4.9) is half times lower compared to the TP P/S force (Figure 4.11).

The sliding-rolling curves regarding the TP and TP P/S start approximately from 0.3. From 40-60˚ of flexion angle, the TP and TP P/S functions begin to increase until they reach the maximum sliding-rolling ratio, 0.7 in the case of the TP model and 0.725 in case of the TP P/S on both medial and lateral side.

The BioMet Oxford model (Figure 4.12) has lower sliding attribute, since between 20-60˚ of flexion angle it only reaches the value of 0.2-0.22. It has also the feature of closely linear growth, with minor irregularities, on both sides.

Among the tested prostheses, this replacement provided the lowest peak sliding-rolling value, namely 0.56. As for the kinetics, the tibiofemoral force (Figure 4.13) has the same magnitude as the BioTech TP P/S (Figure 4.11).

While the evolutions of the sliding-rolling functions are somewhat similar regarding the SZIU, Biotech TP- TP P/S or BioMet Oxford models, the DePuy prosthesis (Figure 4.14) follows a completely different pattern. The curve is practically constant, with less than 5% of periodic deviation. The maximum value of the curve is registered at 23˚ of flexion angle at the medial side where it reaches for a short interval the value of one, which means complete sliding. After that the function decreases to an average 0.75. The tibiofemoral force (Figure 4.15) is similar to the BioMet Oxford model (Figure 4.13).

If we compare the magnitude of the lateral and medial sliding-rolling ratio, a slightly higher percentage of sliding can always be credited to the medial compartment. This difference is quite visible for the DePuy or SZIU prosthesis while it is less obvious concerning the Biotech or BioMet models.

This difference was also confirmed by the study of Wilson et al. [Wilson et al., 1998]: from 0˚ to 5˚ of flexion angle the sliding-rolling ratio at the medial side was significantly higher (approximately 1.5-2 times) compared to the lateral side, between 5˚ and 10˚ was about 1-0.5 times and from 20˚ of flexion angle the difference stays in the range of 5-8%. Since in general the sliding-rolling ratio is slightly (5-8%) higher on the medial side, the medial results were taken as reference functions.

By fitting a third-order function on each medial sliding-rolling curve, and summarizing them in one graph, the following results were obtained (Figure 4.17):

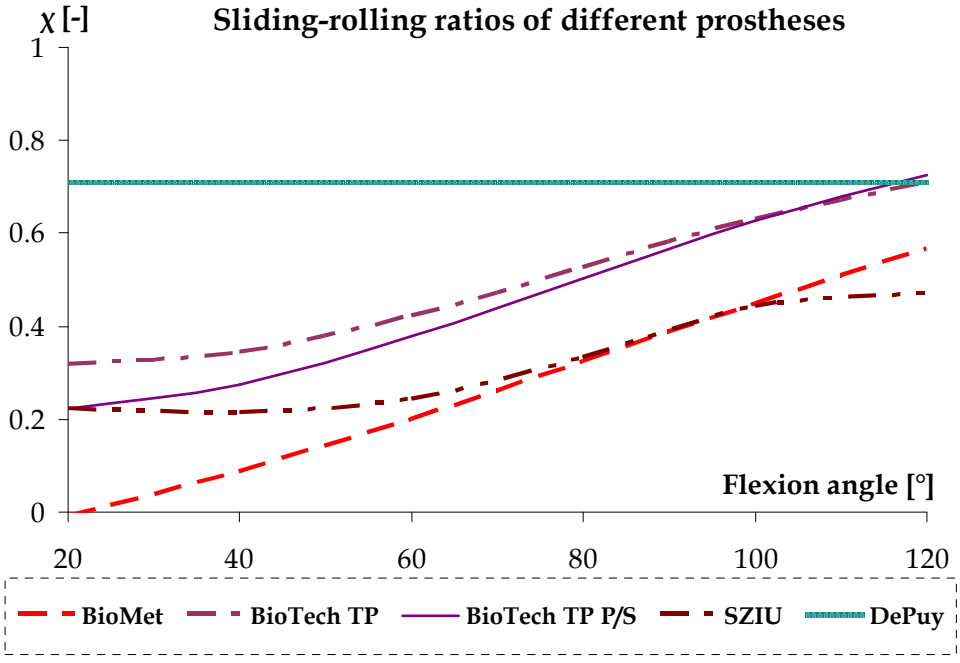

Figure 4.17. Summarized sliding-rolling ratios of the prostheses

From Figure 4.17, a well-visible trend appears along the flexion angle for the SZIU, Biotech TP, Biotech TP P/S and the BioMet Oxford models. The DePuy model although falls completely out of the range, as appears to be a constant function, thus it has been removed from the further investigation.

To generalize the results, the obtained functions have been averaged and the average function has been plotted in Figure 4.18 with the standard deviation.

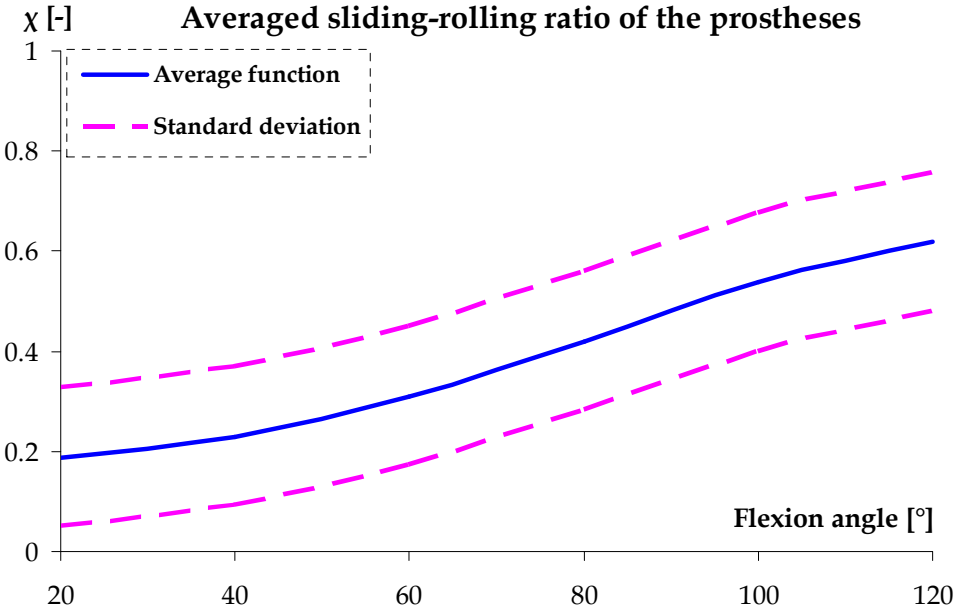

Figure 4.18. Averaged sliding-rolling ratio of the prostheses

The averaged function of the four prostheses (SZIU, Biotech TP, Biotech TP P/S and the BioMet Oxford):

$$\chi(\alpha) = -5.16 \cdot 10^{-7} \cdot \alpha^3 + 1.235 \cdot 10^{-4} \cdot \alpha^2 - 4.113 \cdot 10^{-3} \cdot \alpha + 0.226 \tag{4.3}$$

The function with its standard deviation carves out a well-defined area. Other results from numerical models (ICR approach, semi-3D, etc.) have been added to the obtained functions to see how they correlate with each other (Figure 4.19):

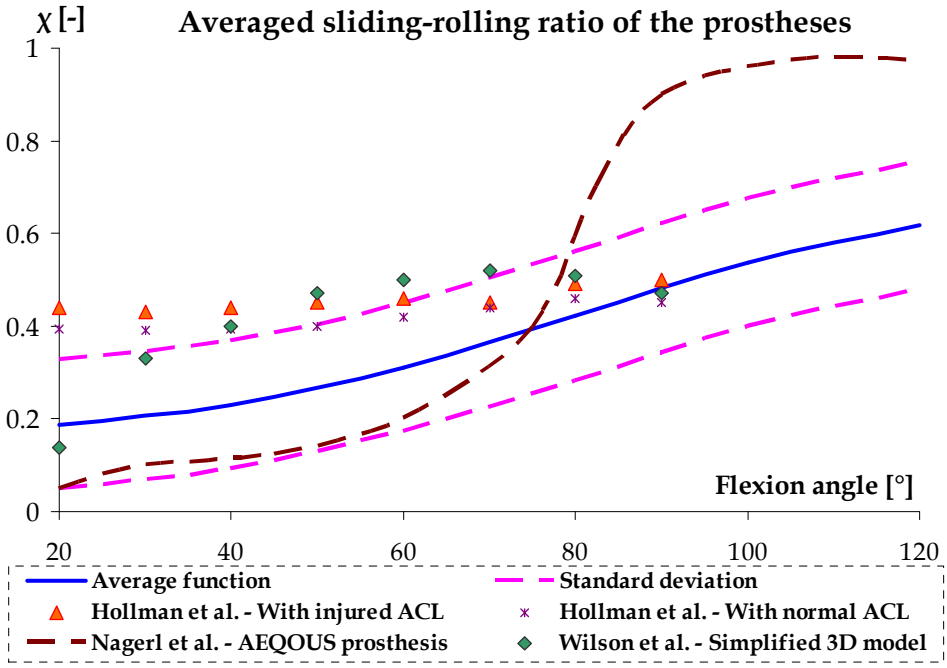

Figure 4.19. Averaged sliding-rolling ratio function with other authors' results

Hollman et al. [Hollman et al., 2002] used the path of instantaneous center of rotation (PICR) method which is a simplified two-dimensional approach that corresponds well with the result of Wilson et al. [Wilson et al., 1998].

Their results situate just a bit higher than the expected domain, and they only reach to 90° of flexion angle.

The difference can be interpreted due to the limitation of their approaches:

Hollman et al. [Hollman et al., 2002] used geometric components which represented averaged joint surface geometry obtained from 3 subjects, sliding and rolling could be calculated only in the sagittal plane, and the joint was considered a single degree of freedom. The carried out motion was a 2-legged sit-to-stand movement.

Wilson et al. [Wilson et al., 1998] carried out passive knee flexion by their model, where the main limitation was the geometry as well, since they used spherical femur condyles with planar tibial condyles.

Both of the authors agreed that their main limitation is the geometry, which might cause that the sliding-rolling ratio is underestimated in the higher flexion angles.

In contrary, Nägerl et al. [Nägerl et al., 2008] used unique prosthesis geometry (AEQUOS-G1), which was designed to maintain primarily rolling attributes during the stance phase in order to avoid wear due to the sliding friction. Their result corresponds well in the lower region, although they assume that the sliding-rolling ratio reaches its maximum already at 90° of flexion angle. A mention must be made: their result represents the result of a single prosthesis.

4.2.2.1. The role of lateral and medial collateral ligaments

As an interesting modelling question, the possible effect of the collateral ligaments has been considered as a factor, which might alter the sliding-rolling ratio. Their important role is undisputable regarding the stability of the knee, but their contribution to the local kinematics (sliding-rolling) is currently unknown. For this reason, three prostheses, with additional collateral ligaments, were examined whether the included ligaments have significant impact on the sliding-rolling between the contact surfaces (Figure 4.20).

Among the prostheses, the SZIU, the DePuy and the Biotech TP P/S models were chosen for further investigation. The SZIU model was considered as being a prototype model while the DePuy and the Biotech TP P/S models for being widely accepted and applied replacements in the practice.

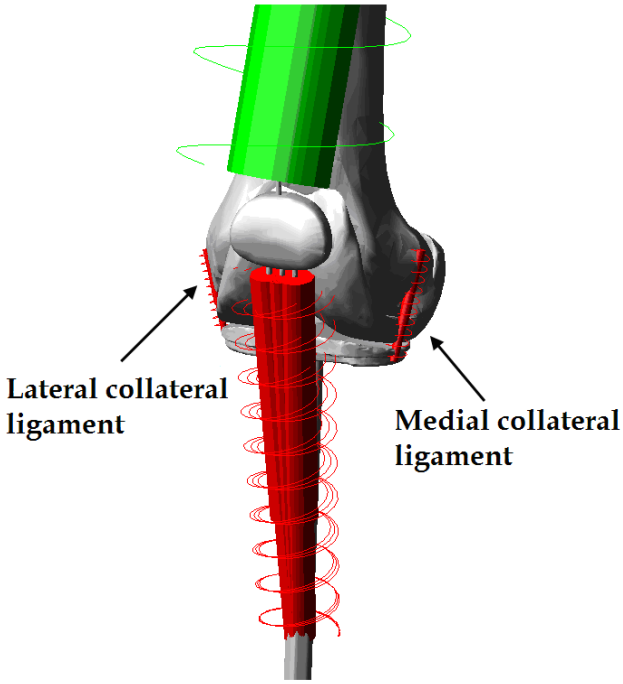

Figure 4.20. MSC.ADAMS model with collateral ligaments

The medial- and lateral collateral ligaments were represented with linear springs with stiffness value of 134 and 114 N/mm and damping constant of 0.15 Ns/mm [Momersteeg et al., 1995]. The contact points were appointed according to the studies of Park et al. [Park et al., 2006] and König et al. [König et al., 2011].

After setting the additional parameters, the simulations were carried out under the same circumstances as before. The following results were obtained:

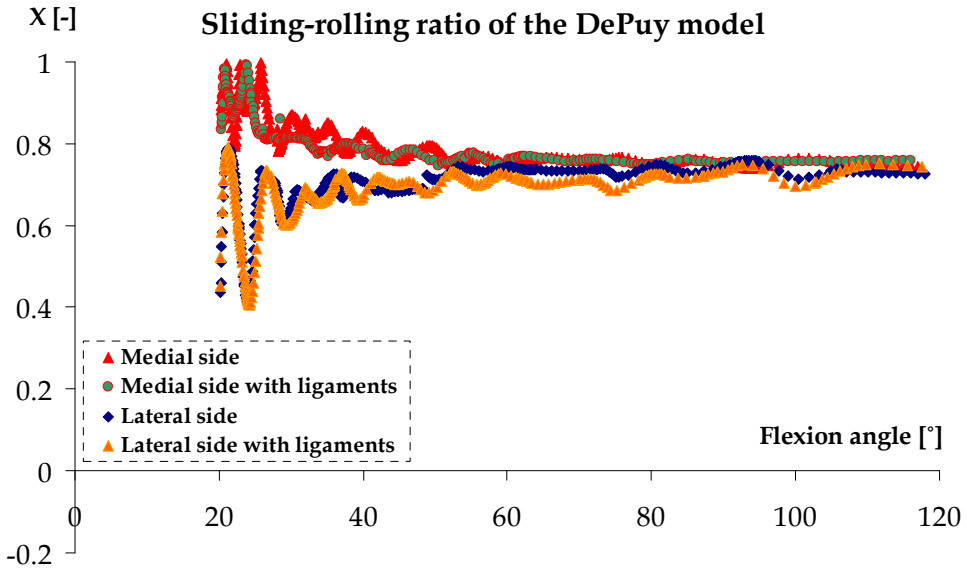

Figure 4.21. Sliding-rolling ratio of DePuy model: with and without collateral ligaments

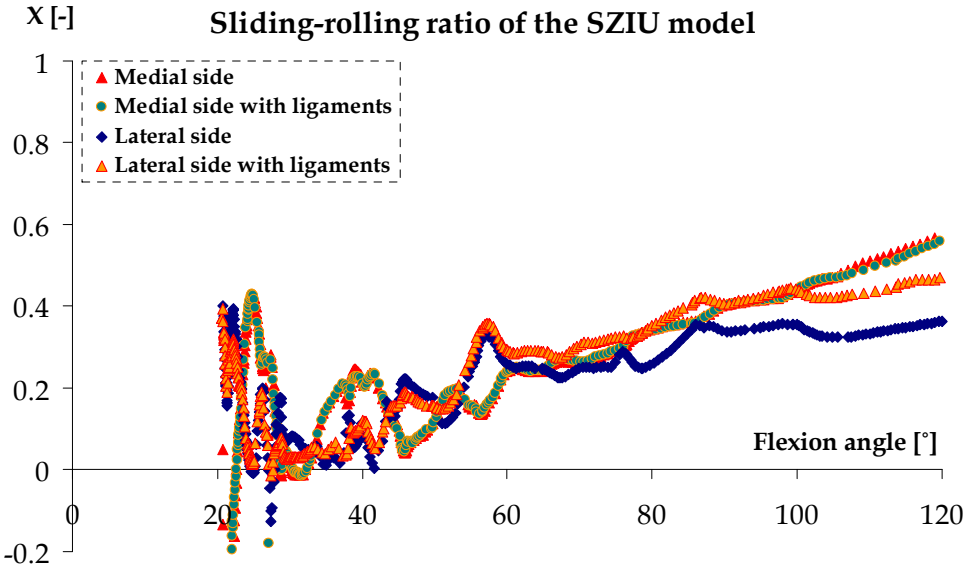

Figure 4.22. Sliding-rolling ratio of SZIU model: with and without collateral ligaments

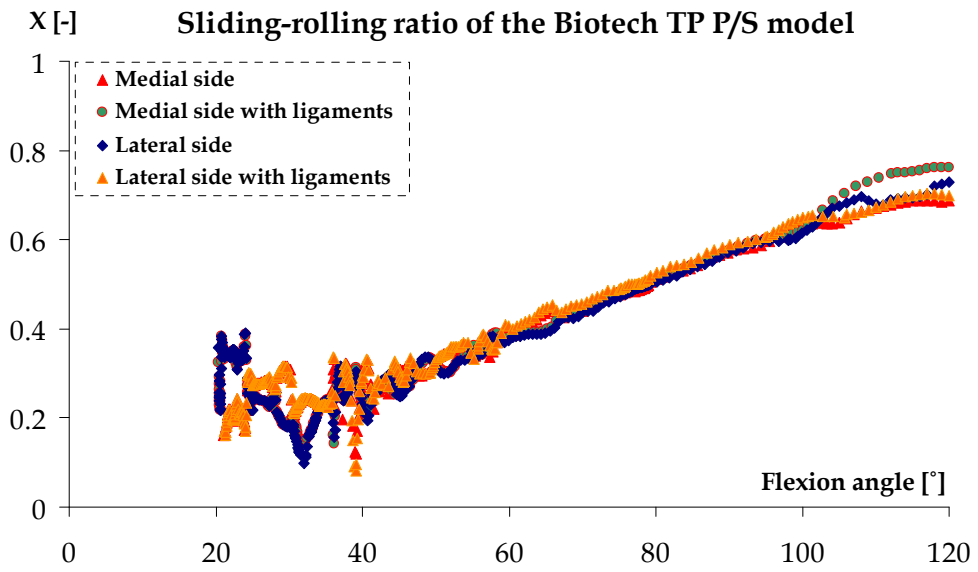

Figure 4.23. Sliding-rolling ratio of Biotech TP P/S model: with and without collateral ligaments

By looking at the DePuy prosthesis (Figure 4.21), no sharp difference can be noticed on the sliding-rolling curves. With or without the collateral ligaments, their magnitude and shape are almost identical.

The SZIU model shows also no remarkable difference on the medial side however some deviation can be observed on the lateral side (Figure 4.22). The sliding-rolling ratios, with and without collateral ligaments, are corresponsive until 60˚ of flexion angle.

Above this certain angle, 5% more sliding appears on the lateral side with collateral ligaments at 60˚ of flexion angle and 10% more at the end phase at 120˚ of flexion angle.

Regarding the Biotech TP P/S replacement, this prosthesis showed also no concrete evidence about the effect of the collateral ligaments on the sliding-rolling phenomenon (Figure 4.23). Up to 105-110˚ of flexion angle the difference is imperceptible, after 110˚ of flexion 8% more sliding appears on the medial side with collateral ligaments and 4% on the lateral side without ligaments. Nevertheless, these differences develop in such a short segment (between 110˚ and 120˚ of flexion angle) combined with very low magnitude that this deviation can be safely disregarded.

As a summary, it can be concluded that except the SZIU model, no concrete evidence could be observed regarding the effect of collateral ligaments on the sliding-rolling ratios. The more observable deviation on the SZIU model is very likely attributed to its design, since the prosthesis at issue is a prototype.

4.3. New scientific results

The new scientific results of this doctoral work can be summarized as follows:

1st Thesis: A new analytical-kinetical model has been created that can provide closed-form solutions regarding the patellofemoral and tibiofemoral forces. The new model takes the horizontal movement of the center of gravity, as a new parameter in the squat literature, into account. It has also been proven by this model that this new parameter has a significant effect on the patellofemoral kinetics.

By taking into consideration the earlier published knee models, a new analytical-kinetical model has been created which involves 7 anthropometrical parameters in order to describe the evolution of the patellofemoral and tibiofemoral forces between 0° and 120° of flexion angle. The model can calculate the forces with respect to standard and non-standard squat.

$$\frac{F_{pt}(\alpha)}{BW} = \frac{\lambda_1(\alpha) \cdot \sin\gamma(\alpha)}{\lambda_p \cdot \sin\beta(\alpha) + \lambda_t \cdot \cos\beta(\alpha)} \tag{3.3}$$

$$\frac{F_{tf}(\alpha)}{BW} = \frac{F_{pt}}{G} \cdot \frac{\cos\beta(\alpha)}{\cos\varphi(\alpha)} + \frac{\cos\gamma(\alpha)}{\cos\varphi(\alpha)} \tag{3.7}$$

$$\frac{F_q(\alpha)}{BW} = \frac{\lambda_3(\alpha) \cdot \sin\left(\alpha - \gamma(\alpha)\right)}{\lambda_f} \tag{3.9}$$

$$\frac{F_{pf}(\alpha)}{BW} = \frac{\sqrt{F_q(\alpha)^2 + F_{pt}(\alpha)^2 - 2 \cdot F_q(\alpha) \cdot F_{pt}(\alpha) \cdot \cos(\beta(\alpha) + \delta(\alpha) + \gamma(\alpha))}}{G} \tag{3.12}$$

Applicabilty limit of the model: $0° \leq \alpha \leq 120°$

2nd Thesis: By means of experimental methods the horizontal movement of the center of gravity during non-standard squat has been experimentally described as a function of flexion angle.

As a parameter in demand for the analytical-kinetical model, the center of gravity functions were determined by experimental methods carried out on 16 human subjects, under non-standard squatting motion. The human subjects had to carry out the movement under certain conditions (stretched out hands, adjusted heels, holding the position for 3 second), thus the functions describe one certain squatting motion.

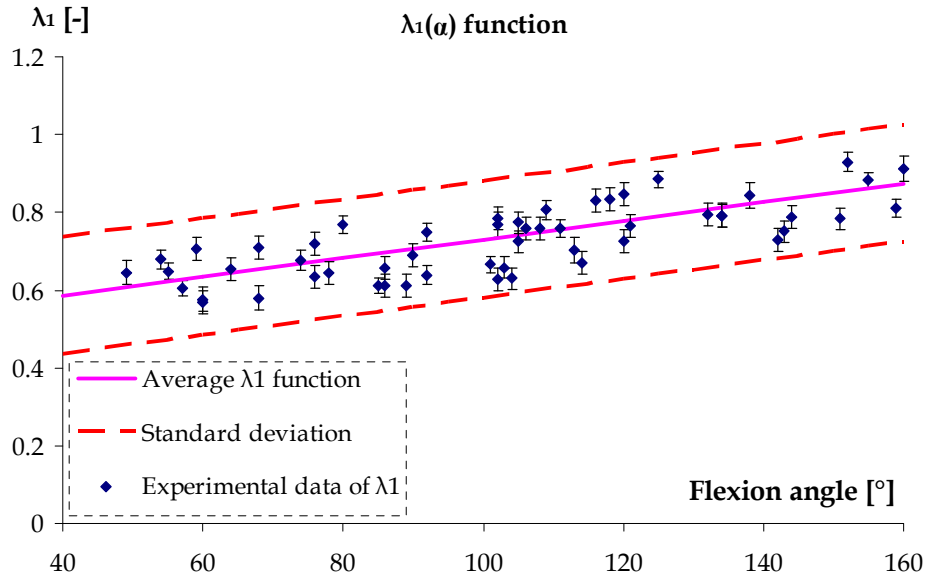

$$\lambda_1(\alpha) = 0.0024 \cdot \alpha + 0.4925 \pm t \cdot s_{\lambda 1} \tag{3.28}$$

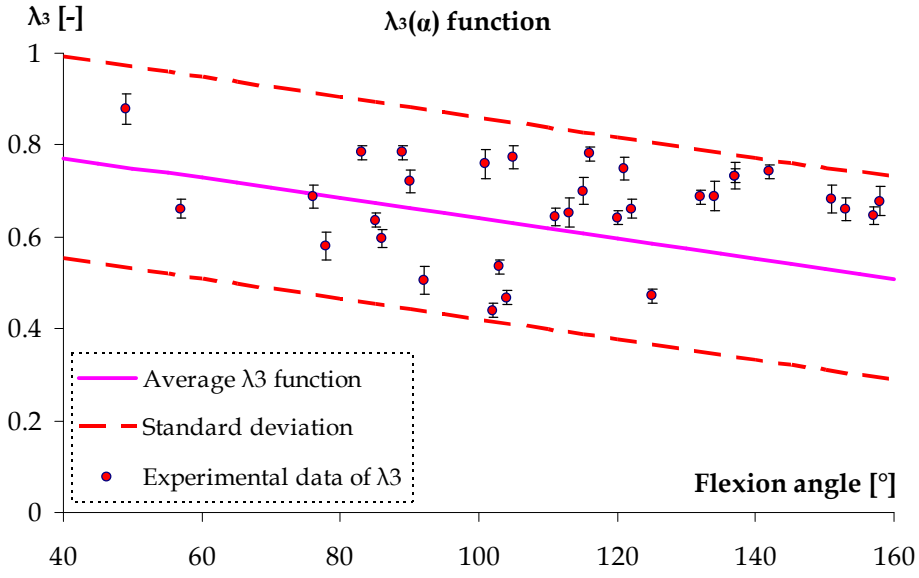

$$\lambda_3(\alpha) = -0.0022 \cdot \alpha + 0.86 \pm t \cdot s_{\lambda 3} \tag{3.29}$$

Observation limit: $40^\circ \leq \alpha \leq 160^\circ$

3rd Thesis: Based on the multibody approach, the sliding-rolling ratio between the contact surfaces has been numerically determined along the complete functional arc with regard to actual prosthesis geometries.

The sliding-rolling ratio (with its maximum and minimum values) on both lateral and medial side has been determined by the use of commercial prosthesis models. Earlier, the ratio was only known in the initial movement ($0^\circ \leq \alpha \leq 20\text{-}30^\circ$) thus now the phenomenon, and its evolution, has been described, under certain circumstances, along the complete functional arc of the knee joint.

$$\chi(\alpha) = -5.16 \cdot 10^{-7} \cdot \alpha^3 + 1.235 \cdot 10^{-4} \cdot \alpha^2 - 4.113 \cdot 10^{-3} \cdot \alpha + 0.226 \tag{4.3}$$

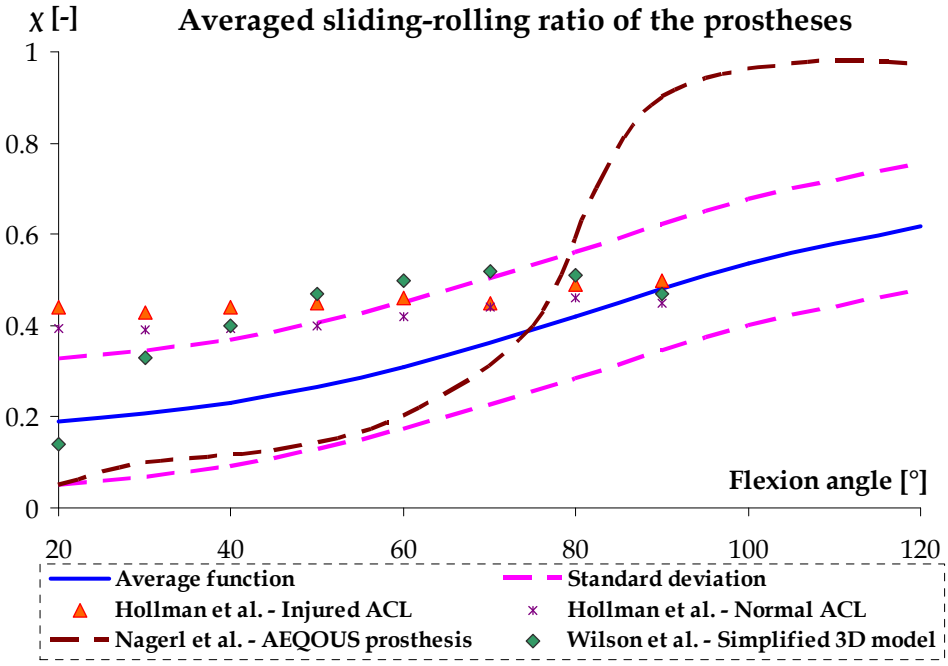

Applicability limit of the model: $20^\circ \leq \alpha \leq 120^\circ$

5. CONCLUSIONS AND SUGGESTIONS

Conclusions regarding the analytical-kinetical model

In summary, a new analytical-kinetical model is presented which draws the attention to the effect of moving center of gravity on the knee joint kinetics. The difference, if this parameter is considered, has been well-demonstrated as the new analytical-kinetical model was compared to the model of Mason et al. [Mason et al., 2008].

Compared to other models, the analytical-kinetical allows the prediction of the patellofemoral, tibiofemoral, patellar tendon and quadriceps forces in the knee joint under standard- and non-standard squatting motion. In addition, while the inverse dynamics method requires expensive measuring system and programs to determine the forces, this new model gives accurate results by simple equations.

The model was derived by equilibrium equations and experimentally determined parameters based on multiple human participants. The obtained results showed good accordance with the compared inverse dynamics results from the available literature.

Among the patello- and tibiofemoral forces, the obtained $\boldsymbol{F_q}(\alpha)$ force function can be extended for further use as an input function for isometric motion, since most descriptive relationships found in the literature provide only the ratio of the patellofemoral forces divided by the quadriceps force.

Suggestions regarding the analytical-kinetical model

The new analytical-kinetical model is a good basis for including other relevant parameters (e.g. the line of action of the quadriceps force is not parallel with the femoral axis, speed-dependent displacement of the center of gravity, etc.) to study the squatting movement. In its current form, it would be also capable to model the ascending and descending motion of rising from a chair if the line of action of the center of gravity, by similar measurement was carried out.

The significance of analytical models is unambiguous since the effect and the mathematical connection of each parameter can be directly observed and studied.

Although the new analytical-kinetical model corresponds well with the results from the literature, an experimental test setup, which includes all the seven parameters (or preferably other optional parameters as well), would be very useful to verify the obtained results by direct measurements.

Among the simplifications, the one degree-of-freedom connection (hinge connection) should be reconsidered in order to make the force prediction more realistic. One possible solution could be the incorporation of the instantaneous contact points between the tibiofemoral and patellofemoral surface similarly to the study of Nisell et al. [Nisell et al., 1986]. By doing so, on the one hand the connection would be more accurately modeled and on the other hand, since contact points would be appointed, connection with friction could be taken into account.

Conclusions regarding the numerical-kinematical model

Sliding-rolling phenomenon related to the human knee joint has been only researched by means of two- or semi-three-dimensional models where the geometry of the knee joint was considerably simplified.

By this new model two, long-standing restrictions in the knee joint modelling were eliminated. These restrictions were were the simplified geometry and the absence of friction. The presented multibody models include both the three-dimensional geometry and the effect of friction as well. Moreover, the effect of collateral ligaments on the sliding-rolling ratio has been also analyzed. The multibody models showed a convincing trend regarding the sliding-rolling ratio, which so far has not been studied in such depth.

By using stereophotogrammetry rendering, several currently used prosthesis geometries were mapped and five multibody models were created in order to analyze the evolution of the sliding-rolling phenomenon.

As a conclusion of the numerical results, an averaged third-order function has been created with its standard deviation along the active functional arc of the knee joint. In addition, the sliding-rolling curves of the individual knee replacements were also plotted in the interest of showing the differences between the examined prostheses regarding the local kinematics. Results from the available literature were plotted together with the obtained numerical results.

By reading the results, we can conclude that the new numerical model and the model of Nägerl et al. [Nägerl et al., 2008] have a somewhat similar trend that starts from moderately low values, which can be interpreted that at lower flexion angle rolling dominates the motion, while at higher flexion angles sliding gradually increases and prevails. This natural transition is well visible in both cases, while it does not appear in the results of Hollman et al. [Hollman et al., 2002], or only slightly in case of Wilson et al. [Wilson et al., 1998] who state that maximum of the sliding-rolling ratio is around 0.4-0.45.

The lack of the transition can be originated in both cases to the simplified geometry and the diversity of the motion, which makes the new numerical model more realistic. In addition, except Nägerl et al. [Nägerl et al., 1998] no authors consider higher sliding-rolling ratio than 0.45, while according to our model the ratio can easily reach 0.6, or in some cases 0.75, between 110˚ and 120˚ of flexion angle.

Another pro beside the new numerical model and the model of Nägerl et al. [Nägerl et al., 1998], that above 90˚ of flexion angle the two other models [Wilson et al., 1998, Hollman et al., 2002] do not provide any information about the sliding-rolling ratio.

The obtained results can be beneficial for the practice in the field of total knee replacements: as it was concluded by McGloughlin and Kavanagh [McGloughlin and Kavanagh, 1998], higher sliding-rolling ratio generates higher wear rate, thus depending on the testing angle, a proper ratio has to be applied during tribological tests.

The currently determined pattern (Figure 4.18), based on the five different prosthesis geometries, can provide a future limit for experimental tests related to applicable sliding-rolling ratio with the actual load. These applicable loads are represented in this thesis as tibiofemoral forces.

Suggestions regarding the numerical-kinematical model

The multibody model includes even more possibilities for further development. In our current model, there are several tasks which should be closely investigated in the near future:

- The cruciate ligaments of the knee joint have not been considered in our simulations, thus it is adequate to complement the multibody model with these ligaments,
- Analysis of the anatomical angles such as the rotation, abduction, adduction,
- The horizontal movement of the center of gravity has not yet been implemented into the multibody model,
- The effect of the ratio of the frictional coefficient on the sliding-rolling pheonomeon has not been investigated (different static/dynamic friction coefficient ratios).

After this small list, let us discuss these options in details.

The task of the ligaments is twofold. Partly, they maintain the stability of the knee joint under various kinds of motions, while they also control it in a certain level. There is a debate about whether the connecting surfaces of the femur and tibia or the ligaments have more control over the carried out movements. By involving the medial and lateral cruciate ligaments, it would be possible to analyze how the local motion, the sliding-rolling ratio, changes and in this manner, conclusions could be drawn about the control role of the ligaments.

Although, no anatomical angles have been studied thoroughly in this thesis, it has been planned to carry out simulations as verification for experimental tests. At the Szent István University, a biomechanical research group is engaged in kinematical testing of both commercial and prototype prostheses. One the one hand, the aim is to measure the rotation, abduction and adduction as a function of flexion angle and the applied load, and on the other hand to classify these prostheses depending on the above-mentioned kinematical quantities. The introduced multibody model, with some modification regarding the initial conditions and the constraints, can be an efficient and versatile tool for such examination.

The horizontal movement of the center of gravity has unequivocal impact on the kinetics of the human knee joint, which has been demonstrated on the analytical-kinetical model. Naturally these results should be expanded to the multibody model as well, therefore it would visible how this new factor influences the sliding-rolling ratio, the contact forces and the anatomical angles.

The impact of different sets of friction conditions on the local kinematics is also an important question which can indirectly provide information about wear. The connection between these important parameters could be unfolded by changing the ratio of the static and dynamic friction.

The connection between the sliding-rolling ratio and the anatomical angles clearly show how much control the surface connection has on the kinematics of the knee joint. By studying this relationship, the ultimate role, or a sort of ratio of the roles could be settled between the ligaments and the connecting surfaces.

6. SUMMARY

In this doctoral thesis, two novel mechanical models were presented: an analytical-kinetical model with regard to the kinetics of the human knee joint under non-standard squatting, and a numerical-kinematical model with regard to the local kinematics of the knee joint under standard squatting.

The new analytical-kinetical model is capable to calculate the patellofemoral, tibiofemoral, patellar tendon and quadriceps forces in the knee joint under different squatting motions. The results of this model showed that a moderate trunk motion, the horizontal movement of the center of gravity, decreases the forces approximately 25% in the knee joint. The published results are in good agreement with the compared inverse dynamics results taken from the literature.

The main advantage and value of the presented model, that while the inverse dynamics method requires expensive measuring system and programs to determine the forces, our new model gives accurate results by simple algebraic equations. Through the approach of the modelling and the creation of the equations, similar modelling issues become more understandable and solvable.

The second aim of the thesis was to unfold the sliding-rolling phenomenon related to the currently applied knee prostheses under standard squatting movement. The phenomenon, which has been so far not studied in such depth regarding knee prostheses, was addressed by means of multibody models, which considered real three-dimensional geometries, the effect of friction between the condyles, and collateral ligaments as well. The sliding-rolling ratio functions, derived from the multibody models, showed a convincing trend.

As a conclusion of the numerical results, an averaged third-order function has been created with its standard deviation along the active functional arc of the knee joint. In addition, the sliding-rolling curves of the individual knee replacements were also determined in the interest of showing the differences between the examined prostheses regarding the local kinematics.

The obtained results can be beneficial for the practice in the field of total knee replacements as well: as it was concluded by McGloughlin and Kavanagh [McGloughlin and Kavanagh, 1998], higher sliding-rolling ratio generates higher wear rate, thus depending on the testing angle, a proper ratio has to be applied during tribological tests.

The currently determined pattern based on the five different prosthesis geometries, can provide a future limit for experimental tests related to applicable sliding-rolling ratio with the actual load. These applicable loads are represented in this thesis as tibiofemoral forces.

7. ÖSSZEFOGLALÁS (SUMMARY IN HUNGARIAN)

Ezen doktori disszertációban két új mechanikai modell került bemutatásra: egy analitikai-kinetikai modell, amely a térdizületben kialakuló erőviszonyokat hivatott vizsgálni nem-standard guggolás során, illetve egy numerikus-kinematikai modell, amely a standard guggolás közben a térdizületben lezajló lokális mozgásokat (csúszva-gördülés) képes meghatározni.

Az új analitikai-kinetikai modell segítségével a patellofemorális-tibiófemorális erők, valamint a patelláris- illetve a quadricepsz szalagban ébredő erők pontosan meghatározhatóak különféle guggoló mozgás során. Az eredmények azt mutatják, hogy a torzó mérsékelt előredőlése – a súlyvonal horizontális irányú elmozdulása – megközelítőleg 25%-al csökkenti a térdizületben ébredő erőket. A közölt eredmények jó egyezést mutatnak az irodalomban található inverz dinamikai mérésekkel.

Legfőbb értéke és előnye a modellnek, hogy míg az inverz dinamikai mérések kivitelezéséhez költséges mérőeszközök és programok szükségesek, addig az újonnan közölt modell megfelelő eredményeket szolgáltat egyszerű algebrai egyenletek segítségével. Emellett, a modellezési eljárás keretében hasonló problémák válnak érthetőbbé és megoldhatókká.

A disszertáció második felében a kereskedelmi protézispárok (femur-tíbia kapcsolat) között fellépő csúszva-gördülés jelenségének meghatározása volt a cél, standard guggoló mozgás során. A jelenség, amelyet ilyen mélységben még nem tanulmányoztak protézisekkel kapcsolatban, multibody modellek segítségével került vizsgálatra, amelyek figyelembe vették a valóságos háromdimenziós geometriát, a súrlódás jelenségét az érintkező felületeken között, valamint a kollaterális szalagokat. A multibody modellek által meghatározott csúszva-gördülési függvények meggyőző trendet mutattak.

A numerikus-kinematikai modell alapján a térdizület teljes funkcionális szakaszára vonatkozóan egy harmadfokú, átlagolt csúszva-gördülési függvény jött létre. Emellett, az egyes protézisek csúszva-gördülési függvénye is közlésre került a különböző protézisek közötti lokális kinematikai különbségek bemutatása céljából.

Az eredményeknek komoly jelentősége lehet a térdizülethez kapcsolódó protézisek területén: McGloughlin és Kavanagh [McGloughlin és Kavanagh, 1998] következtetései alapján a magasabb csúszva-gördülési arány, nagyobb kopást eredményez, így tribológiai vizsgálatok során, a behajlítási szög függvényeként megfelelő csúszva-gördülési arányt kell megadni.

Az öt protézisgeometria alapján meghatározott trend a kísérleti vizsgálatoknál alkalmazott jövőbeni csúszva-gördülési értékekre ad egy alkalmazható határt, a közben fellépő terheléssel együtt. Ezek az alkalmazandó terhelések, tibiofemorális erőként vannak feltüntetve a disszertációban.

APPENDIX

A1. Bibliography

[1] **Abdel-Rahman E. M., Hefzy M. S.**: Three-dimensional dynamic behaviour of the human knee joint under impact loading. *Medical Engineering and Physics*, 20 (4), 276–290, 1998.

[2] **Abe M., Masani K., Nozaki D., Akai M., Nakazawa K.**: Temporal correlations in center of body mass fluctuations during standing and walking. *Human Movement Science*, 29 (4), 556-566, 2010.

[3] **Ahmed A. M., Burke D. L., Yu A.**: In-vitro measurement of static pressure distribution in synovial joints - Part II: Retropatellar surface. *Journal of Biomechanical Engineering*, 105 (3), 226-236, 1983.

[4] **Amis A. A., Farahmand F.**: Biomechanics of the knee extensor mechanism. *The Knee*, 3 (1-2), 73-81, 1996.

[5] **Andriacchi T. P., Andersson G. B. J., Fremier R. W., Stern D., Galante J. O.**: A study of lower limb mechanics during stair climbing. *The Journal of Bone and Joint Surgery*, 62 (5)-A, 749-757, 1980.

[6] **Andriacchi T. P., Dyrby C. O., Johnson T. S.**: The use of functional analysis in evaluating knee kinematics. *Clinical Orthopaedics and Related Research*, 410, 44-53, 2003.

[7] **Andriacchi T. P., Mikosz R. P., Hampton S. J., Galante J. O.**: Model studies of the stiffness charachteristics of the human knee joint. *Journal of Biomechanics*, 16 (1), 23-29, 1983.

[8] **Baldwin M. A., Clary C., Maletsky L. P., Rullkoetter P. J.**: Verification of predicted specimen-specific natural and implanted patellofemoral kinematics during simulated deep knee bend. *Journal of Biomechanics*, 42 (14), 2341-2348, 2009.

[9] **Bandi W.**: Chondromalacia Patellae und Femoro-Patellare Arthrose. *Helvetica Chirurgica Acta*, Suppl. 11, 1972.

[10] **Bishop R. E. D., Denham R. A.**: A note on the ratio between tensions in the quadriceps tendon and infra-patellar ligament. *Engineering in Medicine*, 6 (2), 53-54, 1977.

[11] **Bíró I., Csizmadia B. M., Katona G.**: Sensitivity invsestigation of three-cylinder model of human knee joint. *Biomechanica Hungarica*, 3 (1), 33-42, 2010.

[12] **Blackburn J., Qureshi A., Amirfeyz R., Bannister G.**: Does preoperative anxiety and depression predict satisfaction after total knee replacement? *The Knee*, 19 (5), 522-524, 2012.

[13] **Blankevoort L., Kuiper J. H., Huiskes R., Grootenboer H. J.**: Articular contact in a three-dimensional model of the knee. *Journal of Biomechanics*, 24 (11), 1019–1031, 1991.

[14] **Blunn G. W., Joshi A. B., Lilley A. P., Engelbrecht E., Ryd L., Lidgren L., Walker P. S.**: Polyethylene wear in unicondylar knee prostheses. *Acta Orthopaedica Scandinavica,* 63 (3)*,* 247-255, 1992.

[15] **Blunn G. W., Lilley A. P., Walker P. S.**: Variability of the wear of ultra high molecular weight polyethylene in simulated TKR. *Transactions of the Orthopaedic Research Society*, 40, 177, 1994.

[16] **Blunn G. W., Walker P. S., Joshi A. B.**: The dominance of cyclic sliding in producing wear in total knee replacements. *Clinical Ortopeadics and Related Research*, 273, 253-260, 1991.

[17] **Box G.**: Non-normality and tests on variances. *Biometrika*, 40 (3-4), 318-335, 1953.

[18] **Bresler B., Frankel J. P.**: The forces and moment in the leg during level walking. *Transactions of American Society of Medical Engineers*, 72 (27), 25-35, 1950.

[19] **Buff H. U., Jones L. C., Hungerford D. S.**: Experimental determination of forces transmitted through the patello-femoral joint. *Journal of Biomechanics*, 21 (1), 17-23, 1988.

[20] **Caron O., Faure B., Brenière Y.**: Estimating the centre of gravity of the body on the basis of the centre of pressure in standing posture. *Journal of Biomechanics*, 30 (11-12), 1169-1171, 1997.

[21] **Chao E. Y. S.**: Graphic-based musculoskeletal model for biomechanical analyses and animation. *Medical Engineering and Physics*, 25 (4), 201–212, 2003.

[22] **Chittajallu S. K., Kohrt K. G.**: FORM 2D – A mathematical model of the knee. *Mathematical and Computer Modelling*, 24 (9), 91-101, 1999.

[23] **Churchill D. L., Incavo S. J., Johnson C. C., Beynnon B. D.**: The transepicondylar axis approximates the optimal flexion axis of the knee. *Clinical Orthopaedics*, 356, 111–118, 1998.

[24] **Churchill D. L., Incavo S. J., Johnson C. C., Beynnon B. D.**: The influence of femoral rollback on patellofemoral contact loads in total knee arthroplasty, *Journal of Arthroplasty*, 16 (7), 909-918, 2001.

[25] **Cohen Z. A., Henry J. H., McCarthy D. M., Mow V. C., Ateshian G. A.**: Computer simulations of patellofemoral joint surgery: Patient-specific models for tuberosity transfer. *The American Journal of Sports Medicine*, 31 (1), 87–98, 2003.

[26] **Cohen Z. A., Roglic H., Grelsamer R. P., Henry J. H., Levine W. N., Mow V. C., Ateshian G. A.**: Patellofemoral stresses during open and closed kinetic chain exercises – An analysis using computer simulation. *The American Journal of Sports Medicine*, 29 (4), 480-487, 2001.

[27] **Conceição F., Sousa F., Gonzçalves P., Carvalho J. M., Vilas-Boas J. P.**: In vivo stiffnes evaluation of human tendons. 20th International Symposium on Biomechanics in Sports, ISSN 1999-4168, Cáceres, Spain, 2002.

[28] **Crowninshield R., Pope M. H., Johnson R. J.**: An analytical model of the knee. *Journal of Biomechanics*, 9 (6), 397-405, 1976.

[29] **Csizmadia B. M., Nádori E.**: Mozgástan (Dynamics), Course book. Editor: B. M. Csizmadia, E. Nádori. Nemzeti Tankönyvkiadó (National Course book Press), Budapest, Hungary, 1997.

[30] **Csizmadia B. M., Nándori E.**: Statika (Statics), Course book. Editor: B. M. Csizmadia, E. Nándori. Nemzeti Tankönykiadó (National Coursebook Press), Budapest, Hungary, 2009.

[31] **Csizmadia B. M., Nándori E.**: Modellalkotás (Model creation), Coursebook. Editor: B. M. Csizmadia, E. Nándori. Nemzeti Tankönyvkiadó (National Coursebook Press), Budapest, Hungary, 2003.

[32] **Csizmadia B. M.**: Kísérletek tervezése (Experiment planning), In: Bevezetés a kutatásba (Introduction to research), Coursebook. Editor: László Csorba. GATE Kiadó (GATE Press), Gödöllő, Hungary, 1998.

[33] **D'Lima D. D., Poole C., Chadha H., Hermida J. C., Mahar A., Colwell C. W. J.**: Quadriceps moment arm and quadriceps forces after total knee arthroplasty. *Clinical Orthopaedics and Related Resarch*, 392, 213–220, 2001.

[34] **Dahlqvist N. J., Mayo P., Seedhom B. B.**: Forces during squatting and rising from a deep squat. *Engineering Medicine*, 11 (2), 69-76, 1982.

[35] **Dandy D. J., Desai S. S.**: Patellar tendon length after anterior cruciate ligament reconstruction. *The Journal of Bone and Joint Surgery*, 76 (2)-B, 198-199, 1994.

[36] **Davidson J. A., Mishra A. K., Poggie R. A., Werr J. I.**: Sliding friction and UHMWPE wear comparison between cobalt alloy and zirconia surfaces. *Transactions of the Orthopaedic Research Society*, 38, 404, 1992.

[37] **Dempster W. T.**: Space requirements of the seated operator. Geometrical, kinematic and mechanical aspects of the body with special references to the limbs. *WADC Technical Report*, 55-159, 1955.

[38] **Denham R. A., Bishop R. E. D.**: Mechanics of the knee and problems in reconstructive surgery. *The Journal of Bone and Joint Surgery*, 60 (3)-B, 345-352, 1978.

[39] **Dhaher Y. Y., Kahn L. E.**: The effect of vastus medialis forces on patello-femoral contact: a model-based study. *Journal of Biomechanical Engineering*, 124 (6), 758–767, 2002.

[40] **Didden K., Luyckx T., Bellemans J., Labey L., Innocenti B., Vandenneucker H.**: Anteroposterior positioning of the tibial component and its effect on the mechanics of patellofemoral contact. *The Journal of Bone and Joint Surgery*, 92 (10)-B, 1466-1470, 2010.

[41] **Eames M., Cosgrove A., Baker R**.: Comparing methods of estimating the total body centre of mass in three dimensions in normal and pathological gaits. *Human Movement Science*, 18 (5), 637-646, 1999.

[42] **Ellis M. I., Seedhom B. B., Amis A. A., Dowson D., Wright V.**: Forces in the knee joint whilst rising from normal and motorised chairs. *Engineering Medicine*, 8 (1), 33-40, 1979.

[43] **Ericson M. O., Nisell R.**: Patellofemoral joint forces during ergometer cycling. *Physical Therapy*, 67 (9), 1365-1369, 1987.

[44] **Escamilla R. F., Zheng N., MacLeod T. D., Edwards W. B., Hreljak A., Fleisig G. S., Wilk K. E., Moorman III C. T., Imamura R.**: Patellofemoral compressive force and stress during the forward and side lunges with and without stride. *Clinical Biomechanics*, 23 (8), 1026-1037. 2008.

[45] **Essinger J. R., Leyvraz P. F., Heegard J. H., Robertson D. D.**: A mathematical model for the evaluation of the behaviour during flexion of condylar-type knee prosthesis. *Journal of Biomechanics*, 22 (11-12), 1229-1241, 1989.

[46] **Ethgen O., Bruyere O., Richy F., Dardennes C., Reginster J. Y.**: Health-related quality of life in total hip and total knee arthroplasty. A qualitative and systematic review of the literature. *The Journal of Bone and Joint Surgery*, 86 (5)-A, 963-974, 2004.

[47] **Euler L.**: De aptissima figura rotarum dentibus tribuenda (On finding the best shape for gear teeth). Novi Commentarii academiae scientiarum Petropolitanae, 5, 299-316, St. Petersburg, Russia, 1760.

[48] **Farrokhi S., Pollard C. D., Souza R. B., Chen Y. J., Reischl S., Powers C. M.**: Trunk position influences the kinematics, kinetics, and muscle activity of the lead lower extremity during forward lunge excercise. *The Journal of Orthopaedic and Sports Physical Therapy*, 38 (7), 403-409, 2008.

[49] **Frankel V. H., Burnstein A. H., Brooks D. B.**: Biomechanics of internal dearangement of the knee. Pathomechanics as determined by analysis of the instant centers of motion. *The Journal of Bone and Joint Surgery*, 53 (5)-A, 945-962, 1971.

[50] **Freeman M. A. R.**: How the knee moves. *Current Orthopaedics*, 15 (6), 444-450, 2001.

[51] **Fregly B. J., Besier T. F., Lloyd D. G., Delp S. L., Banks S. A., Pandy M. G., D'Lima D. D.**: Grand challenge competition to predict in vivo knee loads. *Journal of Orthopaedic Research*, 30 (4), 503-513, 2012.

[52] **Frigo C., Pavan E. E., Brunner R.**: A dynamic model of quadriceps and hamstrings function. *Gait & Posture*, 31 (1), 100-103, 2010.

[53] **Frohm A., Halvorsen K., Thorstensson A.**: Patellar tendon load in different types of eccentric squats. *Clinical Biomechanics*, 22 (6), 704-711, 2007.

[54] **Froimson M. I., Ateshian G. A., Soslowskyet L. J.**: Quantification of the surfaces and contact areas at the patellofemoral articulation. Proceedings of the Institution of Mechanical Engineers, International Conference. The Changing Role of Engineering in Orthopaedics. Mechanical Engineering Publications, Suffolk, UK, 73-81, 1989.

[55] **Fukagawa S., Leardini A., Callewaert B., Wong P. D., Labey L., Desloovere K., Matsuda S., Bellemans J.**: Age-related changes in kinematics of the knee joint during deep squat. *The Knee*, 19 (3), 208-212, 2012.

[56] **Gandhi R., Davey R., Mahommed N. N.**: Predicting patient dissatisfaction following joint replacement surgery. *The Journal of Rheumatology*, 35 (12), 2415-2418, 2008.

[57] **Garcia R. M., Kraay M. J., Messerschmitt P. J., Goldberg V. M., Rimnac C. M.**: Analysis of retrieved ultra high molecular polyethylene tibial components from rotating-platform total knee arthroplasty. *Journal of Arhtroplasty*, 24 (1), 131-138, 2009.

[58] **Gard S., Miff S., Kuo A.**: Comparison of kinematic and kinetic methods for computing the vertical motion of the body center of mass during walking. *Human Movement Science*, 22 (6), 597-610, 2004.

[59] **Gear C. W.**: Simultaneous solution of differential-algebraic equations. *IEEE Transactions on Circuit Theory*, 18 (1), 89-115, 1971.

[60] **Gellhorn A. C., Morgenroth D. C., Goldstein B.**: A novel sonographic method of measuring patellar tendon length. *Ultrasound in Medicine and Biology*, 38 (5), 719-726, 2012.

[61] **Gill H. S., O'Connor J. J.**: Biarticulating two-dimensional computer model of the human patellofemoral joint. *Clinical Biomechanics*, 11 (2), 81-89, 1996.

[62] **Girgis F. G., Marshall J. L., Monajem A. R. S.**: The cruciate ligaments of the knee joint - Anatomical, functional and experimental analysis. *Clinical Orthopaedics and Related Research*, 106, 216-231, 1975.

[63] **Gómez-Barrena E., Fernandez-Garciá C., Fernandez-Bravo A., Cutillas-Ruiz R., Bermejo-Fernandez G.**: Functional performance with single-radius femoral design total knee arthroplasty. *Clinical Orthopaedics and Related Research*, 468 (5), 1214-1220, 2010.

[64] **Goodfellow J. W., Hungerford D., Zindell M.**: Patello-femoral joint mechanics and pathology. I. Functional anatomy. *The Journal of Bone and Joint Surgery*, 56 (3)-B, 283-287, 1976.

[65] **Granata K. P., Wilson S. E., Padua D. A.**: Gender differences in active musculoskeletal stiffness. Part I. Quantification in controlled measurements of knee joint dynamics. *Journal of Electromyography and Kinesiology*, 12 (2), 119-126, 2002.

[66] **Grood E. S., Suntay W. J., Noyes F. R., Butler D. L.**: Biomechanics of the knee-extension exercise. Effect of cutting the anterior cruciate ligament. *The Journal of Bone and Joint Surgery*, 66 (5)-A, 725-734, 1984.

[67] **Guess T. M., Maletsky L. P.**: Computational modelling of a total knee prosthetic loaded in a dynamic knee simulator. *Medical Engineering and Physics*, 27 (5), 357-367, 2004.

[68] **Guess T. M., Thiagarajan G., Kia M., Mishra M.**: A subject specific multibody model of the knee with menisci. *Medical Engineering and Physics*, 32 (5), 505-515, 2010.

[69] **Gunston F. H.**: Polycentric knee arthroplasty. Prosthetic simulation of normal knee movement. *The Journal of Bone and Joint Surgery*, 53 (2)-B, 272–277, 1971.

[70] **Gutierrez-Farewik E., Bartonek A., Saraste H.**: Comparison and evaluation of two common methods to measure center of mass displacement in three dimensions during gait. *Human Movement Science*, 25 (2), 238-256, 2006.

[71] **Haines R. W.**: Anatomical note – A note on the actions of the cruciate ligaments of the knee joint. *Journal of Anatomy*, 75 (3), 373-375, 1941.

[72] **Halloran J. P., Easley S. K., Petrella A. J., Rullkoetter P. J.**: Comparison of deformable and elastic foundation finite element simulations for predicting knee replacement mechanics. *Journal of Biomechanical Engineering*, 127 (5), 813–818, 2005a.

[73] **Halloran J. P., Petrella A. J., Rullkoetter P. J.**: Explicit finite element modeling of total knee replacement mechanics. *Journal of Biomechanics*, 38 (2), 323–331, 2005b.

[74] **Hamilton N., Luttgens K.**: Kinesiology: Scientific Basis of Human Motion. Editor: Thalia Dorwick, McGrew and Hill Inc, New York, USA, 2002.

[75] **Hanavan E. P.**: A mathematical model of the human body. *AMRL Technical Report*, 64-102, 1964.

[76] **Hasan S., Robin R., Szurkus D., Ashmead D., Peterson S., Shiavi R.**: Simultaneous measurement of body center of pressure and center of gravity during upright stance. Part I-II. *Gait & Posture*, 4 (1), 1-20, 1996

[77] **Haxton H.**: The function of the patella and the effects of its excision. *Surgery, Gynecology and Obstetrics*, 80, 389-395, 1945.

[78] **HBM**: www.hbm.com, Accessed: 05.01.2010.

[79] **Hefzy M. S., Yang H.**: A three-dimensional anatomical model of the human patello-femoral joint for the determination of patello-femoral motions and contact characteristics. *Journal of Biomedical Engineering*, 15 (4), 289-302, 1993.

[80] **Hirokawa S.**: Three-dimensional mathematical model analysis of the patellofemoral joint. *Journal of Biomechanics*, 24 (8), 659-671, 1991.

[81] **Hollman J. H., Deusinger R. H., Van Dillen L. R., Matava M. J.**: Knee joint movements in subjects without knee pathology and subjects with injured anterior cruciate ligaments. *Physical Therapy*, 82 (10), 960-972, 2002.

[82] **Hood R. W., Wright T. M., Burstein A. H.**: Retrieval analysis of total knee prostheses: a method and its application to 48 total condylar prostheses. *Journal of Biomedical Material Resistance*, 17 (5), 829-842, 1983.

[83] **Huberti H. H., Hayes W. C.**: Patellofemoral contact pressures. *The Journal of Bone and Joint Surgery*, 66 (5)-A, 715-724, 1984.

[84] **Innocenti B., Pianigiani S., Labey L., Victor J., Bellemans J.**: Contact forces in several TKA designs during squatting: A numerical sensitivity analysis. *Journal of Biomechanics*, 44 (8), 1573-1581, 2011.

[85] **Iwaki A., Pinskerova V., Freeman M. A. R.**: The shapes and relative movements of the femur and tibia in the unloaded cadaver knee. *The Journal of Bone and Joint Surgery*, 82 (8)-B, 1189-1195, 2000.

[86] **KALIBER**: http://members.chello.hu/kaliberkft, Accessed: 12.01.2010.

[87] **Karlhuber M.**: Development of a method for the analysis of the wear of retrieved polyethylene components of total knee arthroplasty. Thesis, Technical University of Hamburg, Germany, 1995.

[88] **Kaufer H.**: Mechanical function of the patella. *The Journal of Bone and Joint Surgery*, 53 (8)-A, 1551-1660, 1971.

[89] **Kaufman K. R., An K. N., Litchy W. J., Morrey B. F., Chao E. Y. S.**: Dynamic joint forces during knee isokinetic exercise. *The American Journal of Sports Medicine*, 19 (3), 305-316, 1991.

[90] **Kellett C. F., Short A., Price A., Gill H. S., Murray D. W.**: In vivo measurement of total knee replacement wear. *The Knee*, 11 (3), 183-187, 2004.

[91] **Kelley D. L., Dainis A., Wood G. K.**: Mechanics and muscular dynamics of rising from a seated position, In: Komi PV (ed). International Series on Biomechanics. Proceedings of the 5th International Congress on Biomechanics, Biomechanics V-B. 127-134, University Park Press, Baltimore, USA, 1976.

[92] **Kettelkamp D. B., Johnson R. J., Smidt G. L., Chao E. Y., Walker M.**: An electrogoniometric study of knee motion in normal gait. *The Journal of Bone and Joint Surgery*, 52 (4)-A, 775-790, 1970.

[93] **Klebanov B. M., Barlam D. M., Nystrom F. E.**: Machine Elements: Life and Design, Coursebook. Editor: B. M. Klebanov, D. M. Barlam, F. E. Nystrom. Boca Raton, FL, USA, 2008.

[94] **Komistek R. D., Kane T. R., Mahfouz M., Ochoa J. A., Dennis D. A.**: Knee mechanics: A review of past and present techniques to determine in vivo loads. *Journal of Biomechanics*, 38 (2), 215-228, 2005.

[95] **König C., Matziolis G., Sharenkov A., Taylor W. R., Perka C., Duda G. N., Heller M. O.**: Collateral ligament length change patterns after joint line elevation may not explain midflexion instability following TKA. *Medical Engineering and Physics*, 33 (10), 1303-1308, 2011.

[96] **Krabbe B., Farkas R., Baumann W.**: Influence of inertia on intersegment moments of the lower extremity joints. *Journal of Biomechanics*, 30 (5), 517-519, 1997.

[97] **Kretzer J. P., Jakubowitz E., Reinders J., Lietz E., Moradi B., Hofmann J.**: Wear analysis of unicondylar mobile bearing and fixed bearing knee systems: A knee simulator study. *Acta Biomaterialia*, 7 (2), 710-715, 2011.

[98] **Kulas A. S., Hortobágyi T., DeVita P.**: Trunk position modulates anterior cruciate ligament forces and strains during a single-leg squat. *Clinical Biomechanics*, 27 (1), 16-21, 2012.

[99] **Kulas A. S., Zalewski P., Hortobágyi T., DeVita P.**: Effects of added trunk load and corresponding trunk position adaptations on lower extremity biomechanics during drop-landings. *Journal of Biomechanics*, 41 (1), 180-185, 2008.

[100] **Kurtz S. M.**: UHMWPE Biomaterials handbook. Editor: S. M. Kurtz. Elsevier Inc, San Diego, CA, USA, 2009.

[101] **Kwak S. D., Blankevoort L., Ateshian G. A.**: A mathematical formulation for 3D quasi-static multibody models of diarthrodial joints. *Computer Methods in Biomechanics and Biomedical Engineering*, 3 (1), 41–64, 2000.

[102] **Kwon S. K., Kang Y. G., Kim S. J., Chang C. B., Seong S. C., Kim T. K.**: Correlations between commonly used clinical outcome scales and patient satisfaction after total knee arthroplasty. *The Journal of Arthroplasty*, 25 (7), 1125-1130, 2010.

[103] **Lancin P., Essner A., Yau S-S., Wang A.**: Wear performance of 1900 direct compression molded, 1020 direct compression molded, and 1020 sheet compression molded UHMWPE under knee simulator testing. *Wear*, 263 (7-12), 1030-1033, 2007.

[104] **Laubenthal K. N., Smidt G. L., Kettelkamp D. B.**: A quantitative analysis of knee motion during activities of daily living. *Physical Therapy*, 52 (1), 34-43, 1972.

[105] **Laurent M. P., Johnson T. S., Yao J. Q., Blanchard C. R., Crowninshield R. D.**: In vitro lateral versus medial wear of knee prosthesis. *Wear*, 255 (7-12), 1101-1106, 2003.

[106] **Lemon M., Packham I., Narang K., Craig D. M.**: Patellar tendon length after knee arthroplasty with and without preservation of the infrapatellar fat pad. *The Journal of Arthroplasty*, 22 (4), 574-580, 2007.

[107] **Ling Z-K., Guo H-Q., Boersma S.**: Analytical study on the kinematic and dynamic behaviors of the knee joint. *Medical Engineering and Physics*, 19 (1), 29-36, 1997.

[108] **Loram I. D., Maganerius C. N., Lakie M.**: Human postural sway results from frequent, ballistic bias impulses by soleus and gastrocnemius. *Journal of Physiology*, 564 (1), 295-311, 2005.

[109] **Luyckx T., Didden K., Vandenneucker H., Labey L., Innocenti B., Bellemans J.**: Is there biomechanical explanation for anterior knee pain in patients with patella alta? *The Journal of Bone and Joint Surgery*, 91 (3)-B, 344-350, 2009.

[110] **Manssour H. M., Engin A. E., Akkas N.**: Two-dimensional dynamic modelling of the human knee. *Journal of Biomechanics*, 16 (4), 253-264, 1983.

[111] **Markowski C., Markowski E.**: Conditions for effectiveness of a preliminary test of variance. *The American Statistician*, 44 (4), 322-326, 1990.

[112] **Masani K., Vette A. H., Popovic M. R.**: Controlling balance during quiet standing: Proportional and derivative controller generates preceding motor command to body sway position observed in experiments. *Gait & Posture*, 23 (2), 164-172, 2006.

[113] **Mason J. J., Leszko F., Johnson T., Komistek R. D.**: Patellofemoral joint forces. *Journal of Biomechanics*, 41 (11), 2337-2348, 2008.

[114] **McGloughlin T., Kavanagh A.**: The influence of slip ratios in contemporary TKR on the wear of ultra-high molecular weight polyethylene (UHMWPE): An experimental view. *Journal of Biomechanics*, 31 (Supplement 1), 8, 1998.

[115] **McLain R. F., Bargar W. F.**: The effect of total knee design on patellar strain. *The Journal of Arthroplasty*, 1 (2), 91-98, 1986.

[116] **Miller P. K.**: Biomechanics of the patellofemoral joint. MSc thesis, University of Oxford, Oxford, England, 1991.

[117] **Momersteeg T. J. A., Blankevoort L., Huiskes R., Kooloos J. G. M., Kauer J. M. G., Hendriks J. C. M.**: The effect of variable relative insertion orientation of human knee bone-ligament-bone complexes on the tensile stiffness. *Journal of Biomechanics*, 28 (6), 745-752, 1995.

[118] **Mommersteeg T. J. A., Kooloos J. G. M., Blankevoort L., Kauer J. M. G., Huiskes R., Roeling F. Q. C.**: The fibre bundle anatomy of human cruciate ligaments. *Journal of Anatomy*, 187 (2), 461-471, 1995.

[119] **Morra E. A., Greenwald A. S.**: Patello-femoral replacement polymer stress during daily activities: A finite element study. 56th Annual Meeting of the AAOS, Chicago, IL, USA, 2006.

[120] **Mostamand J., Bader D. L., Hudson Z.**: Reliability testing of the patellofemoral joint reaction force (PFJRF) measurement in taped and untaped patellofemoral conditions during single leg squatting: A pilot study. *Journal of Bodywork & Movement therapies*, 48 (4), 502-506, 2011.

[121] **Mow V. C., Soslowsky L. J.**: Lubrication and wear of joints. In: V. C. Mow, W. C. Hayes: Basic Orthopaedic Biomechanics. Raven Press, New York, USA, 1991.

[122] **MSC.ADAMS** Basic Full Simulation Package: Training Guide. Santa Ana, CA, USA, 2005.

[123] **Nägerl H., Frosch K. H., Wachowski M. M., Dumont C., Abicht Ch., Adam P., Kubein-Meesenburg D.**: A novel total knee replacement by rolling articulating surfaces. In vivo functional measurements and tests. *Acta of Bioengineering and Biomechanics*, 10 (1), 55-60, 2008.

[124] **Nagura T., Matsumoto H., Kiriyama Y., Chaudhari A., Andriacchi T. P.**: Tibiofemoral joint contact force in deep knee flexion and its consideration in knee osteoarthritis and joint replacement. *Journal of Applied Biomechanics*, 22 (4), 305-313, 2006.

[125] **Nakamura N., Ellis M., Seedholm B. B.**: Advancement of the tibial tuberosity. *The Journal of Bone and Joint Surgery*, 67 (2)-B, 255-260, 1985.

[126] **Newton I.**: De analysi per aequationes numero terminorum infinitas. William Jones, London, England, 1711.

[127] **Neyret Ph., Robinson A. H. N., Le Coultre B., Lapra C., Chambat P.**: Patellar tendon length – The factor in patellar instability? *The Knee*, 9 (1), 3-6, 2002.

[128] **Nisell R., Németh G., Ohlsén H.**: Joint forces in extension of the knee. *Acta Orthopaedica Scandinavica*, 57 (1), 41-46, 1986.

[129] **Nisell R.**: Mechanics of the knee: A study of joint and muscle load with clinical applications. *Acta Orthopaedica Scandinavica*, 56 (Suppl. 216), 1-42, 1985.

[130] **Noble P. C., Conditt M. A., Cook K. F.**: Patient expectations affect satisfaction with total knee arthroplasty. *Clinical Orthopaedics and Related Research*, 452, 35-43, 2006.

[131] **Noyes F. R., Wojtys E. M., Marshall M. T.**: The early diagnosis and treatment of developmental patella infera syndrome. *Clinical Orthopeadics and Related Research*, 265, 241-252, 1991.

[132] **O'Brien S. J., Warren R. F., Pavlov H., Panariello R., Wickiewicz T. L.**: Reconstruction of the chronically insufficient anterior cruciate ligament with the central third of the patellar ligament. *The Journal of Bone and Joint Surgery*, 73 (2)-A, 278-286, 1991.

[133] **O'Brien S., Luo Y., Wu C., Petrak M., Bohm E., Brandt J. M.**: Computational development of polyethylene wear model for the articular backside surfaces in modular total knee replacements. *Tribology International*, 59, 284-291, 2013.

[134] **O'Connor J. J., Shercliff T., Fitzpatrick D., Bradley J., Daniel D. M., Biden E., Goodfellow J.**: Geometry of the knee. In: D. Daniel: Knee Ligaments: Structure, function, Injury and Repair. Chapter 10, Raven Press, New York, USA, 1990.

[135] **Özaslan A., İşcan M. Y., Özaslan İ., Tuğcu H., Koç S.**: Estimation of stature from body parts. *Forensic Science International*, 132 (1), 40-45, 2003.

[136] **Pandy M. G., Sasaki K., Kim S.**: A three-dimensional musculoskeletal model of the human knee joint. Part 1: Theoretical construction. *Computer Methods in Biomechanics and Biomedical Engineering*, 1 (2), 87–108, 1997.

[137] **Pandy M. G., Sasaki K.**: A three-dimensional musculoskeletal model of the human knee joint. Part 2: Analysis of ligament function. *Computer Methods in Biomechanics and Biomedical Engineering*, 1 (4), 265–283, 1998.

[138] **Park S. E., DeFrate L. E., Suggs J. F., Gill T. J., Rubash H. E., Li G.**: Erratum to "The change in length of the medial and lateral collateral ligaments during in vivo knee flexion. *The Knee*, 13 (1), 77-82, 2006.

[139] **Perry J., Antonelli D., Ford W.**: Analysis of knee-joint forces during flexed-knee stance. *The Journal of Bone and Joint Surgery*, 57 (7)-A, 961-967, 1975.

[140] **Petersilge W. J., Oishi C. S., Kaufman K. R., Irby S. E., Colwell C. W.**: The effect of trochlear design on patellofemoral shear and compressive forces in total knee arthroplasty. *Clinical Orthopaedics and Related Research*, 309, 124-130, 1994.

[141] **Piazza S. J., Delp S. L.**: Three-dimensional simulation of total knee replacement motion during a step-up task. *Journal of Biomechanical Engineering*, 123 (6), 599–606, 2001.

[142] **Pinskerova V., Iwaki H., Freeman M. A. R.**: The shapes and relative movements of the femur and tibia at the knee. *Der Orthopäde*, 29 (Suppl. 1), 3-5, 2000.

[143] **Pinskerova V., Johal P., Nakagawa S., Sosna A., Williams A., Gedroyc W., Freeman M. A. R.**: Does the femur roll-back with flexion? *The Journal of Bone and Joint Surgery*, 86 (6)-B, 925-931, 2004.

[144] **Plitz W., Bergmann M., Weinmann K. H.**: Der Einfluß von Verschleiß und Positionierung auf die Verankerung von Knieendoprothesen. *Zeitshrift für Orthopädie und Unfallchirurgie*, 121, 476, 1983.

[145] **Plitz W., Hoss H. U.**: Vershleiß und resultierende Beanspruchung auf die Verankerung von Knieendprothesen. *Zeitshrift für Orthopädie und Unfallchirurgie*, 120, 412, 1982.

[146] **Powers C. M., Chen Y-J., Scher I., Lee T. Q.**: The influence of patellofemoral joint contact geometry on the modeling of three dimensional patellofemoral forces. *Journal of Biomechanics*, 39 (15), 2783-2791, 2006.

[147] **Quian S. H., Ge S. R., Wang Q. L.**: The frictional coefficient of bovine knee articular cartilage. *Journal of Bionic Engineering*, 3 (2), 79-85, 2006.

[148] **Radin E. L., Paul I. L.**: A Consolidated Concept of Joint Lubrication. *The Journal of Bone and Joint Surgery*, 54 (3)-A, 607-616, 1972.

[149] **Raphson J.**: Analysis aequationum universalis. London, England, 1690.

[150] **Reilly D. T., Martens M.**: Experimental analysis of the quadriceps muscle force and patellofemoral joint reaction force for various activities. *Acta Orthopaedica Scandinavica*, 43 (2), 126-137, 1972.

[151] **Reinholz A., Wimmer M. A., Morlock M. M., Schnelder E.**: Analysis of the coefficient of friction as function of slide-roll ratio in total knee replacement. *Journal of Biomechanics*, 31 (Supplement 1), 8, 1998.

[152] **Reithmeier E., Plitz W.**: A theoretical and numerical approach to optimal positioning of the patellar surface replacement in a total knee endoprothesis. *Journal of Biomechanics*, 23 (9), 883-892, 1990.

[153] **Ren L., Howard D., Ren L., Nester C., Tian L.**: A phase dependent hypothesis for locomotor functions of human foot complex. *Journal of Bionic Engineering*, 5 (3), 175-180, 2008.

[154] **Reuben J. D., McDonald C. L., Woodard P. L., Hennington L. J.**: Effect of patella thickness on patella strain following total knee arthroplasty. *The Journal of Arthroplasty*, 6 (3), 251-258, 1991.

[155] **Robertson D. G. E., Caldwell G. E., Hamill J., Kamen G., Whittlesey S. N.**: Research Methods in Biomechanics, Editor: L. D. Robertson. Edward Brothers Press, Campaign, IL, USA, 2004.

[156] **Saikko V., Calonius O.**: Simulation of wear rates and mechanisms in total knee prostheses by ball-on-flat contact in a five-station, three axis rig. *Wear*, 253 (3-4), 424-429, 2002.

[157] **Salem G. J., Powers C. M.**: Patellofemoral joint kinetics during squatting in collegiate women athletes. *Clinical Biomechanics*, 16 (5), 424-430, 2001.

[158] **Schindler O. S., Scott W. N.**: Basic kinematics and biomechanics of the patello-femoral joint. Part 1: The native patella. *Acta Orthopaedica Belgica*, 77 (4), 421-431, 2011.

[159] **Schwenke T., Borgstede L. L., Schneider E., Andriacchi T. P., Wimmer M. A.**: The influence of slip velocity on wear of total knee arthroplasty. *Wear*, 259 (7-12), 926-932, 2005.

[160] **Schwenke T., Orozco D., Schneider E., Wimmer M. A.**: Differences in wear between load and displacement control tested total knee replacements. *Wear*, 267 (5-8), 757-762, 2009.

[161] **Scott C. E. H., Howie C. R., MacDonald D., Biant L. C.**: Predicting dissatisfaction following total knee replacement. A prospective study of 1217 patients. *The Journal of Bone and Joint Surgery*, 92 (9)-B, 1253-1258, 2010.

[162] **Sharkey P. F., Hozack W. J., Rothman R. H., Shastri S., Jacobi S. M.**: Why are total knee arthroplasties failing today? *Clinical Orthopaedics and Related Research*, 404, 7-13, 2002.

[163] **Sharma A., Leszko F., Komistek R. D., Scuderi G. R., Cates H. E., Liu F.**: In vivo patellofemoral forces in high flexion total knee arthroplasty. *Journal of Biomechanics*, 41 (3), 642-648, 2008.

[164] **Singerman R., Berilla J., Archdeacon M., Peyser A.**: In vitro forces in the normal and cruciate-deficient knee during simulated squatting motion. *Journal of Biomechanical Engineering*, 121 (2), 234-242, 1999.

[165] **Singerman R., Berilla J., Kotzar G., Daly J., Davy D. T.**: A six-degree-of-freedom transducer for in-vitro measurement of patellofemoral contact forces. *Journal of Biomechanics*, 27 (2), 233-238, 1994.

[166] **Smidt G. L.**: Biomechanical analysis of knee flexion and extension. *Journal of Biomechanics*, 6 (1), 79-92, 1973.

[167] **Smith A. J.**: A study of force on the body in athletic activities with particular reference to jumping. PhD thesis, Leeds, England, 1972.

[168] **Smith J. W.**: Observation on the postural mechanism of the human knee joint. *Journal of Anatomy*, 92 (2), 236-260, 1956.

[169] **Standring S.**: Gray's Anatomy: The anatomical basis of clinical practice, Churchill-Livingstone-Elsevier Press, 40th Edition, Spain, 2008.

[170] **Steele K. M., DeMers M. S., Schwartz M. H., Delp S. L.**: Compressive tibiofemoral force during crouch gait. *Gait & Posture*, 35 (4), 556-560, 2012.

[171] **Stephens L. J.**: Advanced statistics demystified. Editor: Judy Bass. McGraw-Hill Inc, USA, 2004.

[172] **Stiehl J. B., Komistek R. D., Dennis D. A., Keblish P. A.**: Kinematics of the patellofemoral joint in total knee arthroplasty. *The Journal of Arthroplasty*, 16 (6), 706-714, 2001.

[173] **STRYKER®**: http://www.getaroundknee.com/why-stryker, Accessed: 02.02.2013.

[174] **Szendrő P.**: Gépelemek (Machine Elements), Course book. Editor: P. Szendrő. Mezőgazda Kiadó (Agriculturer Press), Budapest, Hungary, 2007.

[175] **Szentágothai J.**: Funkcionális anatómia I. (Functional Anatomy I.), Course book. Editor: Lovass Pál. Medicina Könyvkiadó Zrt (Medicina Press), Budapest, Hungary, 2006.

[176] **Tanaka N., Sakahashi H., Sato E., Hirose K., Isima T.**: Influence of the infrapatellar fat pad resection in a synovectomy during total knee arthroplasty in patients with rheumatoid arthritis. *The Journal of Arthroplasty*, 18 (7), 897-902, 2003.

[177] **Tesio L., Rota V., Chessa C., Perucca L.**: The 3D path of body centre of mass during walking on force treadmill. *Journal of Biomechanics*, 43 (5), 938-944, 2010.

[178] **Thambyah A.**: How critical are the tibiofemoral joint reaction forces during frequent squatting in the Asian populations? *The Knee*, 15 (4), 286-294, 2008.

[179] **Thelen D. G., Chumanov E. S., Best T. M., Swanson S. C., Heiderscheit B. C.**: Simulation of biceps femoris musculotendon mechanics during the swing phase of sprinting. *Medicine and Science in Sport and Exercise*, 37 (11), 1931-1938, 2005.

[180] **Unsworth A., Dowson D., Wright V.**: The functional behaviour of human synovial joints - Part I: Natural joints. *Transactions of the ASME, Journal of Lubrication Technology*, 74 (38), l-8, 1974.

[181] **Van Citters D. W., Kennedy F. E., Collier J. P.**: Rolling sliding wear of UHMWPE for knee bearing applications. *Wear*, 263, 1087-1094, 2007.

[182] **Van Citters D. W., Kennedy F. E., Currier J. H., Collier J. P., Nichols T. D.**: A multi-station rolling/sliding tribotester for knee bearing materials. *Journal of Tribology*, 126 (2), 380-385, 2004.

[183] **Van Eijden T. M. G. J., Kouwenhoven E., Verburg J., Weijs W. A.**: A mathematical model of the patellofemoral joint. *Journal of Biomechanics*, 19 (3), 219-229, 1986.

[184] **Van Ijsseldijk E. A., Valstar E. R., Stoel B. C., Nelissen R. G. H. H., Reiber J. H. C., Kaptein B. L.**: The robustness and accuracy of in vivo linear wear measurements for knee prostheses based on model-based RSA. *Journal of Biomechanics*, 44 (15), 2724-2727, 2011.

[185] **Victor J., Labey L., Wong P., Innocenti B., Bellemans J.**: The influence of muscle load on tibiofemoral kinematics. *Journal of Orthopaedic Research*, 28 (4), 419-428, 2010.

[186] **Vörös I.**: Gépelemek (Machine Elements), Course book. Editor: I. Vörös. Tankönyvkiadó (Course book Press), Budapest, Hungary, 1970.

[187] **Wahrenberg H., Lindbeck L., Ekholm J.**: Knee muscular moment, tendon tension force and EMG during a vigorous movement in man. *Scandinavian Journal of Rehabilitation Medicine*, 10 (2), 99-106, 1978.

[188] **Wang H., Simpson K. J., Chamnongkich S., Kinsey T., Mahoney O. M.**: A biomechanical comparison between the single-axis and multi-axis total knee arthroplasty systems for stand-to-sit movement. *Clinical Biomechanics*, 20 (4), 428-433, 2005.

[189] **Weale A. E., Murray D. W., Newman J. H., Ackroyd C. E.**: The patellar length of the patellar tendon after unicompartmental and total knee replacement. *The Journal of Bone and Joint Surgery*, 81 (5)-B, 790-795, 1999.

[190] **Wehner T., Claes L., Simon U.**: Internal loads in the human tibia during gait. *Clinical Biomechanics*, 24 (3), 299-302, 2009.

[191] **Wilson D. R., Feikes J. D., O'Connor J. J.**: Ligaments and articular contact guide passive knee flexion. *Journal of Biomechanics*, 31 (12), 1127-1136, 1998.

[192] **Wimmer M. A., Andriacchi T. P., Natarajan R. N., Loos J., Karlhuber M., Petermann J., Schneider E., Rosenberg A. G.**: A striated pattern of wear in ultrahigh-molecular-weight polyethylene components of Miller-Galante total knee arthroplasty. *The Journal of Arthroplasty*, 13 (1), 8-16, 1998.

[193] **Wimmer M. A., Andriacchi T. P.**: Tractive forces during rolling motion of the knee: Implications for wear in total knee replacement. *Journal of Biomechanics*, 30 (2), 131-137, 1997.

[194] **Wimmer M. A.**: Wear of polyethylene component created by rolling motion of the artificial knee joint. Shaker Verlag, Aachen, Germany, 1999.

[195] **Winter D. A.**: Moments of force and mechanical power in jogging. *Journal of Biomechanics*, 16 (1), 91-97, 1983.

[196] **Wisman J., Veldpaus F., Jansen J.**: A three-dimensional mathematical model of the knee joint. *Journal of Biomechanics*, 13 (8), 677-685, 1980.

[197] **Wojtys E. M., Oakes B., Lindenfeld T. N., Bach B. R.**: Patella infera syndrome: An analysis of the patellar tendon pathology. *Instructional course lecture*, 46, 241-250, 1997.

[198] **Yamaguchi G. T., Zajac F. E.**: A planar model of the knee joint to characterize the knee extensor mechanism. *Journal of Biomechanics*, 22 (1), 1-10, 1989.

[199] **Zernicke R. F., Garhammer J., Jobe F. W.**: Human patellar tendon rupture: A kinetic analysis. *The Journal of Bone and Joint Surgery*, 59 (2)-A, 179-183, 1977.

[200] **Zheng N., Fleisig G. S., Escamilla R. F., Barrentine S. W.**: An analytical model of the knee for estimation of internal forces during exercise. *Journal of Biomechanics*, 31 (10), 963-967, 1998.

[201] **Zok M., Mazza C., Croce U.**: Total body centre of mass displacement estimated using ground reactions during transitory motor tasks: Application to step ascent. *Medical Engineering and Physics*, 26 (9), 791-798, 2004.

[202] **Zuppinger H.**: Die aktive im unbelasteten Kniegelenk. Wiesbaden, Germany, 1904.

A2. Publications related to the thesis

Peer-reviewed journal publications included in SCI

1. **Fekete G.**, Csizmadia B. M., Wahab M. A., De Baets P.: Experimental determination of horizontal motion of human center of gravity during squatting. *Experimental Techniques*, Accepted, 2011, DOI: 10.1111/j.1747-1567.2011.00768.x. IF: 0.257
2. **Fekete G.**, Csizmadia B. M., Wahab M. A., De Baets P., Katona G., Vanegas-Useche L.V., Solanilla J.A.: Sliding-rolling ratio during deep squat with regard to different knee prostheses. *Acta Polytechnica Hungarica*, 9 (5), pp. 5-24, 2012. IF: 0.385
3. **Fekete G.**, Csizmadia B. M., Wahab M. A., De Baets P., Bíró I.: Simple equations to calculate knee patellofemoral forces during modified squatting. *Dyna Colombia*, Under review, 2013.

Peer-reviewed journal publications

1. **Fekete G.**, Csizmadia B. M., De Baets P., Wahab M. A.: Review of current knee biomechanical modelling techniques. *Mechanical Engineering Letters*, 5, pp. 30-36, 2011.
2. **Fekete G.**, Csizmadia B. M.: Biomechanics of the human knee joint. *Mechanical Engineering Letters*, 1, pp. 146-158, 2008.
3. **Fekete G.**, Csizmadia B. M.: Csúszva gördülés értelmezése a térdízület biomechanikai vizsgálatához. *Gép*, 12 (59), pp. 4-8, 2008.
4. **Fekete G.**, Csizmadia B. M.: Interpretation of sliding-roll phenomena in the examination of knee biomechanics. *Bulletin of Szent István University*, pp. 339-347, 2008.
5. **Fekete G.**, Csizmadia B. M.: Computational human knee joint model for determining sliding-rolling properties. *Scientific Bulletin of Politehnica University Timisoara – Transaction on Mechanics*, 53 (67), Special Issue 1, pp. 305-309, 2008.

Conference Proceedings

1. **Fekete G.**, Csizmadia B. M., De Baets P., Wahab M. A.: Multibody dynamic models in biomechanics: Modelling issues and a new model. *Sustainable Construction and Design*, 3 (2), pp. 128-137, 2012.
2. **Fekete G.**, Csizmadia B. M., De Baets P., Wahab M. A.: Analytical patellofemoral knee models: Past and Present. *Synergy in the technical development of agriculture and food industry*, Gödöllő, Hungary, October 9-16, 2011.
3. **Fekete G.**, Csizmadia B. M., Wahab M. A., De Baets P.: Analytical and computational estimation of patellofemoral forces in the knee under squatting and isometric motion. *Sustainable Construction and Design*, 2 (2), pp. 246-257, 2011.
4. **Fekete G.**, Csizmadia B. M.: Biomechanical research of Szent István University. *Sustainable Construction and Design*, 1 (1), pp. 107-114, 2010.
5. **Fekete G.**, Csizmadia B. M.: Numerical methods for determining local motions of human knee joint. *Zilele Technice Studentesti*, 12, pp. 204-210, Timisoara, Romania, May 11-18, 2008,

6. **Fekete G.**, Kátai L.: MSC.ADAMS programrendszer felhasználása a biomechanikai modellezésben. *Fiatal Műszakiak Tudományos Ülésszaka*, 13, pp. 1-4, Cluj-Napoca, Romania, March 13-14, 2008.

Reviewer for international journals in SCI

1. Experimental Techniques (1)
2. Clinical Biomechanics (1)

A3. Geometric model creation

This method was carried out in Solid Edge V16 and Catia V5R17 and explained step by step:

1. The STL file has to be opened in the CATIA (Figure 1).

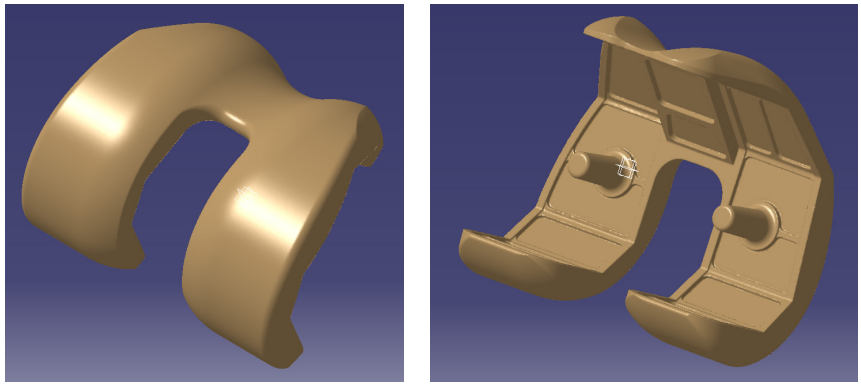

Figure 1. STL files in the Catia

2. Since the STL is only a dot-cloud, a surface has to be fit on the cloud, and from surface, a body has to be converted. Disclosing holes on the surface or other problems have to be repaired in CATIA software.
3. After finishing the surface and body model, the geometric model has to be saved as IGS.
4. Now, the IGS can be opened in Solid Edge. Before opening, make sure that the following options are set as follows (Figure 2 and Figure 3):

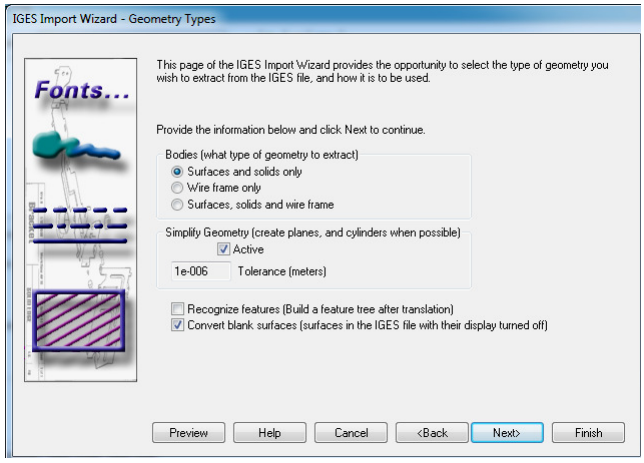

Figure 2. Setting Surface and Solids options in Solid Edge

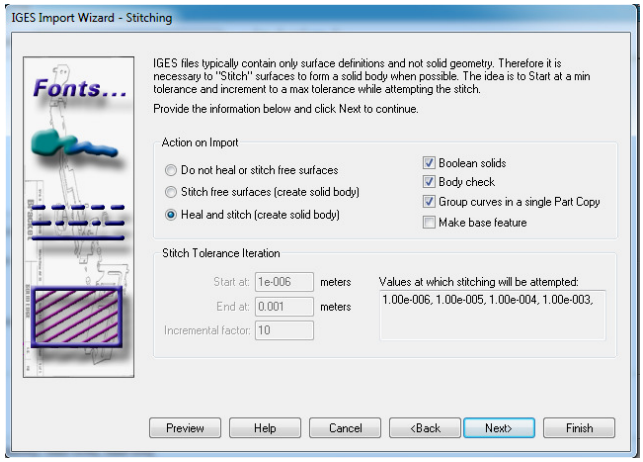

Figure 3. Setting Stitching options in Solid Edge

5. Once you opened the IGS, you have to save it as a PART.
6. Read in the PART and now save it as PARASOLID. Before saving, set in the OPTIONS as follows (Figure 4):

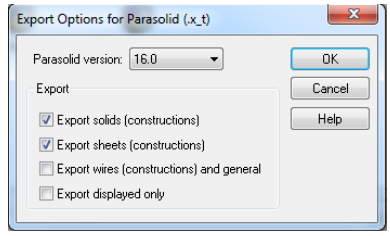

Figure 4. Export options in Solid Edge

7. After setting these options, the IGS can be opened in the Solid Edge (Figure 5).

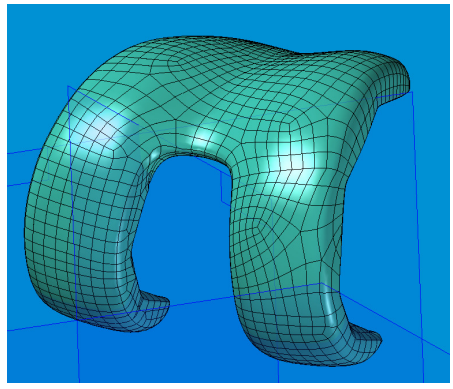

Figure 5. Geometric model in Solid Edge

8. Now it can be saved as PARASOLID and can be imported into the MSC.ADAMS.

A4. Mathematical-anatomical models

Reithmeier and Plitz [Reithmeier and Plitz, 1990] envisaged the effect of the patellar height due to the postoperative problems of patellar replacement. In their earlier studies [Plitz and Hoss, 1982, Plitz et al., 1983], they performed tests on 40 knee prostheses and found heavily damaged prosthetic surfaces. Their mathematical model is based on a parameter study, which describes how the contact forces change as a function of the patellar height (Figure 6).

To formulate their model, they assumed the following simplifications:

a) The bones are considered as rigid bodies,

b) The patellar tendon and the quadriceps tendon are inextensible,

c) Since the prosthesis is symmetrical, the model is planar (two-dimensional),

d) Similarly to the model of Van Eijden et al. [Van Eijden et al., 1986], point contact is considered between the condyles,

e) Friction force between the surfaces is not considered.

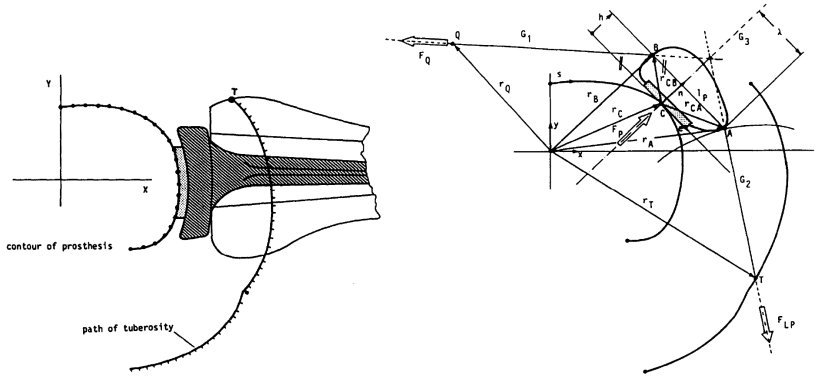

Figure 6. Mechanical model [Reithmeier and Plitz, 1990]

The points of attachment for the patellar tendon and the quadriceps tendon were determined from X-ray images. After deriving and solving the non-linear equation system, which includes seven equations, the authors published the following findings:

I. The authors verified and demonstrated their hypothesis about the significance of the patellar height on the patellofemoral forces.

II. In Figure 7 and Figure 8, it becomes apparent how the patellofemoral force versus quadriceps force and the patellofemoral forces versus patellar tendon force change as a function of flexion angle and patellar height.

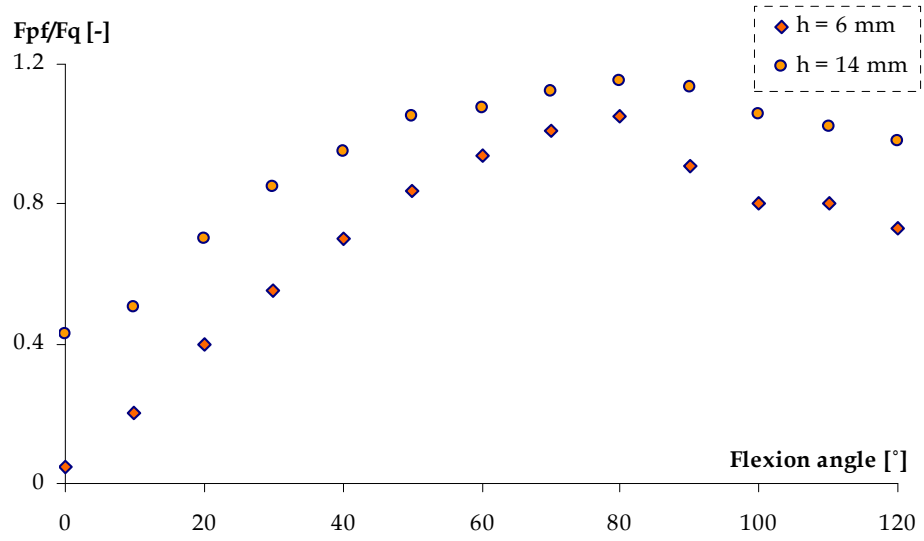

Figure 7. F_{pf}/F_q as a function of flexion angle and patellar height [Reithmeier and Plitz, 1990]

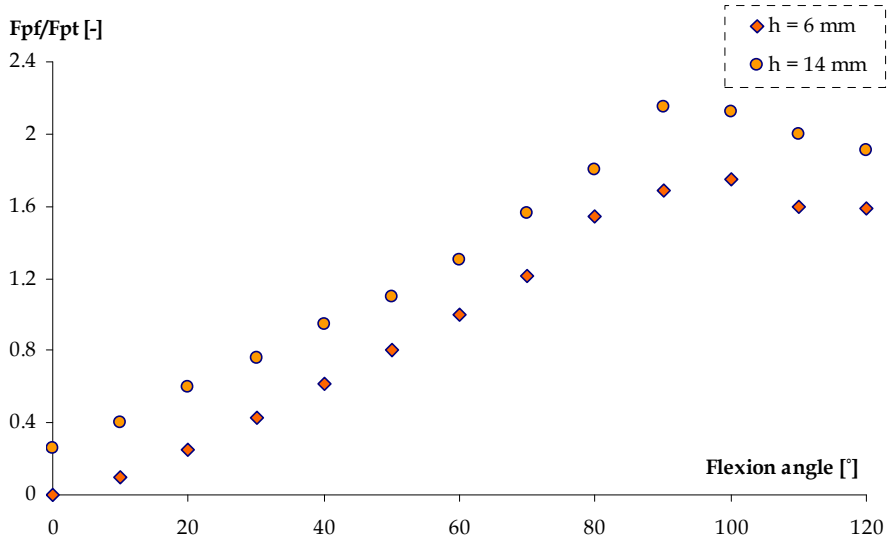

Figure 8. F_{pf}/F_{pt} as a function of flexion angle and patellar height [Reithmeier and Plitz, 1990]

Naturally, some remarks have to be added to the summary of the model:

- The model is very similar to the model of Van Eijden et al. [Van Eijden et al., 1986], although it can only calculate the force ratios, no other relevant kinematic quantities (anatomical angles) can be determined.
- The model is mathematical, but no closed form solution can be obtained, only approximation through iterative methods. This makes the implementation of quick calculations inaccessible.

In the framework of the analytical-kinetical models, except some of the stiffness models, nobody modelled the knee joint in three-dimension, due to several cumbersome factors.

Hirokawa [Hirokawa, 1991] made the first substantial step by creating the first three-dimensional mathematical-mechanical model (Figure 9), which included the articular surface geometry and the mechanical properties of the ligaments.

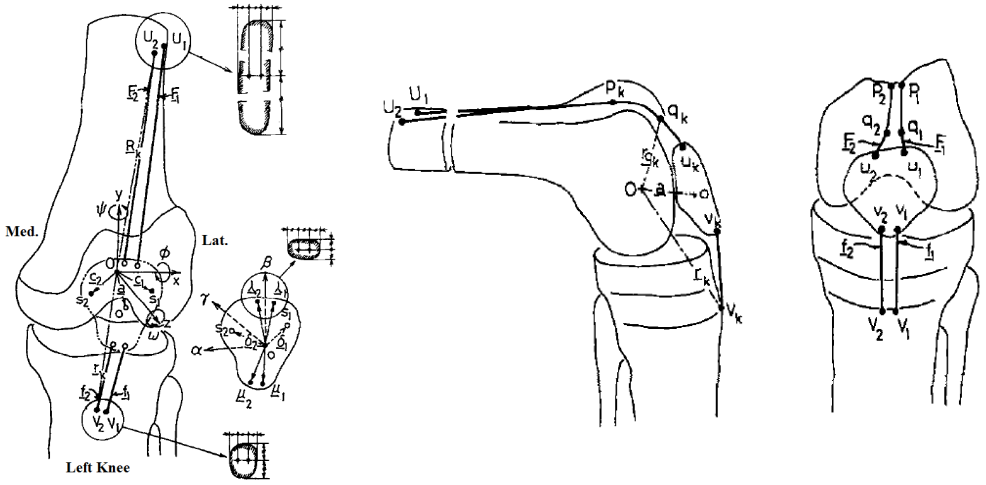

Figure 9. Three-dimensional model [Hirokawa, 1991]

Although Wisman et al. [Wisman et al., 1980] has already published a three-dimensional model, but in their model, the articular shapes were approximated with polynomials that are not able to express precisely the entire patellofemoral surfaces including the patellar mid-ridge and the femoral mid-groove.

The aims of Hirokawa's study were to describe the three-dimensional patellar motion and to calculate the patellofemoral compression force alongside with the patellar tendon force as a function of flexion angle. Since he applied the Hertzian elastic theory, the contact stresses could be estimated as well. During the assembly of the model, the contact points of the quadriceps tendon and the patellar tendon were measured by using three cadaver knees. The four heads of the quadriceps muscle were modelled by two lines, which followed the direction of the vastus intermedius. Two points on the tibial tuberosity represented the attachment of the patellar tendon at the tibia.

Hirokawa described his mathematical model by fourteen non-linear equations with fourteen unknown values. The force of the quadriceps muscle ($\boldsymbol{F_q}$) was a fixed constant for the whole range of knee flexion.

The following findings were derived from Hirokawa's model [Hirokawa, 1991]:

I. The author's results agreed with the results of Van Eijden et al. [Van Eijden et al., 1986] and Yamaguchi and Zajac [Yamaguchi and Zajac, 1989] related to the $\boldsymbol{F_{pf}/F_q}$ and $\boldsymbol{F_{pt}/F_q}$ relationships.

II. The calculated contact stresses in the articular faces correspond very well with other author's result [Ahmed et al., 1983].

III. The author gave a complete and well-based description about the three-dimensional patellar angles (rotation, twist and tilt) as it is seen in Figure 10, Figure 11 and Figure 12.

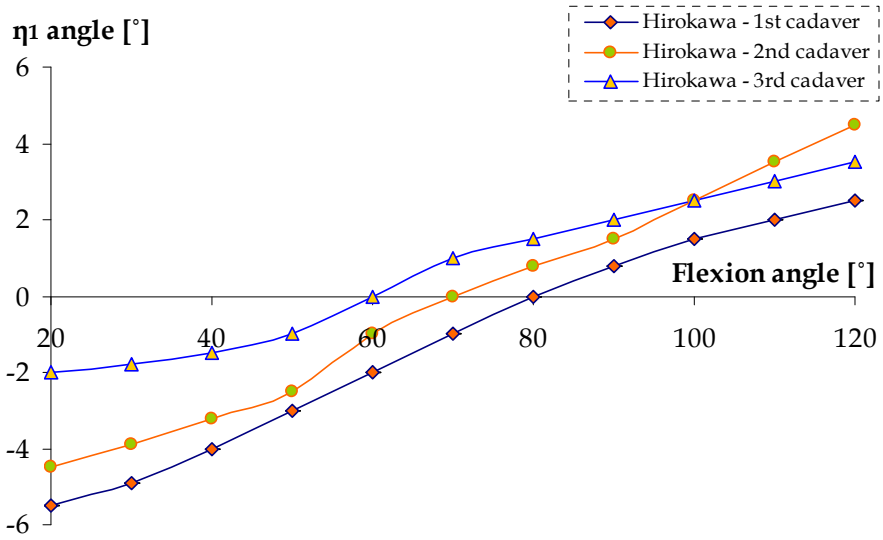

Figure 10. Patella rotation [Hirokawa, 1991]

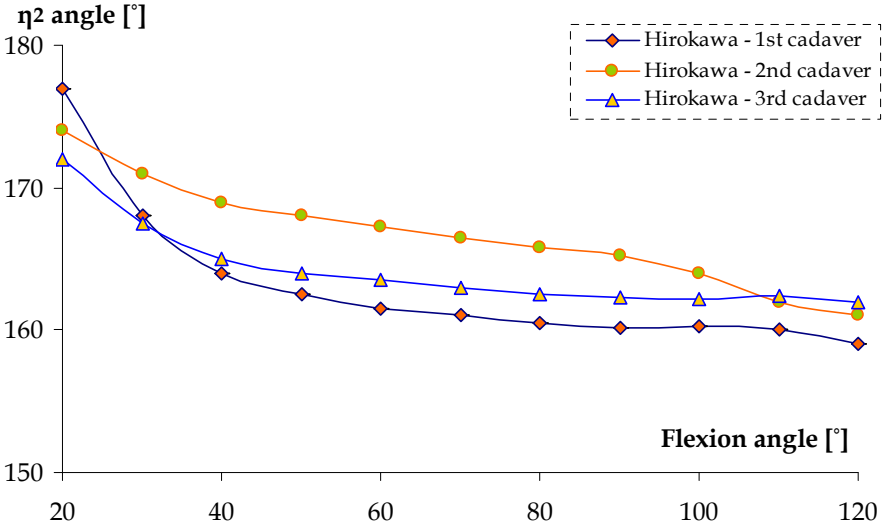

Figure 11. Patella twist [Hirokawa, 1991]

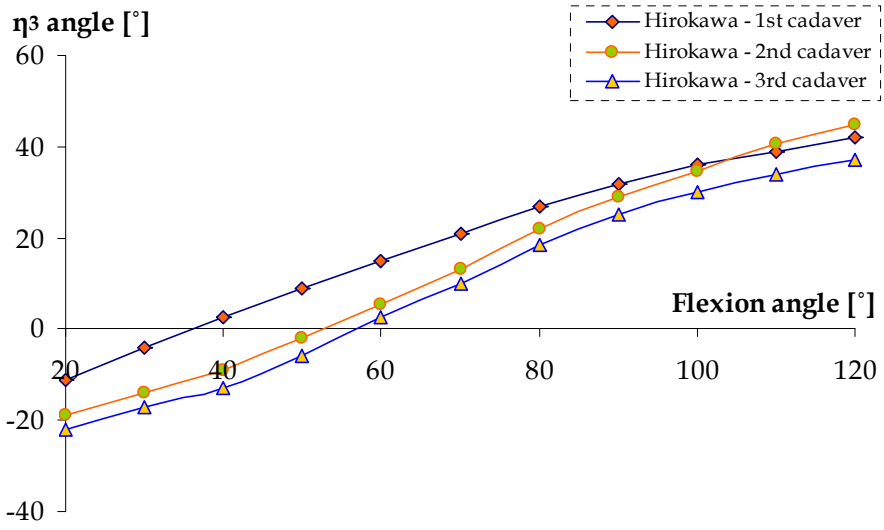

Figure 12. Patella tilt [Hirokawa, 1991]

The following remarks should be addressed to Hirokawa's model [Hirokawa, 1991]:

- Similar to other authors' models [Van Eijden et al., 1986, Yamaguchi and Zajac, 1989, Reithmeier and Plitz, 1990] this mathematical model can only be solved numerically.
- Similar to other models [Van Eijden et al., 1986, Nisell, 1985, Nisell et al., 1986, Yamaguchi and Zajac, 1989] the F_{pt}/F_q and F_{pf}/F_q relationships are derived from a simple knee extension, where F_q is considered as a known external force. This model only enables us to calculate the very same type of motion what was earlier investigated, namely the femur is fixed and the tibia carries out a constrained motion. However, these results agree well.

Hefzy and Yang [Hefzy and Yang, 1993] have also developed a three-dimensional, anatomical-mathematical, patellofemoral joint model that determines how patellofemoral motions and patellofemoral contact force change with knee flexion (Figure 13). Furthermore, a unique two-point contact is assumed between the femur and tibia, on the medial and lateral sides.

The model includes seventeen non-linear equations with seventeen unknowns.

Similar to the other earlier mentioned models, the patellofemoral joint has been modelled as three rigid bodies. The femur was assumed fixed and the patella moved along it. In the analysis, the patellar tendon was assumed to be a rigid ligament whose length remained constant during the motion. The length of the quadriceps tendon was allowed to change as the patella moved along the femur. However, the quadriceps tendon was not allowed to wrap around the femur.

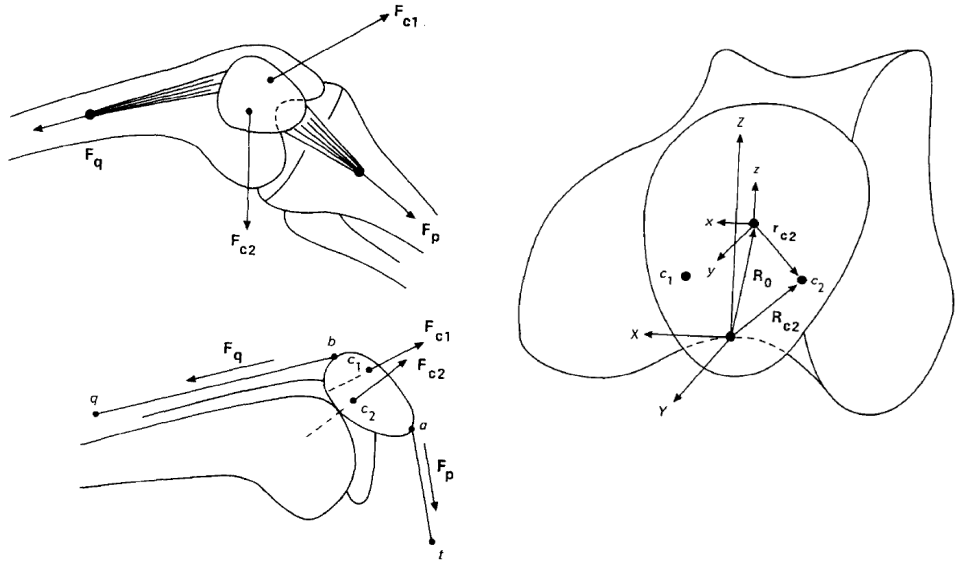

Figure 13. Mechanical model [Hefzy and Yang, 1993]

The major findings of Hefzy and Yang [Hefzy and Yang, 1993] can be summarized as follows:

I. The authors' results agreed less with the results of Van Eijden et al. [Van Eijden et al., 1986] related to the F_{pt}/F_q relationship.

II. The authors' results agreed well with the results of Van Eijden et al. [Van Eijden et al., 1986] related to the angle between the patellar tendon and the patellar axis as a function of flexion angle (Figure 14).

III. The authors' results agreed well with the results of Van Eijden et al. [Van Eijden et al., 1986] related to the angle between the patellar axis and the femoral axis as a function of flexion angle (Figure 15).

IV. The authors' results agreed less with the results of Van Eijden et al. [Van Eijden et al., 1986] related to the angle between the quadriceps tendon and the femoral axis as a function of flexion angle (Figure 16).

V. The authors' results agreed well with the results of Van Eijden et al. [Van Eijden et al., 1986] related to the angle between the quadriceps tendon and the patellar axis as a function of flexion angle (Figure 17).

VI. The authors introduced the contact points in transversal and frontal view of the condyles including the medial and lateral pathways as well (Figure 18).

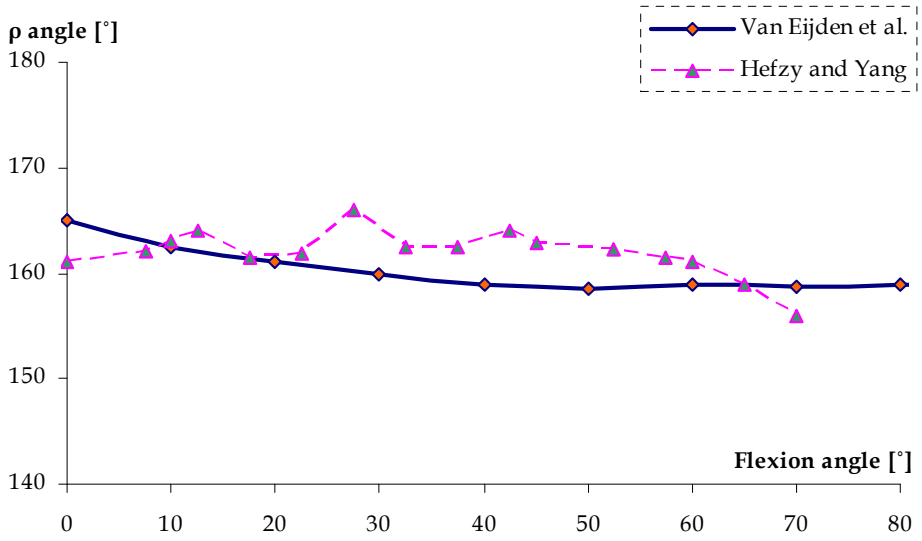

Figure 14. Angle between the patellar tendon and the patellar axis (ρ) [Hefzy and Yang, 1993]

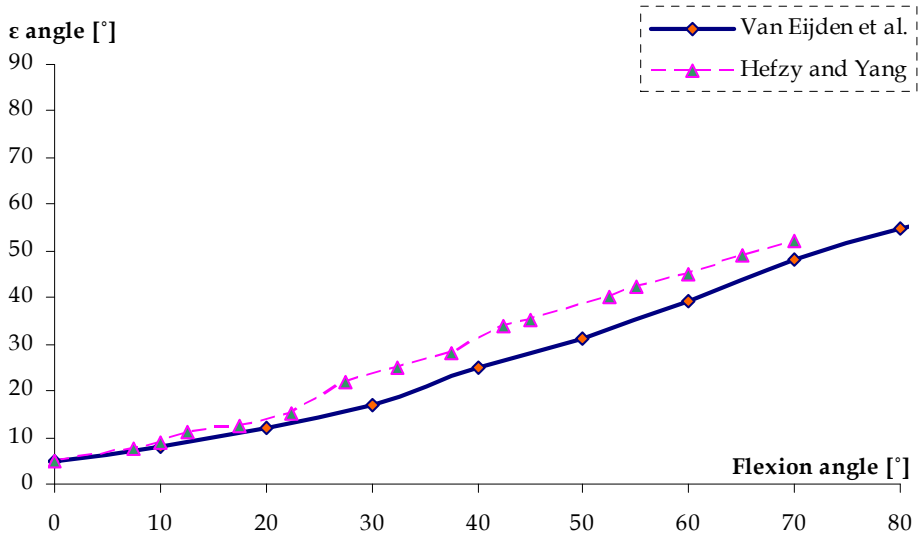

Figure 15. Angle between patellar axis and femoral axis (ε) [Hefzy and Yang, 1993]

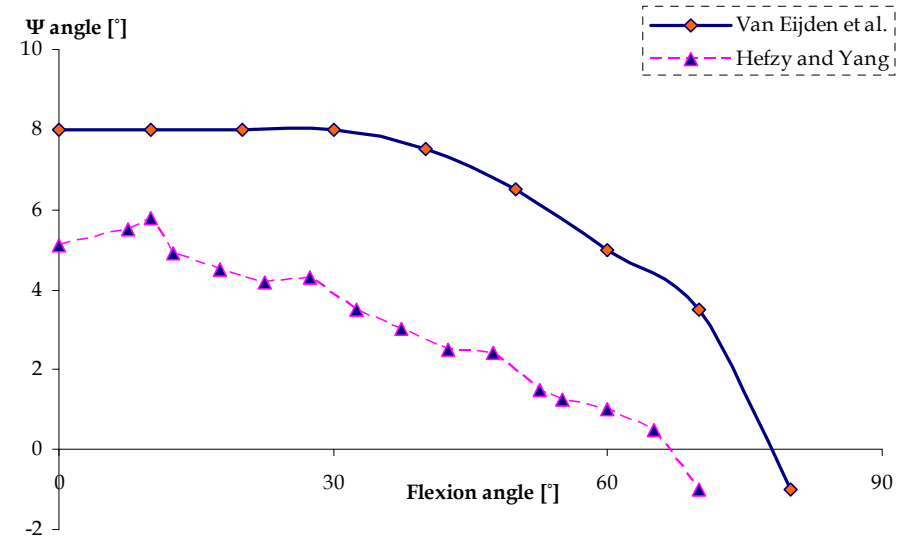

Figure 16. Angle between the quadriceps tendon and the femoral axis (δ) [Hefzy and Yang, 1993]

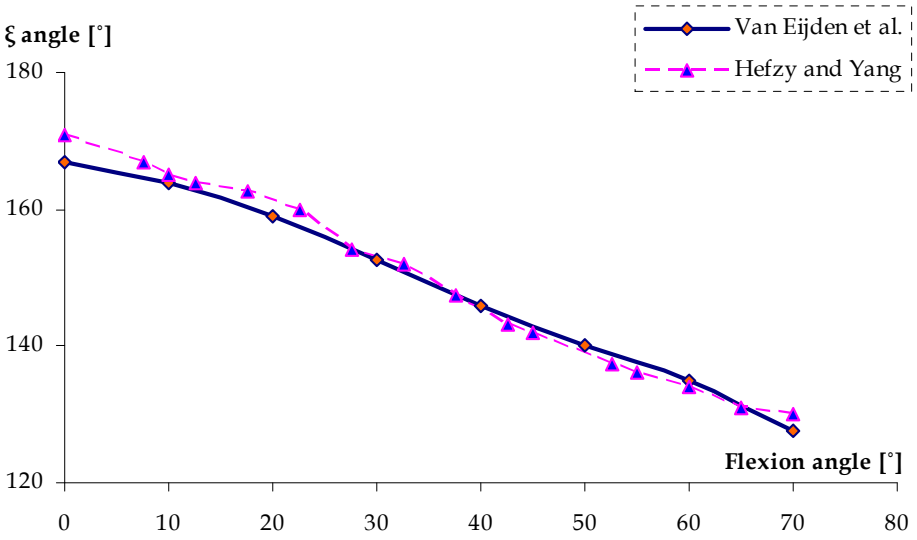

Figure 17. Angle between the quadriceps tendon and the patellar axis (ξ) [Hefzy and Yang, 1993]

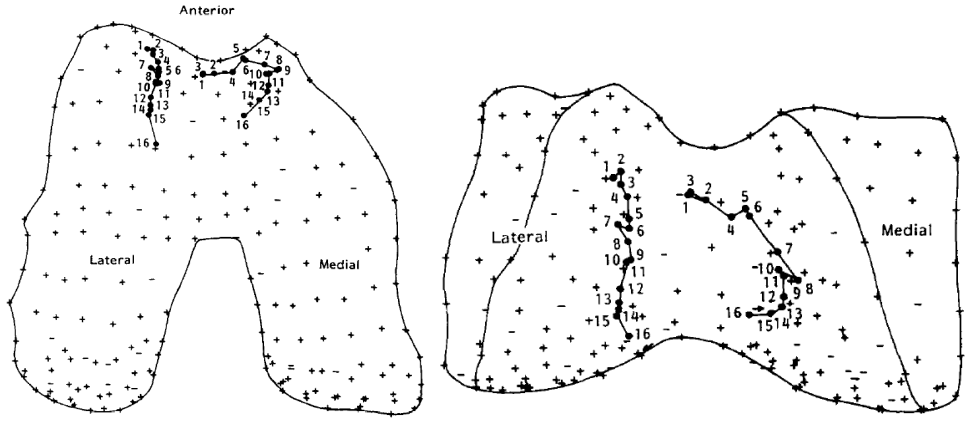

Figure 18. Frontal and transversal view of the contact points [Hefzy and Yang, 1993]

In case of the model of Hefzy and Yang [Hefzy and Yang, 1993] some remarks have to be mentioned as well related to their findings:

- Similar to other models [Van Eijden et al., 1986, Yamaguchi and Zajac, 1989, Reithmeier and Plitz, 1990, Hirokawa, 1991], this mathematical model can only be solved numerically.
- Although their model is three-dimensional, similarly to Hirokawa's model [Hirokawa, 1991], they calculated the parameters only to 72˚ of flexion angle.
- The calculated anatomical angles are mostly in agreement with the two-dimensional model of Van Eijden et al. [Van Eijden et al., 1986], although it seems that the simpler model gives better prediction. In addition, the model of Hefzy and Yang [Hefzy and Yang, 1993] provides solution only to 90˚ of flexion angle.
- The kinetic calculation is not in agreement with the earlier authors [Denham and Bishop, 1978, Van Eijden et al., 1986, Yamaguchi and Zajac, 1989, Hirokawa, 1991], even though the kinematic boundary conditions are the same.
- The Q-angle has not been taken into account, even though the model is three-dimensional.

After a few three-dimensional models, Gill and O'Connor [Gill and O'Connor, 1996] turned back to the two-dimensional modelling (Figure 19) due to the convincing studies of Singerman et al. [Singerman et al., 1994] and Miller [Miller, 1991], who cogently emphasized the importance of the sagittal plane effects in the patellar mechanics.

In the previous studies, related to the two-dimensional modelling, the authors considered contact between the patella and the trochlear groove, although the patella makes contact with the femoral condyles, proven by several authors [Goodfellow et al., 1976, Nakamura et al., 1985, Froimson et al., 1989], at large flexion angle.

The authors stated that the patterns of wear and degeneration of the knee joint depended on both the kinematics and the kinetics of the knee joint. Their purpose was to relate the kinematics and kinetics of the patella to the geometry, the mechanics of the cruciate ligaments, and the tibiofemoral joint. Their model includes the median ridge and the lateral facets, allowing the modelling of the patellofemoral joint at high flexion angles.

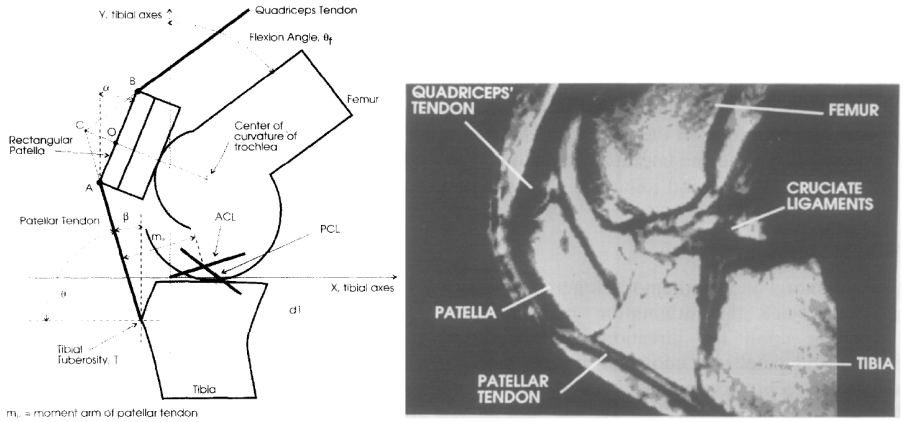

Figure 19. Mechanical model [Gill and O'Connor, 1996]

The authors made the following simplifications and assumptions:

a) Cruciate ligaments from rigid bodies are pin-jointed to the bones,

b) Patellar tendon is inextensible and pin-jointed to the patella and the tibial tubercle,

c) Point contact occurs between patella and femur,

d) Trochlea groove is circular,

e) Patellofemoral and tibiofemoral joints are frictionless. This assumption is made on the basis of extremely low values of joint friction reported by several authors [Radin and Paul, 1972, Unsworth et al., 1974] due to the effect of synovial fluid,

f) The quadriceps tendon is parallel to the femoral axis until wrap occurs (87.5° of flexion angle),

g) The quadriceps tendon and the patellar tendon are in tension,

h) The three forces acting upon the patella, namely the quadriceps tendon force ($\boldsymbol{F_q}$, in this article ***QT***), the patellar tendon force ($\boldsymbol{F_{pt}}$, in this article ***PT***) and the patellofemoral compression force ($\boldsymbol{F_{pf}}$, in this article ***PFCF***) are coplanar and concurrent.

Gill and O'Connor [Gill and O'Connor, 1996] published the following results in their study:

I. The authors' results lie within the area of the result of Van Eijden et al. [Van Eijden et al., 1986], and Yamaguchi and Zajac [Yamaguchi and Zajac, 1989] with regard to the geometric relationships and the $\boldsymbol{F_{pf}/F_q}$, $\boldsymbol{F_{pt}/F_q}$ relationships.

II. The authors' result related to the patellar mechanism angle, which describes the wrapping trend of the femoral tendon, agrees well with the experimental data of Buff et al. [Buff et al., 1988] (Figure 20).

III. The actual moment arm of the patellar tendon changes only slightly compared to the ones found in the literature (Figure 21).

IV. The authors revealed that the length-height of the patella and the radius of the trochlear groove significantly alter the mechanics of the knee joint.

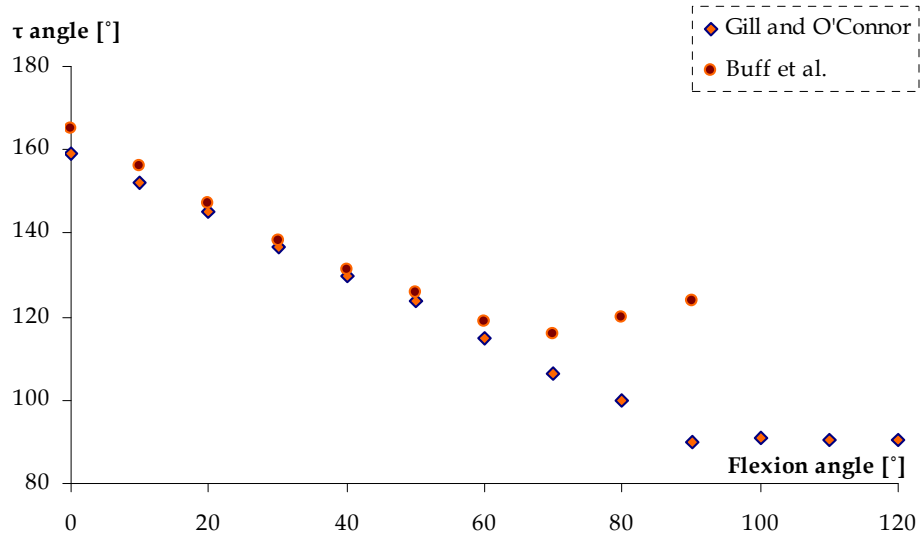

Figure 20. Patellar mechanism τ angle [Gill and O'Connor, 1996]

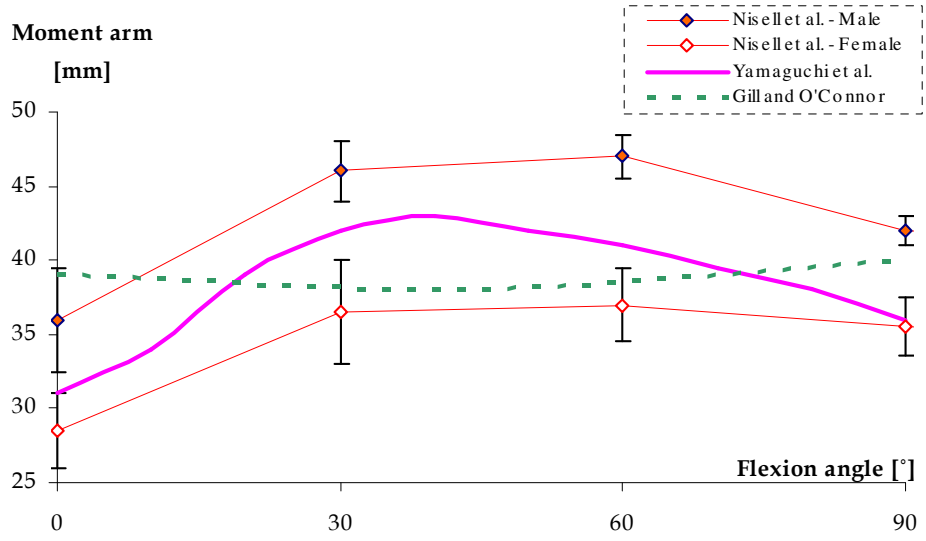

Figure 21. Actual moment arm of the patella [Gill and O'Connor, 1996]

The following remarks have to be mentioned related to the model:

- Similar to other authors [Van Eijden et al., 1986, Yamaguchi and Zajac, 1989, Reitmeier and Plitz, 1990, Hirokawa, 1991, Hefzy and Yang, 1993], this mathematical model can only be solved numerically.
- The model cannot predict the contact forces of the coronal plane. It has to be added that the according to Singerman et al. [Singerman et al., 1994] the forces in that plane are relatively small.
- The shape of the actual moment arm differs significantly compared to other authors' results.

10.14751/SZIE.2013.005

ACKNOWLEDGEMENTS

This PhD work has been carried out at the Department of Mechanics and Engineering Design, Institute of Mechanics and Machinery, Faculty of Mechanical Engineering, Szent István University – Gödöllő, and the Department of Mechanical Construction and Production, Laboratory Soete, Faculty of Engineering and Architecture, Ghent University – Ghent, between 2007 September and 2012 September.

First of all, I would like to express my gratitude to Prof. Dr. Béla M. Csizmadia for the lots of help. I will never forget the late afternoon consultations, when we were looking for the answers of biomechanics by "thinking together". During these conversations, there was always time for discussing the "great questions of life" and step by step, getting to know each other. Wherever life takes me, I will be always proud that I could be his student and I did not only know him as a Professor, but as a fatherly friend.

I would like to thank the help of Prof. Dr. Patrick De Baets for granting me these two years to finish my doctorate. Under his supervision, I could learn the "art of publishing papers" while by his useful comments, I could refine and write a better doctoral thesis.

I express my thanks to Prof. Dr. Magd Abdel Wahab for being able to join the mechanics education of the Ghent University. Thank you for your help in the correction of the papers and for your honest, kind words.

Since I carried out my doctoral work in two countries, I would like to thank the help of all the colleagues from the Department of Mechanics and Engineering Design, Szent István University, and from the Department of Mechanical Construction and Production, Ghent University.

My deepest gratitude is dedicated to my beloved parents, to my mother, Márta Polka, and to my father, Márton Fekete. They brought me up, loved me and made all these things possible beyond their efforts, in order to fulfil my dream. They were the ones, who saw all my steps, stumbles and still always believed in me. God bless you my dear parents.

I would like to express my deepest love and thank to my beloved wife, Evelien Impens. Thank you that you helped me, always loved me and supported me in the hard days. Thank you for being my shelter, my partner, my friend, my all.

Finally yet importantly, I thank the living God this life and all its possibilities that were given to me.